UNIVERSITÀ DEGLI STUDI DI BRESCIA

DOTTORATO DI RICERCA IN INGEGNERIA MECCANICA E INDUSTRIALE

_____

CHIM/07 FONDAMENTI CHIMICI DELLE TECNOLOGIE

CICLO XXXV

_____

VALORIZATION OF BIOMASS WASTE ASH FOR PHOSPHORUS RECOVERY

PhD Candidate:

Laura Fiameni

Supervisor:

Prof. Elza Bontempi

Tutor:

Prof. Laura Borgese

Ai miei genitori,

Per avermi permesso questo percorso di vita

Per aver ambito per me a traguardi sempre più grandi

Per tutta la fiducia che hanno sempre riposto in me

SOMMARIO

Il fosforo (P) è una materia prima critica elencata dall'Unione Europea dal 2017, a causa della sua presenza sulla terra in aree geografiche specifiche sotto forma di roccia fosfatica. Questa distribuzione genera squilibri nella fornitura mondiale dell'elemento, un nutriente essenziale per tutti gli esseri viventi. La questione coinvolge molti aspetti economici e politici, concentrando l'attenzione sulle soluzioni alternative necessarie per la gestione della *supply chain*.

Combinando i principi dell'economia circolare e il processo *end of waste*, sono stati studiati negli ultimi anni diversi tipi di biomasse come fonte secondaria di P. Affrontando anche il problema della gestione degli scarti, anch'esso di grande attualità, la trasformazione dei rifiuti in energia è stata proposta come soluzione congiunta per i due problemi. La conversione termica dei rifiuti da biomassa è una tecnologia sempre più spesso applicata anche per concentrare il P nelle ceneri.

Questo lavoro di tesi è dedicato alla valorizzazione delle ceneri da biomassa per il recupero di P. Dopo un'introduzione sull'argomento (capitolo 1), sono stati investigati due tipi di biomasse: lettiera di pollame (PL) e fanghi di depurazione (SS). Una caratterizzazione completa della cenere di lettiera di pollame prodotta insieme a lolla di riso (RHPLA), derivante da un impianto portoghese, è stata eseguita utilizzando diffrazione a raggi X (XRD), microscopia elettronica a scansione (SEM) accoppiata con EDXS (spettroscopia a raggi X), fluorescenza a raggi X a riflessione totale (TXRF), fluorescenza a raggi X (XRF) e spettrofotometria UV-Vis. Uno studio successivo sulla valorizzazione di RHPLA è stato effettuato esaminando l'estrazione di un ulteriore *eco-material*, diverso dal P. È stato testato il recupero di silice amorfa (SiO_2) da RHPLA, confermando la possibilità di recupero simultaneo di P e SiO_2 nello stesso processo di lisciviazione chimica (capitolo 2). L'ottimizzazione del recupero di P da RHPLA e la valutazione della sostenibilità del processo combinato sono stati completati nel capitolo 3. L'analisi statistica e ambientale della sostenibilità è stata eseguita grazie ad un disegno sperimentale (*design of experiments*) eseguito sulla fase di lisciviazione acida utilizzata per l'estrazione del P. Nel capitolo 4, sono state studiate le ceneri di fanghi di depurazione (SSA) per il recupero di P, conducendo il metodo di estrazione ad umido ad uno stadio successivo, ovvero alla precipitazione di P mediante titolazione alcalina. Durante questa fase, è stata studiata l'influenza del pH di titolazione sul prodotto recuperato, grazie al monitoraggio dell'efficienza di precipitazione di P e degli equilibri chimici in soluzione (software di simulazione Visual MINTEQ). Contemporaneamente, il recupero di SiO_2 è stato testato anche su questo tipo di cenere (SSA) per valutare un'ulteriore valorizzazione del rifiuto.

Proseguendo, il capitolo 5 presenta due casi studio di recupero di P mediante estrazione chimica a umido a partire da diverse biomasse convertite termicamente. La lisciviazione acida e la precipitazione sono state eseguite su due campioni stabilizzati di SSA (con altri sottoprodotti industriali) e su vari prodotti termoconvertiti: cenere, pyrochar e hydrochar di CM e SS. L'efficienza di estrazione di P, l'efficienza di precipitazione di P e il contenuto di metalli pesanti (HM) nei precipitati sono stati

monitorati durante i processi, per valutarne l'efficacia. Infine, nel capitolo 6, il recupero P da SSA è stato effettuato utilizzando un metodo termochimico innovativo, che coinvolge microonde (MW) invece di sistemi di riscaldamento convenzionali. Diversi campioni di SSA mono-inceneriti e co-inceneriti provenienti da un impianto italiano sono stati trattati per confronto mediante MW ed estrazione chimica umida. La solubilità di P in acqua dopo trattamento MW e la co-precipitazione di HM durante l'estrazione sono stati monitorati per verificare l'efficacia delle due procedure.

ABSTRACT

Phosphorus (P) is a critical raw material listed by the European Union since 2017, due to its presence on the earth in specific geographic areas in the form of phosphate rock. This distribution generates imbalances in the worldwide supply of the element, an essential nutrient for all the living beings. Currently the global fertilizer market is still based on the extraction and processing of feedstock, foreshadowing scarcity for the future. The issue involves many economic and policy aspects, focusing attention on necessary alternative solutions for the supply chain management.

Driven by this situation, several actions have been implemented in recent years, seeking to merge governance and scientific implications. P recovery from waste has become a very current topic, of great interest for academic as well as industrial realities. By combining circular economy principles and the end of waste process, different types of biomasses were studied as secondary source of P.

Also facing the problem of biomass waste management, another very topical matter, waste-to-energy transformation was proposed as combined resolution for the two problems. Thermal conversion of the biomass waste, such as incineration, pyrolysis and hydrothermal carbonization, is a technology increasingly often applied.

This work of thesis was addressed to valorization of biomass waste ash for P recovery. After an introduction about the topic (chapter 1), two types of biomasses were used: poultry litter (PL) or chicken manure (CM), and sewage sludge (SS). A complete and novel characterization of rice husk poultry litter ash (RHPLA) deriving from a Portuguese plant was performed using X-ray diffraction (XRD), scanning electron microscopy (SEM) coupled with EDXS (energy dispersive X-ray spectroscopy), total reflection X-ray fluorescence (TXRF), X-ray fluorescence (XRF), and UV-Vis spectrophotometry. Subsequent study on the potential valorization of RHPLA was carried out investigating an eco-material extraction, different from P. Amorphous silica (SiO_2) recovery from RHPLA was tested, confirming the possibility of simultaneous recovery of P and SiO_2 in the same process of chemical leaching (chapter 2). Then, optimization of P recovery from RHPLA and sustainability evaluation of the combined process was completed in chapter 3. Statistical and environmental sustainability analysis was performed thanks to a design of experiment about the acid leaching step used for P extraction. In chapter 4, sewage sludge ash (SSA) was studied for P recovery, conducting the extraction method to a next stage: P precipitation by means of alkali titration. During this step, influence of titration pH on the resulting recovered product was investigated, thanks to the monitoring of P precipitation efficiency and chemical equilibria in solution (simulation software Visual MINTEQ). Concurrently, SiO_2 recovery was also tested on SSA sample to estimate the further waste valorization. Chapter 5 presents two case studies about P recovery by wet chemical extraction from different thermal converted waste streams. Acid leaching and precipitation were performed on two stabilized SSA samples (with other industrial by-products), and on various thermal converted

products: ash, pyrochar and hydrochar of CM and SS. P extraction efficiency, P precipitation efficiency and heavy metals (HM) content in the precipitates were monitored during the processes. In the end, P recovery from SSA was carried out using an innovative thermochemical method, that involves microwaves (MW) instead of conventional heating systems (chapter 6). Mono-incinerated and co-incinerated SSA samples from an Italian plant were treated by means of MW and wet chemical extraction for comparison. P solubility in water after MW treatment and HM co-precipitation during wet chemical extraction were checked to verify the effectiveness of the two procedures.

ACKNOWLEDGEMENTS

I would like to thank all the main figures that in these three years helped me to reach my goals and, above all, to become a researcher.

Professor Roberto Canziani, researcher Andrea Turolla and PhD student Gaia Boniardi, from Politecnico di Milano. It was a pleasure to meet you along my route, and share data, opinions, efforts, a lot of work, but also fun. I understood thanks to you what it means to cultivate a common passion and what is the scientific contamination.

Dr. Bruno Valentim, Dr. Georgeta Predeanu and professor Jale Yanik from DEASPHOR project consortium, for all the advice they gave me and for their commitment to my formation. Thank you so much for all your time spent on me.

All the colleagues from DEASPHOR and PHIGO consortium, who taught me the international side of the research and what it means scientific community.

RINGRAZIAMENTI

Desidero fortemente ringraziare la mia supervisor, professoressa Elza Bontempi, per tutto il lavoro che ha fatto con me e per me in questi anni. Per tutta la fiducia e l'indipendenza che mi ha concesso nell'affidarmi la ricerca. E per la tanta pazienza che ha avuto.

Ringrazio di cuore la professoressa Laura Eleonora Depero, responsabile del laboratorio di ricerca di Chimica per le Tecnologie (C4T), in cui ho lavorato in questi anni e svolto la mia ricerca. Per aver creato e sempre curato un gruppo di ricercatori e ricercatrici da cui ho imparato tanto. Per aver sempre spronato le occasioni di convivialità e di festa, per il riconoscimento di ogni traguardo fatto ad ognuno, e per le tante attività di disseminazione promosse.

Ringrazio entrambe le mie professoresse, per avermi trasmesso la passione per la ricerca, che prima non conoscevo.

Ringrazio i miei colleghi e le mie colleghe, per aver reso la mia quotidianità gioiosa e serena. È una fortuna che non accade in tutti i luoghi di lavoro, e per questo vi ringrazio, perché è stato davvero un piacere passare le mie giornate con voi.

Ringrazio i miei genitori, a cui devo tutto questo.

E ringrazio Antonio, vita mia. Per tutto.

LIST OF ABBREVIATIONS

PR phosphate rocks

P phosphorus

C4T Lab Chemistry for Technologies Laboratory, at University of Brescia

EU European Union

SS sewage sludge

SSA sewage sludge ash

ISSA incinerated sewage sludge ash

WW wastewaters

WWTP wastewater treatment plant

PL poultry litter

PLA poultry litter

RH rice husk

RHPLA rice husk poultry litter ash

CM chicken manure

CMA chicken manure ash

HM heavy metals

S/S solidification/stabilization

WtE waste-to-energy

LCA Life Cycle Assessment

CRM critical raw material

DoE design of experiment

ANOVA analysis of variance

MSW municipal solid waste

MW microwave

TABLE OF CONTENTS

1. INTRODUCTION

1.1. A valuable and critical resource: phosphorus

1.1.1. Deployment and supply of P

Phosphorus (P) is a chemical element diffused in nature in different forms within the life cycles of all living beings. It is essential in biochemical reactions involving genetic material (DNA, RNA), metabolism energy transfer through the adenosine tri/diphosphate (ATP-ADP) cycle, and in structural functions of cell membranes (phospholipids). P is also a fundamental component of bones and teeth, where is present as hydroxyapatite [1].

The natural reserves of this element are phosphate rocks (PR), a sedimentary mineral deposit, that occurs principally as sedimentary marine phosphorites and which take millions of years to form [2]. The largest deposits are located in northern Africa, the Middle East, China, and the United States, with more than 70% of the reserves concentrated in Morocco. The world PR resources are estimated more than 300 billion tons and Figure 1 shows the mining production, with China holding the record of extraction and processing [3].
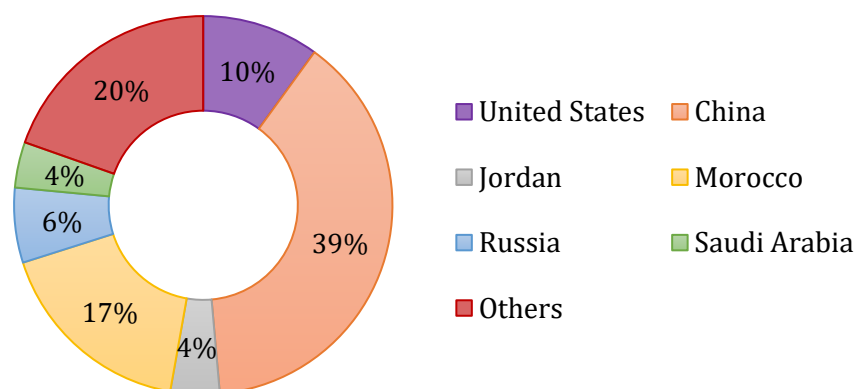
Figure 1.1: *Phosphate rocks (PR) mine production worldwide* [3].

PR and P are considered non-renewable resources, like oil, and in recent decades global attention has been focused on their shortage for next generations [4]. The main use of these two raw materials is the fertilization [5] because the base of the heart's life and biological growth is settled proper on phosphate compounds, more specifically on the bioavailable orthophosphate (PO_4^{3-}) form. PR are extracted from mines and manipulate to manufacture phosphatic fertilizers, such as diammonium phosphate (DAP), monoammonium phosphate (MAP), single superphosphate (SSP) or triple superphosphate (TSP) [6]. Indeed, P is one of the three primary plant macronutrients (P-N-K) that ensures the global food security and the growing of agriculture [7]. According to the Food and Agriculture Organization of the United Nations (FAO), the outlook of P supply in 2022 expressed as P_2O_5 consists of 52 066 thousand tons, versus the outlook of P_2O_5 demand for world fertilizer

production in the same year of 49 096 thousand tons [8]. In addition, world consumption of P_2O_5 for fertilizer production is estimated to have increased by 7% in crop-year 2021 compared to 2020 [3].

Fortunately, despite its scarcity, P can be recovered thanks to its anthropogenic cycle (much faster than the PR formation): after the human extraction from rocks, the element is transformed, spread on the ground, dissolved in rivers and streams, uptake by plants, aquatic and marine animals, algae, and other photosynthetic organisms. The organic decomposition, animal excreta and plants decaying, are at the end and the beginning of the loop, because restore the element to the environment [9–11].

In a world constantly depressed by the huge anthropologic impact on the environment, it is clear, since several years, that is necessary to create a circular economy of the industrial products and by-products for a responsible consumption and production. The challenge interests all the world population and is part of the UN Sustainable Development Goals (SDGs) [12]. This is a fundamental point regarding the P problem, since it is known that there are no substitutes for P in agriculture [3].

1.1.2. The European problem

Compared to the rest of the world, the EU is already challenging with P scarcity due to the geographical distribution of the reserves and the trade monopoly. The European Commission prepares a triennial updated list of critical raw materials (CRMs) for the EU [13] in which P is present since 2017 and PR since 2014. So, the global problem of P supply became more urgent for our continent where P is already listed as CRM and alternative solutions are needed. Sustainable and innovative technologies must be explored to substitute a critical resource in exhaustion, as in the case of lithium (essential to produce rechargeable batteries and for the energy transition) and bauxite (mineral from which aluminum is extracted), listed for the first time in the last CRMs EU report, in 2020.

The depletion of natural resources is a very current topic that concerns not only the present materials procurement, but also the future policy decisions, considering all the environmental effects and earth changes. In the *Circular Economy Action Plan* adopted on 11 March 2020 [14], the European Commission promotes access to alternative feedstock sources such as sustainable biomass. The aim is to reduce greenhouse gas (GHG) emissions and landfilled wastes because in the future, biomass will play an important role in renewable and sustainable energy development. In particular, the agricultural and livestock sector has a key role in the growth of the bioeconomy, since it is a major producer of biomass for feed, food, and energy [15]. In 2018 the European consumption of inorganic P fertilizers was 1.13 million tons [16], and Turkey, France, Spain, Poland, Italy, Germany, Romania, United Kingdom and Hungary were the main countries with a consumption higher than 50 000 tons per year.

Therefore, the most affordable solution, in terms of environmental and economic impact, is to recover and recycle CRMs from other secondary sources.

1.2. Secondary P sources

1.2.1. The most accessible sources: biomass waste

Based on what explained in section 1.1.1., all the biological material, generated by plants, animals and humans, can be the most widespread and most accessible P source. From here, the possibility to not limit the supply of a such precious element only as product from extraction of PR but recover it from waste [17]. Biological waste, such as biomass, can therefore close the P cycle, providing an opportunity for the future [18] and delivering a possibility of application in the fertilizer industry [19]. P recovery from waste is an emerging practice that aims to restore P present in organic waste streams, conserving resources and reducing the environmental impact of P mining. Especially, P recovery and recycling from biomass waste and wastewater has been much studied during the last 25 years, and many publications and reviews were made especially in the last 15 years. Recently a very complete work of Hisao Ohtake and Satoshi Tsuneda [20] collects useful information on the element availability, the production and the application in the world, the development of P-recycling, the analysis of Circular Economy and Life Cycle Assessment (LCA), the recovery methodologies from different waste, and the different processes and plants, always comparing the situation of Europe and Japan. A large part of the work is dedicated to raw materials/waste and treatments to recover P from them. More in general, in literature, some main biomass waste was found very capable alternative P source, as long as its uncontrolled dispersion in the environment is avoided and a specific end of waste criteria are identified [21]. They are sewage sludge (SS) originating from wastewater treatment plant (WWTP), animal manure, animal by-products and slaughterhouse waste (e.g., meat and bone meal) and food waste [11][22][23][24]. In this paragraph, particular attention will be paid to the two specific biomasses addressed in this thesis: sewage sludge and animal manure.

Sewage sludge

SS can be a by-product of municipal or industrial WWTPs, and the high levels of P in it were already studied for recovery through added biological and chemical operations at various steps of the WW treatment [25]. SS were widely studied for double scope: initially P was an annoying element because it generated eutrophication [26] and had to be removed from the water purification line and sludge, and after it became a precious element for its role in agriculture and its shortage [27,28]. Interestingly, in literature, on this point, the research has moved from "P removal" to "P recovery". During the last decades, sewage sludge production in Europe has rapidly increased (from 7.8 to 10 million tons) [29], and in the Italian and European context, SS production and disposal is a very current problem, with environmental and economic repercussions. The large amount of waste to be treated makes landfill disposal a no longer viable solution. Alternative methods have been proposed: agricultural use, compost and incineration are the most used. According to Eurostat data reported in **Figure 1.2**, EU countries have very different destination (and policy) for SS; for example, Greece, Italy, Malta, Bosnia-

Herzegovina, Romania, and Croatia, maintains landfill as major disposal route, while The Netherlands, Germany, Slovenia, and Switzerland use incineration as the most common treatment [30]. Also, the past widespread agricultural use of SS is now often restricted due to its large concentrations of HM, pathogens and toxic organic compounds [31], favouring alternative solutions for waste management such as mono incineration. In this view, only high-quality sludge should be directly applied in agriculture while sending to mono-incineration the remaining amount for both material and energy recovery. However, incineration does not remove most of the HM contained in SS, and depending on local legislation, may constitute a regulatory constraint also for the direct application of SSA as a fertilizer on crops [32].
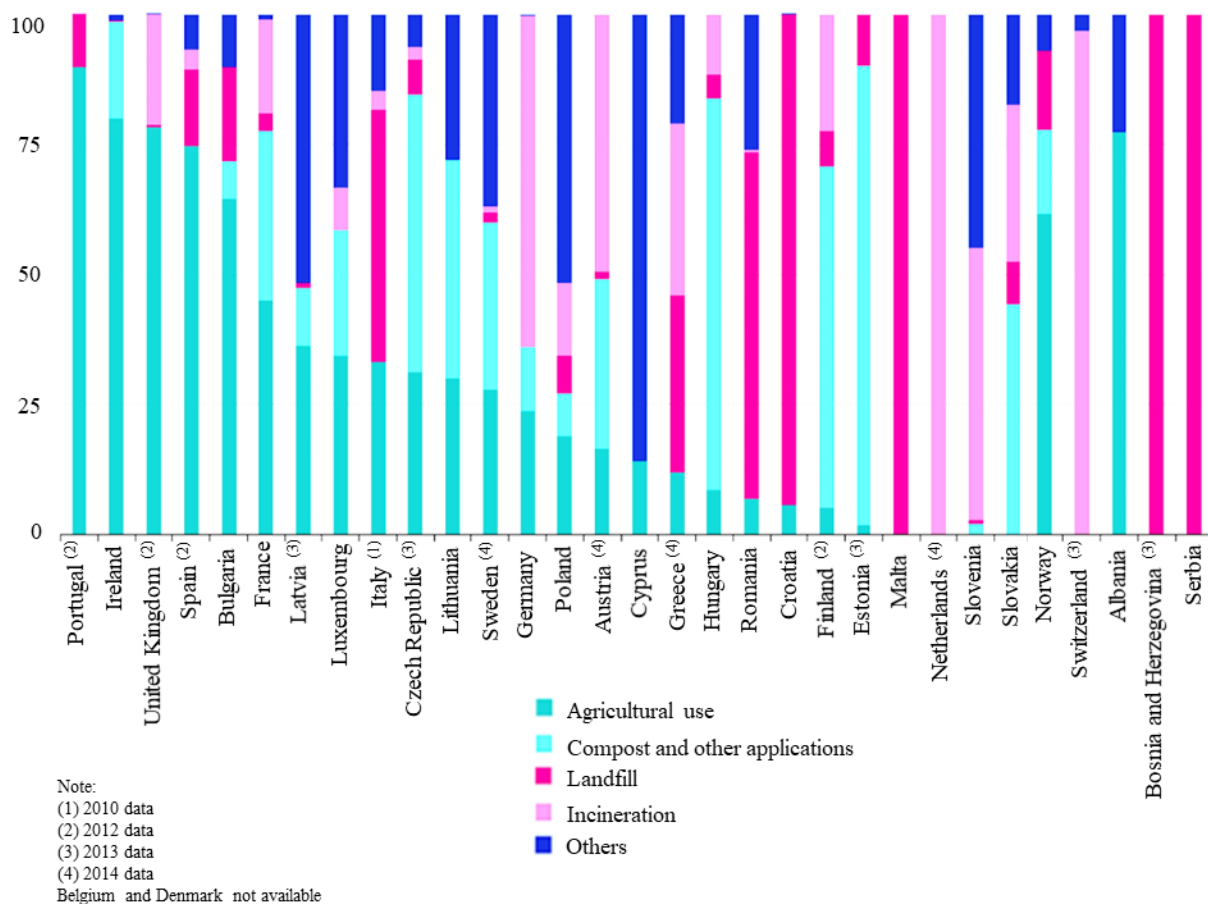
Figure 1.2*: Sewage sludge percentage of disposal in the EU countries, from Eurostat 2019. (1) 2010 data, (2) 2012 data, (3) 2013 data, (4) 2014 data. Data for Belgium and Denmark not available* [30]*.*

Animal manure

During the period 2016–2019, in Europe (EU-27) and UK, 1.4 billion tons of animal manure were produced annually from farmed animals including cattle, pigs, sheep, goats and poultry [33]. Animal manure is widely used as organic fertilizer, directly applied to soils and is often present in excess in intensively farmed areas [33][34][22]. The solution to this excess accumulation is to transport the manure to regions with less production or invest in the nutrient's extraction from the animal waste,

since the movement is costly and inefficient due to the high amount of moisture present in almost all animal excrement. The characteristics of P in the animal manure [35] are relevant for undertaking the study of P-recovery, and literature already presents examples of alternative P supply in agri-food sector, where the element can be recovered as struvite from breeding and dairy processing wastes, and used as a fertilizer [36,37]. In particular, compared to the other waste streams, poultry litter (PL) (i) has a high N and P content, (ii) is relatively dry and consequently more adequate for energy recovery and (iii) it is easier to transport [38]. In this way, PL and chicken manure (CM) become a valuable provider not only of P, but also N and C according to the technology adopted for the handling [39].
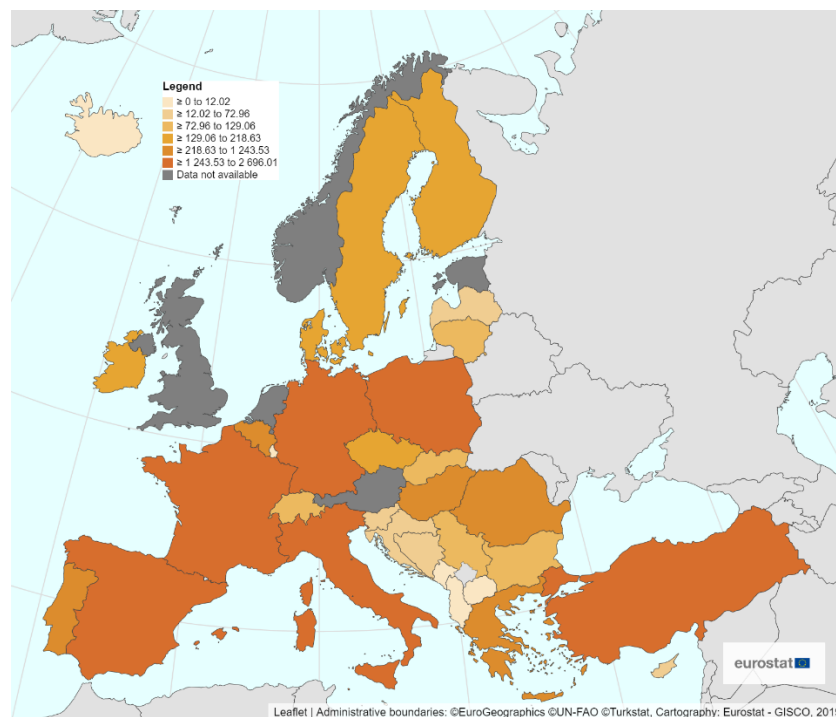
Figure 1.3: Annual production of poultry meat in 2020 in the EU countries, expressed in thousand tons [40].

Considering the production of poultry meat in the EU in 2020, **Figure 1. 3** shows visual data expressed in thousand tons. Spain, France, Italy, Germany, Poland and Turkey have a national poultry meat production over 1.2 million tons per year, with almost a double production in Poland (2.7 million tons) and Turkey (2.2 million tons) compared to the other countries. These considerations confirm the very current issue that the management of large volumes of PL and CM can generate, as of SS.

1.2.2. Advantages of thermal conversion

Using the term biomass, is implied to identify an organic and non-fossil material used for production of biofuels, and therefore of energy [41]. For this scope, biomass is converted in a proper plant for heat production or electricity generation.

Regarding SS, the literature about thermochemical treatments is wide considering that the management of this waste has been the focus of research since the beginning of the 21st century [42][43] driving the implementation of thermal conversion techniques in function of P recovery [44–46]. In particular, thermal conversion of SS allows the safe handling of biological waste that is otherwise hazardous due to pathogens and the reduction of its volume and mass facilitating transport and reuse [47,48]. Mono-incineration of SS in specific waste-to-energy (WtE) plants is an option that allows the recovery of both energy and matter, minimizing the amount of final waste, and reducing the global carbon footprint of this cycle by recycling the waste resulting from incineration and applying carbon capture systems. The product generated, the incinerated sewage sludge ash (ISSA), is the most popular in various European countries, where the incineration practice is common. The leading countries are Netherlands, Belgium, Germany, Austria and Turkey where the incineration of SS coming from urban WWTPs in 2018 was respectively equal to 89%, 76%, 74%, 53% and 49% of the total sludge disposal [29]. The P content in ISSA varies greatly depending on the nature of SS, but it was estimated up to 12% [49], close to the value of PR, between 2 and 18 % [50]. Anyway, studies of pyrolysis and hydrothermal carbonization (HTC) of SS are similarly diffused in view of P recovery from SS [51–54].

On the other side, to identify the more advantageous transformation to implement for PL, more recent studies on management and valorization of the waste have been done [55,56]. Composting, anaerobic digestion and direct combustion were proposed to reuse PL [57], recognizing satisfactory calorific values of this biomass, suitable to the use as energy feedstock [58–60]. Nusselder et al. [38] demonstrated with LCA that PL thermal conversion is the best environmentally friendly method for the management of this waste, because a low environmental impact and elimination of organic pollutants can be achieved by thermal treatments. Thus, the ashes from the incineration, the poultry litter ash (PLA), are rich in P [61,62] and their high potential for reuse is very appealing [63,64] so much so that PLA was already proposed as alternative P source [65–67]. PLA has a P content between 4 and 11%, because P is concentrated in the solid matter during the combustion, even if the loss of N and C occurs, both important elements in fertilizers [61,68].

In this work, the samples investigated are coming from PL (or CM) and SS. The selection of these biomasses was ruled by all the aspects described above, and by the possibility of collecting samples.

1.3. The main P recovery technologies

1.3.1. Wet chemical extraction

The wet chemical extraction is a simple and largely applied method, that requires a solvent (extractant) left in contact with the solid sample, to favor the dissolution of nutrients and soluble salts. It can be easily implemented in laboratory and scaled-up in a pilot plant, adjusting different variables, such as contact time, liquid to solid (L/S) ratio, temperature, extractant concentration, and type of mixing. Unfortunately, without a selective operation, not only main elements like Al, Ca, Fe, K, Mg and P are leached, but also a certain amount of HM. The mixture is then filtrated or separated, and the leachate stored for subsequent step of P precipitation. The natural by-product is the solid residue free of P and soluble components. For SSA, which has been extensively studied, the most common method for P-recovery is acid lixiviation because of its simplicity, high efficiency, and low costs [69–74]. For PLA, the main advantage of this procedure is given by the low content of HM compared with SSA [75] and so, all the problems of contaminant co-dissolution are, in this case, overcome.

The principle behind the wet chemical extraction of P from biomass ash is very similar to the traditional industrial method use for P extraction from PR. But if in the second case the practice was experimented and refined for several years, in the first case continuous improvements and studies must be done, to obtain a purified and suitable P product. The research in this sense is only in a former stage and needs to test a lot of different biomass and procedure to find the best solution. Biomass ash is chemically and mineralogically more complex than PR, and often differs from each other according to the origin; for this reason, the research takes a careful material characterization as primary step.

A specific study of Fahimi et al. based on carbon footprint and embodied energy involved in the different technologies proposed for P recovery, confirms that wet chemical extraction is the more sustainable method [76]. Also, Egle et al. came to the same conclusion through a techno-economic assessment [77].

1.3.2. Thermochemical treatment

The thermochemical treatment provides the mixing of the biomass ash with a chemical additive, such as mainly carbonates and sulfates [78][46,79,80][81,82], or chlorides [83][84–86], and the following heating up to 500 - 1200°C [44]. This operation ensures the conversion of the low plant available P compounds present in the ash, to the more soluble form. Simultaneously, the HM content is reduced by the volatilization during the heating process and the treated biomass ash is transformed in a P fertilizer with great potential as raw material [87][88].

The main downside of this technique is the high operational costs due to energy consumption performed with a traditional furnace, but the right balance between energy dosage, cost of chemicals and P bioavailability of the final product, can benefit the process [89].

In this research work, both recovery techniques described above were tested. In the first part, wet-chemical extraction was performed on the samples, while in the second part, an innovative and low-power consumption thermochemical treatment was adopted. Starting from literature already available for SSA, a procedure for P leaching from PLA was proposed, while at the same time a pioneering microwave patented process for P-recovery was suggested. The aim is to build operative methods where all the steps are designed to be as sustainable as possible, and the by-products adapted for a safe reuse.

1.4. Italian situation

In this frame, Italian situation about P recovery from combusted biomass needs to be analyzed from different points of view. The municipal solid waste (MSW) incineration is a common and well-known practice [90], and according to the scientific community, monitored mono-incineration of (urban and biomass) waste in specific WtE plants for energy and matter recovery, is a good solution for manage the existing waste. Nevertheless, the national public opinion express strong concerns about fumes emitted by chimneys, even if they are properly treated to remove pollutants. The public perception is that they are worse than greenhouse emissions from landfilled wastes, maybe because the former are visible, and the latter are not. Moreover, the population does not support the construction of new WtE plants. It is also necessary to consider the difficulty of technology transfer of a completely new way of processing waste: Italy has 37 efficient WtE plant for the handling of MSW, 26 of which are located in the north of the country. 20 of these plants are settled in only two regions: Lombardia and Emilia Romagna [91,92]. The adaptation of these plants for different input materials i.e., biomass waste such as SS and PL, seem to be the easier and fastest decision. In Italy actually we have some situations of co-combustion of SS with MSW [93,94], and few cases of SS mono-incineration plants in Bologna [95], Prato [96], and Milano [97][98]. The project Biopiattaforma guided by CAP Holding is a virtuous example of integrated approach to overcome the public opinion hesitations. The further step, at the centre of today's research, is the subsequent P and nutrient recovery from the ashes.

To have a clear idea of the current situation, the national SS production is 3.9 billion tons per year, with high production concentration in the region Lombardia (where Milano and Brescia are located), that has 10 million inhabitants and generates 770 thousand tons of SS every year [99]. Less than 15 % of this SS is incinerated because spreading on crops is very common, together with composting and biochemical treatments [100]. Furthermore, starting from 2019 many industrial SS were excluded from the agronomic practice due to recent regulation (d.g.r. 1777/2019) and now, more urgently than before, we need to find a proper way to manage the waste.

As Italian researchers, we are trying to lead the country towards the good practice shown by other European countries, to propose sustainable solutions from an economic and environmental point of view. To follow up the European policy, Italy must create and spend efforts in this current topic, complementing this type of research by policy makers and regulatory authorities. In this view, the creation of an appropriate Italian legislation on this subject must comply the European trend and the continuous recent developments encouraged by the EU commission. The European Sustainable Phosphorus Platform (ESPP) [101] works incessantly for strengthening of the international network and sharing of technologies. Based on these actions, also Italy generated a national platform for P management and recovery, led by the Italian National Agency for New Technologies, Energy and Sustainable Economic Development (ENEA) [102]. Starting from 2023, the activities of the national platform will be relaunched by the Ministry of Environment and Energy Security.

The first hurdle to overcome is the awareness of the problem we are experiencing, for the supply of this and other valuable raw materials, and the decision to invest resources and energy in finding solutions ahead of time. Italy is not able to decide immediately which technology to use for P recovery, but rather in the phase of cognizance that the problem must be addressed starting from the transformation and exploitation of waste. Once widespread the waste processing method will be possible to experiment with the most suitable recovery method in a large industrial scale.

Believing in a future circular management of MSW and biomass waste in Italy, this doctoral research wants to give an overview of the P recovery alternatives deriving from SS and PL mono incineration.

1.5. Research approach

1.5.1. Methodology and statement of originality

This three-year work could take advantage of several inputs, including expertise, multidisciplinary skills, ash samples and analytical instrumentations, thanks to the international and national partnerships in the frame of various projects.

The final output of the research is a set of data in part generated in first person in the Chemistry for Technologies Laboratory (C4T Lab) at University of Brescia, where this work was conducted, and in part generated by the partners. The collaboration with different teams has allowed the sharing of the results and the creations of joint publications.

The PhD fellowship was half funded by the European **project DEASPHOR** "Design of a product for substitution of phosphate rocks", under the scope of the ERA-MIN2 Joint Call (2017) on raw materials for sustainable development and the circular economy (ref. n. ERA-MIN-2017_40) [103]. The project was coordinated by Dr. Bruno Valentim, Faculty of Sciences of Porto University (PT) and the main objective was the recycling of P from aviary litter ash as a substituting material of phosphate rocks. The principal tasks in charge of the University of Brescia, team led by Professor Elza Bontempi, were the sampling and chemical characterization of the ash, the P-extraction efficiency evaluation in function of the fertilizing potential, the zero-waste assessment based on silica utilization and the environmental evaluation starting from the carbon footprint considerations. All these results are presented in chapter 2 and chapter 3, based on two scientific publications as first author, two scientific publications as co-author, and two poster presentations as first author at international conferences.

Concurrently to this research, a collaboration with Politecnico di Milano, Department of Civil and Environmental Engineering (DICA) has been driven, in the frame of the Italian **project PerFORM WATER 2030** (ID 240750) [104] directed by Gruppo CAP. The research was activated under the scope of Regione Lombardia Call on Agreements for Research and Innovation (POR FESR 2014–2020). The project intended to face the Italian challenges of the public water management sector, and the partnership with the team of Politecnico di Milano led by prof. Roberto Canziani, was focused on P recovery from sewage sludge ashes and valorization of the by-products after the extraction. The results of this work are presented in chapter 4 and partially in chapter 5, based on two scientific publications as co-author, and two poster and oral presentations as first author at international conferences.

In addition, in the last year of the doctoral program, it was possible to further expand the collaborations. The C4T Lab was in charge of P recovery from sewage sludge ashes and valorization of other raw materials present in the ashes, within the Italian **project FANGHI** (ID 1178787) [105] led by A2A Ambiente S.p.A. The research was activated in the frame of Regione Lombardia Call "Research and

Innovation Hub" (POR FESR 2014-2020). The aim of the project was the experimentation of advanced forms of sewage sludge management thanks to the establishment of a hub in Lombardia (northern Italian region) for the development of the territory. At the same time, University of Brescia, through Professor Elza Bontempi, was involved in the European **project PHIGO** "Thermal Processing of P-rich ashes aiming for HIGH-GRADE PHOSPHORUS Products", under the scope of the ERA-MIN3 Joint Call (2021) on raw materials for the sustainable development and the circular economy (ref. n. JTC-2021_035) [106]. The project is coordinated by Dr. Guozhu Ye from Swerim (SE) with the principal goals oriented to the optimization of the biowastes incineration step and to the development of a sustainable technology for an efficient thermal P-extraction from P-rich ashes. The results of participation in these projects are presented in chapter 6, based on a scientific publication as first author.

Overall, the work reported in this thesis is the outcome of the interweaving of several studies regarding P and eco-materials recovery from biomass waste, which involved many partners, many insights and trials, and different methods of recovery. This type of approach to research has permitted access to samples and instrumentations otherwise inaccessible, creating a productive network that can guarantee the basis for an exchange of information and experience aimed at the sustainability of the supply and distribution of resources in the EU. The cooperation and continuous dialogue with colleagues have allowed a progress of the research in function of a wider vision of the national and international situation about the topic.

1.5.2. Objectives

The research objectives are directly correlated to the tasks and objectives assigned to C4T Lab during the collaboration within the international and national project cited in the section 1.5.1. Specifically:

  I.   Characterization of RHPLA in view of its use as secondary P source;

 II.   Optimization of P extraction by wet-chemical method from RHPLA, based on environmental and efficiency parameters;

III.   Evaluation of the recovery of additional material (amorphous silica) from RHPLA and ISSA after P wet chemical extraction, in a zero waste perspective;

 IV.   Investigation of P precipitation from the ISSA leachate in function of the HM minimization, for potential application as fertilizer;

  V.   Study of advanced solutions for P-rich biomass waste management, including different thermal treatments and stabilization of HM by pozzolanic reactions before the P recovery step;

 VI.   Testing of an innovative and sustainable technique, based on thermochemical conversion of the P-rich biomass ashes, to increase P solubility and bioavailability.

More in general, this work of thesis would like to be the foundation for a conscious choice for the investment of resources and technologies by institutions and companies, especially in the national

context. SS plays a leading role in the panorama of P recovery for a long time, due to the attendant and very current issue of the management of this waste. WWTPs, in which SS is produced, are part of the primary water system of each country, and minimization of the SS volume through incineration in WtE plants would be the best solution for both problems: SS disposal and P supply. On the other side, different biomass waste (PLA, CMA) can be likewise a valuable alternative P resources, and it may be time to concentrate energies also in this direction.

In a global vision of transition to a greener and sustainable reality [107], this research is guided by a model of circular economy and environmental protection and suggests technological innovation to prevent depletion of a critical element, and reuse of the process by-products.

1.5.3. Outline

As already described in the section 1.5.1., the thesis is organized on the experiments carried out within the different research projects and collaborations. Each chapter, except chapter 1, is structured as a scientific report, with its own introduction, materials and methods part, results and discussion part, and conclusion.

- Chapter 1: Introduction
- Chapter 2: Rice husk poultry litter ash characterization and valorization – DEASPHOR project
- Chapter 3: Optimization of P recovery from RHPLA and sustainability evaluation of a zero-waste process - DEASPHOR project
- Chapter 4: Sewage sludge ash study for P recovery and waste valorization – collaboration with Politecnico di Milano in the frame of PerFORM WATER 2030 project
- Chapter 5: P recovery by wet chemical extraction from different thermal converted waste streams - collaboration with Politecnico di Milano in the frame of PerFORM WATER 2030 project and collaboration with EGE University (TR) from the consortium of DEASPHOR project
- Chapter 6: P recovery from SSA by innovative thermochemical treatment and comparison with wet chemical extraction – FANGHI project and PHIGO project

2. POULTRY LITTER ASH CHARACTERIZATION AND VALORIZATION

Abstract

This chapter is focus on the characterization of a specific type of PLA, coming from an industrial Portuguese power plant, using the traditional techniques already reported in literature for other biomass waste ash, such as ISSA. After this stage, the possibility of recovering different eco-materials from the ash was studied. Manure, and more in general biomass, contains large amounts of macronutrients and other elements that may be recycled, in the frame of zero waste concept. The main attractive reuse for the recovered products is the fertilizer production, especially for P which is listed as a CRM due to its high demand and limited availability in Europe. On the other side, often the ash residue after P removal remain without a specific destination, and it be considered as a useless by-product. To ensure, not only the sustainability of the food chain, but also the principles of circular economy, this research focuses on the extraction and recovery of amorphous silica (SiO_2) from rice husk poultry litter ash (RHPLA). Two different extraction procedures are proposed and compared, and the obtained silica is characterized. This work shows that SiO_2 can be recovered as an almost pure material rendering the residual ash free of P thanks to an acid leaching. Therefore, it also addresses the option of more specific P recovery from RHPLA through wet-chemical extraction. In this way RHPLA could be a good secondary P source and recovered SiO_2 could be tested for HM stabilization in different matrices, such as municipal solid waste incinerated fly ash (MSWI-FA), thanks to the occurrence of pozzolanic reactions.

Keywords

Poultry litter ash characterization

Ash residue valorization

Silica extraction

P recovery

Scientific contribution

This chapter is based on the following publication, whose form have been adapted for reasons of consistency with the structure of this doctoral thesis. The content reported in this chapter is the result of my own work, including literature review, data curation, formal analysis, investigation, methodology, visualization, and writing. Any work made by others is attributed to the original author in the text.

o **Fiameni L.**, Assi A., Fahimi A., Valentim B., Moreira K., Predeanu G., Slăvescu V., Vasile B. Ş., Nicoară A. I., Borgese L., Boniardi G., Turolla A., Canziani R., Bontempi E., Simultaneous amorphous silica

and phosphorus recovery from rice husk poultry litter ash. *RSC Advances* (2021), **11**, 8927-8939. https://doi.org/10.1039/d0ra10120f

2.1.   Introduction

Considering PLA as a great asset for P supply, in this work a specific type of rice husk poultry litter ash (RHPLA) is studied. Every year around the world, approximately 3×10^7 tons of biomass waste is produced from rice husk (RH) [108]. RH is the coating of a seed and is a by-product of the grinding process that separates the rice grain; it has been proposed as an alternative to wood shavings and sawdust as bedding material in poultry houses [109,110]. In this way RH is mixed with PL, generating a difficult waste to separate, so that it becomes part of the biomass manure used as fuel for combustion. The incinerated product is RHPLA.

As already studied, RHPLA is mainly composed of K, P, Ca, S, and Si, where the amount of amorphous component is higher than 60% [75]. Obviously, in such a complex waste, containing several phases and different elements (also in low quantities), it is hard to define the exact amorphous composition. But literature reports that the combustion of RH, produces essentially amorphous silica (SiO_2) [111].

It is important to highlight that the depletion of natural resources, such as PR, requires the continuous improvement of recovery strategies, with an emphasis on the recovery of all the waste components, especially when they derive from incineration processes [30]. In particular, recently a new idea was developed in terms of Azure Chemistry [112], with the aim to not only replace CRMs with valorized wastes (i.e. secondary materials) but also to strive for simultaneous recover and recycle of the by-product derived from the CRM extraction and subsequently use it in other applications [75,113]. In this context, creative approaches are mandatory as a driving force not only to find suitable and sustainable ways to proceed in the recovery of CRMs but also to propose new and high-value applications for the recovered materials [114] that are defined eco-materials. Eco-materials improve environmental protection and respect the sustainability pillars while maintaining accountable performances [115–119][115–119].

In this way, RHPLA is not only considered a secondary P source, but also a field of other possible eco-materials. This is the case of SiO_2 contained in the ashes, that can be recovered. Silica recovered from RH has gained attention over the years due to its various applications and the virtuous example of the circular economy that it represents. Fillers, additives, desiccants, adsorbents, catalysts, mesoporous materials, nanocomposites, ceramics, biomedical sector, and heavy metal stabilization of incineration waste, are some of the fields in which value-added silica from RH could found application [116,120–123].

The overall objective of this work is to propose an eco-material extraction (SiO_2) from RHPLA, that can be made in combination with P recovery. RHPLA, and more in general PLA, is a type of waste that obtained visibility for reuse in a recent period, and for this reason, it is necessary to start from the ash characterization, performed in the first part of the chapter. **Table 2.1** shows the P and Si content in different biomass ash reported in literature. It is evident that P can be equally concentrate in both fly

and bottom ash, while SiO_2 is more present in bottom ash, especially if the combustion system is made of a fluidized bed with sand as bedding material.

Table 2.1: Phosphorus (P_2O_5) and silicon (SiO_2) content in biomass ash. * mean value, ** data converted with conversation factors $P/P_2O_5 = 0.436$, $Si/SiO_2 = 0.468$.

Biomass ash	P_2O_5 %		SiO_2 %		Reference
	Fly ash	Bottom ash	Fly ash	Bottom ash	
Poultry litter ash	16.17 *, **	11.47 **	7.37*, **	19.66 **	[124]
	-	12.16 **	-	-	[125]
	-	22.00 *, **	-	-	[61]
	-	19.38 **	-	-	[63]
	22.71	-	3.19	-	[126]
Animal by-products (meat bone meal ash)	22.45 **	25.96 *, **	-	-	[61]
	32.50	-	1.80	-	[126]
	-	30.94 **	-	4.36 **	[127]
Pig manure ash	-	22.80 *	-	13.30 *	[126]
Wood ash	0.69 **	3.21 **	7.69 **	12.39 **	[128]

2.2.   Materials and methods

2.2.1.   Sampling

RHPLA was sampled at "Campoaves, S.A." (Figueira da Foz, Portugal) from an incineration plant designed for the combustion of PL in a chain grate stoker with an over-fire airflow which regulates the temperature for combustion at ~1000 °C. The fuel is composed of rice husk poultry litter (the rice husk is provided from rice fields which are in the surrounding area close to the plant) and woodchips on a 70:30 ratio. The generated ash consists of bottom ash (BA) accumulated in a wet tank in an open-air storage area close to the plant, economizer fly ash (ECO), and fly ash captured by a multicyclone system (MCYC).

The conditions of the boiler are variable and change from month to month. On average, the plant generates 156 tons of ash/month. The amount of ash sampled reflects the specific conditions implemented on the day of sampling. After 5 h, the samples were collected in thick plastic bags. Approximately 327 kg of BA was collected at the water tank exit, 5 kg of ECO was collected from a duct connected to the economizer with an exit point near to the BA outlet, and 10 kg of MCYC was collected from the multicyclone hopper. The samples were dried for 24 h in aluminium trays inside an oven operating at 50 °C, as described by Fahimi et al. (2020) [75] and Andò (2020) [129]. After drying, the samples were manually divided into representative fractions through the coning method and then further divided into representative 100 g sub-samples using a riffle splitter. The ashes were then sent to C4T Lab where they were grounded, and finally sieved to obtain four different fractions: <300 μm, 300-500 μm, 500-1400 μm, >1400 μm. The sieving was manually carried out with a set of ASTM International standard sieves: 50 mesh (300 μm), 35 mesh (500 μm), and 14 mesh (1400 μm).

2.2.2.   Characterization techniques

For the structural characterization of the raw ashes and the amorphous silica fraction obtained from the raw ashes, X-ray diffraction (XRD) analysis was conducted. XRD measurements were performed by a PANalytical X'Pert PRO diffractometer (PANalytical, Malvern, UK), equipped with a Cu Kα anode and operating at a voltage of 40 kV and a current of 40 mA. For the phase identification, Philips X'Pert software was used (associated with the crystallography open database COD) as described by Assi et al. (2019) [130]. Morphological and dimensional characterization of the ash and silica powder samples were performed through scanning electron microscopy (SEM) (LEO EVO 40, Carl Zeiss AG, Milan, Italy), coupled with an EDXS (energy dispersive X-ray spectroscopy, Oxford instruments, Wiesbaden, Germany) probe for elemental analysis and semiquantitative chemical characterization. The material topography was analyzed using the secondary electron (SE) mode. Total reflection X-ray fluorescence (TXRF) technique was used for elemental analysis in solution. A stock solution of 1 g/L Ga in nitric acid (Ga-inductively coupled plasma (ICP) Standard Solution, Fluka, Sigma Aldrich) was used as the internal standard. Approximately 0.010 g of 100 mg/L of Ga solution prepared from the stock solution

was added to the samples and properly diluted with MQ water to obtain a final concentration of 1 mg/L Ga in 1 mL specimens. The specimens were then homogenized using a vortex shaker for 1 min at 2500 rpm [117]. For each specimen of the leachate solution, a 10 μL drop was deposited on three different plexiglass reflectors and dried on a hot plate at 50 °C under a laminar hood. Each reflector was irradiated for 600 s of live time using an S2 Picofox system (Bruker AXS Microanalysis GmbH, Berlin, Germany) equipped with a Mo tube (operating at 50 kV and 750 mA) and a silicon drift detector (SDD). An instrumental software with a routine deconvolution based on mono-element profiles was applied to evaluate the peak areas and analyze the TXRF spectra. Since lighter elements such as P and S can be underestimated by the TXRF analysis under the reported experimental conditions [131], a dedicated calibration curve was developed for S and P to correct for matrix effects following the approach reported by Borgese et al. (2018) [132].

Element concentrations present in the acid leaching solution were converted into extracted mass using **Equation (2.1)**:

$$\text{Extracted mass (mg/Kg)} = (C \cdot DF \cdot V)/m \qquad\qquad \textbf{(2.1)}$$

in which:

C = concentration of the analyte in solution (mg/L)

DF = dilution factor

V = volume of extractant (mL)

m = mass of ash weighed for the test (g)

For qualitative and quantitative X-ray fluorescence (XRF) analysis of the elements, an X-ray Sequential Fluorescence Spectrometer Thermo Scientific ARL PERFORM'X equipped with an X-ray tube with Rh anode and Be window of 30 μm was used. The entire surface of the sample was analyzed in a dry He flow. Phosphorus quantification was performed via UV-Vis chemical method. The method was developed following the Romanian standardized method [133]. RHPLA raw samples were prepared at a grain size of less than 0.2 mm and the amount was 0.1 g with a 0.0001 g measured accuracy. Then, RHPLA samples were solubilized with a mixture of concentrated acids 2:1/H_2SO_4: HNO_3. To prevent the colorimetry operation, the silicic acid that produces the opaque solution was removed by filtration. The analysis was carried out by adding ammonium molybdate and H_2SO_4 6N solutions. The P concentration in the filtrate was encapsulated in phosphomolybdate $[(NH_4)_6Mo_7O_{24} \cdot 4H_2O]$ and the absorbance of the resulting blue solution was measured at 700 nm wavelength by JASCO V570 UV-VIS spectrophotometer at UPB - CPMTE laboratory. The measurements were done in 2 cm thick cuvettes. As a reference, a blank solution of the reagents, without the ash, passed through all the analytical steps was used. The spectrophotometer was set to perform three readings and the average was taken. On

the calibration curve with a 0.993 regression coefficient, the P content corresponding to the extinction obtained on the spectrophotometer was read.

The P content in ash was calculated using **Equation (2.2)**:

$$\% \text{ P} = (e / m) \cdot 100 \tag{2.2}$$

in which:

e = P content, mg (read on the calibration curve).

m = mass of the ash sample in the 50 mL colorimetric solution, mg.

2.2.3. SiO_2 and P extraction

Procedure A

Procedure A was conducted using the method proposed by Bosio et al. (2014) [134] and Kamath et al. (1998) [135]. 50 g of each ash sample was placed in a beaker and 416 mL of 1 mol/L NaOH solution was added. Constant stirring was maintained at 100 °C for 1 h. The solutions from samples ECO and MCYC containing sodium silicate **Reaction (2.3)**, still warm, were filtered under slight suction through Whatman filter paper grade 589/2 white ribbon filter ashless (pore size 4-12 μm). However, the filtration of the BA sample was slow and difficult, and it was first filtered through a Whatman filter paper grade 589/1 black ribbon ashless (pore size 12-25 μm) before passing to the finer porosity. Sedimentation, which led to phase separation, was useful for better percolation. The BA sample leachate was clear but dark brown in colour, while the other solutions were clear and colourless.

$$SiO_2(s) + 2\ NaOH(aq) \rightarrow Na_2SiO_3(aq) + H_2O(l) \tag{2.3}$$
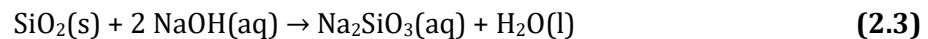
After filtration, 60 mL of 1 mol/L H_2SO_4 solution was slowly added, at room temperature and constant stirring, to each 200 mL of leachate. Chemical conditions of the reaction govern the kinetic, the mechanism of hydrolysis, and the condensation processes [136]. Therefore, the gel formation was controlled by pH measurement to reach the best endpoint of the gelling reaction. The acid solution was further added dropwise until a pH of 9.8 was reached, and then the titration was stopped. A volume ranging between 20 and 40 mL, depending on the ash leachate, was added after the first H_2SO_4 addition. The formation of silica gel from the sodium silicate solution was performed in accordance with **Reaction (2.4)**.

$$Na_2SiO_3(aq) + H_2SO_4(aq) \rightarrow SiO_2(gel) + Na_2SO_4(aq) + H_2O(l) \tag{2.4}$$
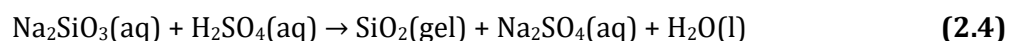
After 7 days of aging, the gels were completely formed, however, they were still mixed with reaction water. A centrifuge (Eppendorf, Centrifuge 5804 R) was used to separate the gel from the solution. The mixture was transferred to a 50 mL centrifuge tube and centrifuged at 1000 rcf for 10 min at 20 °C.

The supernatant was separated and stored in a polyethylene tube, while the gel was dried with an electric oven at 120 °C for 7-10 h (halogen convection furnace Bonny 2172339, Kooper, Rome, Italy). The final BA silica gel was brown, while the other two gels were whitish, even after drying. For subsequent XRD analysis, the gels were grounded using a mixer mill MM 400 (Retsch, Haan, Germany).

Procedure B

The second procedure is based on work from Santana Costa et al. (2018) [137]. 30 g of each ash was placed in a beaker with a 1 mol/L HCl solution at a liquid-to-solid (L/S) ratio of 10 and constantly stirred at room temperature for 2 h. After this period, the acid leachates of ECO and MCYC were filtered under slight suction through Whatman filter paper grade 589/2 (pore size 4-12 μm) and stored in polyethylene tubes for further TXRF analysis. The solid residues were washed with MQ water until a constant pH was reached, dried, and then the washed water was stored separately in polyethylene tubes. It was not possible to filter the BA acid suspension due to its fine porosity and the sample was instead centrifuged at 20 °C for 20 min at 1000 rcf with a 50 mL centrifuge tube (Eppendorf, Centrifuge 5804 R). The supernatant was separated and stored in a polyethylene tube for further TXRF analysis. The solid residue was washed with MQ water until a constant pH was reached, dried, and then, by using the procedure described previously, separated from the wash waters, and stored in polyethylene tubes.

All the solid samples after acid pre-treatment were dried in an electric oven at 120 °C for 9 h (halogen convection furnace Bonny 2172339, Kooper, Rome, Italy). A weight loss of 64.1 % for BA and ECO and 72.8 % for MCYC was recorded.

To conform with **Reaction (2.3)**, these samples were reacted with a 4 mol/L NaOH solution, in an L/S ratio of 10, under constant stirring at 80 °C for 4 h. At the end of the reaction, the mix was allowed to cool and settle at room temperature for 24 h.

The separation of sodium silicate solutions from the solid residues was performed under slight suction through Whatman filter paper grade 589/2 and 589/1 (pore size 4-12 μm and 12-25 μm). The solid residues were then washed with MQ water until a constant pH was reached, dried with an electric oven (halogen convection furnace Bonny 2172339, Kooper, Rome, Italy), and stored in plastic bags. The washing waters were stored in polyethylene tubes. During the procedure, a volume loss for the sodium silicate solutions was recorded: 25% for ECO and MCYC and 40% for BA.

To comply with **Reaction (2.4)**, a 5 mol/L H_2SO_4 solution was added dropwise to each 50 mL of sodium silicate solution, under constant stirring at room temperature, in order to lower the pH to 9.8 and to form the gel. After the period of aging, the silica gel separation from the reaction water was carried out in the same way as described in procedure A. A Neya centrifuge model 16-R was used, operated at 5000 rpm for 20 min at 25 °C. Subsequent drying in the oven lasted 5-6 h. The BA silica gel

was brown, while the ECO and MCYC gels were whitish. For subsequent XRD analysis, the gels were ground with a mixer mill MM 400 (Retsch, Haan, Germany).

2.3.   Results and discussion

2.3.1.   Rice husk poultry litter ash (RHPLA) characterization

Figure 2.1 shows the XRD patterns of the raw RHPLA (BA, ECO, and MCYC) compared to the same samples after the acid pre-treatment step of procedure B. As shown in **Figure 2.1A** (spectrum BA-A), BA contains quartz [SiO_2], sylvite [KCl], and arcanite [K_2SO_4] as identified by the main peaks at 26.62°, 28.31° and 30.77° in 2ϑ (2 theta) respectively. All the other crystalline phases are phosphate compounds of Na, Ca, K, and Mg namely sodium hydrogen phosphate [NaH_2PO_4], sodium-calcium phosphate [$Na_2CaP_2O_7$], calcium phosphate [$Ca_3(PO_4)_2$], sodium hydrogen phosphate hydrate [$Na_3HP_2O_7(H_2O)$], and potassium magnesium orthophosphate hydrate [$KMgPO_4(6H_2O)$]. The presence of a broad band in all the XRD patterns BA-B (**Figure 2.1A**), ECO-B (**Figure 2.1B**), and MCYC-B (**Figure 2.1C**) between 15 and 35° in 2ϑ, demonstrates that an amorphous phase is also present in these samples [135]. The broad X-ray diffraction halo in the XRD pattern is typical for amorphous compounds [138]. Consequently, even if this type of bottom ash (BA) was characterized for the first time by the XRD technique, the presence of an amorphous phase can be assumed seeing as it has already been reported for fly ash with the same origin by Fahimi et al. (2020) [75]. This amorphous component in all the samples may consist of both silicon oxide, widely found and studied for ash originating from rice husk combustion [139–141], and P phases, as confirmed by the Raman and XRD analyses made by Fahimi et al. (2020) [75] and Stammeier et al. (2018) [142]. The spectrum BA-B in **Figure 2.1A** shows that after the acid leaching, the initial complex matrix loses its soluble components, maintaining only two crystalline phases: quartz [SiO_2] and sylvite [KCl]. The compound KCl is present in a different crystalline phase from the raw BA sample seeing as it shows the main peak at 34.88° in 2ϑ which was previously absent. Also, the differences between the crystalline phases in BA-A and BA-B (**Figure 2.1A**) suggest that phosphate soluble compounds are leached by HCl. The same can be assumed for the ECO and MCYC samples.

Spectrum ECO-A (**Figure 2.1B**) and spectrum MCYC-A (**Figure 2.1C**) show that ECO and MCYC, similar to BA, contain quartz [SiO_2], sylvite [KCl], and potassium sulphate (or arcanite) [K_2SO_4] as identified by the same main peaks found in BA-A (26.6°, 28.3° and 30.8° in 2θ). All the raw samples contain the same crystalline phosphate phase: sodium hydrogen phosphate [NaH_2PO_4]. Sodium calcium phosphate [$Na_2CaP_2O_7$] was observed in MCYC as well as in the BA sample, while hydroxyapatite [$Ca_{10}(PO_4)_6(OH)_2$] was found only in ECO (**Figure 2.1B** ECO-A). Hydroxyapatite and sylvite were previously found in similar wastes [143] and some of the detected crystalline phases are those previously found by Fahimi et al. (2020) [75]. Lastly, Periclase [MgO] was found in both fly ash samples (spectra ECO-A and MCYC-A in **Figure 2.1B-C**). After the acid pre-treatment, spectra ECO-B and MCYC-B (**Figure 2.1B-C**) show the presence of an amorphous phase and remaining crystalline phases quartz/silicon oxide [SiO_2] and bassanite [$Ca_2(SO_4)yH_2O$]. A residual amount of potassium
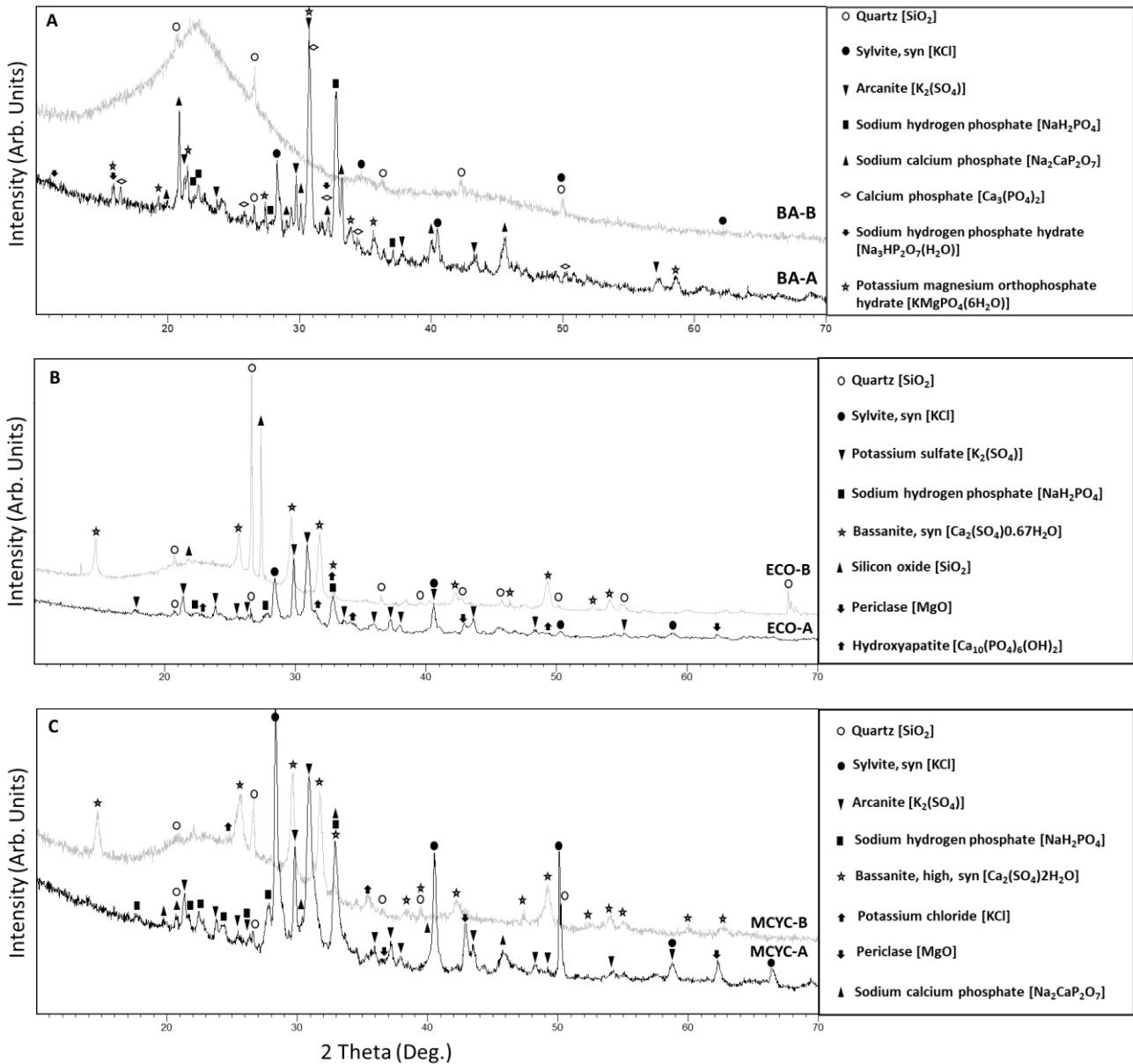
Figure 2.1*: XRD patterns obtained for the samples BA (A), ECO (B) and MCYC (C): raw RHPLA in black (BA-A, ECO-A, MCYC-A) and raw RHPLA after the acid leaching with HCl 1 mol · L⁻¹ for procedure B in grey (BA-B, ECO-B, MCYC-B).*

chloride [KCl] was detected for MCYC-B (**Figure 2.1C**) in a phase very similar to that found in BA-B (**Figure 2.1A**). Similar to BA, after the acid treatment, phosphatic compounds are absent in ECO and MCYC.

The crystalline phase identification is conforming to the XRF data reported in **Table 2.2** for each raw RHPLA and its corresponding ash after acid leaching with procedure B. The raw ashes formed from the combustion of three main fuels: rice husk, poultry droppings, and wood chips that have high concentrations of silicon (SiO_2), phosphorus (P_2O_5), and calcium (CaO) respectively. However, as shown in **Table 2.2**, the main constituent of these samples is potassium (K_2O). Additionally, SO_3, MgO,

Na$_2$O, and Cl are present in lower concentrations. Other metals, such as Al$_2$O$_3$, MnO, Fe$_2$O$_3$, NiO, CuO, and ZnO are present in negligible amounts. These results confirm the importance of recovering both P and silicon (Si) from this waste typology.

Table 2.2: *XRF chemical composition of raw RHPLA and raw RHPLA after acid leaching with HCl 1 mol/L in procedure B. nd: not detected. Others contains: TiO$_2$, Cr$_2$O$_3$, Rb$_2$O, BaO, SrO, Br, V$_2$O$_5$ and SeO$_2$.*

	BA		ECO		MCYC	
	raw RHPLA	leaching HCl 1 mol/L	raw RHPLA	leaching HCl 1 mol/L	raw RHPLA	leaching HCl 1 mol/L
Compositions	**Results in wt %**					
Na$_2$O	2.91	nd	2.88	nd	2.95	nd
MgO	5.83	1.01	3.90	0.49	6.15	0.94
Al$_2$O$_3$	0.84	1.03	0.43	0.66	0.64	4.50
SiO$_2$	10.26	56.67	12.76	47.96	9.86	32.04
P$_2$O$_5$	18.89	6.60	12.67	3.58	17.62	21.41
SO$_3$	7.23	14.82	17.20	27.52	13.82	17.10
Cl	1.34	6.89	2.42	1.52	3.52	0.45
K$_2$O	30.72	4.10	33.10	1.33	28.28	3.85
CaO	18.60	3.52	12.02	13.17	14.13	13.34
MnO	0.58	0.21	0.36	0.10	0.48	0.32
Fe$_2$O$_3$	1.19	2.83	0.64	1.95	0.97	3.93
NiO	0.01	0.02	0.01	0.01	0.01	0.01
CuO	0.11	0.49	0.07	0.26	0.08	0.24
ZnO	0.30	0.25	0.43	0.13	0.36	0.42
Others	0.17	0.53	0.09	0.27	0.11	0.38

XRF analysis of ash samples after acid pre-treatment reported in **Table 2.2**, also corroborates the previous hypothesis that P-compounds are leached by HCl, while Si remains in the matrix and is purified for subsequent recovery. As shown in **Table 2.2**, during the leaching process, BA lost P$_2$O$_5$, K$_2$O, and CaO, while maintaining SiO$_2$, SO$_3$, and Cl. In ECO evident leaching of K$_2$O, P$_2$O$_5$, and other minor components occurred. However, SiO$_2$, SO$_3$, and CaO remain in high percentages in the sample. For MCYC, the P-leaching was not so effective, and the amounts of P$_2$O$_5$, SiO$_2$, and SO$_3$ in the RHPLA residues remain quite high (P$_2$O$_5$ at 21.41%). The leaching of K$_2$O occurred. According to the results expressed as w/w% it can be observed that the major content of SiO$_2$ after the acid pre-treatment is detected in BA. After acid leaching with HCl 1 mol/L as described in procedure B, BA seems more purified compared to ECO and MCYC because most of the components are contained in minor concentrations. However, the BA complex matrix, rich in organic matter and hydrocarbon compounds, is not the best starting material for silica recovery, due to its composition and dark colour, as seen during the experimental.

The quantification of P by XRF and chemical method is reported for comparison in **Figure 2.2**. The UV-Vis method was adapted for phosphorous quantification in the ash [133]: it was considered suitable for RHPLA since it is a material with high P content and the method is based on colorimetric tests to

obtain the extinction values on the calibration curve. XRF results reveal, in the three raw RHPLA, a P content between 4.9 and 7.1 %, while UV-Vis data between 3.9 and 7.9 %.

In **Figure 2.3** an image for each RHPLA sample (scale bar 2 mm), BA (**A**), ECO (**B**), MCYC (**C**), is provided. For points P.1 (**Figure 2.3B**) and P.2 (**Figure 2.3C**) respectively located in the ECO and MCYC samples, a higher magnification analysis was carried out as reported in **Figure 2.3D** and **Figure 2.3E**. The chemical composition measured with EDXS of points P.1, P.2, P.3, P.4 is shown in the spectra below. Phosphospheres were identified in ECO (**Figure 2.3B** P.1) and MCYC (**Figure 2.3C** P.2) and are distinguishable due to their (spherical) shape and semi-smooth surface which was covered with micrometric particles of other elements. Although the phosphosphere shown in **Figure 2.3E** is very "clean" compared to the phosphosphere in **Figure 2.3D**, their respective compositions reported in spectra P.1 and P.2 are relatively similar. The main constituent element for these two points, besides O and K, is P. Other spheres like these were detected during the analysis and their dimensions vary from less than 100 to 300 μm. Like findings made by Fahimi et al. (2020) [75], the two fly ash samples (ECO and MCYC) consist of micrometric and supermicrometric (<10 μm and >10 μm respectively) P-rich morphotypes. Valentim et al. (2016) [144] reported that Si-, Ca-, K- and Mg-phosphospheres (P-rich glassy spheres) are a type of amorphous material that can frequently be observed in biomass fly ash. Points P.3 and P.4 (**Figure 2.3D** and spectra P.3 and P.4) show high concentrations of Si and O, and their surfaces are covered mainly with K but also with Na, Mg, P, S, Cl, and Ca. So finally, the presence of an amorphous P-phase (P.1 and P.2) and an amorphous Si-phase (P.3 and P.4) are reconfirmed by the SEM-EDXS analysis.
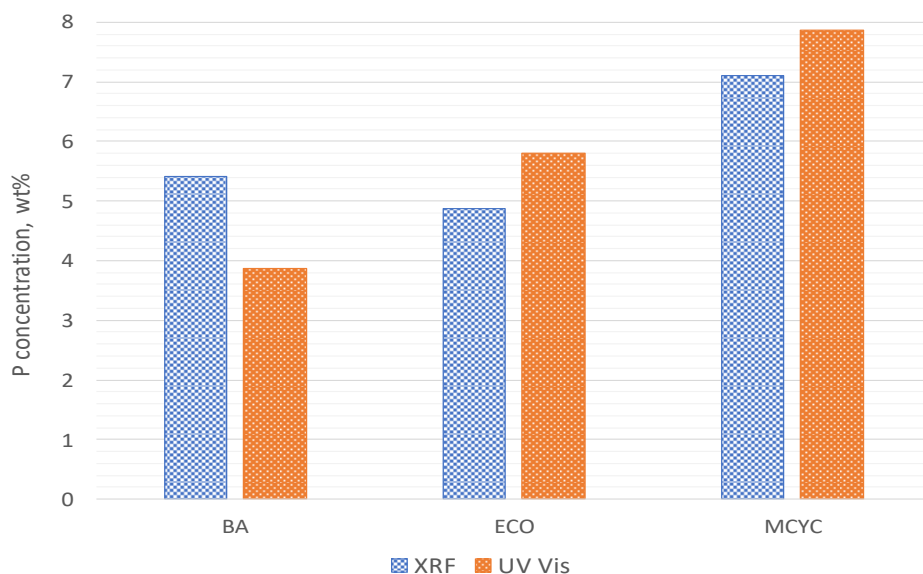
Figure 2.2: Comparison of XRF and UV-Vis results for P quantification in raw RHPLA.
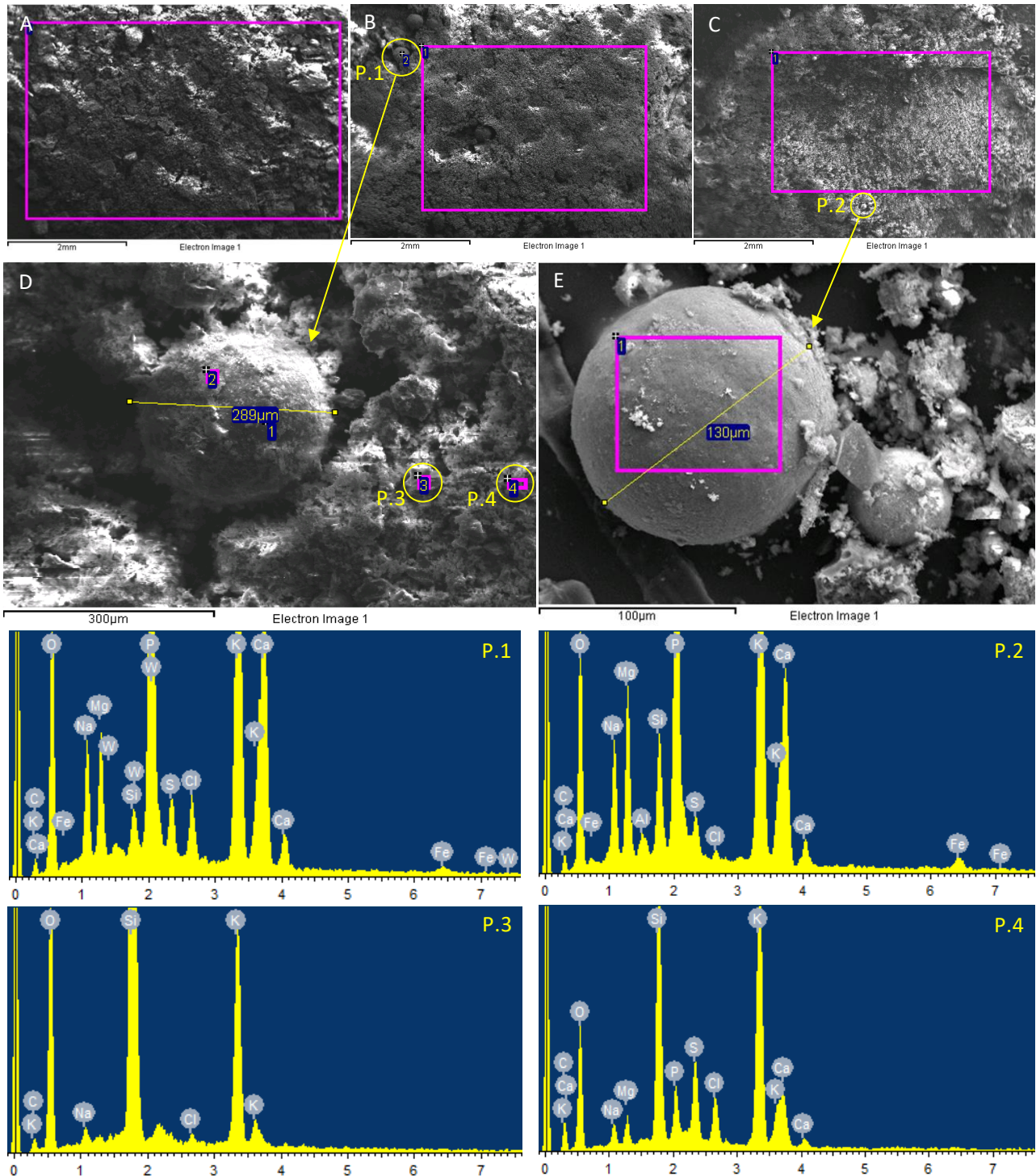
Figure 2.3 *: SEM images of raw RHPLA: BA (A), ECO (B), MCYC (C) with a scale bar of 2 mm. Micrometric spherical morphotypes marked with P.1 and P.2 and their magnification shown in (D) and (E). EDXS chemical composition of the points P.1, P.2, P.3 and P.4 in the spectra below.*

2.3.2. Silica characterization

As previously mentioned, the XRF analysis in **Table 2.2** shows a significant reduction or total leaching of P_2O_5 and alkali metals, while SiO_2 remains in the matrix. The acid pre-treatment of procedure B therefore allows the lowering of salt contents in the final dried silica, as shown by the XRD analysis in

Figure 2.4. **Figure 2.4A** shows that, for silica recovered with procedure A, thernadite and sodium sulphate [Na_2SO_4] as well as potassium sodium sulphate phases were identified. It should be noted that there are several crystalline phases for procedure A, while for procedure B (**Figure 2.4B**), the final product is contaminated only by thernadite and sodium sulphate with the same chemical formula [Na_2SO_4]. The presence of these compounds is justified by **Reaction (2.4)** where Na_2SO_4 is a reaction product together with SiO_2. During the aging of the gel, a certain amount of Na_2SO_4, soluble in the reaction solution, may be trapped in the hygroscopic silica network, and then recrystallized during drying.

Moreover, from the XRD analysis of recovered silica from procedure B (**Figure 2.4B**), an amorphous phase is identified from the broad halo present in all the XRD patterns from about 15 to 35° in 2theta. These assessments suggest that procedure B was more effective and data in **Table 2.3** validate this hypothesis. XRF analysis of the six samples of recovered amorphous silica provided in **Table 2.3,** indicates that the SiO_2 content in the gels from procedure A was very low compared to procedure B. Na_2O, SO_3 and K_2O contaminate amorphous silica A much more than the amorphous silica B. The absence of an acid pre-treatment in procedure A leads to P_2O_5 still being present in the final amorphous recovered product, wasting P and contaminating the silica. On the other hand, SiO_2, Na_2O, and SO_3 are the significant components of amorphous silica B, and the only crystalline phase detected by XRD, namely thernadite/sodium sulphate [Na_2SO_4] (**Figure 2.4B**), justifies the presence of sodium and sulphur in the XRF analysis of these samples. As reported in **Table 2.3**, ECO B has the highest silica content at 80.30%. Nevertheless, all the samples produced with procedure B show higher values of SiO_2% due to the low presence of crystalline phases compared to the silica from procedure A that contains a lot of salts. This means that procedure B allows the obtainment of an almost pure final product in three steps: acid leaching pre-treatment, **Reaction (2.3)** and **Reaction (2.4)**.

Due to the origin of the silica gel from this type RHPLA, then dried to amorphous silica, a valuable option of re-use can be HM stabilization in municipal solid waste incinerated fly ash (MSWI-FA) as already studied [123,145,146].
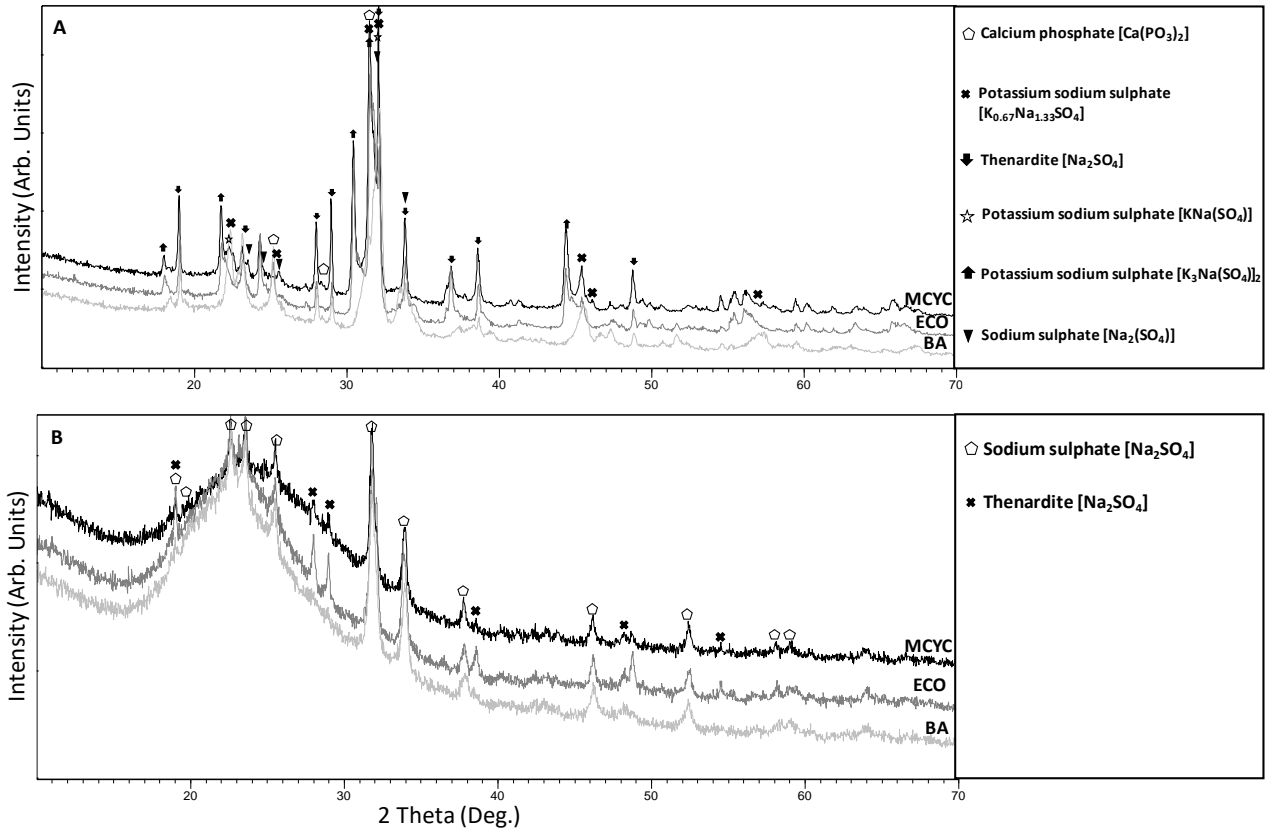
Figure 2.4: XRD patterns of silica obtained from procedure A (A) and from procedure B (B): silica BA in grey, silica ECO in dark grey, silica MCYC in black.

Table 2.3: XRF chemical composition of recovered amorphous silica using procedure A and B. nd: not detected. Others contains: Fe₂O₃, ZnO, CuO, MnO and BaO.

	Procedure A			Procedure B		
	Silica BA	Silica ECO	Silica MCYC	Silica BA	Silica ECO	Silica MCYC
Compositions			Results in wt %			
SiO_2	23.38	14.98	21.70	77.48	80.30	73.11
Na_2O	22.99	19.39	16.89	9.29	8.68	9.30
SO_3	35.35	39.08	35.17	10.67	9.32	5.78
P_2O_5	3.68	2.93	4.61	0.09	0.08	0.30
K_2O	11.08	20.53	17.65	0.12	0.08	1.05
Cl	0.71	1.43	2.31	0.08	0.04	0.02
CaO	0.59	0.01	0.01	0.09	0.03	0.02
MgO	0.54	0.45	0.40	0.13	nd	nd
Al_2O_3	0.52	0.11	0.18	0.42	0.20	8.30
Others	0.13	0.06	0.03	0.47	0.15	1.05

2.3.3. Acid leachate characterization

In procedure B for silica extraction, a pre-treatment with 1 mol/L HCl solution was used, as proposed by Alvarez et al. (2015) [147], to obtain better results in terms of purity of the extracted silica. As is well known for other different starting materials, such as ISSA, the most common method for P-recovery is acid leaching [69–71]. The choice to use HCl as an extractant in this work was done in accord with the reference article on which the procedure B was based [137], following literature about ISSA: Hong et al. (2005) [148], Biswas et al. (2009) [73], Xu et al. (2012) [149], Petzet et al. (2012) [72] and the recent Semerci et al. (2020) [150], that demonstrates the effective recovery of P with HCl.

Moreover, a recent paper [76] shows that wet chemical leaching approaches appear to be the most sustainable method for P extraction from ISSA and the current research proceeds in this direction.

The main advantage of the proposed method is that the RHPLA contains low quantities of HM compared to ISSA. In particular, great attention to fertilizer regulations (the first area of interest for the application of recovered P) must be given regarding maximum concentrations of As, Cd, Hg, Cr (VI), Ni, Cu, Pb, and Zn [151,152]. Regulation (EC) No 2003/2003 of the European Parliament and of the Council relating to fertilizers [153] at the time of this research, in 2020, was the reference to be complied about fertilizer market. Regulation (EC) No 2003/2003 was then repealed with effect from 16 July 2022 by regulation (EU) 2019/1009 laying down rules on the market availability of EU fertilizing products [154]. **Figure 2.5** highlights the concentration of the elements of interest for the discussion, in the acid leaching solution, derived from TXRF results.
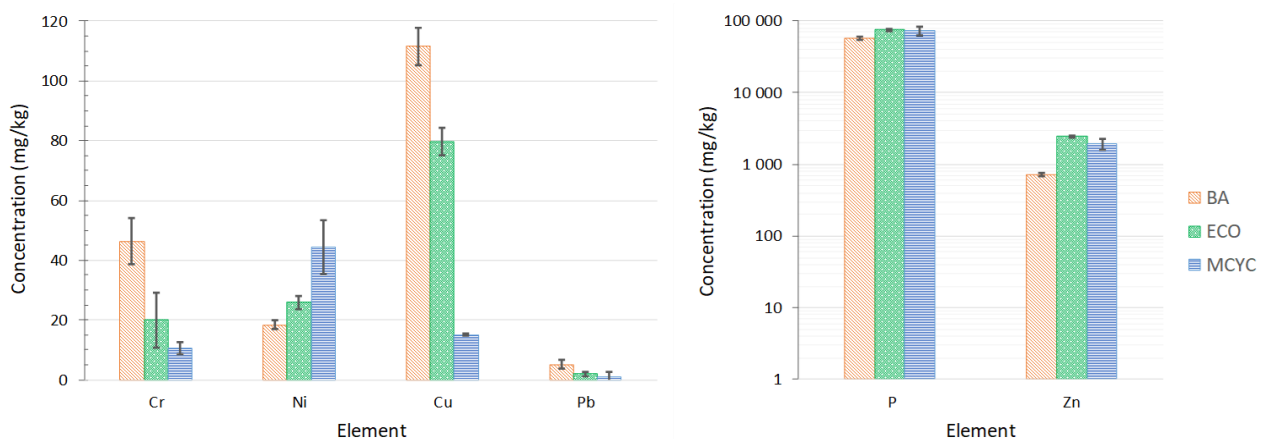
Figure 2.5: *TXRF analysis of acid leachate with HCl 1 mol · L⁻¹ for the three RHPLA under examination: BA in orange, ECO in green and MCYC in blue. P and contaminants of interest for the preparation of fertilizers are reported.*

As shown in **Figure 2.5**, P is detected between 57 and 75 g/Kg, or 5.7 and 7.5 % in the three RHPLA leachate samples. Considering the different nature of the analytical techniques used to quantify P (XRF in the solid, UV-Vis in the digested sample, and TXRF in the leachate), the P extraction efficiency is not

reported for instrumental consistency reasons. In the following chapters of this thesis, the choice of a single analytical technique for P quantification, before and after extraction, was considered in order to calculate the extraction efficiency. The choice of technique was dictated essentially by two factors: reliability of the result according to the matrix effect and availability of the instrumentation for repeated analyses. Arsenic (As), cadmium (Cd), and mercury (Hg) were not detected in the leachates. Total chromium (Cr) was quantified but TXRF analysis provides an elemental analysis that cannot discriminate between elemental speciation. To set the precise value of hexavalent chromium in the samples, different analytical techniques are required. In any case, the highest concentration of total chromium is recorded for BA at about 46 mg/Kg. Nickel (Ni) in MCYC is present at more or less 44 mg/Kg, copper (Cu) is detected in concentrations ranging between 15 and 112 mg/Kg, while lead (Pb) is present in BA at more or less 5 mg/Kg. Contrary, zinc (Zn) shows the following concentrations: about 0.7 g/Kg for BA, about 2.5 g/Kg for ECO, and about 1.9 g/Kg for MCYC, attesting as the main contaminant metal in the leachates. Consequently, the use of P recovered from RHPLA to prepare fertilizers or soil improvers, through the precipitation of a solid product from the RHPLA acid leachate, shall be developed to keep Zn within the legal limit. So, the leaching with an acid that has a high P extraction capacity, but not preferred in literature for ISSA due to metal leaching [74,155], may be a good solution for P-recovery from RHPLA for fertilizer applications, because the main limitation is only provided by Zn concentration in the solution. The P thus extracted may undergo the same treatments already studied for ISSA [156,157] and recently proposed for PL [158], to obtain a novel product and a novel eco-material for the fertilizer industry. Regarding the discussion on HM content in the leachates, a more precise evaluation can be made only considering the content of these metals, not in the leached but in the precipitate obtained in a subsequent step, in order to be able to compare these values with those reported by the regulation. This part of the research will be better addressed in the next chapters.

It is evident that the proposed procedure is suitable to promote P separation before proceeding with silica recovery and the two stages can be studied with a mutual approach as already achieved for ISSA [159,160]. This first attempt of double recovery (P and SiO_2) from raw RHPLA could also present the opportunity for the reuse of RHPLA residual. The alkali leaching step with NaOH in the silica recovery procedure could leave a certain amount of Si-amorphous phase in the matrix: this may suggest a more in-depth study of extraction efficiency or a new study for further application of the RHPLA residual in Portland cement-based materials [161] as already proposed for ISSA [162,163].

2.4.   Conclusions

The three RHPLA under study (BA, ECO and MCYC) were found to be composed of P between 5,5% and 8,2%, and SiO_2 between 9,9 % and 12,8%, according to XRF analysis. A thorough characterization via XRD and SEM-EDXS analyses of RHPL bottom ash (BA) were made. The results show that BA is composed of different crystalline phosphate compounds namely: sodium-calcium phosphate $[Na_2CaP_2O_7]$, calcium phosphate $[Ca_3(PO_4)_2]$, sodium hydrogen phosphate hydrate $[Na_3HP_2O_7(H_2O)]$, and potassium magnesium orthophosphate hydrate $[KMgPO_4(6H_2O)]$. In all the ash samples (BA, ECO and MCYC), together with quartz, sylvite, and arcanite, phosphate is present as sodium hydrogen phosphate $[NaH_2PO_4]$, while hydroxyapatite emerges only in the ECO sample. Amorphous phases of both Si and P are present in ECO and MCYC and phosphospheres were identified. The XRD analysis clearly shows these amorphous phases are purified from the soluble forms after procedure B acid leaching. EDXS analysis confirms that P, Na, Mg, S, K, and Ca are leached by the acid, while Si remains in the solid matrix. Therefore, in procedure B, Si and P were extracted separately and acid leaching was essential to obtain purified dried silica. The best result was obtained for sample ECO (about 80% SiO_2 grade). It can be concluded that procedure B can be a combined process to recover firstly P and then silica in two subsequent steps, confirming the chance of recovering more than one eco-material from the biomass waste ash. In conclusion, considering this process as a flow that produces, respectively, acid leachate containing P, RHPLA residues, and SiO_2, it can be further reported that:

i.   The acid leachate contains a very small quantity of contaminants (As, Cd, Hg, Ni, and Pb) compared to the ISSA leachate, leading to the conclusion that RHPLA is a good secondary source of P that can be precipitated to obtain an eco-material candidate for industrial mineral fertilizer production, with particular attention to Zn concentration.

ii.   RHPLA residues can be used as a binder in porous materials to improve mechanical performance or can be studied for further application in the Portland cement industry.

iii. The dried amorphous silica can be tested for the stabilization of HM in MSWI-FA, thanks to pozzolanic reactions.

The next research focused on the optimization of procedure B to find the best conditions for the acid leaching to reach a good yield for P recovery (chapter 3) and on the possibility of obtaining SiO_2 at the same time as P from ISSA (chapter 4). Further studies are needed to better understand the composition and behaviour of RHPLA residues as additive in the building sector, and to evaluate the properties of SiO_2 as HM stabilizer.

Acknowledgements

3.   OPTIMIZATION OF P RECOVERY FROM RHPLA AND SUSTAINABILITY EVALUATION OF A ZERO-WASTE PROCESS

Abstract

The overall objective of this chapter is to combine the study of an efficient procedure for P recovery from RHPLA, through acid leaching in view of subsequent P precipitation, with the development of an industrial cost-effective and environmentally sustainable method. It is essential to plan all the steps of the recovery process in order to limit the creation of scraps, evaluating the impact in terms of carbon footprint and embodied energy. Considering the simultaneous P and SiO_2 recovery from RHPLA studied in chapter 2, this work arises precisely from those results. A statistical approach, combined with a sustainability evaluation (ESCAPE approach) for the recovery of eco-materials from RHPLA, is presented. The design of experiment (DoE) method was applied to maximize the P extraction using hydrochloric acid (HCl), with the aim to minimize the contamination that can occur by leachable HM present in RHPLA, such as zinc (Zn). Two independent variables, the molar concentration of the acid, and the liquid-to-solid ratio (L/S) between the acid and the ash, were used in the experimental design to optimize the operating parameters. The statistical analysis showed that a HCl concentration of 0.34 mol/L and an L/S ratio of 50 are the best conditions to recover P with low Zn contamination. On the other side, sustainability analysis has shown that 1 mol/L of HCl and L/S ratio equal to 10 are the most sustainable operating conditions, when the recovery starts from RHPLA that has a minimum P content of 10%. Concerning the SiO_2, its content in RHPLA is too low to consider the proposed recovery process advantageous from an environmental and economic point of view. However, based on the analysis, this process should be sustainable to recover SiO_2 when its content in the raw starting material is more than 80%.

Keywords

Poultry litter ash
P extraction efficiency optimization
Sustainability analysis
Design of experiments

Scientific contribution

This chapter is based on the following publication, whose form have been adapted for reasons of consistency with the structure of this doctoral thesis. The content reported in this chapter is the result of my own work, including literature review, data curation, formal analysis, investigation, methodology, visualization and writing. Any work made by others is attributed to the original author in the text.

o **Fiameni L.**, Fahimi A., Marchesi C., Sorrentino G. P., Zanoletti A., Moreira K., Valentim B., Predeanu G., Depero L. E., Bontempi E., Phosphorous and silica recovery from rice husk poultry litter ash: a sustainability analysis using a zero-waste approach. *Materials* (2021), **14** (21), 6297. https://doi.org/10.3390/ma14216297

o **Fiameni L.**, Fahimi A., Marchesi C., Sorrentino G. P., Zanoletti A., Moreira K., Valentim B., Predeanu G., Depero L. E., Bontempi E., Phosphorous and silica recovery from rice husk poultry litter ash: a sustainability analysis using a zero-waste approach. *Materials* (2021), **14** (21), 6297. https://doi.org/10.3390/ma14216297

3.1. Introduction

As displayed in chapter 2, recycling and recovery of resources from waste and industrial by-products are priority goals that can be achieved by applying circular economy principles. Especially in the last years, probably due to the great upheaval produced by the COVID-19 pandemic, the reduced geographic availability of mined materials has more highlighted the urgency to improve resource sustainability [164–166].

Thus, great attention is devoted to the "zero waste strategy", which is defined, by the Zero Waste International Alliance (ZWIA), as "designing and managing products and processes systematically to eliminate the waste and materials, conserve and recover all resources and not burn or bury them" [167]. The final aim is to reduce the waste that is landfilled and promote an overall responsible management of materials. Obviously, new technologies are needed to support the decision makers in developing suitable policies towards the transition to a circular economy, like new ideas for by-products reuse [168][169][170].

The conclusions of the previous chapter drove the research towards a more in-depth study of P recovery from RHPLA, verified as a P-rich waste [171,172]. The use of biomass ash to recover P, in this specific case adopting wet-chemical extraction to obtain P-concentrated leachate from RHPLA, is considered a winning strategy for saving natural resources and implementing an industrial symbiosis, where the waste from one industry can be considered a resource for another industry [173,174]. Acting in this way, the anthropogenic P cycle can be seen as a natural ecosystem, where there are no wastes, but only resources and products, just like in a cradle-to-cradle model [175].

Since literature about P recovery from PLA is lacking because this biomass got attention in more recent times for P recovery, the corresponding method was study based on ISSA. Several wet-extraction procedures have been proposed to recover P from ISSA [69,76,176,177], especially due to the low energy requirement and to the ease of application to different samples, as described in section 1.3. However, attention must be paid to HM (such as Pb and Zn), often present in ISSA, which may limit the use of the products as fertilizers [178–180].

To investigate for the first time the wet-chemical extraction of P from RHPLA, optimization using a statistical model has been chosen as study method to ensuring the effectiveness and efficiency of the procedure, mimicking what already proposed in literature for P separation from different waste streams [181][182]. The response surface method (RSM) is a powerful tool to analyze independent variables and to predict the observed response, as exactly and precisely as possible, at points within the experimental domain where no experiments were performed, thus finding the best conditions under uncertainty conditions, reducing the ambiguity. In particular, the design of experiments (DoE) method has already been used in environmental studies for the optimization of P recovery [159,183,184][185]. Design-based modelling of experiments can be an effective instrument to assess

the feasibility of a chemical process, since it allows to understand the effect of critical parameters, such as the concentration of the extractant, and the liquid-to-solid ratio between ash and extractant. In this study, the goal is to provide a cost-effective and sustainable option to tackle the problem of the co-dissolution of trace elements with P, aiming to P maximization and HM minimization at the same time [186].

In addition, RHPLA also contains silica (SiO_2) that can be extracted through an alkali leaching. As described in chapter 2, SiO_2 is a raw, valuable material used in pharmaceuticals, cosmetics, paints, semiconductors, catalysts, glass, and adsorbent products. In particular, recovered SiO_2 was proposed for stabilizing HM in fly ash [187][188][145][189], providing a solution to another environmental problem beyond P management. Therefore, recovering two different eco-materials from the same waste fits perfectly into the zero-waste concept exposed before.

But is the simultaneous recovery of P and SiO_2 from RHPLA environmentally sustainable? This was the starting point for the work presented in this chapter, trying to understand the feasibility of the proposed process not only from the technological point of view, but also in terms of environmental sustainability. It was considered necessary to evaluate the viability of the overall recovery process because the use of chemicals and/or high-energy treatments can jeopardize the environmental benefits of the eco-material recovery. Some publications, that were the cue for this work, had already evaluated the sustainability of the recovery strategies for different materials, such as ISSA and spent lithium-ion batteries [190–192][193] [194]. The ESCAPE (standing for Evaluation of Sustainability of material substitution using CArbon footPrint by a simplified approach) method, proposed by Elza Bontempi [195] [196] was used for sustainability analysis. With this approach, the potential environmental impact of a material extracted from a secondary source can be compared with the corresponding material from a natural source, considering the energies (embodied energy) and the emissions (carbon footprint) involved in the production of the material. As results of this analysis, a sustainability indicator is generated, so-called SUB-RAW index.

Therefore, the sustainability evaluation of the procedure B (to obtain simultaneously P and SiO_2 gel from RHPLA) presented in the previous chapter, was studied. The DoE applied to the process, based on the central composite design (CCD), integrates as responses (i) the amount of P recovered (as a nutrient to be maximized), (ii) the amount of Zn (as a typical heavy metal to be minimized) and (iii) the SUB-RAW index (as environmental indicator of sustainability to be maximized). Thus, an overall study is proposed, which combines the statistical and environmental approaches, allowing the optimization of the recovery process at the laboratory scale.

3.2. Materials and methods

3.2.1. Sampling

Ash samples were collected at the incinerator of Campoaves (Figueira da Foz, Portugal) and their detailed characterization is reported in chapter 2. The RHPLA consists of both bottom and fly ashes, but in this study, only fly ash was used as collected from the economizer system and named ECO. This waste was mainly composed of potassium (K_2O = 33.1%), sulphur (SO_3 = 17.2%), phosphorus (P_2O_5 = 12.7%) and calcium (CaO = 12.0%), with a SiO_2 content greater than 12.5% [172]. For this work the ash was re-prepared as follows: after sampling, the ash was oven-dried at 50 °C until a constant weight was reached, then manually sieved using a 0.5 mm mesh. The size fraction > 0.5 mm was placed in a water column, the sunk and floating particles were then collected and oven-dried at 50 °C until a constant weight was reached. **Figure 3.1** shows the XRF composition of ECO bulk sample before the dry and wet separation. Compared to the previous analysis, total composition is quite different but in the same order of magnitude: K_2O = 30.2%, SO_3 = 13.7%, P_2O_5 = 16.2%, CaO = 16.8% and SiO_2 = 10.4%. The heterogeneity of ash sample is a common issue, due to different fractions present in the sample and due to the variability of fuel for combustion. In **Figure 3.2** the chemical composition of the elements of interest for each fraction is specified. The investigation of simultaneous P and SiO_2 recovery, avoiding the Zn contamination, has brought to the choice of sample ECO SINK from fraction > 500 μm for this work, because of higher P and Si content in the raw sample (P_2O_5 = 21.3% and SiO_2 = 23.3%).
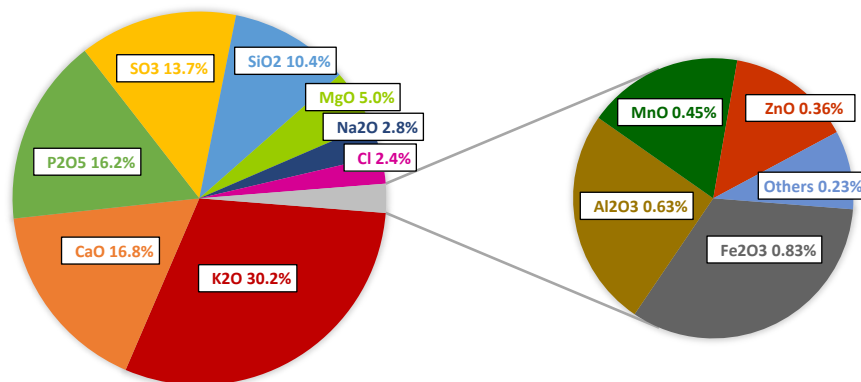

Figure 3.1: XRF composition of ECO bulk sample before the dry sieving and wet separation.
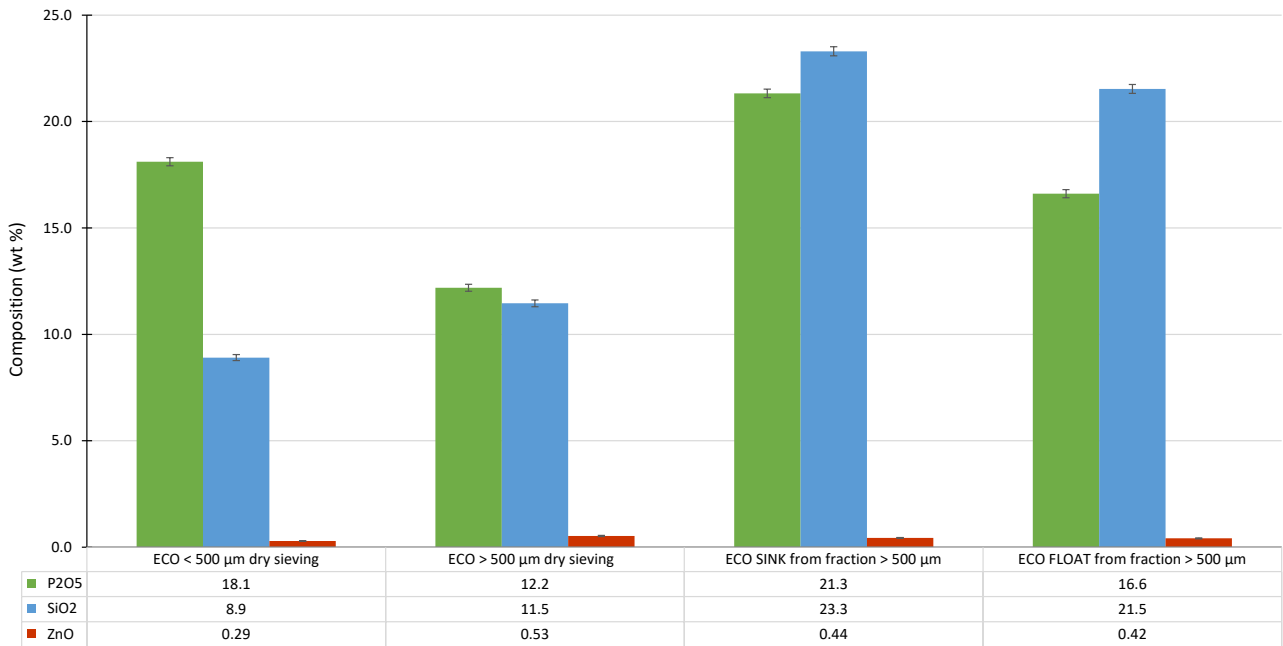
Figure 3.2: *XRF composition of ECO ash fractions generated by dry sieving and wet separation.*

The selected fraction, simply named ECO, was used for the leaching experiments, considering ZnO content quite high (0.44 % from XRF analysis in **Figure 3.2**, that is circa 3500 mg/Kg of elemental Zn) but aware that the analytical technique on solid cannot be very sensitive for low concentrations of trace elements, like other metals in addition to Zn that may compromise the use of recovered P as fertilizer i.e. As, Cd, Hg, Cr(VI), Ni, Cu, Pb [154]. For this reason, during the research another analytical technique was used for Zn quantification.

3.2.2. Recovery process under study and preliminary experimental assessments

Figure 3.3 shows the P and SiO_2 recovery scheme, composed of two leaching processes, as described in detail in chapter 2 (procedure B) [172]. The first process (in blue in **Figure 3.3**) is the RHPLA acid leaching by HCl (1 mol/L), that aims to recover P. The second process (in green in **Figure 3.3**) is composed of several steps to recover the residual SiO_2 as SiO_2 gel by using NaOH (4 M) and H_2SO_4 (5 M).

Figure 3.3: *P (1) and SiO$_2$ (2) simultaneous recovery process from RHPLA.*

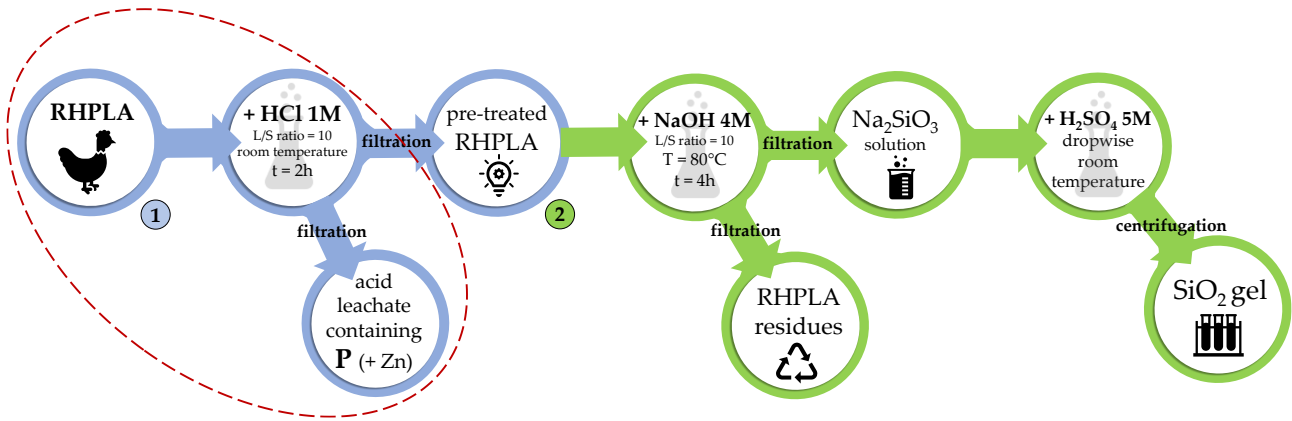The recycling of macronutrients contained in PLA, e.g., P and potassium (K), for application as fertilizers, was already suggested [124], emphasizing the need for an optimized recovery method that considers the legal constraints of HM content in the recovered materials. Therefore, the extraction of P from the ash by a wet chemical method was investigated considering the first process proposed in **Figure 3.3**, where acid leaching technology was used as pre-treatment for the subsequent recovery of amorphous SiO$_2$. Hydrochloric acid was chosen based on previous results, and to propose a first attempt regarding the investigation of P recovery through acid leaching of RHPLA. This method is already applied for ISSA, for which a broad combination of types and concentrations of extractant, liquid-to-solid (L/S) ratio and contact time was already investigated in literature [197] It was shown that an equilibrium time of 2 h is usually appropriate. Thus, contact time was fixed at 2 h, while the effect of the acid concentration and the L/S ratio on the recovery efficiency was evaluated. The parameters were optimized to obtain a solution with the highest P content and the lowest Zn contamination. The tests were performed using 5 g of ECO sample stirred with HCl solution for 2 h at room temperature. Afterwards, the samples were filtered through a nylon membrane with a pore size of 0.45 μm, and the leachate solutions were analyzed. The second process was not experimentally tested for optimization, focusing the attention on the P recovery, while it was considered in the sustainability evaluation of the potential overall recovery (see section 3.3.3.).

3.2.3.   Characterization techniques

After the acid leaching, P concentrations on the eluate were evaluated by the spectrophotometric UV-Vis method proposed in section 2.2.2 and adapted from the Romanian standardized method [133]. The procedure of P quantification was adopted for the ECO mineralized sample and for all the leachates, appropriately diluted. Spectrophotometry measurements were performed by a QE65000 spectrophotometer (Ocean Optics) in the C4T Lab suitable for measuring absorbance in the visible and near-infrared regions of the spectrum, using a polystyrene cuvette (10 mm optical path). A blank

solution prepared with the same quantities of reagents and a suitable volume of MilliQ water was used as a reference. The calibration curve (absorbance vs P content in mg/L) was obtained by standard solutions of potassium dihydrogen phosphate (KH_2PO_4). P extraction efficiency (PEE) was calculated as reported in **Equation (3.1)**:

$$PEE \, (\%) = (C_{P, \, leached} / C_{P, \, ash}) \cdot 100 \tag{3.1}$$

in which:

$C_{P, leached}$ = P concentration in the leached ash (mg/Kg) converted from (mg/L) using **Equation (2.1)**

$C_{P, ash}$ = P concentration in the mineralized ash (mg/Kg) converted from (mg/L) using **Equation (2.1)**

Zn quantification was performed by TXRF (Total Reflection X-ray Fluorescence) analysis. ECO specimen was digested, and the Zn concentration (mg/kg) was evaluated. The procedure for sample preparation was mentioned by Assi et al. [198]: namely, 0.25 g of ash sample was placed in a teflon vessel with a mixture of 6 mL of HNO_3 (≥65%), 2 mL of HCl (37%) and 2 mL of HF (48%) and digested (twice as replicate to confirm the numerical output data) using a CEM SPD automated microwave digestion system (CEM, Charlotte, NC, USA). The complete digestion of the ash was realized thanks to an automatic procedure, with the following temperature ramp: 10 min to reach 200 °C, then 10 min at 200 °C, and in the end 10 min to bring the temperature back to room temperature. Finally, the digested mixtures were transferred to 50 mL polyethylene flasks and diluted to the mark with MilliQ water. A stock solution of 1 g/L Ga in nitric acid (Ga inductively coupled plasma (ICP) standard solution, Fluka, Sigma Aldrich, Darmstadt, Germany) was used as internal standard and the analysis preparation followed the same procedure described in section 2.2.2. The specimens were prepared considering the linearity range of quantification as mentioned by Borgese et al. [132]. Zn extraction efficiency (ZEE) was calculated as reported in **Equation (3.2)**:

$$ZEE \, (\%) = (C_{Zn, \, leached} / C_{Zn, \, ash}) \cdot 100 \tag{3.2}$$

in which:

$C_{Zn, leached}$ = Zn concentration in the leached ash (mg/Kg) converted from (mg/L) using **Equation (2.1)**

$C_{Zn, ash}$ = Zn concentration in the digested ash (mg/Kg) converted from (mg/L) using **Equation (2.1)**

3.2.4. Design of Experiments (DoE)

Response surface tool is a set of experimental design methodologies that allow the response of a system to be studied in a clearer and more understandable way. Thus, the influence of several variables on the response of interest is investigated and the response can be optimized [199]. A face-centered central composite design (CCD) was adopted for the experiments, in order to investigate the optimal conditions for a chosen response and the curvature of the model between the factors [200].

The experiments were organized into 17 tests, with the following two factors being investigated: the molar concentration of the leaching agent (A) and the L/S ratio (B). In detail, two replicates of factorial points and five for central points were carried out. The choice of this design was based on a balance between good timing feasibility in the laboratory and an acceptable statistical power of the model. HCl concentration was considered in the range of 0.1–1 mol/L and L/S ratio in the range of 10–50 mL/g. Details of the 17 trials are outlined in **Table 3.1**. The considered responses were P and Zn concentrations, and the SUB-RAW indexes. The goal was to maximize the amount of P and the SUB-RAW index, and to minimize the Zn content. Design Expert 12.0.0 (Stat-Ease Inc., Minneapolis, USA) was used for performing statistical analysis in accordance with principles of the analysis of variance (ANOVA).

Table 3.1: Experimental design for P and Zn extraction with hydrochloric acid (HCl).

Run Order	HCl Concentration [mol/L]	L/S Ratio [mL/g]
1	0.55	30
2	0.55	10
3	0.1	10
4	0.55	50
5	0.1	50
6	0.1	50
7	1	30
8	0.1	30
9	1	10
10	1	50
11	1	50
12	0.1	10
13	0.55	30
14	0.55	30
15	0.55	30
16	1	10
17	0.55	30

3.2.5. ESCAPE approach for sustainability evaluation

ESCAPE is based on the SUB-RAW index, a simple, direct, and versatile dimension-less index, which allows the environmental impact evaluation of waste or by-product materials if used in substitution of natural resources. Moreover, it was recently used to examine different P recovery strategies from ISSA [76]. The SUB-RAW index is based on the following two parameters [196]: (i) the embodied energy (EE) that includes the energies directly and indirectly needed for the production of 1 kg of material, and (ii) the carbon footprint (CF) that represents the equivalent mass of greenhouse gases released into the atmosphere when 1 kg of material is produced (equivalent kg of CO_2). The parameters are calculated in MJ and $kgCO_2$, respectively. They can be normalized to a reference system defined

arbitrarily, and in this study, the EE and CF are normalized with respect to 1 kg of P produced (for process 1) and 1 kg of SiO_2 produced (for process 2).

The EE and CF of reagents are reported in several databases and in this work CES Selector 2019 integrated with its commercial database [201] and open LCA [202] with free database from Ecoinvent v. 3.3 [203] were used. The "Eco Audit Tool" of CES Selector 2019 combines user-defined input with EE and CF values, processing energy and transport type to create the energy breakdown [204]. This tool was used for the calculation of EE and CF associated with the total operating power consumption (expressed in Watt, W) for moving mechanical components (mixers, crushers, mills, vacuum filters, etc.) or heating (for thermal treatments). The associated EE and CF of chemicals and water dosage were also considered.

The EE and CF parameters can be evaluated for each step of the considered technology, and the SUB-RAW index was calculated by using **Equation (3.3)** [196], as follows:

SUB-RAW index = [log(EE_{RAW})/(MJ/kg) − log(EE_{SUB})/(MJ/kg) + log(CF_{RAW}) − log(CF_{SUB})]/2   **(3.3)**

EE_{RAW} and CF_{RAW} are the EE (MJ/kg) and CF ($kgCO_2$/kg) of the reference process, i.e., P extraction from the PR, or the SiO_2 extraction from diatomite (DE) while EE_{SUB} and CF_{SUB} are the EE (MJ/kg) and CF ($kgCO_2$/kg) of the P or SiO_2 extraction process from the RHPLA, intended as substitute of the original process from natural resources. The logarithm in the formula allows a direct and simple comparison considering an average of the environmental emission impact and energy consumed. If the SUB-RAW index has a positive result, the proposed substitute material can be considered as more sustainable than the reference material. On the contrary, a negative index means that the proposed material is more onerous than the reference material.

In this work, the SUB-RAW index was applied for the sustainability evaluation of the two recovery processes (1 and 2) explained in **Figure 3.3**.

3.3. Results and discussion

3.3.1. Experimental results

Figure 3.4 presents the P extraction efficiency (PEE) and Zn extraction efficiency (ZEE) for the 17 experiments. The maximum PEE value, equal to 76.5%, is reached by test n. 4 (HCl 0.55 mol/L, L/S = 50), but at the same time, the ZEE is over 70%. The minimum values for ZEE (<5%) are obtained in tests n. 5 and 6, in which the PEE values are between 35% and 40%. It was reported that, for ISSA, the chemical composition and the phases of the ash can significantly affect the extraction efficiency. Thus, the same operating conditions applied to different ashes do not guarantee similar results [197]. For the same reason, the investigation of the acid leaching behavior of one sample of RHPLA was screened especially under different conditions. The low value obtained for PEE, compared to the higher PEE obtained from HCl leaching of ISSA [73,74,159,205], suggests that polyphosphate and organophosphorus compounds can only be determined via phosphomolybdate complexation if they are converted to molybdate reactive orthophosphate, formed by sulfuric acid hydrolysis [206]. For the same reason, investigating the sulfuric lixiviation of RHPLA should be an advantageous forthcoming activity. In any case, PEE > 75% is a good result compared to the yield obtained from ISSA with HCl by Liu Y. and Qu H. in 2016 [160]. However, in tests n. 2, 3, 5, 6, 8, 12, and 16, PEE is greater than ZEE.
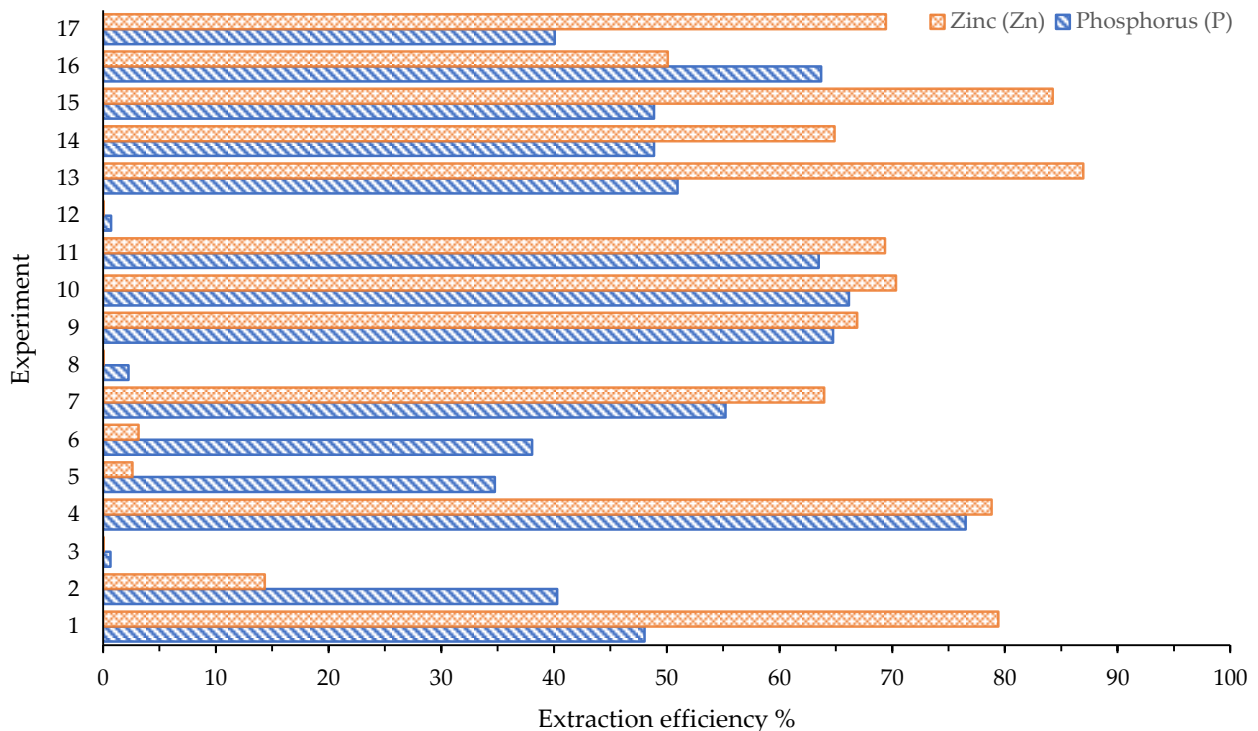

Figure 3.4: Extraction efficiency for phosphorus (P) and zinc (Zn), obtained from the results of colorimetric and TXRF analysis of the acid leachates.

3.3.2. Statistical analysis

The data shown in **Figure 3.4** were submitted to ANOVA. During the preliminary statistical evaluation, test n. 2 was identified as an outlier, both for the P and Zn concentration obtained after acid leaching, probably due to the sampling. Therefore, the data of test n. 2 were not included.

P extraction

To assess the capability and feasibility of the model, the correlation coefficient (R^2) and the analysis of variance were considered. The correlation coefficient was 0.985, while the adjusted R^2 and predicted R^2 values were 0.98 and 0.97, respectively; therefore, the model can be reliable and stable. The model equation was a second-order polynomial with also the interaction term, as reported in **Equation (3.4)**:

$$Y_1 = b_0 + b_1X_1 + b_2X_2 + b_{12}X_1X_2 + b_{11}X_1^2 + b_{22}X_2^2 \qquad \textbf{(3.4)}$$

where b_i are the coefficients for linear effects, b_{ij} are the coefficients of the interaction term, and b_{ii} are the coefficients for squared effects. Y_1 is the response variable of PEE, and X_i are the independent variables. The response surface for PEE is presented in **Figure 3.5** while **Figure 3.6a** represents the predicted values using the model versus the experimental values of PEE.
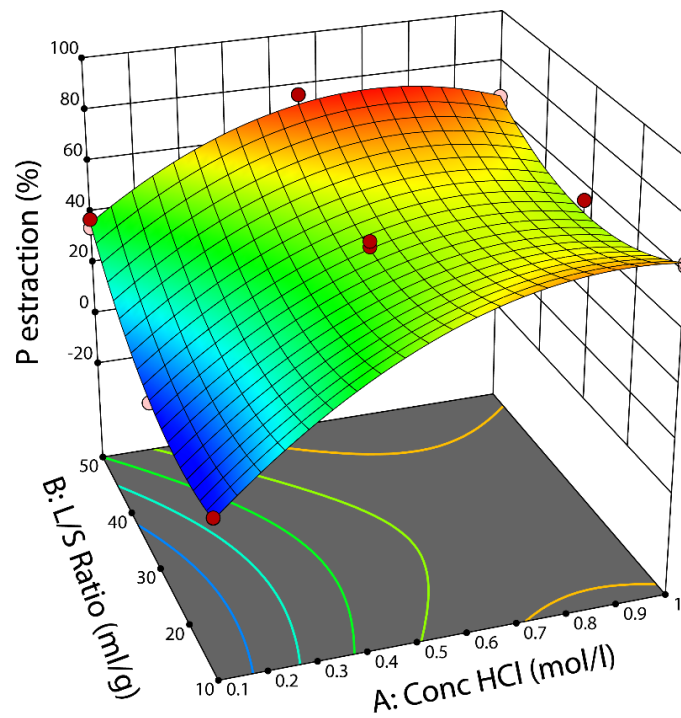

Figure 3.5*: Response surface plot of PEE (P extraction efficiency %) to evaluate the effects of HCl concentration and L/S ratio.*
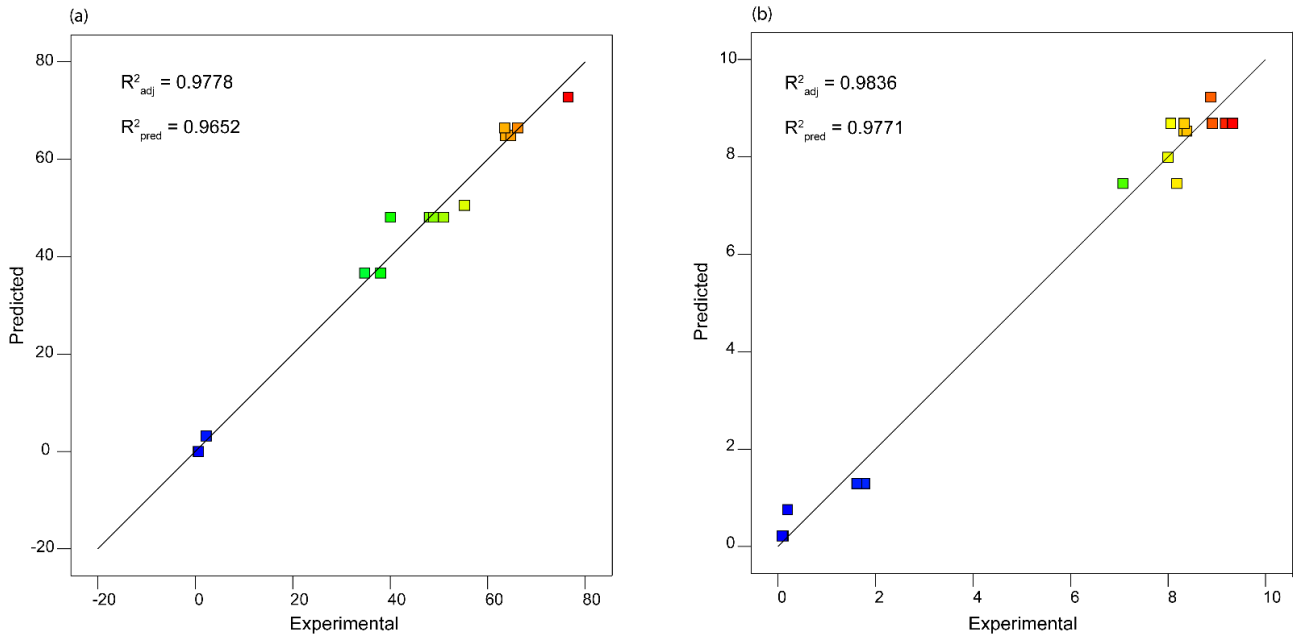
Figure 3.6: *Comparison of the experimental results with predicted results by the model. P extraction (**a**) and Zn extraction (**b**). The points are colored on a scale according to the considered response starting from blue (minimum value) to red (maximum value).*

The ANOVA for the regression model is presented in **Table 3.2**. The Fisher test value (F-value) for the model was found to be 133.13; this means that the model was highly significant, with a *p*-value less than 0.0001. In this case, A, B, AB, A^2, and B^2 are significant model terms. Finally, the lack of fit F-value of 2.32 implies that the lack of fit is not significantly relative to the pure error. There is a 16.06% chance that such a large lack of fit F-value could occur due to the noise (Design Expert 12.0.0, Stat-Ease Inc., Minneapolis, MN, USA).

Table 3.2: *ANOVA analysis for response surface second-order model. The considered response is the efficiency of P extraction. A = HCl concentration, B = L/S ratio, DF = degrees of freedom, SS = sum of squares, MS = mean square. (a) = significant at the 5% probability level, (b) = not significant at the 5% probability level.*

Source	DF	SS	MS	F-Value	*p*-Value
Model	5	8488.23	1697.65	133.13	<0.0001 (a)
A	1	5610.70	5610.70	439.98	<0.0001
B	1	779.21	779.21	61.10	<0.0001
AB	1	616.73	616.73	48.36	<0.0001
A^2	1	1004.99	1004.99	78.81	<0.0001
B^2	1	538.90	538.90	42.26	<0.0001
Residual	10	127.52	12.75	-	-
Lack of Fit	2	46.80	23.40	2.32	0.1606 (b)
Pure Error	8	80.72	10.09	-	-

Zn extraction

The second goal of the process was to minimize the Zn extraction. The correlation coefficient (R^2) and ANOVA were used to test the feasibility and the reliability of the model. The R^2 calculated in fitting was 0.99, while the adjusted and predicted R^2 were 0.98. Thus, the model can be considered reliable and stable. To correlate the response of Zn extraction and the independent variables a second-order polynomial equation was used. It is worth noting that, in this case, a transformation of response was required due to the non-normality distribution of the residuals with the original response; more specifically, a square root transformation was used. The second-order equation used for the prediction of the response is presented in **Equation (3.5)**:

$$Y_2 = b_0 + b_1X_1 + b_2X_2 + b_{11}X_1^2 \tag{3.5}$$

where b_i are the coefficients for linear effects and b_{ii} are the coefficients for squared effects. Y_2 is the response variable of ZEE, and X_i are the independent variables. The response surface for ZEE is presented in **Figure 3.7**.
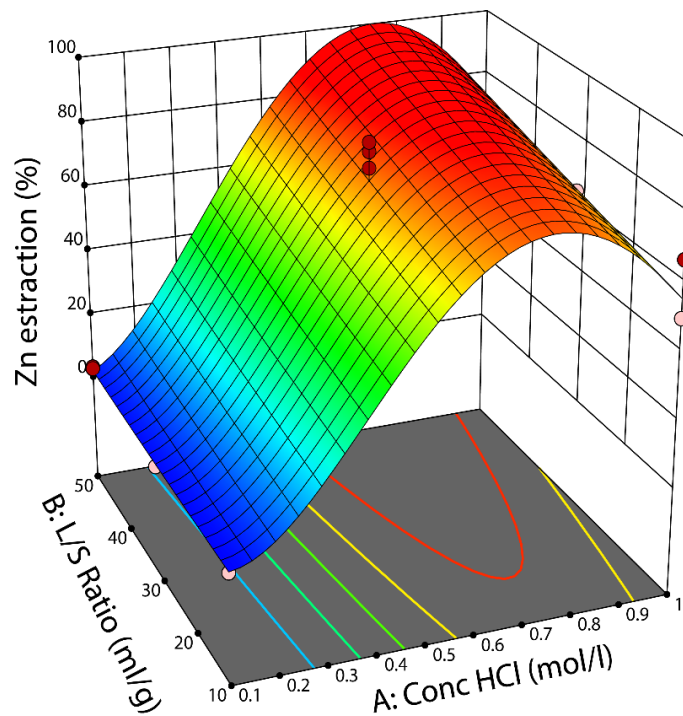
Figure 3.7: *Response surface plot of ZEE (Zn extraction efficiency %) to evaluate the effects of HCl concentration and L/S ratio.*

In **Figure 3.6b**, the predicted values using the model versus the experimental values for ZEE are shown, while the ANOVA is presented in **Table 3.3**. Since the model F-value is 300.07, the model is significant; this is confirmed by the *p*-value less than 0.0001. In this case, A, B, and A² are significant

model terms, as indicated by the *p*-value. As for the P extraction, the lack of fit is not significantly relative to the pure error, as confirmed by the F-value of 1.03 and the p-value greater than 0.05.

Table 3.3: ANOVA analysis for response surface second-order model. The considered response is the efficiency of Zn extraction. A = HCl concentration, B = L/S ratio, DF = degrees of freedom, SS = sum of squares, MS = mean square. (a) = significant at the 5% probability level, (b) = not significant at the 5% probability level.

Source	DF	SS	MS	F-Value	*p*-Value
Model	3	206.32	68.77	300.07	<0.0001 (a)
A	1	130.98	130.98	571.50	<0.0001
B	1	2.56	2.56	11.17	0.0059
A^2	1	69.03	69.03	301.20	<0.0001
Residual	12	2.75	0.23	-	-
Lack of Fit	4	0.93	0.23	1.03	0.4488 (b)
Pure Error	8	1.82	0.23	-	-

SUB-RAW Index

In the DoE study, the SUB-RAW index was calculated for the 17 tests and considered in the optimization, together with the PEE and ZEE percentages. The input parameters were always the HCl molar concentration and the L/S ratio. Considering the SUB-RAW index as a response, the ANOVA results are presented in **Table 3.4**. The model is significant (F-value = 117.12), but the lack of fit is also significant (F-value = 7.77). This means that the model cannot optimize the response. Thus, the model fails to adequately describe the functional relationship between the experimental factors and the response. This inconsistency is probably due to the procedure of the SUB-RAW index calculation that was considered as an experimental result, such as PEE and ZEE, when this index comes from a numerical computation. Therefore, the model cannot be constructed in a reliable way because a thorough study for the possible use of SUB-RAW index in a statistical design is necessary. These whole considerations could be a good starting point for forthcoming studies, especially for the development of a standard method of SUB-RAW index calculation, that is not trivial if made in a non-computerized way. The calculations are different for any process under study, because include many and many values of EE and CF, one for each experimental stage e.g., stirring, heating, centrifugation, drying etc., depending on different instrumentations and their power consumptions, chemicals used, and duration of the reaction. In this specific study, SUB-RAW indexes of the laboratory scale process described in chapter 2 (procedure B) were calculated, considering every single experimental step. The sustainability evaluation through the ESCAPE approach of the same process scaled-up in a pilot or industrial plant, could return totally different SUB-RAW values because the equipment involved would be different. It is important to note then that ESCAPE method already considers many variables and its

use in this specific DoE may not be easy due to the additional relation with other variables (HCl concentration and L/S ratio).

Table 3.4: *ANOVA analysis for SUB-RAW index response obtained from the reprocessing of the experimental data. A = HCl concentration, B = L/S ratio, DF = degrees of freedom, SS = sum of squares, MS = mean square.*

Source	DF	SS	MS	F-Value	*p*-Value
Model	5	6.57	1.31	117.12	<0.0001
A	1	2.26	2.26	201.39	<0.0001
B	1	0.58	0.58	51.67	<0.0001
AB	1	3.35	3.35	298.65	<0.0001
A^2	1	0.33	0.33	29.36	0.0003
B^2	1	0.55	0.54	48.78	<0.0001
Residual	10	0.11	0.01	-	-
Lack of Fit	2	0.07	0.04	7.77	0.0133
Pure Error	8	0.04	0.005	-	-

Response optimization

Since the SUB-RAW index cannot be optimized, optimization was only considered for PEE and ZEE. The model was validated considering these two factors, with the aim of maximizing the P extraction and, simultaneously, minimizing the Zn content. The optimization had to consider that the factors A and B are directly correlated with both responses. A good compromise was found in the following conditions: HCl concentration of 0.34 mol/L and L/S ratio of 50. In these conditions, 61.3% of PEE and 44.2% of ZEE can be reached.

3.3.3. Sustainability analysis

Since the statistical evaluation of the SUB-RAW index was not reliable, a comparison between the most sustainable test and the most efficient test was considered. The sustainability analysis of the 17 tests (in terms of EE and CF) was performed and compared to the similar process reported by Habashi et al. [207], in which the P is recovered from PR. According to **Equation (3.3)**, the 17 SUB-RAW indexes were calculated. All the values are reported in **Table 3.5**, and the best SUB-RAW index is obtained by test n. 9 (HCl 1 mol/L and L/S 10 mL/g, PEE around 65%), with a value equal to −0.34. Unfortunately, no SUB-RAW value is positive, showing that the proposed process is no more sustainable than the original one. It must be taken into account that the calculation of the original process is made only based on the information obtained from the literature without knowing in detail the equipment used as it was for the process on the laboratory scale implemented in first person.

Table 3.5: *SUB-RAW indexes calculated for all 17 tests.*

Run Order	HCl Concentration [mol/L]	L/S Ratio [mL/g]	SUB-RAW index [/]
1	0.55	30	-0.76
2	0.55	10	-0.43
3	0.1	10	-2.04
4	0.55	50	-0.70
5	0.1	50	-0.78
6	0.1	50	-0.76
7	1	30	-0.84
8	0.1	30	-1.87
9	1	10	-0.34
10	1	50	-0.96
11	1	50	-0.98
12	0.1	10	-1.97
13	0.55	30	-0.74
14	0.55	30	-0.75
15	0.55	30	-0.72
16	1	10	-0.37
17	0.55	30	-0.82

Table 3.6 shows the results of EE and CF, concerning the P recovery from PR as raw material and from RHPLA using the parameters of tests n. 4 (the most efficient) and n. 9 (the most sustainable). Test n. 4 showed the highest PEE (76.5%), despite a less sustainable SUB-RAW index (−0.70) than that obtained in test n. 9. The reference process [207] showed a % of P recovery of about 99% (out of the 13.62% available in the PR), thanks to the involvement of beneficiation agents that were not considered in the SUB-RAW calculation, because no data regarding their concentration were reported by the reference. However, despite the negative SUB-RAW index, in terms of the EE and CF referred to the starting material (1 kg of RHPLA), test n. 9 requires lower EE (28.2 MJ/kgRHPLA) and CF (1 kgCO$_2$/kgRHPLA), in comparison to the reference process (EE$_{RAW}$ = 60.99 MJ/kgPR and CF$_{RAW}$ = 2.08 kgCO$_2$/kgPR). Since the approach requires a final normalization step from 1 kg of RHPLA to 1 kg of recovered material (P), the lower P grade contained in RHPLA (about 9% according to XRF analysis in **Figure 3.2**) leads to a negative SUB-RAW index. This problem would be overcome if this analysis had considered other types of agricultural animal-derived ashes, such as meat and bone ash, which has a P content of about 18% [22].

Table 3.6*: Data results of the embodied energy (EE) and carbon footprint (CF) for the raw process (RAW) and the new proposed process (SUB) related to wet-chemical extraction from RHPLA; it shows the comparison between the most efficient trial in terms of PEE (test n. 4) and the most sustainable trial (test n. 9) relative to the other trials.*

Considered processes and materials	EE_{RAW} (MJ/kgPR)	CF_{RAW} (kgCO$_2$/kgPR)	EE_{SUB} (MJ/kgRHPLA)		CF_{SUB} (kgCO$_2$/kgRHPLA)	
			Test n. 4	Test n. 9	Test n. 4	Test n. 9
Thermal and mechanical process	4.43	0.25	3.80	3.80	0.19	0.19
Chemical reagents	30.51	1.82	31.94	11.62	1.90	0.69
Water dosage	26.06	0.01	39.37	12.75	0.75	0.15
Total	60.99	2.08	75.11	28.17	2.84	1.02

In **Figure 3.8a**, PR and test n. 9 are compared. It results that the chemicals and water quantities represent the greatest contributions to EE, whereas, for CF, the contribution of chemicals is more relevant compared to the contribution of the thermal and mechanical treatments, and the quantity of water used.
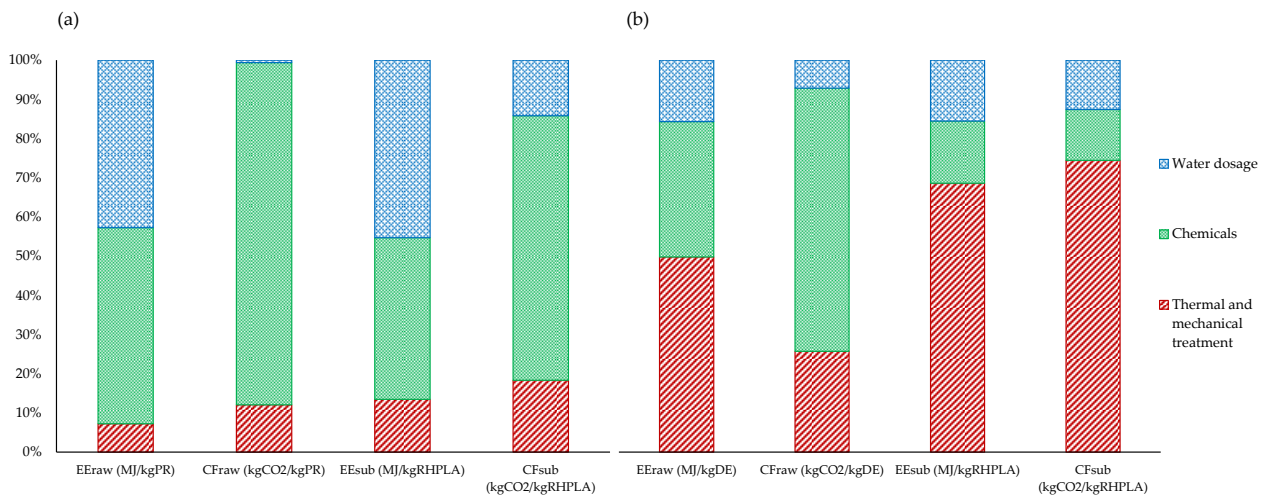

Figure 3.8*: Bar chart results of the embodied energy (EE) and carbon footprint (CF) for the raw process (RAW) and the new proposed process (SUB), showing the relative contribution of the single procedure steps (water dosage, chemical reagents, thermal and mechanical treatment). (**a**) Represents the case of test n. 9 in process 1 (devoted to P recovery), while (**b**) represents process 2 (devoted to silica recovery).*

In **Table 3.7** are presented the values of EE and CF of the second process, to recover SiO$_2$, that are 128 MJ/kgRHPLA and 6 kgCO$_2$/kgRHPLA, respectively. The identified reference process considers the extraction of SiO$_2$ from the DE [208], since it has been suggested to be one of the most promising, stable, and steady sources of SiO$_2$. The calculated values of EE_{RAW} and CF_{RAW} for the reference process are 99 MJ/kgDE and 10.37 kgCO$_2$/kgDE, respectively. These EE and CF values calculated for the raw process and for the process proposed for recovering SiO$_2$ from RHPLA are comparable. More than 50% of the EE of both processes is due to the mechanical and thermal treatments, and the value of EE_{SUB} is

greater by about 38 MJ/kg, in comparison to the value corresponding to EE_{RAW}. But the value of EE_{SUB} could be easily decreased by about 17 MJ by using an electric oven instead of a halogen furnace. Furthermore, the data presented in the reference process [208] did not mention the necessary step of drying the material before the alkaline treatment, weighing it properly, and defining the correct L/S ratio. Considering these facts, in terms of sustainability, the two processes are comparable. In **Figure 3.8b**, it is shown that, for the extraction process of SiO_2 from RHPLA, the highest contribution to both EE_{SUB} and CF_{SUB} is due to the thermal and mechanical treatments. Instead, in the reference process, only EE is determined by thermal and mechanical treatments, while the CF value is mainly related to the use of chemicals.

Table 3.7: *Data results of the embodied energy (EE) and carbon footprint (CF) for the raw process (RAW) and the new proposed process (SUB) for SiO_2 recovery from RHPLA.*

Considered processes and materials	EE_{RAW} (MJ/kgDE)	CF_{RAW} (kgCO$_2$/kgDE)	EE_{SUB} (MJ/kgRHPLA)	CF_{SUB} (kgCO$_2$/kgRHPLA)
Thermal and mechanical treatment	49	3	87	4
Chemicals	34	7	20	1
Water dosage	16	1	20	1
Total	99	10	128	6

If 1 kg of extracted SiO_2 was considered, since, in RHPLA, the extraction efficiency is about 20% [209] (out of the 13% available in RHPLA), and in the DE, the extraction efficiency is about 31% [208] (out of the 80% available in DE), the SUB-RAW index would be negative (-0.9). Thus, the results suggest that the recovery process from RHPLA is less sustainable than the original one from diatomite but was calculated that if the waste contained 80% of SiO_2, the SUB-RAW index would be close to zero.

3.4. Conclusions

This work has reported a novel integrated approach that aimed to evaluate the potential correlation between the input parameters (HCl molar concentration and L/S ratio) and the responses (PEE, ZEE and SUB-RAW index), in the frame of P and SiO_2 recovery from RHPLA by wet-chemical extraction. This was also the first study on the possibility of recovering P from RHPLA, minimizing the metal contamination, and considering at the same time the statistical optimization of the process and its environmental impact.

The good stability of the statistical models for PEE and ZEE allowed the optimization of the process to be appraised, in terms of the maximization of P recovery and minimization of the main HM (Zn). The operating conditions suggested by the experimental design are 0.34 mol/L HCl concentration and 50 L/S ratio, to allow PEE equal to 61.3% and ZEE equal to 44.2%. On the other hand, SUB-RAW index could not be optimized by DoE due to a significant lack of fit in the model, preventing the description of functional relationship between the experimental factors and the response. However, sustainability analysis has shown that the most sustainable operating conditions can be achieved by adopting 1 mol/L of HCl and a L/S ratio equal to 10, realizing a PEE of about 65%.

The results show that the global process for amorphous SiO_2 recovery from RHPLA is less sustainable compared to the corresponding SiO_2 extraction from raw material diatomite, because the SiO_2 content in RHPLA is too low. Environmental sustainability of the proposed recovery process could be achieved in the case in which the by-product material reaches a SiO_2 content of about 80%.

In conclusion, from an environmental point of view, a good practice to manage RHPLA can consist of P recovery by wet chemical extraction, to eventually address the solid residual as a building material (for example, for cement production), due to its content of SiO_2. More in general, this novel approach that integrates statistical methods and the SUB-RAW index may strongly contribute to evaluating the sustainability of any recovery process.

Future studies are mandatory for further optimization of the P recovery process from RHPLA after the acid leaching step. Beyond the result of ESCAPE analysis on sustainability of the P recovery in terms of SUB-RAW index, it is important to highlight that this waste stream has the advantage of being a by-product that is more environmentally affordable than raw material (PR), which must be mined, physically treated, and milled.

Acknowledgements

4. SEWAGE SLUDGE ASH STUDY FOR P RECOVERY AND WASTE VALORIZATION

Abstract

The work addressed in this chapter aims to perform a preliminary SSA characterization in view of simultaneous P and amorphous SiO_2 recovery. SSA was already widely studied for P recovery by wet-chemical extraction, deepening the investigation of P precipitation after lixiviation, and SSA residue re-use. The most common application for ash residue is construction industry, with particular attention to the study of pozzolanic reactivity and silicates action. As for the previous chapters, the idea was to give new life to waste by generating new eco-materials, as alternative to the already known practices.

P dissolved in solution after acid leaching was precipitated at different pH values with alkali titration, to create iron/aluminum/calcium phosphate product for fertilizer applications. SiO_2 was recovered in subsequent steps using the method described in chapter 2 with potential as adsorbent for the removal of drugs from wastewater, or additive for solidification/stabilization of HM in other hazardous waste. Tests were performed on three SSA, collected from both Italian and German treatment plants. P extraction efficiency (PEE) ranges about 58 and 87%, while the subsequent P precipitation efficiency (PPE) from the leachate varies between 30 and 98% depending on type of ash but especially on pH conditions. From the precipitation tests, pH 4 and 5 turned out to be the most suitable values for ensuring good P content, comparable with commercial P fertilizers. At the same time, speciation of the recovered P-precipitates was studied with the simulation software Visual MINTEQ to better understand the chemical composition of phosphatic compounds at different precipitation pH. Moreover, qualitative analysis has shown the satisfying quality of the recovered SiO_2, minimally contaminated with salts, and the SiO_2 extraction efficiency (SEE) was attested around 45 %.

Keywords

Sewage sludge ash characterization
Silica extraction
P wet chemical extraction
Simulation of precipitation equilibrium

Scientific contribution

The samples analyzed in this chapter were collected thanks to the collaboration with Politecnico di Milano in the frame of the PerFORM WATER 2030 project, as mentioned in section 1.5.1. The content reported in this chapter is the result of my own work, including literature review, data curation, formal analysis, investigation, methodology, visualization, and writing. Any work made by others is attributed to the original author in the text. Some results presented here are also based on the following

publication, whose form have been adapted for reasons of consistency with the structure of this doctoral thesis.

o   Boniardi G., Turolla A., **Fiameni L.**, Gelmi E., Malpei F., Bontempi B., Canziani R., Assessment of a simple and replicable procedure for selective phosphorus recovery from sewage sludge ashes by wet chemical extraction and precipitation. *Chemosphere* (2021), **285**, 131476. https://doi.org/10.1016/j.chemosphere.2021.131476

4.1.   Introduction

SSA has a very prominent position in P recovery research compared to PLA, and different studies were already performed on the ash characterization, nutrients extraction, and re-use. As already mentioned, the zero-waste approach was not limited to safe waste management, which is mostly landfilled, but also requires facilitating the recycling of waste ash. The first application for this type of incinerated biomass is the building sector, and it is currently proposed for cement-based materials, as in past years, aiming to a conscious and sustainable construction practice [210–215][193][49,216–219].

In a recent work of the last year [220], the sustainable and the most common applications for incinerated sewage sludge ash (ISSA) are explained: blended binder by lime activation (lime-pozzolan cements), adsorption of pollutants (HM) in wastewater, recycling into construction materials (concrete-related products and ceramics), and stabilization/solidification of contaminated soil to transform low-quality soils into valuable construction materials. Stabilization/solidification (S/S) is the widely studied practice of employing cementitious materials to reduce the leachability of hazardous constituents and it is adopted for hazardous waste control. In the S/S mechanism, chemical and physical reactions are involved, allowing the immobilization of specific components, solidifying, or encapsulating them [221]. All these applications are possible precisely because of the high silicon content of ISSA, together with calcium (to form calcium silicates), characteristic elements for cement hydration and pozzolanic reactivity. In **Figure 4.1** are presented the main mechanisms of S/S promoted by ISSA as suggested by Zhou Y. et al. [220].
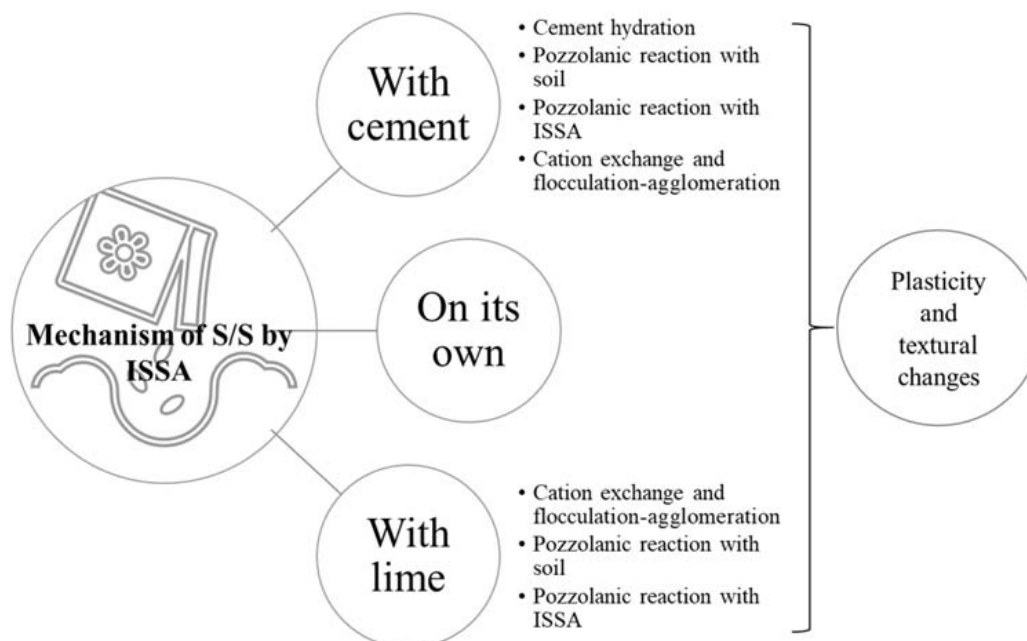

Figure 4.1: Main reaction mechanisms of solidification/stabilization with inclusion of incinerated sewage sludge ash [220].

This specific S/S properties of ISSA has brought over the years also to study the application of this waste for the stabilization of HM in other hazardous waste, such as municipal solid waste incinerated fly ash (MSWI-FA) [30,222][223][224].

In the work of Donatello S. and Cheeseman C.R. [225] the re-use options for ISSA as cement-based material are detailed: into sintered materials, such as bricks, tiles and pavers, or lightweight aggregates, into glass–ceramics products, into lightweight aerated cementitious materials, into Portland cement during the manufacturing process, or as additive to Portland cement itself. Then an entire paragraph is dedicated to the phosphate recovery from ISSA, paying particular attention to the recovery via acid leaching, and the recycling of acid insoluble ISSA residue. Thus, in the research, the focus on ISSA re-use was moved to the destiny of ash residue after P recovery, wondering if its potential in the construction sector was still valid. Different publications were made on this topic [162,163,226,227], highlighting promising effects of ISSA residue in blended cements but without conclusive and consistent findings about compressive strengths and pozzolanic activity.

Starting from these considerations, and aware of the need to suggest a comprehensive solution for the P recovery process from SSA, that also regards the residual ash management, SiO_2 recovery was proposed. Based on the chemical composition of SSA after acid leaching for P recovery, rich of insoluble Si but poor of Ca compounds (necessary for cement application), a new path for SSA residue re-use was tested. Also in this case, SiO_2 recovery is an attempt of zero-waste approach to obtain more added-value products from the same waste, compared to the common destination of the residue ash (landfill) due to its not yet verified suitability in the construction sector. For example, an already known application for recovered SiO_2 could be as adsorbent for the removal of drugs or HM from wastewaters [228–231]. This study is even more important considering the spread that is having P recovery from SSA through wet-chemical extraction.

Therefore, as direct consequence of the study conducted on RHPLA in chapter 2 and chapter 3, the effort of simultaneous P and SiO_2 recovery from SSA was conducted. A first and preliminary trying was conducted on a SSA sample adopting the same operating procedure B described in chapter 2. Then, the P extraction study on other 3 SSA samples was driven by the extensive literature available, leading to the choice of the optimized method offered by Fang L. et al. [70]: 0.2 mol/L of sulfuric acid H_2SO_4 at L/S ratio of 20 and contact time of 2 h. At this stage, the SSA residue after acid leaching was subjected to SiO_2 extraction. Moreover, compared to the process adopted for RHPLA, a next step was added: the subsequent P recovery from the acid leachate was performed by alkali precipitation, screening the best pH value to reach a satisfying P precipitation efficiency. The experimental results were then compared with the simulated results gained from an equilibrium simulation software, Visual MINTEQ.

A brief characterization of the ash was carried out before the experimental part, with the instrumentation available at the C4T Lab. For the complete and joint characterization of the samples, refer to the publication cited in section 4.

4.2. Materials and methods

4.2.1. Sampling

For this research samples were kindly provided by the Department of Civil and Environmental Engineering (DICA) of Politecnico di Milano, as part of PerFORM WATER 2030 project. Three samples of sewage sludge (SS), S1, S2 and S3, were sampled from the output of two thermal driers at two full-scale WWTPs located in the metropolitan area of Milan, Italy. S1 and S2 were collected from the same plant at different times of the year (in the month of August and December respectively), knowing that the nature of municipal wastewater at different sampling times produces dissimilar SS. S1, S2 and S3 were incinerated at laboratory scale at 900 °C for 2 h in a laboratory standard muffle (LT 9/12 SKM Nabertherm, Germany), avoiding excessive gas emissions with a prior heating of the SS on hot plates under the hood for 2 h (heating curve from 100 to 500 °C) and manual mixing. Another ISSA sample, S4, was instead collected from the electro-filters of a mono-incineration plant located in the city of Karlsruhe (Germany); the plant consisted of a fluidized bed reactor, with a combustion temperature between 850-950 °C.

4.2.2. Characterization techniques

For structural characterization and crystalline-phase identification of the samples, X-ray diffraction (XRD) was used, while the morphology of the samples was assessed by scanning electron microscopy (SEM) coupled with an EDXS (energy dispersive X-ray spectroscopy) probe as described in section 2.2.2. Chemical analysis of the digested and leachate solutions was carried out using TXRF (Total Reflection X-ray Fluorescence). The sample preparation and subsequent analysis was described in section 2.2.2 and section 3.2.3.

Table 4.1 shows the techniques available for the characterization of the solid and liquid samples at the different stage of the recovery process.

Table 4.1: Characterization techniques used in each step of the simultaneous P and SiO$_2$ recovery from SSA. * Missing XRD analysis for precipitate at pH 2, due to the very small amount of solid that prevented the complete characterization.

Sample	Raw SSA	Acid leaching	Precipitation at different pH	P-precipitates	Recovered silica
S1	XRD, SEM-EDXS, digestion + TXRF	TXRF, SEM-EDXS on residue	/	/	SEM-EDXS XRD
S2	XRD, SEM-EDXS, digestion + TXRF	TXRF	TXRF on each filtrate at different pH	XRD for each precipitate at different pH	XRD
S3	XRD, SEM-EDXS, digestion + TXRF	TXRF	TXRF on each filtrate at different pH	XRD for each precipitate at different pH *, SEM-EDXS for each precipitate at different pH	XRD
S4	XRD, SEM-EDXS, digestion + TXRF	TXRF	TXRF on each filtrate at different pH	XRD for each precipitate at different pH *, SEM-EDXS for each precipitate at different pH	XRD

4.2.3. SiO$_2$ and P extraction

For sample S1 was adopted the same procedure B explained in section 2.2.3., using HCl 1 mol/L, L/S ratio of 10 and contact time of 2 h at room temperature for acid pre-treatment. This preliminary test was conducted to assess the experimental feasibility of SiO$_2$ recovery from the ash residue after P extraction. For sample S2, S3, S4, based on literature [70], the method was refined in the first recovery step, adopting 0.2 mol/L of H$_2$SO$_4$, L/S ratio equal to 20 and contact time of 2 h. All the leachates were analyzed with TXRF, as well as the digested samples, and P extraction efficiency (PEE) was calculated in accordance with **Equation (3.1)**.

For all the SSA samples, SiO_2 recovery on ash residue was performed with the same steps described in the **Reaction (2.3)** (NaOH 4 mol/L, L/S ratio of 10, constant stirring at 80 °C for 4 h) and **Reaction (2.4)** (H_2SO_4 5 mol/L added dropwise to the sodium silicate leachate, under constant stirring at room temperature, to reach pH 9.8 for gel formation). The dried amorphous silica obtained, was characterized with SEM-EDXS, IR or XRD analysis. When possible, SiO_2 extraction efficiency (SEE) was calculated based on the SiO_2 content in the ash residue after acid leaching, following **Equation (4.1)**:

$$\text{SEE (\%)} = (SiO_{2\ recovered}/\ SiO_{2\ ash\ residue}) \cdot 100 \qquad \textbf{(4.1)}$$

in which:

$SiO_{2\ recovered}$ = mass of the dried amorphous silica recovered at the end of the process (g)

$SiO_{2\ ash\ residue}$ = mass of SiO_2 present in the ash residue according to semi-quantitative analysis (g)

4.2.4. P precipitation

For sample S2, S3, S4 a further study of P recovery was conducted, testing the precipitation of iron/aluminum/calcium phosphate compounds thanks to an alkali titration of the acid leachate as suggested in literature [155,156,232,233]. Seven aliquot of 50 mL of each P-rich leachate, was precipitated in batch conditions at room temperature by gradual addition of lime solution $Ca(OH)_2$ 1% w/w reaching different pH values, from 2 to 8. The titrated solutions were left to rest for 2 h to allow the precipitate formation, then the suspension was filtered through a 0.45 µm nylon membrane, the solid precipitate was dried in the oven for about 10 h at 100 °C, and finally weighed. P content in the precipitates was estimated with a mass balance calculation, thanks to the TXRF elemental quantification (mg/L) in each filtrate at different pH. Percentage of P in each precipitate ($P_{precipitate}$) can be calculated using the **Equation (4.2)**:

$$P_{precipitate}\ (\%) = C_{P,\ precipitate}/10000 \qquad \textbf{(4.2)}$$

In which:

$C_{P,\ precipitate}$ = P concentration in the precipitate (mg/Kg), calculated by the **Equation (4.3)**:

$$C_{P,\ precipitate}\ (mg/Kg) = [(C_{P,\ leachate} \cdot V_{leachate}) - (C_{P,\ filtrate} \cdot V_{titration})]/m_{recovered} \qquad \textbf{(4.3)}$$

In which:

$C_{P,\ leachate}$ = P concentration in the acid leachate (mg/L)

$V_{leachate}$ = volume of acid leachate used for each precipitation test (L)

$C_{P,\ filtrate}$ = P concentration in the filtrate solution after precipitate separation (mg/L)

$V_{titration}$ = volume of titration solution ($V_{leachate}$ + $V_{titrant}$) (L)

m $_{recovered}$ = mass recovered for each precipitate (Kg)

Moreover, using the same terms, P precipitation efficiency (PPE) at different pH values was calculated following the **Equation (4.4)**:

$$PPE\ (\%) = [1 - (C_{P,\ filtrate} \cdot V_{titration})/(C_{P,\ leachate} \cdot V_{leachate})] \cdot 100 \qquad \textbf{(4.4)}$$

In addition, all the precipitates were analyzed with XRD to identify crystalline composition. **Figure 4.2** summarizes the experimental procedure adopted for this study.
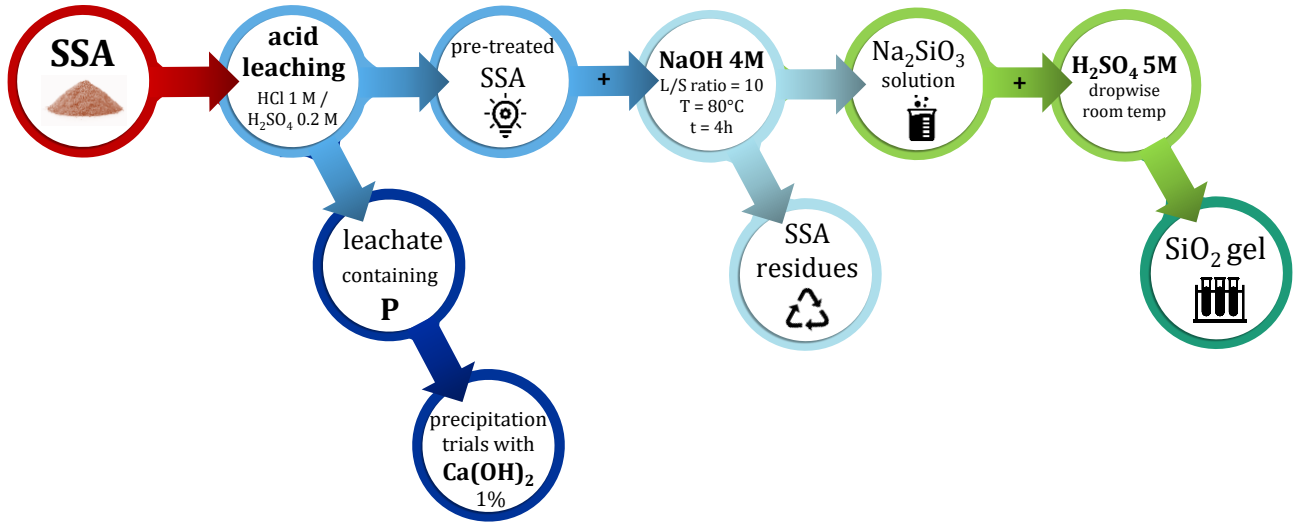

Figure 4.2: *Scheme of the recovery process adopted for SSA samples S1-S4.*

4.2.5.   Equilibrium simulation

For an in-depth understanding of the precipitation mechanism in function of induced pH of the solution, a simulation software was adopted. PHREEQC [234] and Visual MINTEQ [235] are the most used [236][237], especially in the study of P precipitation as struvite $MgNH_4PO_4 \cdot 6(H_2O)$ from wastewaters, digestates or leachates [238–241]. Additionally, Visual MINTEQ was already proposed for ion equilibrium investigation during P precipitation from acid leachate of biomass ash [127,155,158]. For this purpose, the software (ver. 3.1) was adopted as chemical equilibrium model for the calculation of element speciation and solubility equilibria. In particular, the solution saturation condition can be described by the saturation index (SI), as reported in **Equation (4.5)**. It is defined as the ion activity product (IAP) of constituent ions of a compound over equilibrium solubility product (K_{sp}) of the compound.

$$SI = \log\ (IAP/K_{sp}) \qquad \textbf{(4.5)}$$

Equation (4.6) defines IAP, where [A], [B], [C] and [D] indicate ion activity, while a, b, c, d are stoichiometric coefficients.

$$IAP = [C]^c[D]^d/[A]^a[B]^b \qquad \qquad (4.6)$$

When IAP is lower than K_{sp}, the generated value will be negative (SI < 0), which means that the solution is undersaturated and the solid should not be able to form. Conversely, with IAP greater than K_{sp}, positive SI would be obtained (SI > 0) that reflect oversaturated conditions, in which compounds could be precipitated into solution. If instead the values of IAP and K_{sp} were equal, it would be a state of equilibrium (SI = 0). Due to the complex composition of P extracts, SI values simulated by Visual MINTEQ for each potential precipitate were studied starting from concentrations of elements in the acid leachate solutions. **Table 4.2** reports elemental concentration detected in solutions after P wet-chemical extraction by TXRF and used as inputs for ion concentrations in Visual MINTEQ. This analytic technique allows to obtain with high precision the concentration of all the elements with higher atomic weight of silicon (Si). Unfortunately, the concentration of aluminum (Al) can therefore not be considered completely reliable, because of the experimental conditions, but to assess the equilibrium of phosphatic compounds in solution, this data has also been included among the inputs.

Table 4.2: Elemental concentration in acid leachates after P extraction, obtained from TXRF analysis. nd = not detected, < LOQ = under limit of quantification.

	Sample S2			Sample S3			Sample S4		
Element	average (mg/L)		uncertainty	average (mg/L)		uncertainty	average (mg/L)		uncertainty
Al	441	±	139	437	±	72	862	±	40
P	2376	±	587	2630	±	304	3715	±	400
S	3471	±	1474	4400	±	558	3256	±	285
K	41	±	5	264	±	29	142	±	9
Ca	386	±	62	475	±	50	564	±	109
Ti	1.1	±	0.6	5.2	±	0.9	14	±	6
V	1.09	±	0.02	1.40	±	0.17	0.67	±	0.40
Cr		< LOQ		0.97	±	0.08	0.77	±	0.22
Mn	90	±	4	15.14	±	0.85	103	±	9
Fe	160	±	5	526	±	11	652	±	16
Ni	0.88	±	0.28	0.83	±	0.08	0.80	±	0.11
Cu	11.94	±	0.52	16.86	±	0.68	25.7	±	1.4
Zn	35	±	1	94	±	5	87	±	4
As	2.27	±	0.07	0.46	±	0.08	1.18	±	0.18
Br		nd			nd		0.95	±	0.10
Rb		nd		1.01	±	0.09	0.40	±	0.03
Sr	6.25	±	0.87	6.51	±	0.71	6.8	±	1.5
Pb		< LOQ		0.39	±	0.02		< LOQ	
U	1.11	±	0.08	1.42	±	0.10		nd	

Moreover, the initial pH value of each leachate was considered:

- Sample S2 = pH 1.24
- Sample S3 = pH 1.22
- Sample S4 = pH 1.67

The pH was adjusted in the software by adding corresponding concentration of H^+ and SO_4^{2-} in the component list, simulating the addition of H_2SO_4 used for acid lixiviation. At the end, the simulation can be generated via the *multi-problem/sweep* function, selecting the *titration* function. It is possible to enter the volumes related to both the solution to titrate and the titrant and define the chemical composition and the concentration of the titrant ($Ca(OH)_2$ 1%). Even if the experimental tests were performed until pH 8 for P precipitation, simulation was brought up to pH 12.

4.3. Results and discussion

4.3.1. SSA characterization

Figure 4.3 shows XRD patterns of raw SSA samples and the corresponding identified crystalline phases. The crystalline composition is quite similar for all SSA, despite the different origins: quartz [Si_2O] and hematite [Fe_2O_3] were clearly detected in the four samples, according to literature results [216] for ISSA deriving from multi-cyclone units and baghouse dust filters. XRD analysis reveals that the main form of crystalline P present in all samples, is calcium hydrogen iron phosphate [$Ca_9FeH(PO_4)_7$], while anhydrite [$CaSO_4$] was identified in all samples except S3. In this sample two other minor compounds were detected: aluminum phosphate [$AlPO_4$] and aluminum silicate hydroxide [$Si_2Al_2O_5(OH)_4$]. The presence of calcium hydrogen iron phosphate [$Ca_9FeH(PO_4)_7$] shows that iron (Fe), used during the chemical precipitation of phosphorus in all the WWTPs, results the main element bounded with P and Ca, to form a crystalline phosphate. Ash samples S1, S2, and S3, are more easily identifiable as bottom ash, because of their preparation in a muffle furnace and collection. Instead, their crystalline composition is not so far from the fly ash samples S4. Indeed, even if with different methods, the incineration process for all the specimen was performed between 850 and 950°C. Was already demonstrated that calcination temperatures of SS affect the crystallization process, transforming amorphous content in crystalline and identifiable phases as temperatures rise [242,243] really demonstrates how complex the mineralogical composition of SS bottom ash can be, but in this case, the laboratory combustion process led to products more similar to industrial fly ash.
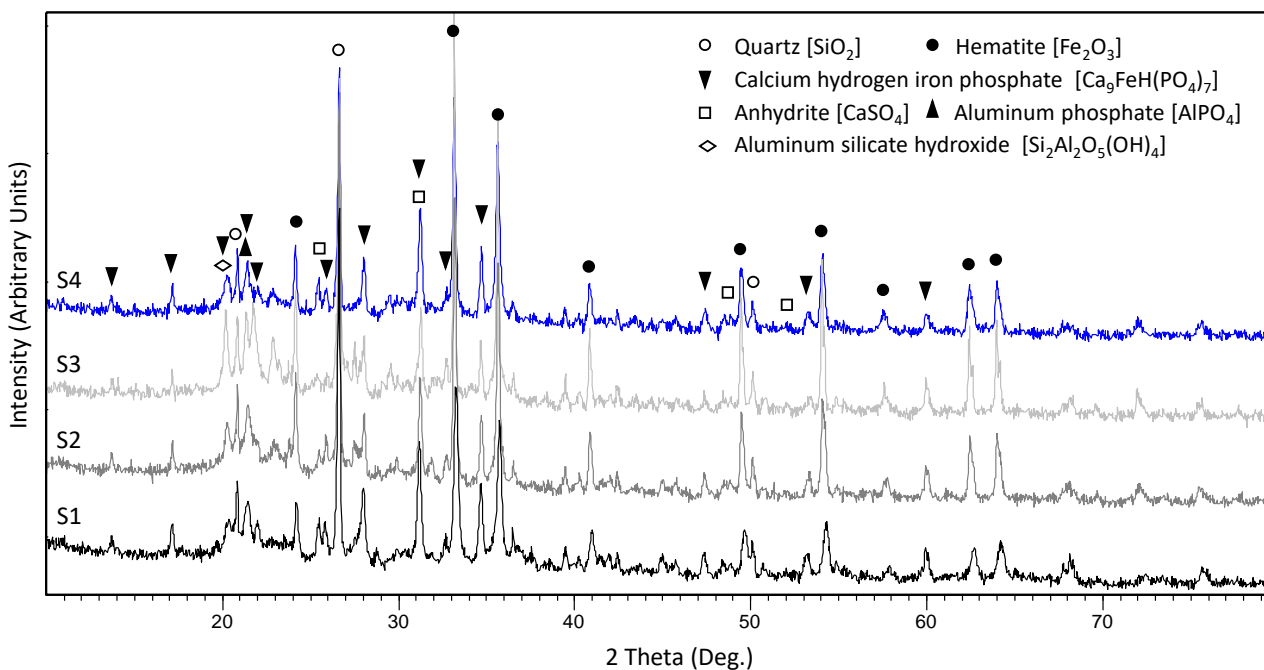

Figure 4.3: XRD patterns obtained for SSA raw samples S1-S4.

To evaluate the chemical composition of the SSA, a semi-quantitative analysis was performed with EDXS during SEM scanning, used for morphology and surface structure investigation. The list of constituent elements is reported below, from the highest to the lowest value, and graphically shown in **Figure 4.4:**

S1: O > Fe > Si > Ca > P > Al > Mg > K > Na > Ti > S,

S2: O > C > Fe > Si > P > Ca > Al > K > Mg > Na > Ti,

S3: O > Fe > Si > P > Ca > Al > C > Mg > K > Ti,

S4: O > Fe > Ca > P > Si > Al > Zn > K > Mg > Ti > S.

In all samples, the presence of oxygen (O) predominates, and iron is the main constituent element, as it appears also from the reddish colouring of SSA and from XRD identification of hematite. Moreover, literature [216,242] shows that for SSA obtained at 900°C (as happened for S1-S4), the main expected crystalline phosphate compound is whitlockite [$Ca_9(MgFe)(PO_4)_6PO_3OH$]. The absence of this compound in the XRD identification, could be explained by the negligible amount of magnesium (Mg) compared to Fe and Al, as highlighted by EDXS results in **Figure 4.4**. The amount of Mg, K, Ti, Na, S and Zn is very low in each SSA, while Al, Si, P and Ca are distributed in the samples in variable proportions. Interestingly in S1, S2 and S3, the amount of Si is considerable (the most abundant after Fe), while in S4 the amount of Ca is higher. Si content ranges between 7.5 % and 10.4 % in the four SSA. The EDXS identification of Fe, Si, P, Ca and Al as primary elements in SSA corroborates the XRD crystalline phases attribution reported in **Figure 4.3**.
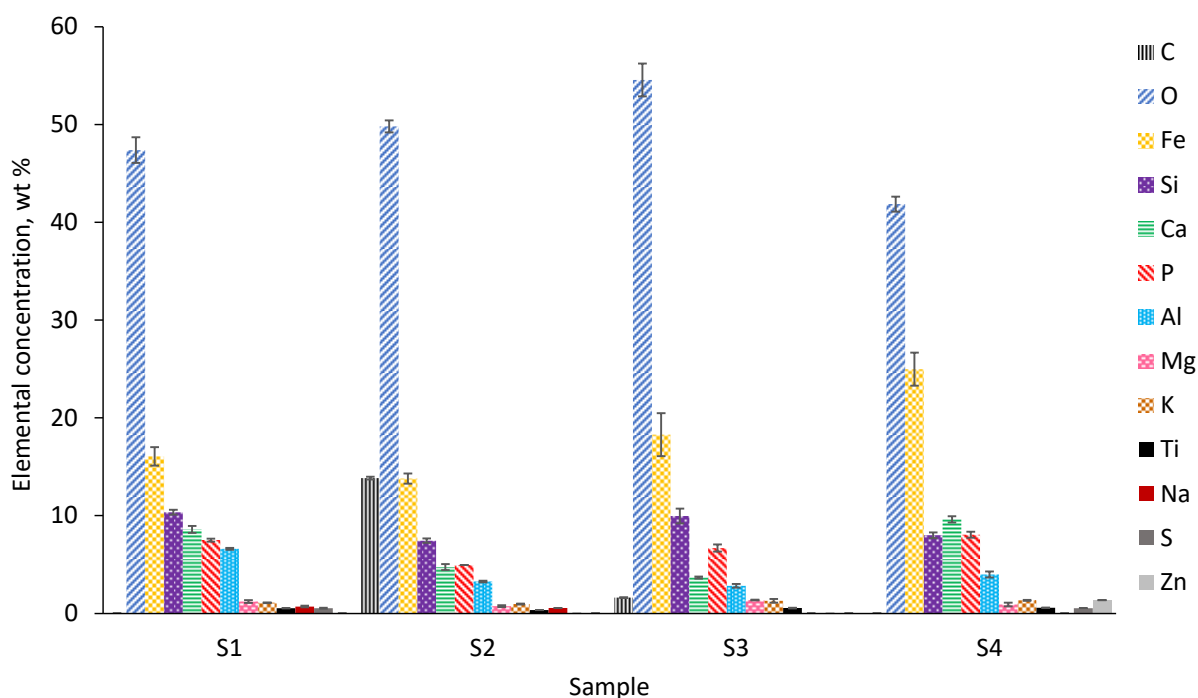

Figure 4.4: *Elemental concentrations in SSA samples (S1-S4) from EDXS analysis.*

The particle morphology of the samples is presented in **Figure 4.5**, where images with same magnification are reported (scale bar 700 μm). In addition, **Figure 4.6** shows SEM images of further magnification: scale bar 100 μm for S1 and S4 and scale bar 30 μm for S2. Irregular shapes and smooth microscales can be noted; the surfaces appear rough but with defined edges. Chemical analyses by EDXS were also made on some spots, reported in **Figure 4.6** with the corresponding spectra: three representative regions for S1 (1A, 2A and 3A), three for S2 (1B, 2B and 3B) and four representative regions for S4 (1C, 2C, 3C and 4C). For sample S1, in the region 1A, Si and Al can be detected, followed by P, while Ca and Fe are minor elements. Similar considerations can be done for the regions 2A and 3A, where though is evident that Ca and Fe signals increase. Also, Mg and Ti can be clearly distinguished in 3A. Regarding sample S2, in point 1B can be recognized a microsphere, consisting primarily of Fe and Ca, with lower quantities of Si and P. Region 2B is mainly composed of Si, while region 3B equally consists of Si and Fe, with high intensity also of P, Al, K and Ca. On the other side, for sample S4, the region 1C exhibit a very high signal of P, although Fe and Ca are present predominantly, followed by Si and Al. In this region, in addition to Mg and K, Zn and Ti can also be recognized. Indeed, presence of Zn in sample S4 can be noted also in **Figure 4.4**. Analogous comments can be made for the region 2C where Fe signal is very intense, followed by P, Ca, Al, Si, Mg, K respectively. The region 3C is an example of different composition, closer to the Italian samples: Ca and Fe signals have relevant intensities, even if Si, Al, and P peaks show higher intensities. K, Mg and Na are present marginally, while gold (Au) detected during analysis, is due to sample preparation. In the end, the region 4C, imitates the elemental distribution of 1C. SEM-EDXS analysis demonstrates that the composition of all the four ashes is chemically similar and confirm the high contribution of P in all samples.
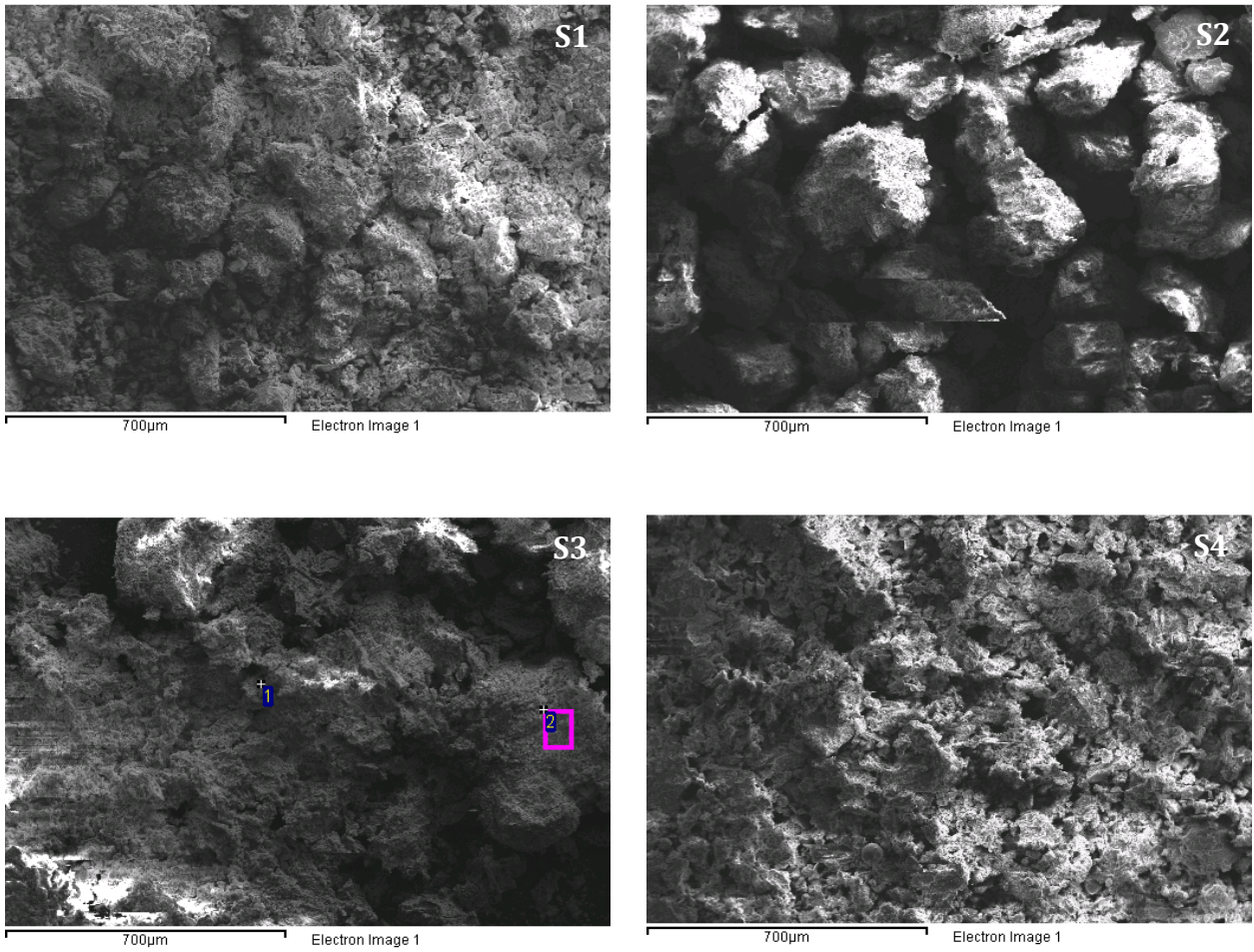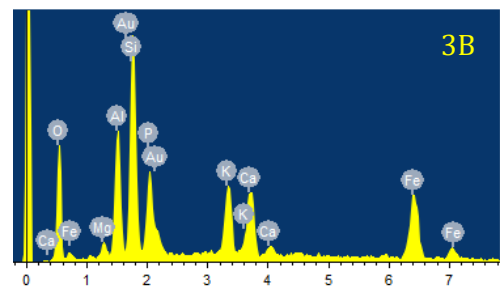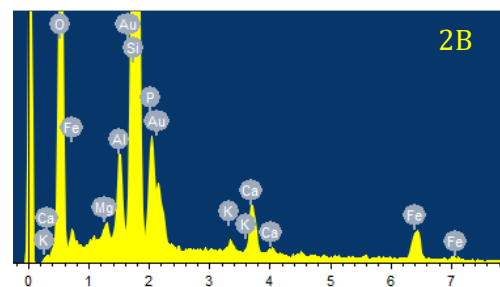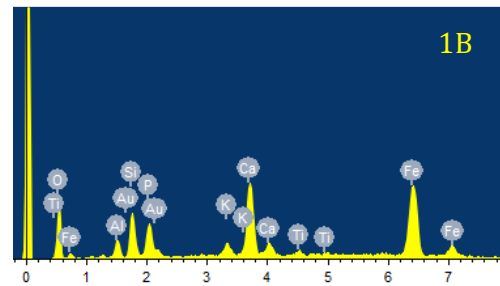
Figure 4.5: SEM images of raw SSA (S1-S4), scale bar 700 μm.
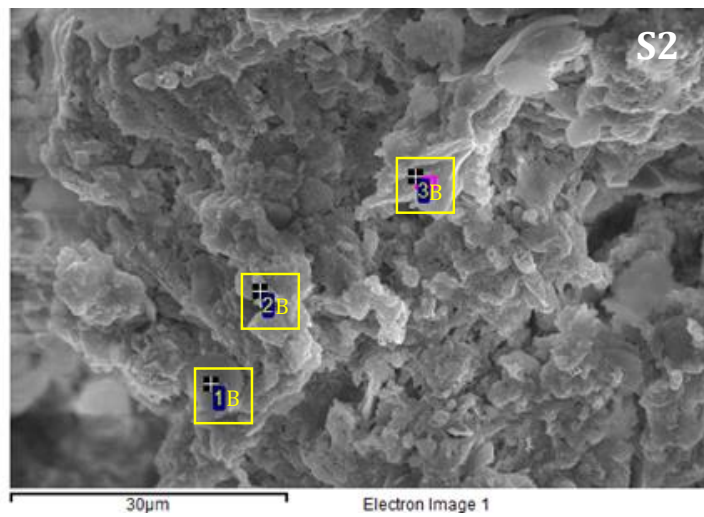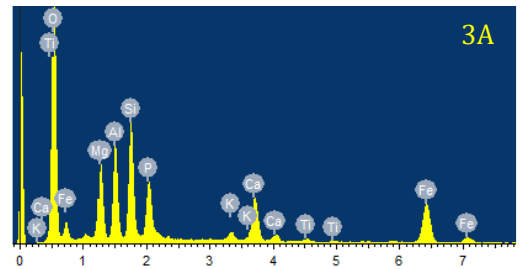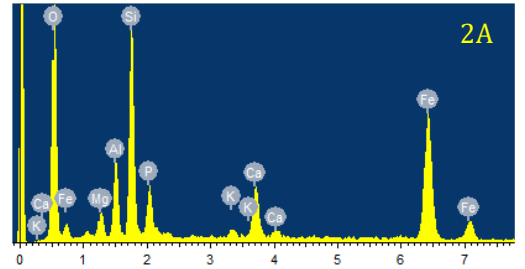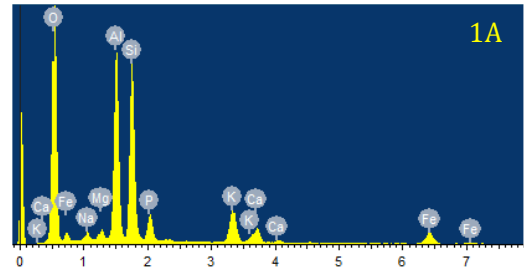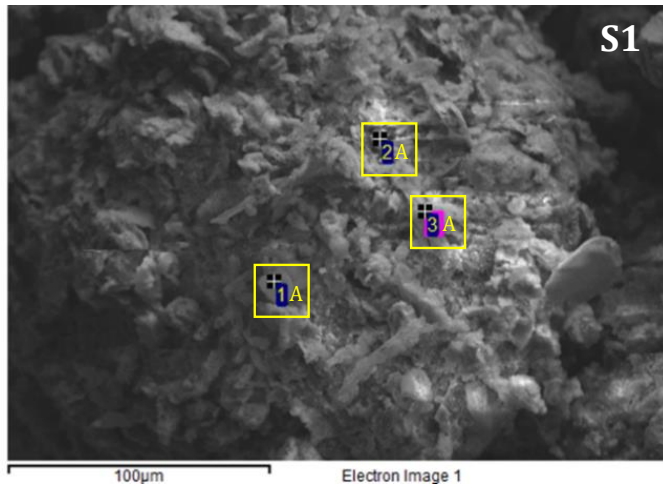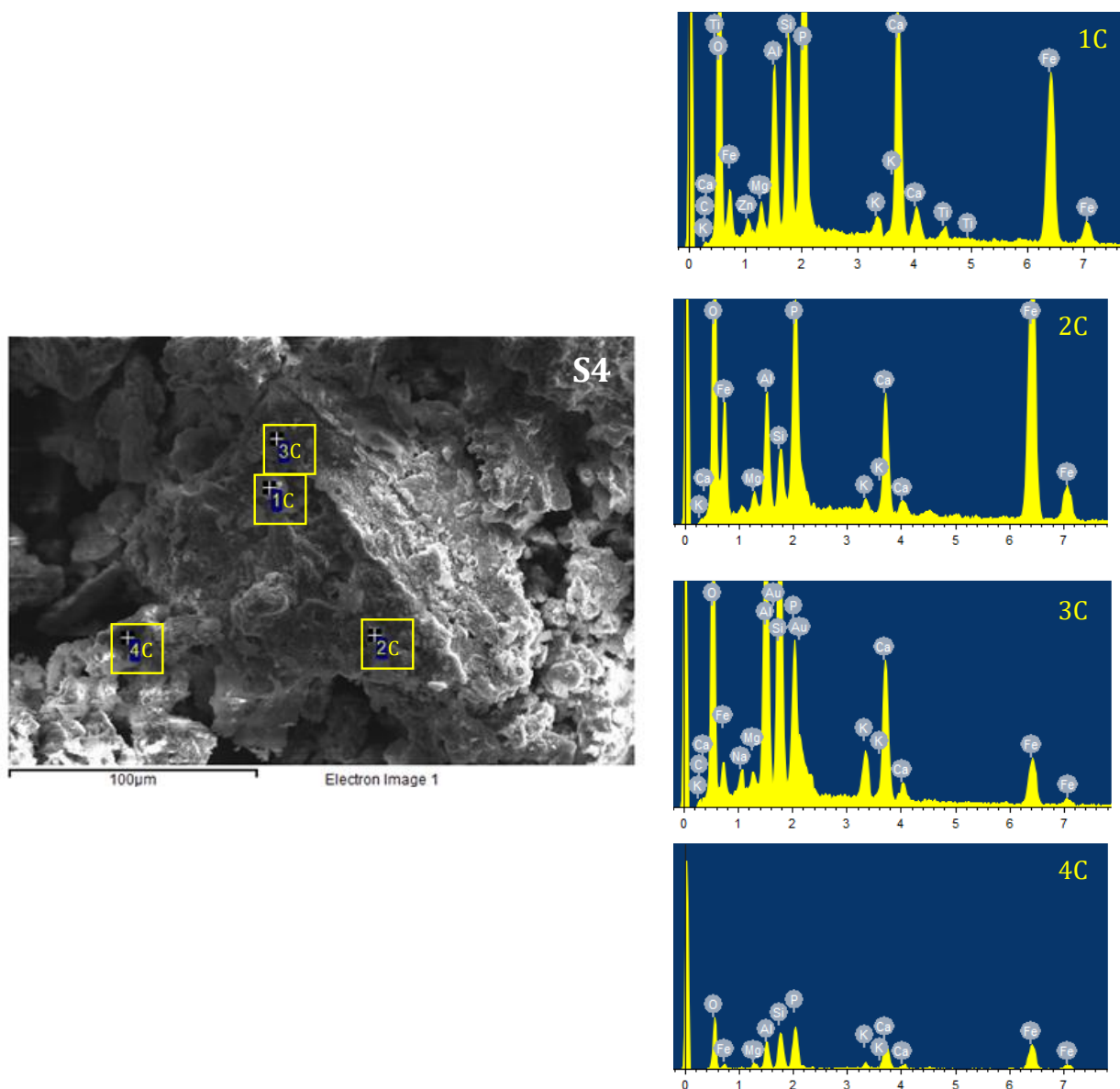
Figure 4.6: *SEM images of raw SSA (S1, S2 and S4), scale bar 100 or 30 μm, and corresponding EDXS spectra: 1A, 2A, 3A for S1; 1B, 2B, 3B for S2;1C, 2C, 3C, 4C for S4.*

4.3.2. SiO$_2$ and P extraction

The preliminary evaluation of the appropriateness of performing the simultaneous P and SiO$_2$ recovery from SSA, was carried out based on the results obtained from S1 processing. The acid treatment with HCl 1 mol/L allowed to obtain an ash residue free of P, as confirmed by EDXS analysis in **Figure 4.7**. Comparing this figure with **Figure 4.4**, it can be noted that Ca and P, main constituents of S1, are completely leached, while Fe, Si and Al remain the primary elements in the ash residue. Their concentration (wt %) is higher in **Figure 4.7** due to the substantial weight loss that occurs during leaching. SiO$_2$ extracted in following steps was also characterized with SEM-EDXS analysis as shown in **Figure 4.8**. **Figure 4.8** reports the chemical composition of the solid: O, Na, Al and Si are detected in the ground product (image on the left), in addition to S in the clump (image on the right). In

comparison with SiO_2 recovered from RHPLA (chemical composition reported in **Table 2.3** in chapter 2), SiO_2 recovered from SSA is more contaminated by Na, S and Al. The presence of Na and S can be justified by the formation of Na_2SO_4 during the gelling of SiO_2 as stated in **Reaction (2.4)** and as confirmed by the XRD analysis of the recovered silica from S1, reported in **Figure 4.9**. **Figure 4.9** shows that the amorphous phase (identified by the broad band between 15 and 35° in 2ϑ) is contaminated by two crystalline forms of Na_2SO_4. Instead, Al could be present as Al_2O_3, the oxide form corresponding to SiO_2, and extracted with Si due to similar behavior that usually brings these two elements to coexisting (e.g., aluminum-silicates in ceramics, refractories, zeolites or aluminates and silicates in concrete-based material). Moreover, Al content in raw SSA is greater than in raw RHPLA, where Al is almost absent (see **Table 2.2**), confirming that the proposed recovery procedure is not selective enough to obtain pure Si from SSA. More studies could be done in this sense, to improve the Si purification or to investigate the potential applications of a SiO_2-Al_2O_3 amorphous gel. SiO_2 extraction efficiency (SEE) for S1 was calculated using **Equation (4.1)** and Si content in the residue ash = 15.40 % from EDXS analysis (**Figure 4.7**). Deriving the total amount of SiO_2 in the residue ash = 32.95 % based on moles of Si and considering the starting mass of residue ash used for silica recovery (17.00 g), 5,60 g resulted as total mass of SiO_2 in the residue ash. The extraction process allowed to obtain 2.56 g of dried SiO_2, therefore a SEE equal to 45.71 % was reached. This type of calculation is approximate, since it assumes that all Si in the residue ash is in the form of SiO_2. In conclusion, even if without a satisfying yield of extraction as much as the common yield obtained for P recovery, it was demonstrated the possibility of extracting SiO_2 from SSA. To enhance the result, a study on the optimization of operating leaching conditions could be made as further research activity. Images of the products resulting from the process are displayed in **Figure 4.10**.
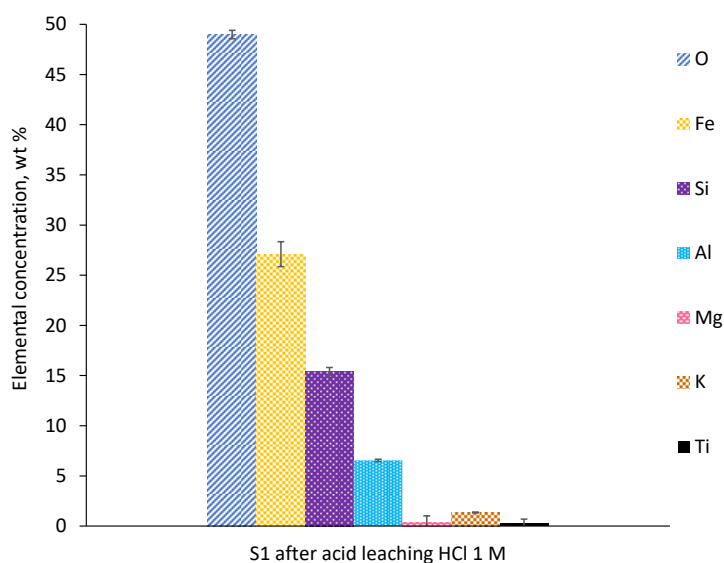
Figure 4.7: *Elemental concentrations in S1 residue after acid leaching from EDXS analysis.*

O	Na	Al	Si
% wt			
58.8	8.7	6.4	26.0

O	Na	Al	Si	S
% wt				
55.9	11.8	5.2	21.4	5.6
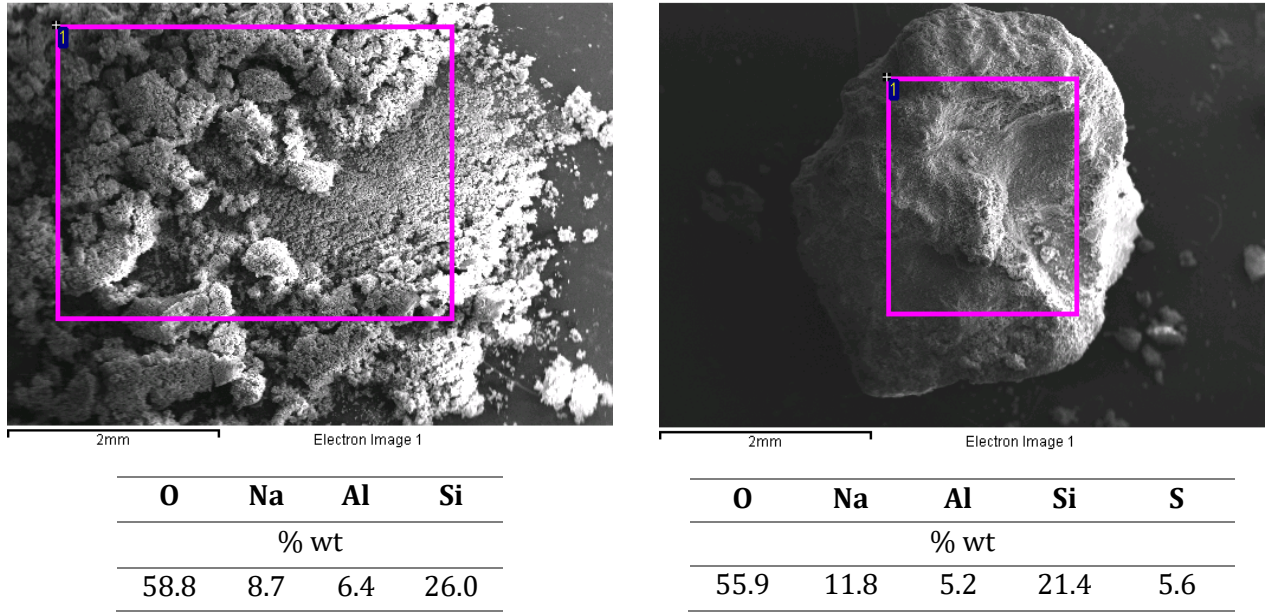
Figure 4.8: SEM images of recovered SiO₂ from S1 (scale bar 2 mm) and corresponding EDXS semi-quantitative analysis in the area marked in purple.
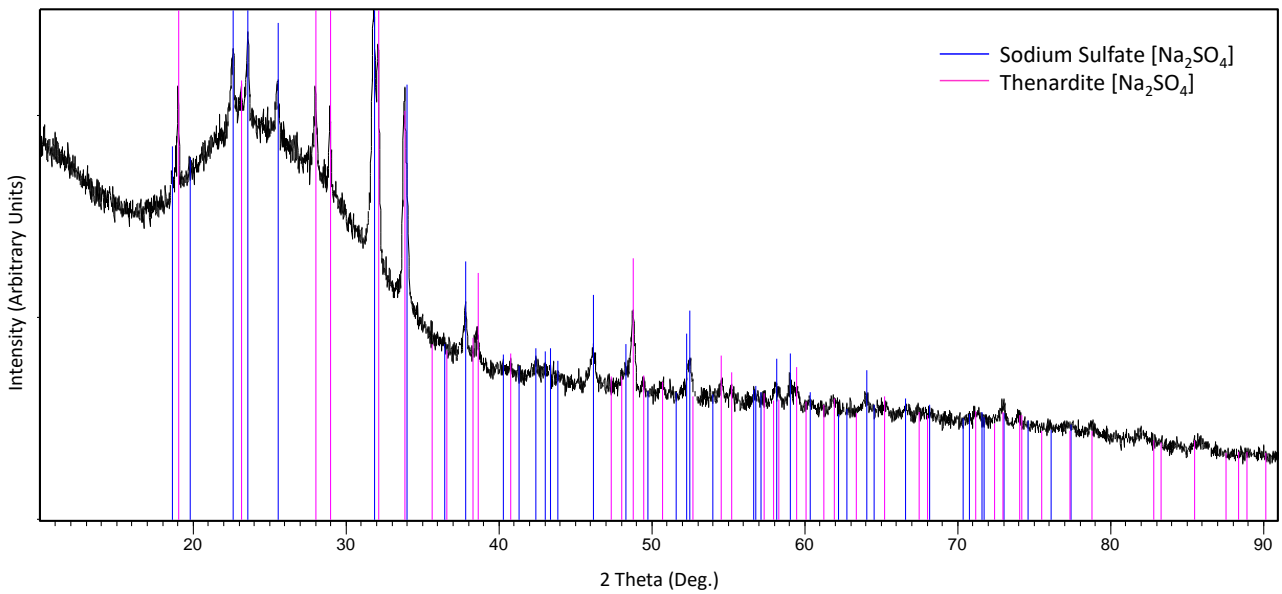
Figure 4.9: XRD patterns of amorphous silica recovered from S1.
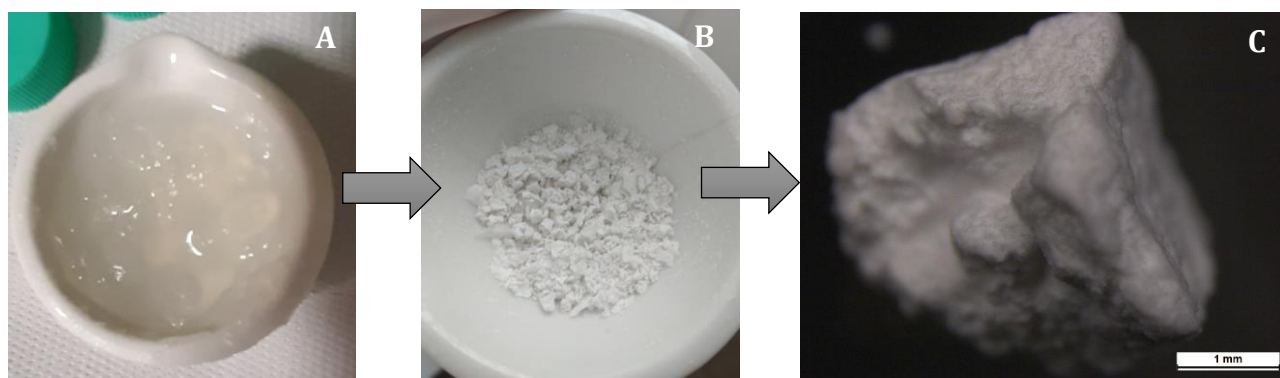
Figure 4.10*: Images of the recovered SiO_2 in form of gel (A), dried powder (B) and observed under the optical microscope (C).*

Regarding SiO_2 extraction from S2, S3 and S4, qualitative analysis (XRD) was performed on the recovered products. **Figure 4.11** shows that the SiO_2 extracted has completely amorphous composition (absence of crystalline peaks) suggesting a minimal contamination of sodium sulfate Na_2SO_4, while it was present in the XRD patterns of SiO_2 recovered from S1 (**Figure 4.9**) and from RHPLA (**Figure 2.4**).
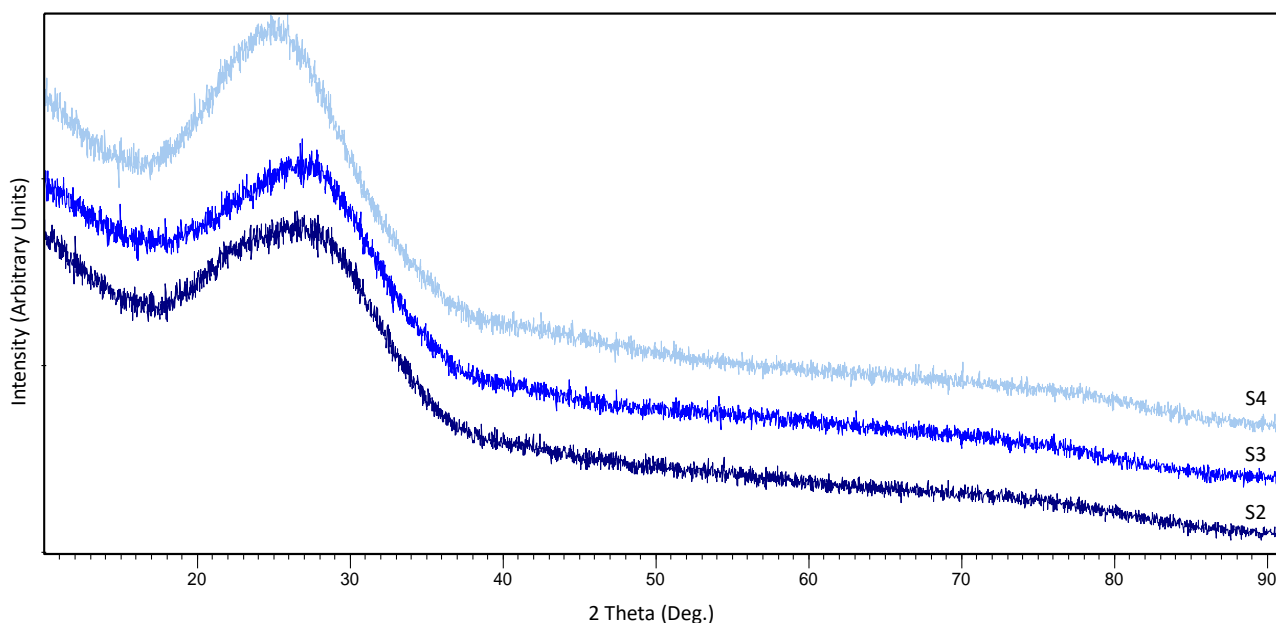
Figure 4.11*: XRD patterns of amorphous silica recovered from S2, S3 and S4.*

Discussing about P extraction through acid leaching, **Figure 4.12** shows the P content analyzed in the sample (orange dots) and the PEE for the four SSA (green bars) calculated according to **Equation (3.1)**. Extraction efficiency was total for S1, where HCl 1 mol/L was used. Indeed, also **Figure 4.7** confirmed that P was no more present in the ash residue after the leaching. Although the high PEE for S1, the switch between HCl and H_2SO_4, acid concentration and L/S ratio for the leaching of the other

samples was experimented in accordance with literature examples and in view of HM control during P recovery. On this stage, only PEE was monitored to focus on the precipitation trials, but aware of the HM co-dissolution issue with a very strong acid (HCl 1 mol/L), a weaker but still effective method was chosen. From **Figure 4.12** can be noted that PEE of S2, S3 and S4 is ascending, while the samples manifest almost the same P content in the matrix (8.3 %, 8.3 % and 8.5 % respectively). A satisfying PEE is reached for S4 at 87.4 %.
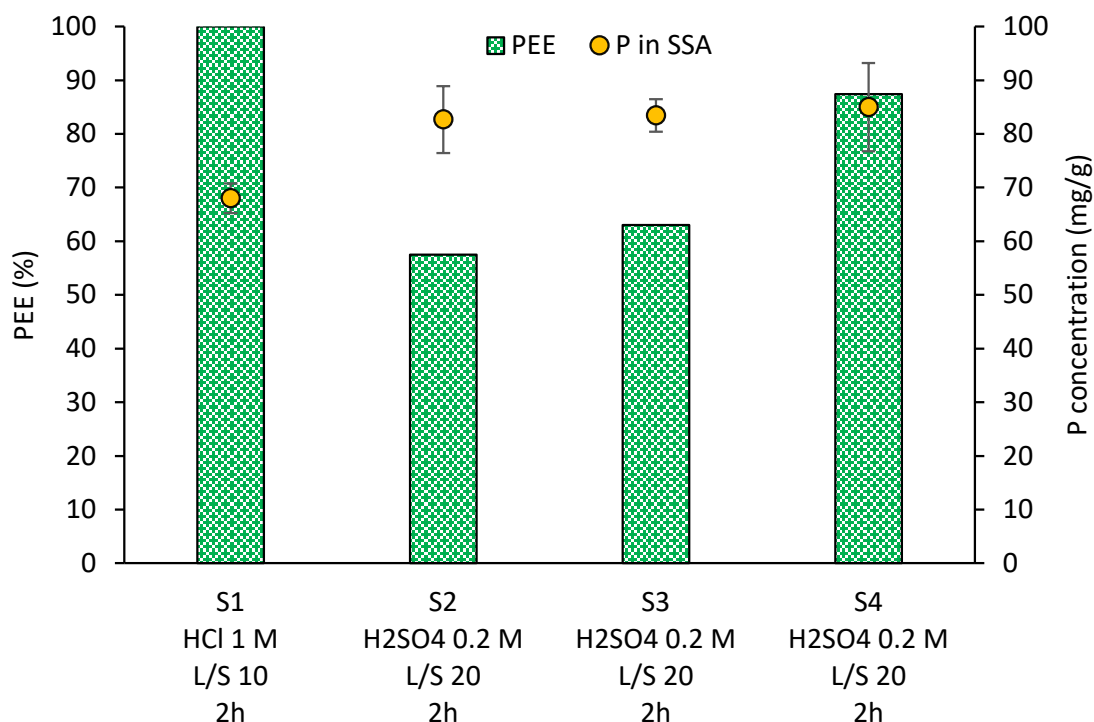
Figure 4.12: P extraction efficiency (PEE) for sample S1-S4 (green bars) in function of operating conditions (type of leaching acid; L:S ratio and contact time) and P content in SSA (orange dots) quantified after sample digestion and TXRF analysis.

4.3.3.   P precipitation and simulation of solubility equilibrium

Figure 4.13 shows the recovered mass (g) of precipitate at different pH starting from 50 mL of acid leaching of each sample. An increasing trend in function of increasing pH is recorded: very little precipitate recovered at acid pH, with 0.4 – 0.7 g between pH 4 and 5, and about 4.0 g at pH 8. It is clear that toward the neutral and basic pH, the equilibrium in solution leads to the precipitation of more species.
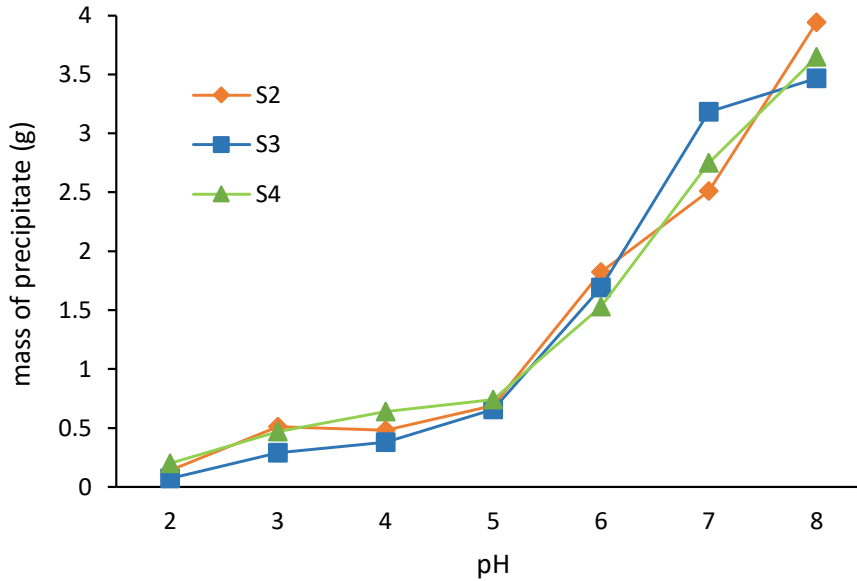
Figure 4.13*: Mass of precipitate recovered at different pH.*

Figure 4.14 shows the P content in each precipitate (squares) obtained from **Equations (4.2) and (4.3)** and the PPE (circles) calculated with **Equation (4.4)**. P content in precipitates decreases in function of pH, with highest values at acid pH, a marked decline from pH 6, and lowest value at pH 8. Although the high P content in precipitates at pH 2, the very small amount of recovered solid at this pH (< 0.2 g according to **Figure 4.13**), does not make these precipitates a viable alternative to commercial fertilizers. In addition, just a maximum PPE of 40% can be achieved, leaving a large amount of dissolved P in solution. On the other side, the PPE increases visibly with increasing pH, showing the maximum efficiency at pH 8. The highest PPE for S2, S3 and S4 is recorded at 94.0%, 94.7% and 97.6% respectively at pH 8, with the maximum P content in the S4 precipitate equal to 5 %. Finally, pH 4 and 5 turned out to be the most suitable values for all the three samples, ensuring a good balance between PPE and P concentration in the precipitates. This consideration was made to favour precipitates with a high P content over a greater amount of recovered mass.
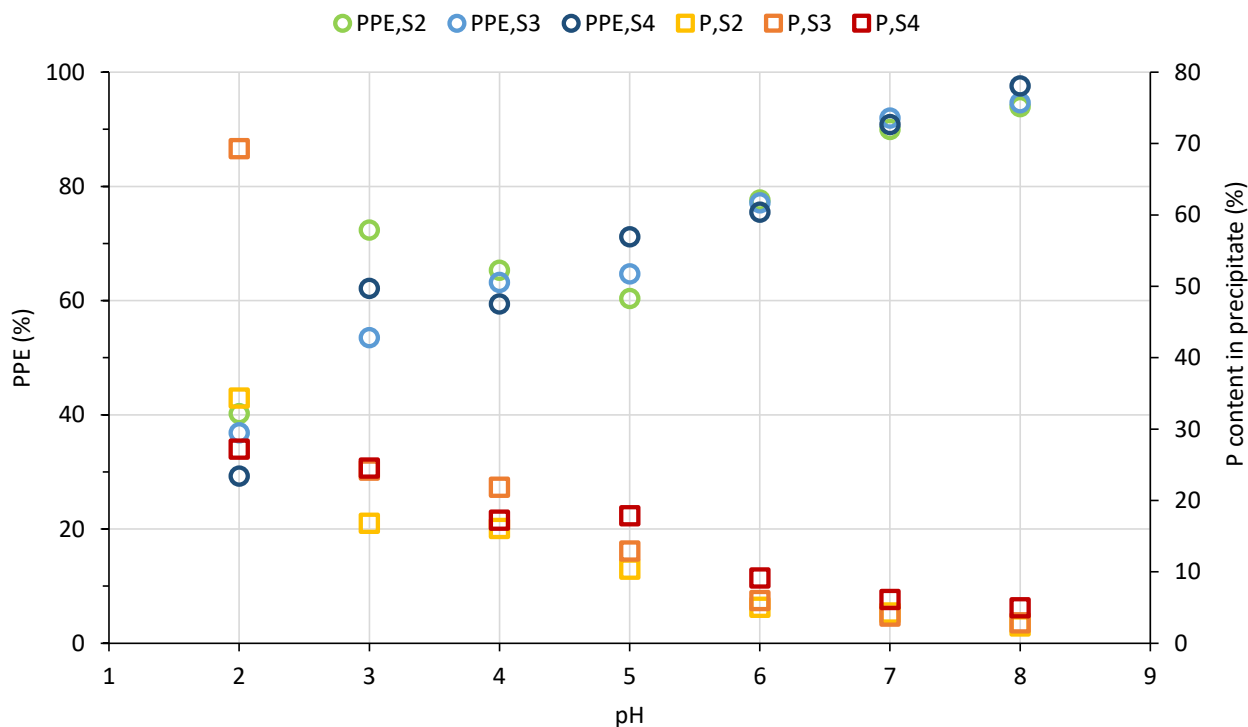
Figure 4.14*: P precipitation efficiency (PPE) (circles) and P content in the precipitates (squares) for each sample at different pH.*

Figure 4.15 shows the comparison between P content and PPE for the three samples at pH 4 (left) and pH 5 (right). The first green bar at the top represents the P content in commercial fertilizer triple super phosphate (TSP), fixed at 19-20% [153]. Precipitates at pH 4 show a P concentration very close to TSP, exceeding it in sample S3. Instead, at pH 5 the P content is slightly below, but the PPE is increased. On the other hand, phases identification after XRD analysis couldn't find any crystalline P compounds in the precipitates at pH 4 and 5. It is important to highlight that equilibrium time during the precipitation and crystallization kinetics during the aging of the solids are two decisive factors: more studies in this direction could be a good tool to better understand the speciation of P in the precipitates.
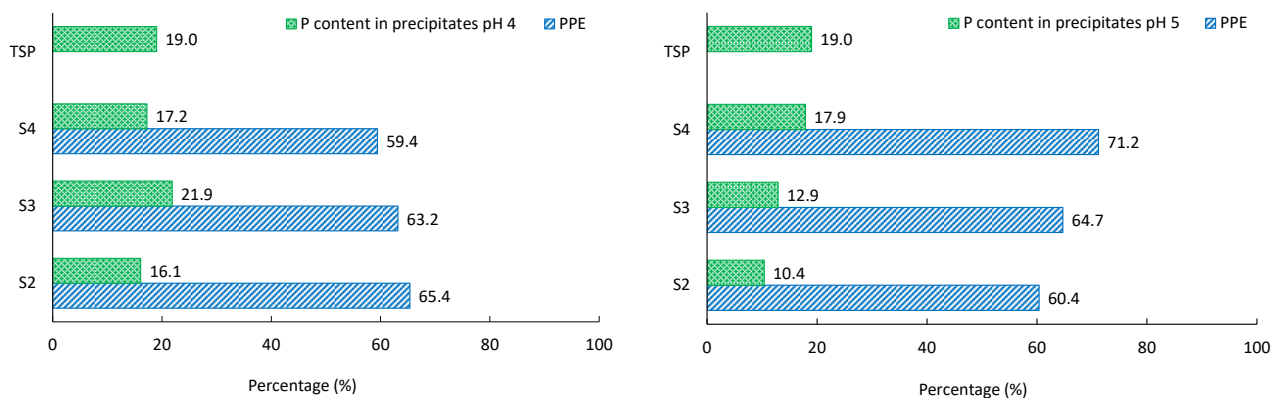
Figure 4.15*: Comparison between P content in precipitates (green bars) and PPE (blue bar) at pH 4 (left) and pH 5 (right), for each sample. TSP = triple super phosphate commercial fertilizer.*

Nevertheless, some considerations on chemical equilibria can be done based on the results coming from the modelling software. Using CHEAQS Pro, another computer program for calculating chemical equilibria in aqueous systems, Kalmykova [232] declared that $Al_3(PO_4)_2(OH)_3(H_2O)_5$ and $Fe(II)_3(PO_4)_2(H_2O)_8$ can be precipitated by maintaining the leachate pH between 3 and 4, while at pH 4, $AlPO_4$ and $Ca_5(PO_4)_3(OH)$ can be obtained. Kalmykova also states that in solution the consumption of hydroxide ions starting from pH 4, implies formation of solid phosphate compounds of Mg and Ca, such as $MgHPO_4$ and $Ca_3(PO_4)_2$. Consequently, the selective formation of the P-precipitates (Al-P, Fe-P or Ca-P) can be achieved by pH control and stoichiometric addition of Al, Fe or Ca to the leachate [69]. **Figure 4.16** shows the possible P-precipitates achievable during the titration of the S2 leachate, calculated by Visual MINTEQ. The trend and the phosphatic compounds identified for S3 and S4 were similar, so just one figure was reported. Considering the specific amount of each element (P, Al, Fe and Ca) at different pH, the simulation confirms that at pH 4 the most probable precipitates are $FePO_4 \cdot 2H_2O$ (Sterngite), $AlPO_4 \cdot 2H_2O$ (Variscite) and $AlPO_4 \cdot 1.5H_2O$, due to SI > 0. At pH 5, several Ca-P precipitates are added, the most likely of which is $Ca_5(PO_4)_3OH$ (Hydroxyapatite), as reported by Kalmykova [232]. SI of Al-P and Fe-P compound then decreases over pH 7, while all the Ca-P precipitates became more and more likely starting from pH 5. The simulation from pH 9 to pH 12 confirms that pH 8, the last point used for experimental titration, is also the last point where all the Al-P, Fe-P and Ca-P compounds are simultaneously precipitable (all SI > 0). Despite this, the total amount of P in the precipitates at pH 8 is lower than the P content in precipitates at pH 4 – 5 (**Figure 4.14**), making these recovered products not so appealing. This point could be explained by the presence of several other precipitated compounds at pH 8, that are not P-phases.
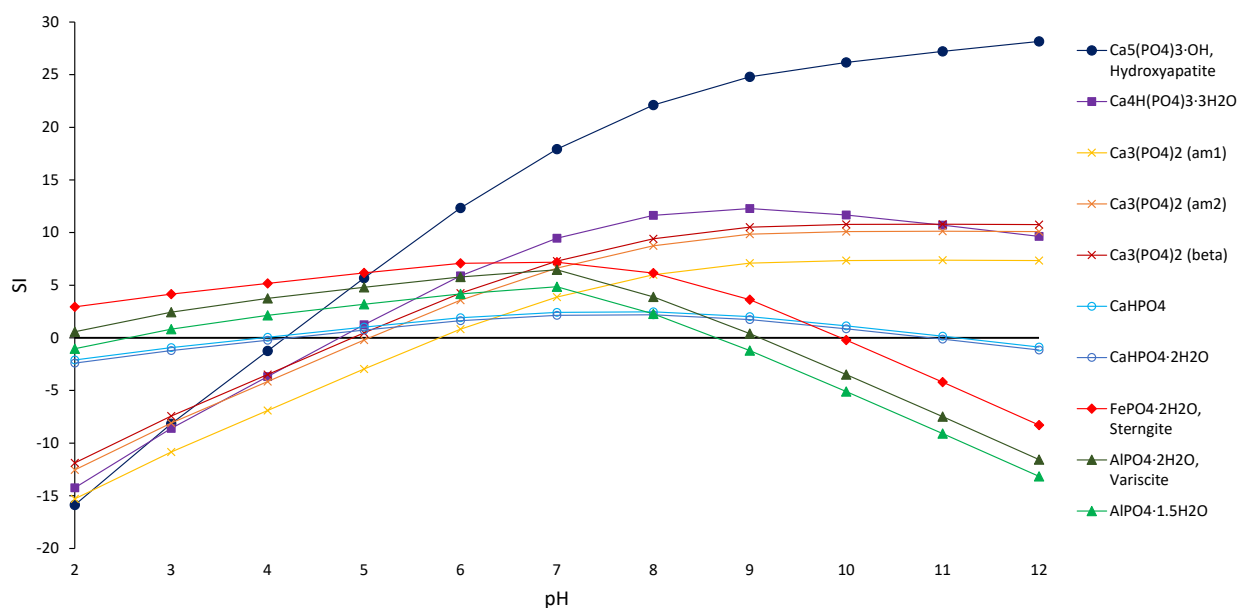
Figure 4.16*: Simulation obtained with Visual MINTEQ of phosphatic compound saturation index (SI) during the titration of S2 leachate.*

Indeed, **Figure 4.17** shows XRD patterns of sample precipitates at pH 8, where only crystalline calcite ($CaCO_3$) is identified. This suggests that CO_2 dissolved in solution, that generates carbonate ion CO_3^{2-} during aqueous dissociation, can participate to the solid formation during the titration with $Ca(OH)_2$. It is also plausible to think that increasing pH over 8 (more alkaline solution) more calcite is formed, affecting the total amount of recovered product and the P content in it. In the simulation model, ion CO_3^{2-} concentration in the starting acid leachate was not considered, because it is not obtainable from TXRF analysis. Further simulation could focus also on the amount of CO_2 dissolved in solution (considering the pressure and the temperature of the system that impact on the gas solubility in water). The ion carbonate CO_3^{2-} concentration can be derived theoretically using Henry's Law for CO_2 solubility in water, or experimentally through the alkalinity test of the solution after the precipitation and filtration of the phosphatic compounds. In this way could also quantified the amount of precipitated calcite at basic pH, allowing to adjust the operating conditions (e.g., pressure, temperature, closed or open system) to achieve the most suitable purpose (high P content in the precipitate).

Figure 4.18 shows the speciation of ion phosphate PO_4^{3-} (left) and ion calcium Ca^{2+} (right) dissolved in solution after the titration of S2 at pH 8, resulting from Visual MINTEQ simulation. More than 50 % of PO_4^{3-} is present as $CaHPO_4$, demonstrating that Al-P and Fe-P compounds are not favourite at this pH. However, more than 45 % of calcium (deriving from the titrant) is present as free ion Ca^{2+}, about 20 % as $CaHPO_4$ and more than 26 % as $CaSO_4$. This suggests that, even if any crystalline phase of $CaSO_4$ was identified in precipitates at pH 8 (**Figure 4.17**), this compound can be present in the solid, increasing the total mass recovered. In fact, both anhydrite ($CaSO_4$) and gypsum ($CaSO_4 \cdot 2H_2O$) have SI > 0 at pH 8, according to Visual MINTEQ prediction, and these precipitates can be easily generated by the neutralization reaction between sulfuric acid (H_2SO_4) used for the SSA leaching and calcium hydroxide ($Ca(OH)_2$) used for titration.
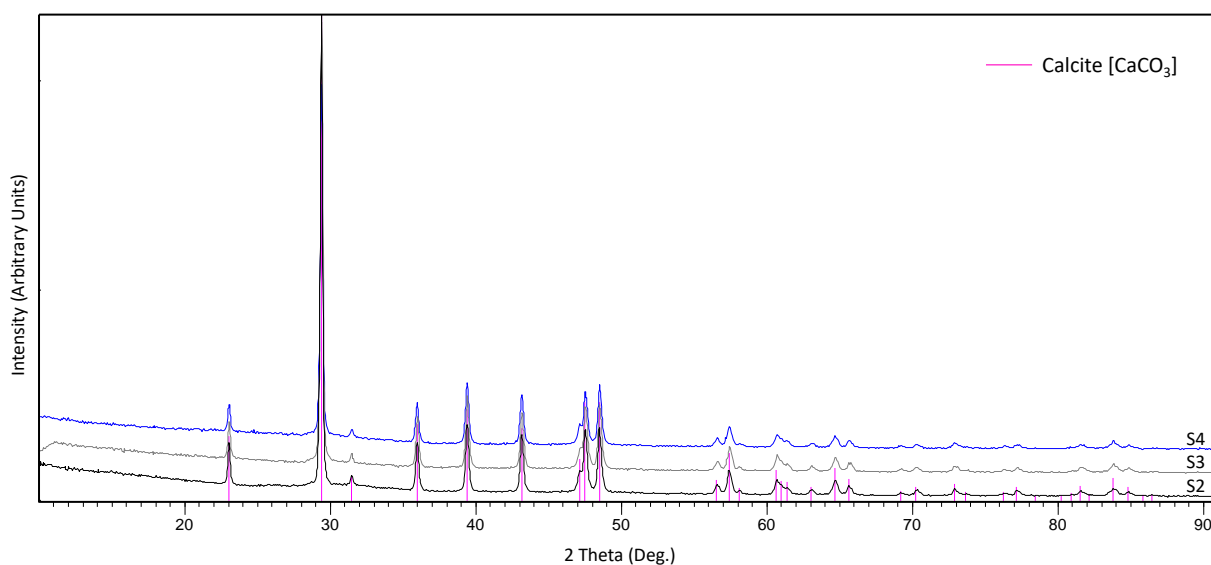
Figure 4.17: *XRD patterns of precipitates recovered from S2, S3 and S4 at pH 8.*

PO_4^{3-} speciation (%)

Ca^{2+} speciation (%)

- HPO4 2- ■ CaHPO4 (aq) ■ CaPO4- ■ Others

- Ca 2+ ■ CaSO4 (aq) ■ CaHPO4 (aq) ■ CaPO4- and CaH2PO4+

Figure 4.18: Percentage of total concentration of ion phosphate (left) and ion calcium (right), intended as dissolved species, resulting from Visual MINTEQ simulation for S2 titration at pH 8.

4.4.   Conclusions

The research conducted in this chapter started from the physical-chemical characterization of four SSA samples (S1-S4), as preliminary and necessary action to the most thorough study of simultaneous P and SiO_2 recovery. XRD, SEM-EDXS and TXRF analysis after solid digestion were performed on the raw samples. Quartz [Si_2O], hematite [Fe_2O_3], calcium hydrogen iron phosphate [$Ca_9FeH(PO_4)_7$] and anhydrite [$CaSO_4$] were identified as main phases in the samples, that have similar crystalline composition. Aluminum phosphate [$AlPO_4$] and aluminum silicate hydroxide [$Si_2Al_2O_5(OH)_4$] were also detected as minor compounds. Silicon content recognized by EDXS ranges between 7.5 % and 10.4 % for the four samples, while P concentration in the matrix after digestion and TXRF analysis was recorded from 6.8 % to 8.5 %. P wet-chemical extraction was completed with HCl 1 mol/L and L/S ratio of 10 on S1, and with H_2SO_4 0.2 mol/L and L/S ratio equal to 20 on S2, S3 and S4. The PEE equaled 100% in the first case and reached the best result of 87.4 % for S4 in the second case. The subsequent valorization of the residue ash after P recovery was made through the SiO_2 extraction as alternative to the common destination of SSA in construction materials. For S1 a SEE of 45.7% was reached, confirming the feasibility of the procedure for SSA with a first encouraging result, considering the absolute novelty of the treatment. The amorphous gel extracted from S1 turned out to be partially composed also by Al and contaminated by crystalline sodium sulfate Na_2SO_4, while SiO_2 recovered from S2, S3 and S4 presented a total amorphous structure under XRD analysis, without contamination of crystalline Na_2SO_4. This second result demonstrates that is possible to obtain a SiO_2 gel from SSA purer than that recovered from RHPLA. In any case, more improvements could be done to the procedure, to minimize Al content in the final product or to investigate the selective recovery of a SiO_2-Al_2O_3 amorphous gel.

In the end, a further research stage was conducted about the precipitation trials of phosphatic compounds from solution. An alkali titration of the acid leachates was carried out on samples S2, S3 and S4, achieving different pH values and investigating the solubility equilibrium through the Visual MINTEQ simulation software. Studying th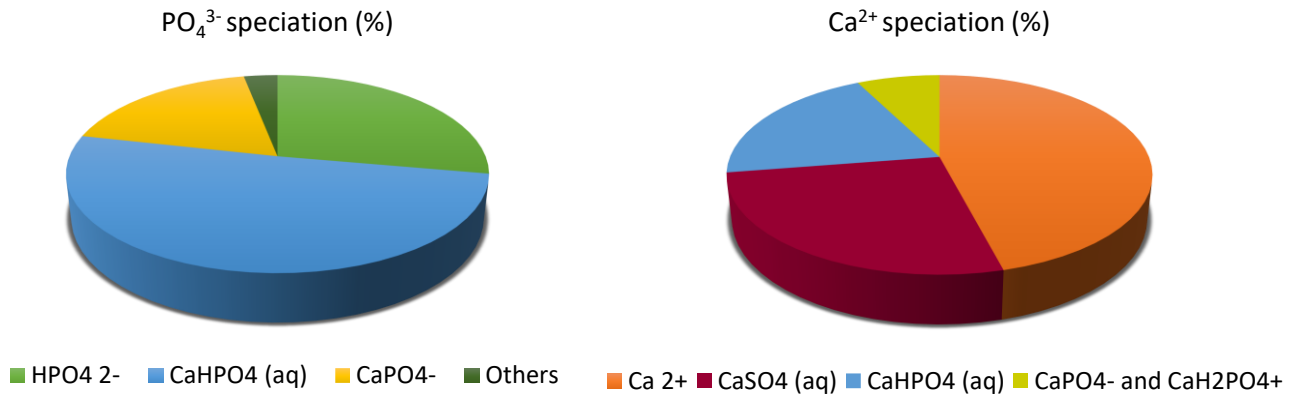e PPE and the final P concentration in the precipitates, acid pH resulted not so appealing due to low amount of recovered product, while basic pH appeared problematic due to co-precipitation of other solid phases different from P compounds. In conclusion, pH 4 and 5 proved to be the best conditions for a good balance between PPE and P content in precipitates. Simulation confirmed what already reported in literature: Al-P and Fe-P compounds are precipitable at acid pH, while Ca-P compounds are more likely starting from pH 7.

5.   P RECOVERY BY WET CHEMICAL EXTRACTION FROM DIFFERENT THERMAL CONVERTED WASTE STREAMS

Abstract

This chapter is devoted to alternative roads for biomass waste management thanks to thermal conversion and subsequent P recovery. Two different studies about P recovery through wet chemical extraction and precipitation were performed on various thermal converted waste streams: Italian sewage sludge (SS), Portuguese poultry litter (PL), and Turkish chicken manure (CM) and sewage sludge (SS).

In the first part of the work two SSA from an Italian pilot plant, bottom ash (BA) and cyclone fly ash (CYC) very rich in Pb and Zn, were investigated. The relevant amount of P in the samples (circa 8% for BA and 10% for CYC) suggested researching a new way to handle the waste, rather than dispose of it. The reuse of other waste to stabilize pollutants, was the choice: BA and CYC were mixed with coal fly ash (CFA) and silica fume (SF), together with flue gas desulfurization ash (FGD) and poultry litter ash (PLA), a type of ash rich in P and poor in HM. After the stabilization, acid leaching was performed on the samples, followed by precipitation trials of P at different pH values, monitoring the co-precipitation of HM. This was a first attempt of repurpose a highly contaminated waste, unsuitable for direct P wet chemical recovery.

In the second part of the work different types of thermal treatments were performed on the original feedstocks, Turkish chicken manure (CM) and sewage sludge (SS), followed by the material characterization, wet-chemical extraction, and precipitation of P-rich products from the leachates. The thermal treatments carried out consisted of incineration (INC), pyrolysis (PYR) and hydrothermal carbonization (HTC). The novelty of the study consists in directing the wet chemical P recovery on two biomasses, thermo-converted with multiple techniques, and investigating the different P extraction efficiencies. The final precipitates were also characterized to estimate the P content for a possible reuse as fertilizers.

Keywords

Biomass waste streams: sewage sludge, chicken manure, poultry litter

Thermal conversion: hydrothermal carbonization, pyrolysis, incineration

P wet chemical extraction and precipitation

Heavy metals stabilization

Scientific contribution

The samples analyzed in this chapter were collected thanks to the collaboration with Politecnico di Milano in the frame of the PerFORM WATER 2030 project, and with EGE University (TR) from the consortium of DEASPHOR project as mentioned in section 1.5.1**.** The content reported in this chapter is

the result of my own work, including literature review, data curation, formal analysis, investigation, methodology, visualization, and writing. Any work made by others is attributed to the original author in the text. Some results presented here are also based on the following publication, whose form have been adapted for reasons of consistency with the structure of this doctoral thesis.

o   Boniardi G., Turolla A., **Fiameni L.**, Gelmi E., Bontempi E., Canziani R., Phosphorus recovery from a pilot-scale grate furnace: influencing factors beyond wet chemical leaching conditions. *Water Science & Technology* (2022), **85** (9), 2525–2538. https://doi.org/10.2166/wst.2022.132

5.1. Introduction

5.1.1. P-rich biomass ash storage as heavy metals stabilization

Since no updated and working plants for P recovery from ashes are active in Europe [244], the current fate of biomass ash is limited by the high HM content. Two paths are today possible: ash disposal and ash storage. The limitations of the first choice are that (i) the waste must respect legal limits about the leaching tests in water that simulates rain runoff in landfill (Italian DM 27 09 2010 for leaching test) and that (ii) mixing P-rich ashes with other waste prevents P recovery. On the other side, ash storage can be a transition period for the development of industrial-scale P recovery processes, that guarantee specific deposits for ashes and specific regulations. Considering ash storage the best practice in order not to lose the P present in the ash, during that period also solidification/stabilization (S/S) of HM in the biomass P-rich ash can take place, exploiting other waste. As explained in section 4.1., this process is typical of the building materials since pozzolanic reactions, which trap HM, occur. Toxic elements can be immobilized and settled in the cement hydration products (i.e., insoluble calcium silicate hydrate, AFt-(ettringite), and AFm-(monosulfate), while the alkaline system for the solidified body can prevent the infiltration of other contaminants [220,245]. Moreover, S/S can include carbonation reactions thanks to the presence of alkaline compounds that produce carbonates after environmental CO_2 entrapment. Starting from this point, biomass ash is mixed with other waste or by-products, that are source of hydroxides of alkali metals and silica, promoting reuse of industrial by-products and CO_2 sequestration [223]. About this, in 2020 the research group C4T Lab filed an Italian patent for the stabilization of co-incinerated SSA, using recovered raw materials without commercial reagents (patent IT201900006651A1).

In the first part of this chapter, a collaboration with Politecnico di Milano to stabilize two SSA highly contaminated with HM is presented. The intent, after the mixing of SSA with other by-product ashes to enhance carbonation and pozzolanic reaction, was to try the P recovery from the stabilized waste. Wet chemical extraction followed by precipitation was performed on the stabilized samples and variations in P and HM leachability was calculated and normalized to the raw ash mass to assess the suitability of the proposed method.

5.1.2. Alternative thermal treatments for biomass waste

The biomass WtE experience has become a relevant field of study in recent years. As mentioned in section 1.2.2., incineration is not the only way to treat biomass.

In recent years slow pyrolysis have been developed for converting various types of biomass to energy, while preserving and concentrating non-volatile nutrient elements [246]. Particularly from manure pyrolysis, the resulting char is used as slow-release fertilizer that contain bioavailable P [247–250]. When applied in soil, the solubility of P in recycled P fertilizers, especially those produced by thermal treatments, depends also on soil properties and soil pH [32,251,252]. Therefore, further research is

needed to clarify the P fertilizer value of pyrolyzed biomass as well. Moreover, pyrolysis has been proven a promising approach to effectively convert most of organic matter to bio-energy fuels (e.g., gases and bio-oils) and high-quality biochar. The biochar has been gathering increased attention for use in soil fertility enhancement, soil remediation, and pollution removal from aqueous solutions as a cost-effective sorbent [253,254]. The relative fractions of P in solid, liquid, and gas phases are related to P speciation and treatment conditions (primarily temperature). For instance, when SS is pyrolyzed at low heating temperatures with slow heating rate (250–600 °C), the phosphate mass predominantly remains in the solid products, and P recovery in the solid phase is close to 100% [255–257].

On the other side, hydrothermal carbonization (HTC), also referred as wet torrefaction, is the most common technique for thermochemical conversion of biomass waste in water at temperatures between 180 and 260 °C, from 5 min to several hours at pressures above 1 MPa [258]. The carbonaceous product deriving from the process is called hydrochar, that is generated together with a large amount of liquid phase (process water) and little gas (mainly CO_2) [259]. HTC was employed on animal manures, including PL, for P recovery [260–262]. Sun et al. also produced hydrochar from PL and identified it as a good soil amendment and an effective sorbent for potentially hazardous organic compounds [263]. Moreover, HTC treatment can be proposed to release phosphate from SS, based on the presence of P-binding metals (Fe and Ca) [264].

Regarding the incineration process, in literature, recovery of P is widely studied for SS, especially starting from the ash, with even industrial processes both for thermal (e.g. AshDec-Outotec, Kubota) [45,126] and for wet chemical approaches (e.g. EcoPhos, Leachphos) [265].

In the second part of this chapter, P recovery by wet chemical extraction of ash, pyrochar and hydrochar obtained from CM and SS was investigated. How much P extraction efficiency can be achieved by means of acid leaching on the products? How much P can be precipitated from the different thermal converted product?

5.2. Materials and methods

5.2.1. Solidification/stabilization of HM in SSA

Sampling and characterization

For this research samples and raw samples analysis were kindly provided by the Department of Civil and Environmental Engineering (DICA) of Politecnico di Milano, as part of PerFORM WATER 2030 project. SS from municipal wastewater was dried, pelletized and incinerated at 850 °C in a pilot-scale grate furnace located close to Milan (San Giuliano Milanese, Italy) and engineered by VOMM Impianti e Processi SpA (Rozzano, Lombardy, Italy). With this specific technology, differently from the fluidized bed combustion system previously studied, 90% of the ash is accumulated at the end of the grid as bottom ash (BA), while fly ash is subsequently captured at the exit of cyclone system (CYC). In this work, the third campaign of sampling from April 2021 was studied. Campaign lasted about 10 days, in which ashes were sampled three times a day (at the beginning, at the middle and at the end of the operation), and investigated samples, BA and CYC, come from the mean samples. BA was ground by a manual mortar before investigation [266]. Both SSA were very rich in P, but also contaminated of HM, especially CYC, as confirmed by the chemical composition of the ash reported in **Table 5.1** and performed by Politecnico di Milano. The promising and good P concentration in CYC (> 10 %) is affected by the high concentration of Pb (> 0.6 %) and Zn (almost 1.5 %).

Table 5.1: SSA composition provided by Politecnico di Milano. Total P content was evaluated using Hach Lange LCK 348 analytical kits and spectrophotometric analysis, after acid mineralization according to EN 15956 (CEN 2011), while other elements were determined by ICP-MS (Agilent, 7700 Series) analysis, according to UNI EN ISO 17294-1 (2007).

Element	Unit	BA			CYC		
P		8.97	±	1.27	10.40	±	1.50
Fe		2.02	±	0.30	1.71	±	0.20
Al		8.30	±	1.17	9.36	±	1.30
Ca	%	7.49	±	1.07	8.83	±	1.20
K		0.52	±	0.07	0.54	±	0.08
Mg		1.26	±	0.20	1.28	±	0.20
Na		0.36	±	0.06	0.29	±	0.04
As		38.2	±	5.4	228	±	32
Cd		0.19	±	0.03	139	±	20
Co		12.8	±	1.8	12.1	±	1.7
Cr		218	±	31	423	±	60
Cu		1279	±	181	1185	±	168
Hg	mg/Kg	0.55	±	0.08	0.57	±	0.08
Ni		469	±	66	586	±	83
Pb		84.6	±	12.0	6318	±	894
Sb		7.2	±	1.0	9.3	±	1.3
Tl		0.20	±	0.03	0.56	±	0.08
V		53.1	±	7.5	45.5	±	6.4
Zn		1631	±	231	14792	±	2092

The two ashes were also characterized with XRD e SEM-EDXS techniques, as described in the previous chapters. **Figure 5.1** shows images from SEM scanning and semi-quantitative elemental composition detected by EDXS. The Zn content in CYC is so high that it is also clearly detected by EDXS as reported in the chart.
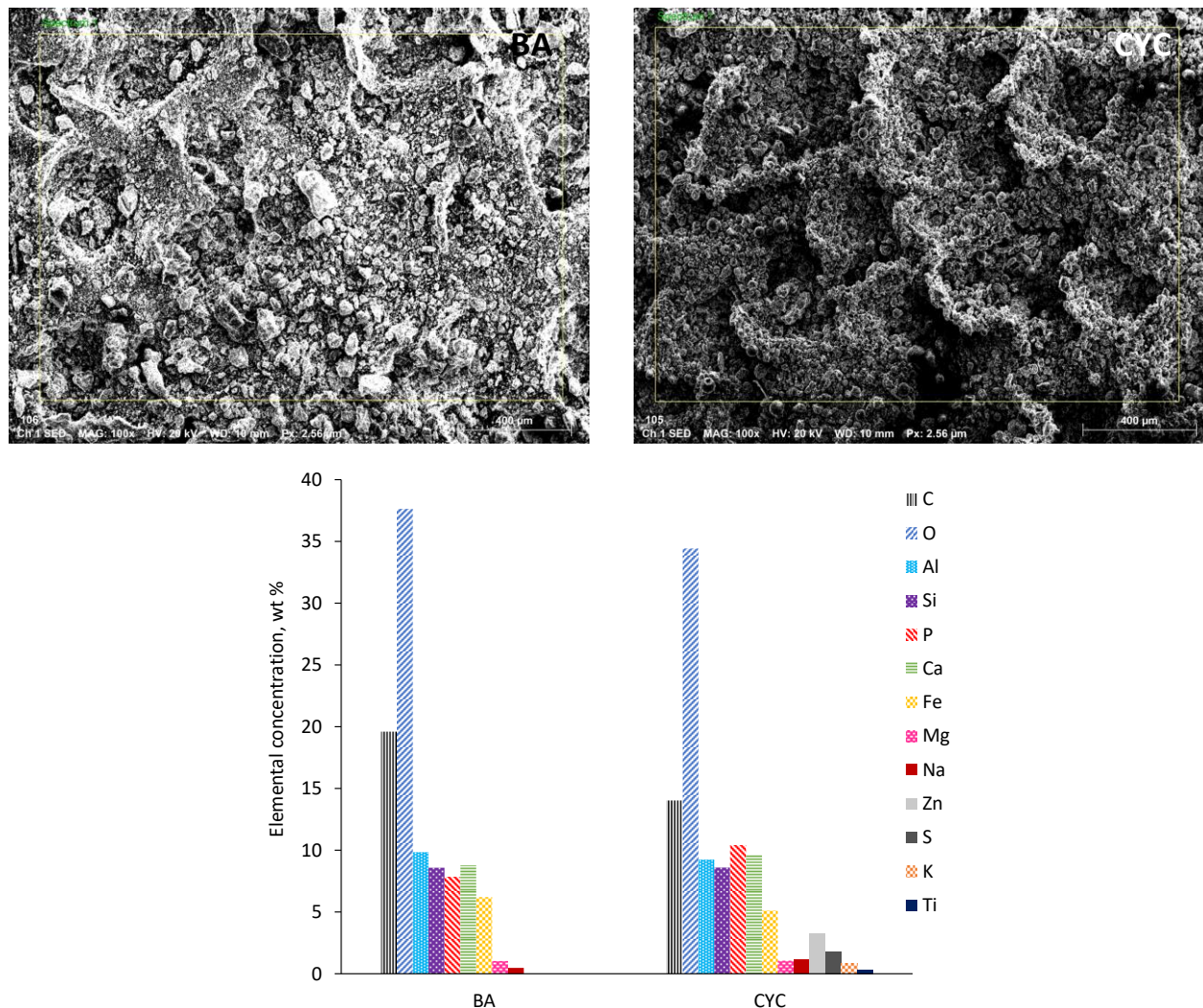
Figure 5.1: SEM images of BA (left) and CYC (right), scale bar 400 μm, and EDXS chemical composition (below).

Table 5.2 reports crystalline phase identification assigned after XRD analysis. A similar crystalline composition was distinguished for BA and CYC: quartz [SiO_2] was detected as main phase, with a little part of tridymite (polymorphic form of [SiO_2]) in CYC, followed by a phosphate phase, namely calcium hydrogen iron phosphate [$Ca_9FeH(PO_4)_7$] in BA and whitlockite [$Ca_8FeOH(PO_4)_6 \cdot 10H_2O$] in CYC. Iron oxide or hematite [Fe_2O_3] was identified in both samples, and small peaks revealed the presence of anhydrite [$CaSO_4$] in CYC. Similar results were reported by Gorazda et al. (2017) [267]: P in SSA was present as calcium phosphate, iron as hematite, and aluminum as anorthite. Quartz and tridymite were also identified. In line with literature and presented experimental results, Abis et al. (2018) [268] indicated quartz, hematite and whitlockite as the main crystallized minerals in SSA.

Table 5.2*: Crystalline phase identification from XRD analysis.*

Crystalline phase	BA	CYC
Quartz [SiO_2]	X	X
Tridymite [SiO_2]		X
Calcium hydrogen iron phosphate [$Ca_9FeH(PO_4)_7$]	X	
Whitlockite [$Ca_8FeOH(PO_4)_6 \cdot 10H_2O$]		X
Iron oxide/Hematite [Fe_2O_3]	X	X
Anhydrite [$CaSO_4$]		X

HM stabilization and P recovery

As anticipated in the introduction, the SSA samples were mixed with other waste, source of hydroxides of alkali metals and silica, to promote reuse of industrial by-products, CO_2 sequestration, HM stabilization and enhancement of P recovery via wet chemical extraction. The selected materials for stabilization, and corresponding quantities were:

- SSA (BA and CYC) from mono incineration pilot plant in Milan (Italy) – 100 g
- coal fly ash (CFA) from a coal thermal power plant in Brescia (Italy) – 24 g
- silica fume (SF) from metallurgical company in Brescia (Italy) – 15 g
- flue gas desulfurization ash (FGD) from coal thermal power plant in Brescia (Italy) or poultry litter ash (PLA), namely ECO sample (SINK from fraction > 500 μm) studied in chapter 3, from Portuguese mono-incineration plant – 30 g

Procedure was suggested by the research of Fahimi et al. (2020) [75]: the mix of dry powders was created, then around 170 mL of MilliQ water was added, it was mixed for other 20 minutes, and in the end, it was aged in laboratory in the open air for three months at room temperature. **Table 5.3** reports the scheme of recipes preparation: recipes n.1 and n.2 refer to CYC, while recipes n.3 and n.4 refer to BA. PLA was present in recipes n.1 and n.3, while FGD was substituted in recipes n.2 and n.4, This exchange was made to evaluate the simultaneous PLA ability of HM stabilization and P recovery promotion (adding more P to the matrix). For each recipe (1, 2, 3 or 4) two different treatments were used for the aging: all the time at room temperature (letter A after the recipe number) or in oven at 120°C for the first 4 hours (letter F after the recipe number). The process effectiveness was proved with leaching test CEN EN 12457-2:2004 in MilliQ water according to Bontempi et al. (2010) [123] after one month of stabilization (acronym 1M after the recipe number means first month), two months (2M) or three months (3M). After solubility tests, Politecnico di Milano kindly analysed P content in water using Hach Lange LCK 348 analytical kits and spectrophotometric technique, and ICP-MS (Agilent, 7700 Series) analysis for HM determination. Based on the results of HM leachability in water, the best recipes were chosen and acid leaching on the stabilized samples followed by precipitation trials of P at different pH values were performed.

Table 5.3: Recipes preparation for stabilization trials. CYC = SSA cyclone fly ash, BA = SSA bottom ash, CFA = coal fly ash, PLA = ECO poultry litter ash, SF = silica fume, FGD = flue gas desulfurization ash.

Recipe n.	1				2				3				4			
Component	CYC	CFA	PLA	SF	CYC	CFA	FGD	SF	BA	CFA	PLA	SF	BA	CFA	FGD	SF
Mass (g)	100	24	30	15	100	24	30	15	100	24	30	15	100	24	30	15

Figure 5.2 shows the timeline of the work, with all the steps performed during the stabilization aging and after the choice of the best recipes for P recovery.
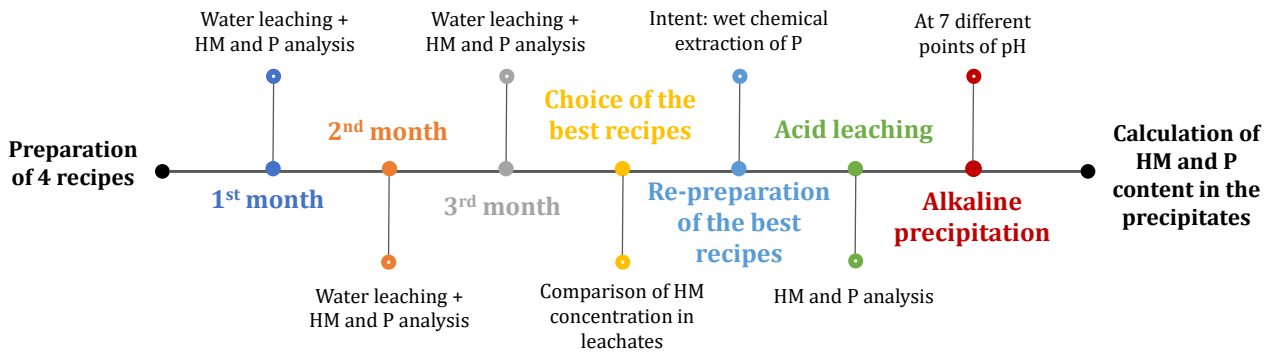
Figure 5.2: Scheme of the workflow.

Wet chemical extraction and precipitation of P were performed according to the procedure described in section 4.2.3. and 4.2.4.: acid leaching with 0.2 mol/L of H_2SO_4, L/S ratio equal to 20 and contact time of 2 h, and P precipitation on 7 different aliquots of acid leachate through alkali titration with lime solution $Ca(OH)_2$ 1% w/w to reach pH values from 2 to 8. At this stage of the research, particular attention was addressed to HM content in the precipitates. Acid leachate analysis was performed by Politecnico di Milano, while TXFR analysis of the filtrate solution after solid separation, was carry out at C4T Lab to quantify HM in precipitates. Concentration of HM in the precipitates ($C_{HM, precipitate}$) was calculated in accordance with **Equation (5.1)**:

$$C_{HM, precipitate} \ (mg/Kg) = [(C_{HM, leachate} \cdot V_{leachate}) - (C_{HM, filtrate} \cdot V_{titration})]/m_{recovered} \qquad (5.1)$$

In which:

$C_{HM, leachate}$ = heavy metal concentration in the acid leachate (mg/L)

$V_{leachate}$ = volume of acid leachate used for each precipitation test (L)

$C_{HM, filtrate}$ = heavy metal concentration in the filtrate solution after precipitate separation (mg/L)

$V_{titration}$ = volume of titration solution ($V_{leachate} + V_{titrant}$) (L)

$m_{recovered}$ = mass recovered for each precipitate (Kg)

In addition, in this case P concentration in the precipitates was analysed directly, without mass balance: the precipitates were mineralized according to EN 15956:2011 and the solution analysed with UV-Vis spectrophotometric Hach Lange LCK 348 kits at C4T Lab. P precipitation efficiency (PPE) was then calculated comparing the total amount of P in the acid leachate (mg) and the amount of P in the recovered precipitates (mg). Extraction efficiency of P (PEE) and other HM was calculated based on **Equation (3.1)** and **(3.2)**.

5.2.2. P extraction from ashes, pyrochars and hydrochars

Sampling, thermal conversion and P recovery

For this research sampling, thermal conversion, and P wet chemical extraction were performed by the Department of Chemistry of the Faculty of Science of Ege University (Izmir, Turkey), as part of DEASPHOR project.

CM was produced and dried in the "Gures Poultry" factory in Manisa, Turkey, while SS came from the "Çiğli Wastewater Treatment Plant" in İzmir, Turkey. Both the feedstock samples were prepared for the further processes in the Department of Chemistry of the Faculty of Science of Ege University (Izmir, Turkey). SS was dried at 105°C for 4 days before the use.

The thermal treatments carried out on CM and SS consisted of incineration (INC), pyrolysis (PYR) and hydrothermal carbonization (HTC). Before the treatments the CM and SS were dried and ground. For the INC, CM and SS were placed into crucibles and introduced in the muffle furnace preheated to 700 °C. The samples remained in the muffle for 4 hours and were cooled in a desiccator. The solid products obtained from this process were named ash (-A). For the PYR, CM and SS were placed in the reactor. Nitrogen gas (N_2) was passed into the reactor, heated to 300°C. The reactor was kept at constant temperature for 1 hour, and after that, it was turned off for cooling. The solid products obtained from this process were named pyrochar (-P), ready for subsequent characterization. For the HTC, CM and SS were put into the reactor with distilled water at a 1:5 (w/w) ratio. The reactor reached 220°C and remained at constant temperature for 1 hour. Vacuum filtration was done to separate the solid and liquid phases in the cooled reactor. The solid products obtained from this process were named hydrochar (-H) and were left to dry in an oven at 105 °C for 24 hours.

The wet extraction was performed via acid leaching, using a H_2SO_4 solution 0.1 mol/L. A liquid to solid (L/S) ratio (mL/g) of 100 was used for the ashes, and a L/S ratio of 50 for pyrochars and hydrochars. The samples were shaken under constant stirring for 2 hours; then they were left to rest for 2 hours and filtered. Solid residues (R-) remaining in the filtrate were collected and analysed. The liquid leachates were titrated until pH 8 with a NaOH solution 1 mol/L. After 4 hours, the precipitation step was completed: the solid and liquid phases were separated by centrifugation. The solid precipitates (P-) had a gelatinous consistency and were left to dry in an oven at 105 °C for 24 hours before the characterization. **Table 5.4** reports a sample list with corresponding acronyms.

Table 5.4*: Sample list and acronyms according to the corresponding origin and thermal treatments applied.*

	Thermal treatment					
	Incineration (INC)		Pyrolysis (PYR)		Hydrothermal carbonization (HTC)	
Feedstocks	SS	CM	SS	CM	SS	CM
Raw samples	SSA	CMA	SSP	CMP	SSH	CMH
Residues	R-SSA	R-CMA	R-SSP	R-CMP	R-SSH	R-CMH
Precipitates	P-SSA	P-CMA	P-SSP	P-CMP	P-SSH	P-CMH

Characterization

Material characterization was completed at C4T Lab (Italy) on all the raw samples (-A, -P, -H), on all the residues after leaching (R-), and on all the precipitates (P-). Analytical techniques used for this scope were described in section 2.2.2. P quantification was carried out using the spectrophotometric chemical method, X-ray diffraction (XRD) analysis was used for the crystalline phases identification and scanning electron microscopy combined with energy-dispersive X-ray spectrometry (SEM-EDXS) was applied to confirm the previous results. P extraction efficiency (PEE) was calculated thanks to **Equation (5.2)**:

$$\text{PEE (\%)} = 100 - [(C_{P,\,residue} \cdot 100)/C_{P,\,raw}] \qquad\qquad \textbf{(5.2)}$$

In which:

$C_{P,\,residue}$ = P concentration in the residue (R-) after the acid leaching (mg/Kg)

$C_{P,\,raw}$ = P concentration in the raw sample before the acid leaching (mg/Kg)

5.3. Results and discussion

5.3.1. HM stabilization in SSA with PLA to enhance P recovery

The selection of the best recipe was made in function of HM leachability in water according to the European standard procedure CEN EN 12457-2:2004, comparing the leaching test results of the raw samples (CYC or BA) with the leaching results of the stabilized samples. **Figure 5.3** shows data for CYC, while **Figure 5.4** reports data for BA. For both CYC and BA, the most leachable metals are Zn and Ni, especially for CYC. Zooming in the results for CYC (**Figure 5.3** at the bottom), it is evident that the stabilization of Ni is total, as for Zn, except in two samples (3M_1A and 3M_2F). The samples that don't stabilize HM were immediately excluded. On the other hand, all BA recipes promote stabilization (**Figure 5.4**), excluding 3M_3A and 1M_4F, and except for Cr which increases slightly, as in CYC stabilized samples. The increase in Cr concentration in both stabilized arrays is probably due to the high concentration of this element in a component of the recipes, that is CFA, as confirmed by **Figure 5.5** on the left. There is also an interesting remark regarding the P solubility in recipe 4 (stabilized sample of BA) that increase during the 3 months of stabilization, as shown in **Figure 5.5** on the right. In conclusion, it can be said that PLA (present in recipes n.1 and n.3) stabilizes metals such as FGD (present in recipes n.2 and n.4). In particular PLA was chosen as a component thanks to the support of the European project DEASPHOR and because it is very rich in Si and Ca, useful for the stabilization reactions, as much as it is in P. Furthermore, the only contaminant present is Zn.
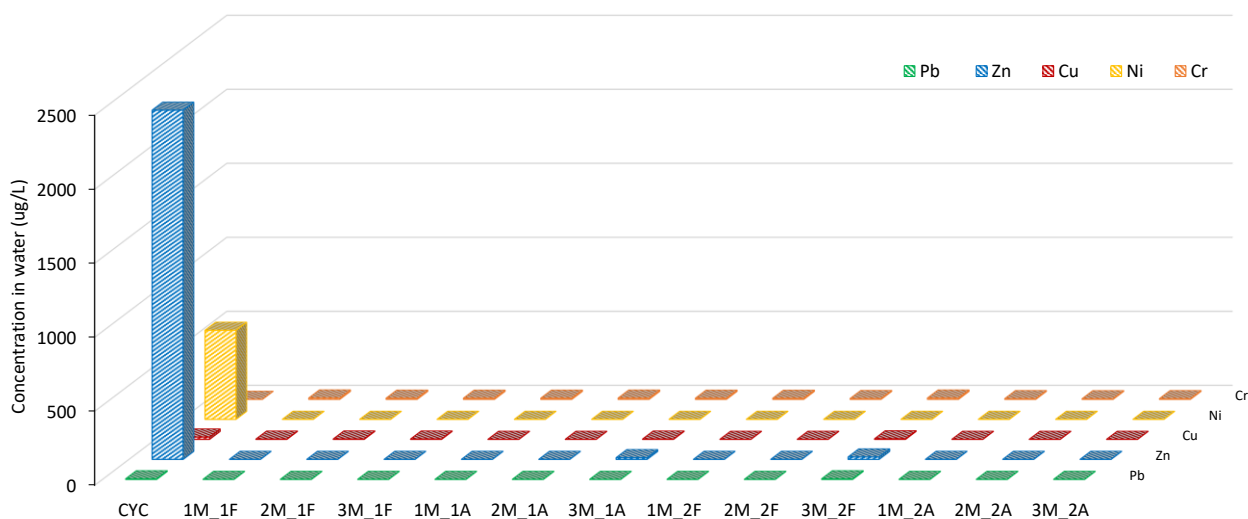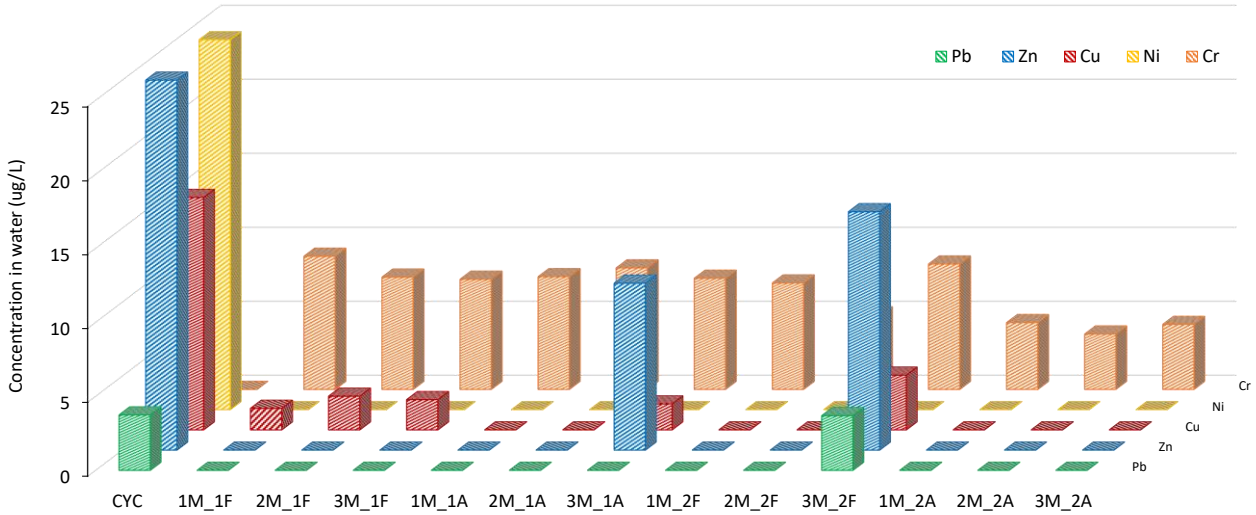
Figure 5.3: Above, results of leaching test in water for raw CYC and corresponding stabilized samples. Below a zoom of the leaching test results.

Figure 5.4: Results of leaching test in water for raw BA and corresponding stabilized samples.
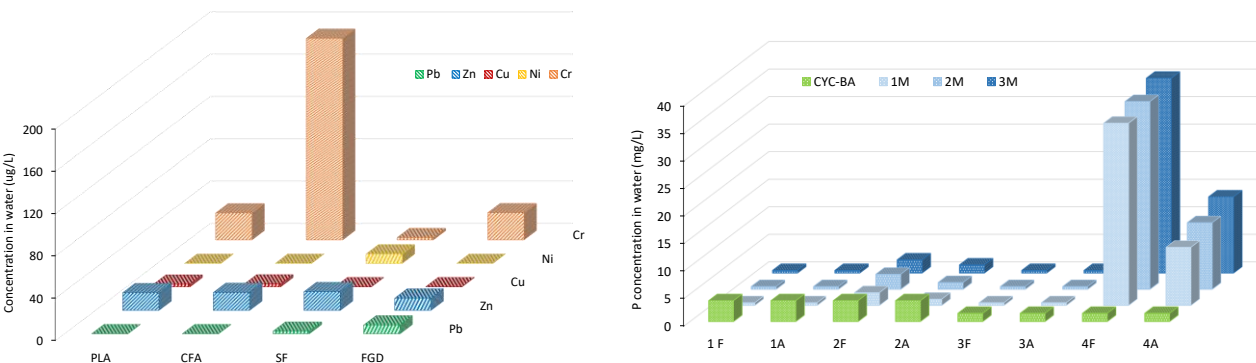
Figure 5.5: Results of leaching test in water for raw PLA, CFA, SF and FGD (left) and P concentration in the leachates of each stabilized samples compared with the raw (CYC or BA) samples (right).
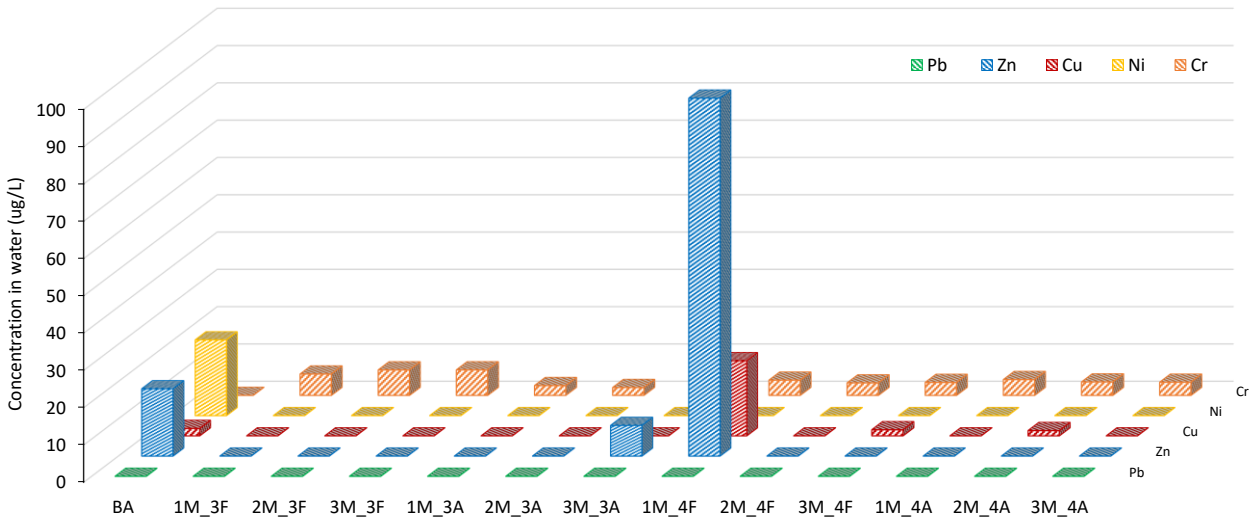
The best selected recipes were 1M_1A and 1M_2A for CYC and 1M_3A for BA, on which acid wet chemical extraction was performed. In **Figure 5.6** the extraction efficiency (EE) of P and HM, normalized on the raw sample mass, is reported. The normalization was made to evaluate whether the other ingredients contributed to increase or decrease the EE. To do this, the results of the acid leaching of the only and same mass of the raw samples inserted in the recipes were compared with the results of the acid leaching of the stabilized samples. **Figure 5.6** (on the left) shows element EE normalized on the raw sample mass: for 1M_3A (blue bar) there is an increase in PEE compared to the BA raw sample (light blue bar) that reaches almost 100 %. Unfortunately, an increase of EE is also recorded for all the metals in the stabilized BA samples. PPE in stabilized CYC samples is not increased (red and orange bars) compared to the raw CYC (yellow bar). On contrary, HM extraction is increased in 1M_2A and 1M_1A, except for Cu. **Figure 5.6** (on the right) shows the variation of EE compared to the acid leaching of the raw sample, in percentage: PEE increases by almost 30 % in 1M_3A from BA (blue bar) and for CYC there is a reduction in Cu EE for both the stabilized samples (red and orange bars).
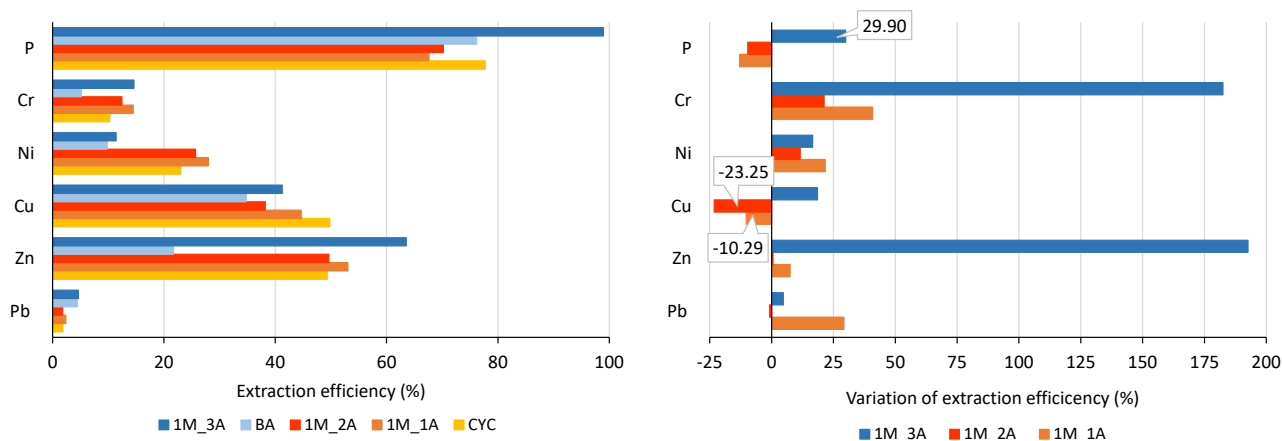
***Figure 5.6**: Extraction efficiency normalized on the raw sample mass (left) and increase or reduction of extraction efficiency compared to the acid leaching of the raw sample (right).*

The alkaline precipitation was performed only on samples 1M_1A and 1M_3A, to focus the study on the influence of PLA on the final P concentration in the precipitates. Seven different pH values were investigated, from 2 to 8. **Figure 5.7** displays the final results about the HM content in the precipitates from 1M_1A (from the CYC): Zn and Pb (purple and green line), the main contaminants for which stabilization procedure was studied, were precipitated in almost all the recovered products above the legal limit fixed by the EU Regulation 2019/1009 [154] detailed in **Table 5.5**. Zn exceeds the limit starting from pH 4, with the higher concentration at pH 5, while Pb at pH 2, 3 and 4. Moreover, As (blue line) is abundantly higher the legal limit in all the precipitates. For these reasons, the products cannot be considered suitable for fertilizer sector and no further analyses were carried out.

Figure 5.7: *HM concentration in the precipitates (calculated from mass balance) coming from acid leaching and alkali titration of 1M_1A, stabilized sample of CYC.*

Table 5.5: Contaminants limit values in fertilizers and soil improvers [154].

Contaminant	Concentration (mg/kg) dry matter				
	Fertilizer			Soil improver	
	Organic	Organo-mineral	Inorganic macronutrient	Organic	Inorganic
Cadmium (Cd)	1,5	3 ** 60 mg/kg phosphorus pentoxide (P_2O_5) ***	3 ** 60 mg/kg phosphorus pentoxide (P_2O_5) ***	2	1,5
Hexavalent chromium (Cr VI)	2	2	2	2	2
Mercury (Hg)	1	1	1	1	1
Nickel (Ni)	50	50	100	50	100
Lead (Pb)	120	120	120	120	120
Inorganic arsenic (As)	40	40	40	40	40
Copper (Cu)	300	600*	600*	300	300
Zinc (Zn)	800	1500*	1500*	800	800

* These limit values shall not apply where copper (Cu) or zinc (Zn) has been intentionally added to an organo-mineral fertilizer or an inorganic macronutrient fertilizer for the purpose of correcting a soil micronutrient deficiency and is declared in accordance with Annex III.

**Where an organo-mineral fertilizer or an inorganic macronutrient fertilizer has a total phosphorus (P) content of less than 5 % phosphorus pentoxide (P_2O_5)-equivalent by mass.

*** Where an organo-mineral fertilizer or an inorganic macronutrient fertilizer has a total phosphorus (P) content of 5 % phosphorus pentoxide (P_2O_5)-equivalent or more by mass ('phosphate fertilizer').

On the other side, **Figure 5.8** reports the results for the precipitates from 1M_3A, the BA stabilized sample. All the recovered products at different pH comply with the legal limits for HM, and so P content in them was investigated. The results are shown in the table in the right in the figure: the P content in the precipitates manifest higher value at pH 5, as already noted in chapter 4. This value, express as phosphoric anhydrite is very close to the P content of commercial single superphosphate

fertilizer (SSP P_2O_5 = 16 %). PPE increases by increasing the pH of the precipitation, reaching almost 100 % at pH 8, confirming what already studied in chapter 4. Considering the precipitate at pH 5 the most promising product, P bioavailability in citric acid 2 % was tested on it, according to EN 15920:2011. The obtained 99.5% of bioavailability confirms a very good result.

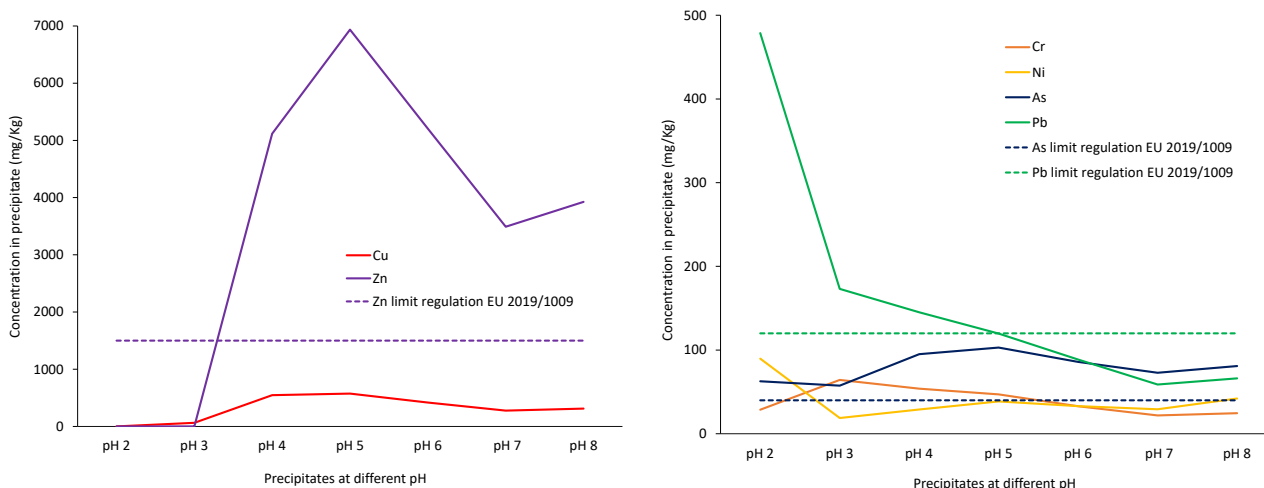| pH	P in the precipitate	P_2O_5 in the precipitate	PPE
	%		
pH 2	1.32	3.03	4.53
pH 3	6.18	14.16	55.81
pH 4	6.59	15.08	59.20
pH 5	7.13	**16.32**	75.54
pH 6	5.99	13.73	79.79
pH 7	4.48	10.26	74.57
pH 8	4.99	11.43	**95.95**
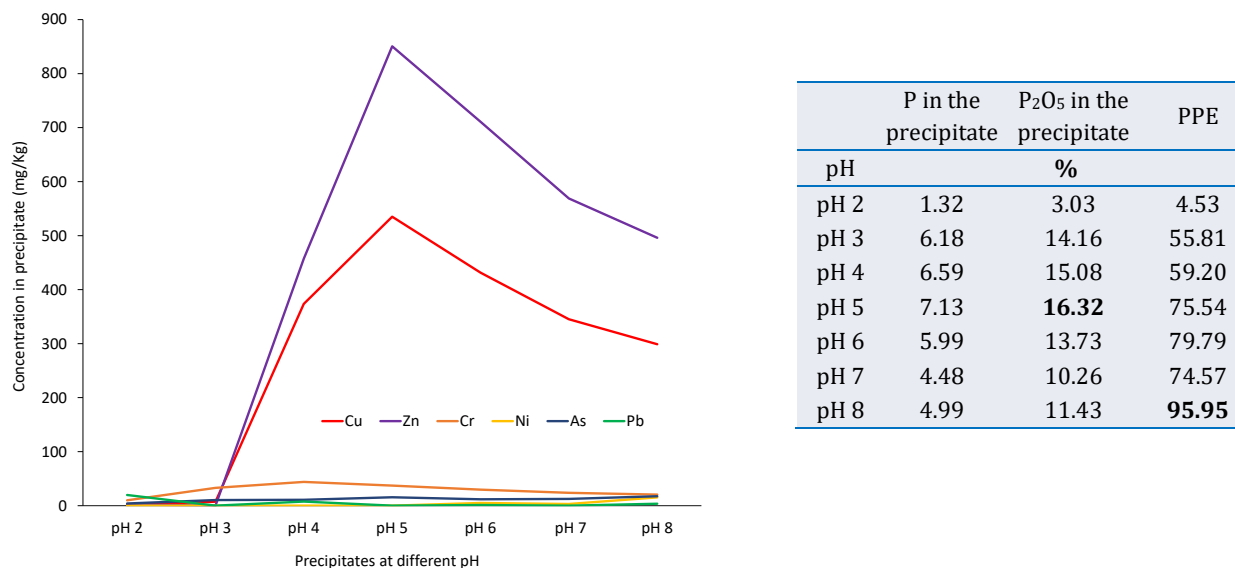
Figure 5.8*: HM concentration in the precipitates (calculated from mass balance) coming from acid leaching and alkali titration of 1M_3A, stabilized sample of BA. P concentration in precipitates (table on the right) and PPE calculated after mineralization of the products according to EN 15956:2011.*

5.3.2.   Comparison of the P recovery effectiveness from different biomass waste and different thermal treatments

The P content in the thermally converted products reported in **Table 5.6** demonstrates that incineration is the best treatment to concentrate P in the solid, especially compared with pyrolysis where the same amount of dried feedstock was used (approximately 20 g). SSA and CMA present the higher P concentration (2.65 % and 5.64 % respectively), revealing the CM more promising as P secondary source. Even if CMH manifests a quite satisfying P content compared to the other samples., this result could be dependent on the dried feedstock mass used in the HTC experiment (approximately 40 g). Certainly, a repetition of each thermal conversion experiment using the same feedstock mass and verifying the P content also in the feedstock as well, could returns a more complete evaluation of the best techniques. It should also be considered that the analysis of P concentration in SS and CM should be accomplished in an appropriate biological laboratory which was not available at the time of the research.

Table 5.6: *P content in thermally converted products quantified with UV-Vis spectrophotometric method.*

	Thermal treatment					
	Incineration (INC)		Pyrolysis (PYR)		Hydrothermal carbonization (HTC)	
Raw samples	SSA	CMA	SSP	CMP	SSH	CMH
P %	2.65	5.64	1.24	0.65	0.87	2.33

Table 5.7 shows the main crystalline phases identified after XRD analysis on all the raw samples. The results confirm the presence of P crystalline compounds, except in CMP. Hydroxaypatite is present in CMA and CMH, chlorapatite in SSA and $AlPO_4$ in SSP and SSH. Comparing the type of samples there are phases common to several products. Calcite $CaCO_3$ is present in all the thermo-converted CM samples, because in the poultry farming, the bedding material consists mainly of eggshells, while quartz SiO_2 was detected in all the SS products. XRD analysis on the residues after the acid leaching (R-samples), not reported here, confirmed that crystalline compounds remaining in the solids were mainly calcium sulphate hydrate or gypsum ($CaSO_4 \cdot 2H_2O$), calcium carbonate ($CaCO_3$) and quartz (SiO_2), in accordance with the acid used and the dissolution of phosphate phases.

Table 5.7: *XRD phase identification in thermally converted products (raw samples).*

	Thermal treatment					
	Incineration (INC)		Pyrolysis (PYR)		Hydrothermal carbonization (HTC)	
Crystalline phase/Raw samples	SSA	CMA	SSP	CMP	SSH	CMH
Hydroxaypatite		X				X
Chlorapatite	X					
$AlPO_4$			X		X	
Quartz SiO_2	X		X		X	
$CaMg(SiO_3)_2$	X					
Calcite $CaCO_3$		X	X	X	X	X
CaO		X				
$Ca(OH)_2$		X				
Sylvite KCl		X		X		
MgO		X				
Dolomite			X			
Anhydrite	X					
K_2SO_4		X				

The PEE calculated with **Equation (5.2)** is displayed in **Figure 5.9**, demonstrating a high extraction efficiency for the HTC samples (CMH and SSH), very close to 100 %. A good PEE was also recorded for the INC samples (CMA and SSA), reaching a yield > 90 %. For both PYR samples (CMP and SSP) the data were not so satisfying, but anyway higher than 60 %. The results obtained for the ash samples

were optimal compared with the PEE of RHPLA achieved in chapter 3 (around 75 %) and with the PEE of SSA recorded in chapter 4 (at most 87 %). A consideration must be done regarding the leaching method, that was different for each case:

1. RHPLA was leached with HCl 1 mol/L, L/S ratio = 10, t = 2 h, room temperature;
2. Italian SSA was leached adopting H_2SO_4 0.2 mol/L, L/S ratio = 20, t = 2 h, room temperature;
3. Turkish CMA and SSA were leached with H_2SO_4 0.1 mol/L, L/S ratio = 100, t = 2 h, room temperature;

Based on the circular economy principles, it is necessary to find a suitable method to not use chemicals too concentrated (case 1), or too high volumes of extract (case 3). Future studies in this direction needed to be aware of finding the right balance.
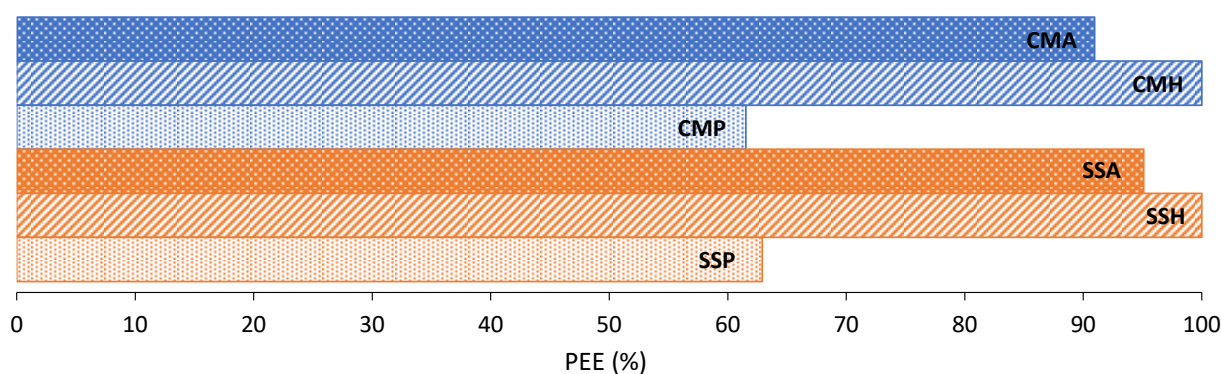
Figure 5.9: P extraction efficiency (PEE) calculated from UV-Vis P quantification before and after acid leaching.

Figure 5.10 shows the P content in precipitates obtained from the UV-Vis analysis of the solids: results range between 7.0 and 9.4 %. P precipitates deriving from CM (P-CMs) are more concentrated in P than precipitates from SS (P-SSs), and P precipitates from PYR contain more P than precipitates from INC and HTC, even if the PEE was lower. Precipitation is affected by many parameters: surely temperature and chemicals used, but also by resting time (equilibrium, 4 h in this experiment) and pH. As demonstrated in chapter 4, P precipitation efficiency (PPE) can be mostly affected by the pH adopted for the titration, and at pH 8, used in this experiment, the higher PPE can be reached. For a complete study, perspectives for the future should include investigation of HM content at this pH. Regarding the percentage of P in the precipitates, the results seem to be quite satisfactory, based on regulation (EC) n. 2003/2003 relating to fertilizers [153]. In ANNEX I (List of types of EC fertilizers, section of inorganic straight primary nutrient fertilizers - phosphatic fertilizers) the minimum content of P (percentage by weight express in % P_2O_5) is listed for each fertilizer in use. Converting the presented data of P % in P_2O_5 % with the conversion factor P_2O_5 = 2.29 · P, a range of 16 – 21.5 % P_2O_5 is obtained. These results are comparable with the single superphosphate (SSP 16 % P_2O_5) listed in the

regulation. Moreover, to facilitate the use of precipitates in fertilizer sector, P-bioavailability tests should be performed in accordance with fertilizers regulations (water, citric acid or ammonium citrate are the most used methods). SEM-EDXS semi-quantitative analysis (not reported here and used to confirm the previous results) returned a higher concentration in the precipitates, up to 15% for P-CMs and up to 10% for P-SSs, showing that P-CMs are mainly made up of P and Ca, while P-SSs are also made up of Fe and Al.

Figure 5.10*: P content in the precipitates analysed with UV-Vis method.*

5.4.   Conclusions

The research conducted in the first part of this chapter led to the following conclusions:

- o The stabilization procedure proposed, using PLA in substitution of FGD, can prevent leaching into water of HM present in SSA highly contaminated.
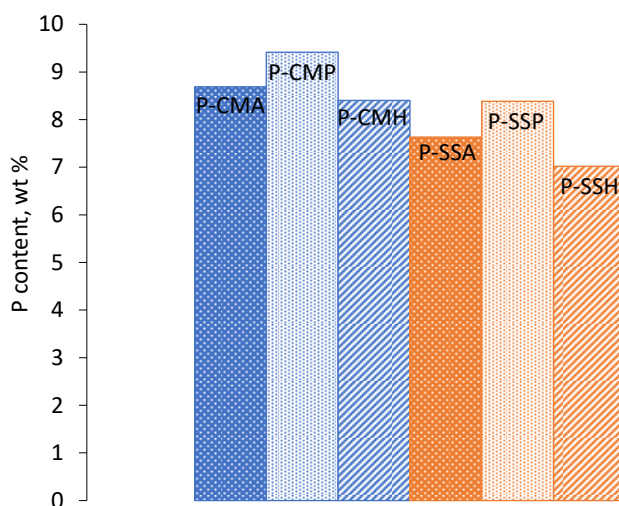
- o During the acid leaching of the stabilized samples 1M_1A and 1M_2A (from CYC raw sample) the reduction in EE of HM was observed for Cu, but not for the most concentrated Zn and Pb.

- o In the acid leaching of 1M_3A (from BA raw sample) the EE of P increases by 30%, guaranteeing the achievement of 100% PEE (normalized on the raw BA mass), probably due to the presence of PLA in the recipe. For Cr and Zn in 1M_3A there is a significant increase in EE, that does not affect the subsequent P recovery.

- o Precipitates from CYC stabilized sample were contaminated by Pb, Zn or As exceeding the legal limits at each pH, but the products recovered from BA stabilized sample were free of HM at each pH and PPE was close to 96 % for pH 8.

- o The best precipitate was identified at pH 5 with a P content comparable to the commercial fertilizers (P_2O_5 = 16,3 %) and with a P bioavailability in citric acid 2 % equal to 99,5 %.

In the end, this work was a preliminary study about the HM stabilization processes that can be performed during the storage period of the SSA, instead of landfill disposal. This practise can be an economically and environmentally sustainable solution, which can easily be realized at low cost while awaiting development of dedicated plants for P extraction. It would be considered advantageous to create separated storage for SSA (with only other selected by-products and ashes that can enhance HM stabilization) to subsequently recover P.

The research conducted in the second part of this chapter compares the P recovery efficiency from two type of biological waste: CM and SS. Thermal treatments (INC, PYR, HTC) were performed on the raw waste and the differences regarding P content and characterization were listed. Ash samples were the more concentrated in P, compared to pyrochars and hydrochars. In any case, thermal converted products from CM were richer of P. Hydroxyapatite, chlorapatite and $AlPO_4$ were identified as main crystalline phosphate compounds in the products. An acid leaching followed by an alkali titration allowed to obtain P-rich precipitates. PEE for the HTC samples was total (100 %), followed by an excellent result also for the INC samples (PEE > 90 %). For PYR samples, a quite satisfying PEE was recorded higher than 60 %. P content in the precipitates was achieved up to 9.4 %, higher than the P content present in the commercial SSP fertilizer, and precipitates from PYR contain more P than the others, even if the PEE was lower. In general, P precipitates deriving from CM are richer in P than precipitates from SS. Perspectives for the future should include optimization of the extraction procedure and study of the P bioavailability in the precipitates, for application as fertilizers.

Acknowledgements

6. P RECOVERY FROM SSA BY INNOVATIVE THERMOCHEMICAL TREATMENT AND COMPARISON WITH WET CHEMICAL EXTRACTION

Abstract

In this chapter two different methods of P recovery were compared: wet chemical extraction and thermochemical microwave assisted treatment. The same SSA samples, deriving from a WtE Italian plant, were treated using the two techniques. Acid leaching and alkali precipitation were used for the chemical method as explained in chapter 4, paying particular attention, in this stage of the research, to the HM content in the P precipitates. Comprehensive considerations were done about the P recovery efficiency and the origin of the ash: mono-incinerated or co-incinerated with secondary solid fuel (SSF) coming from MSW. In addition, on the first SSA co-combusted sample received, a feasibility check of SiO_2 recovery after P extraction was performed with the same procedure used in chapter 4.

On the other side, this work proposes the thermochemical treatment of SSA made by using a microwave oven, associated with a devoted patented chamber by means of a hybrid heating mechanism. The treatment, after the addition of Na-based and carbon additives to SSA, promotes the formation of $CaNaPO_4$ compound, with reduced leaching of HM and increased bioavailability and solubility of P. This treatment offers a new breakthrough in recovering P from SSA opening new possibilities in terms of sustainability.

Keywords

Sewage sludge ash

P recovery

Thermochemical microwave treatment

Wet chemical extraction and precipitation

Scientific contribution

This chapter is partially based on the following publication, whose form have been adapted for reasons of consistency with the structure of this doctoral thesis. The content reported in this chapter is the result of my own work, including literature review, data curation, formal analysis, investigation,

methodology, visualization and writing. Any work made by others is attributed to the original author in the text.

o **Fiameni L.**, Fahimi A., Federici S., Cornelio A., Depero L. E., Bontempi E., A new breakthrough in the P recovery from sewage sludge ash by thermochemical processes. *Green Chemistry* (2022), **24**, 6836-6839. https://doi.org/10.1039/D2GC02328H

6.1. Introduction

The enhancement of the P product resulting from the wet chemical extraction and precipitation from biomass ash, is influenced by many variables. The nature and the origin of the biomass affects the total concentration of nutrients and HM in the ash. A clear example is given by the comparison between the two ashes investigated during this research: PLA and SSA. In the first case, due to the animal origin and the direct exploitation of the litter or manure in WtE plants, the HM contamination is very low. But in the case of SSA, the variability of urban (and industrial) WW, and different period of the year in which SS collection from the WWTP is made, generate more problems and more pollutants in the SSA. For example, in literature Zn concentration in PLA was recorded at most 2500 mg/Kg [171] but more than 7000 mg/Kg in SSA [49]. This is also confirmed by the data reported in the previous chapters, where Zn content was detected 3500 mg/Kg in the ECO sample of RHPLA in chapter 3 but has exceeded 14000 mg/Kg in the CYC sample of ISSA in chapter 5. The contamination is a big impediment for the safe reuse of the recovered P precipitates in the fertilizer market that has strict regulation [154]. In particular, maximum concentrations of Cu, Zn, As, Cd, Hg, Ni and Pb, must be controlled in fertilizer regulation [152]. Especially for SSA, despite its promising potential as secondary raw material to produce P-fertilizers, it generally does not contain bioavailable phosphate phases, and leachable HM are often found. Thus, P in SSA generally results poorly available to plants, and the ash cannot be directly reused in agriculture [78].

For this reason, not all the biomass ash are suitable for the wet chemical extraction of P, and an alternative method of recovery must be considered if refined steps in the traditional leaching procedure are not implemented. According to literature, the other feasible procedure at laboratory scale is the thermochemical treatment of the biomass ash, which can ensure a second utilization also of the more contaminated ash [269]. In this way the ash could became a raw fertilizer material thanks to the conversion of P compounds, present in the solid matrix, in more soluble mineral phases [78]. Whitlockite type $Ca_{3-x}(Mg, Fe)_x(PO_4)_2$ phase, that is the main P-bearing phase in SSA [82], can be converted into buchwaldite ($NaCaPO_4$), when SSA is thermally annealed in the presence of certain sodium compounds [270]. Buchwaldite has the advantage of being bioavailable, which was demonstrated by evaluating its high solubility in ammonium citrate [271]. The process reported by Smol at al. [81] consists of an addition of sodium compounds (Na additive) and a reducing agent (dry sewage sludge) to the SSA samples and using a muffle furnace to reach 1000°C for a defined retention time. The presence of Na in reducing system allows the transformation of insoluble phosphates in soluble buchwaldite $NaCaPO_4$.

At the same time, as explained in section 1.3.2., thermal processes would be very efficient in reducing the HM load by their separation via the gas phase. For example, metals with higher vapor pressures in comparison to the respective oxides (Hg, Pb, and Cd) can partly evaporate or sublimate, with the possible their recovery in conventional gas cleaning systems. However, the literature tends to

associate thermochemical treatment processes with high energy demand. As result, the potentialities of P-resource recovery offered by this method are still considered not attractive.

This research presents for the first time a recent advance in thermochemical process integration with microwave (MW), which can promise a reduction of energy consumption in comparison to classical thermal treatments and may represent a suitable alternative to the use of wet chemical processes for P-extraction. The MW has two main advantages: a) the energy usually necessary to heat the chamber is saved (only the sample is heated), and b) the heating process requires less time and less energy than traditional heating technologies [272]. Then the use of MW heating represents a potential eco-friendly treatment with a major trend toward sustainable development.

In this chapter, as consequence of the previous research conducted on the wet chemical procedure for P recovery, an optimized technique of acid leaching and subsequent alkali precipitation was selected and tested on several SSA. To do this, a first sample of SS co-combusted with municipal solid waste (MSW) was screened. As performed in chapter 4, the SSA resulting from co-combustion, was subjected to a simultaneous P and SiO_2 recovery and further P precipitation at different pH. In this case, in addition to PPE, also the HM concentration in the P precipitate was monitored, to consciously choose the best recovery conditions. After this first check, a specific set of parameters was adopted for the other samples, commenting on the results based on the origin of the ash (co-incinerated or mono-incinerated SSA).

On the other side, was possible to investigate the same samples with an innovative microwave thermochemical method, that was patented within the C4T Lab. In this case, the effectiveness of the process was validated with P solubility tests in water, and XRD analysis to verify crystalline structure transformation.

6.2.   Materials and methods

6.2.1.   Sampling

All the samples investigated in this chapter were provided by the company A2A Ambiente S.p.A., as part of FANGHI project. Three different sampling campaigns were operated in the Italian WtE plant located in Corteolona (Lombardy, Italy), owned by the company. The plant, consisting of a fluidized bed combustion system, is normally destined to MSW and secondary solid fuel (SSF) incineration. In the frame of the research, several trials of co-combustion of SSF and SS, and mono-incineration of SS were performed. **Table 6.1** reports description and images of the SSA samples as collected from different sampling spots inside the plant, and their acronyms. In the first campaign two samples from co-combustion were collected: BA_C1 and R-BA_C1. In the second campaign eight samples of SSA were provided, coming from mono-incineration (CYC-FA_M2, BO-FA_M2 and BA_M2) and co-incineration (BO-FA_C2, CYC-FA_C2, BF-FA_C2 and BA_C2). In the end, for the third campaign, the last four mono-incinerated SSA were collected: CYC-FA_M3, BO-FA_M3, BF-FA_M3 and BA_M3. Depending on the aspect of the raw ash, as necessary, the samples were dried in electric oven at 100°C for 12 h and sieved and ground with mill Retsch MM400. Especially the co-combusted ash, needed separation of ferrous (nails and screws) and glass debris before the grinding.

Table 6.1: Description of the collected SSA samples. BA = bottom ash, FA = fly ash, C1 = co-combustion 1st campaign, M2 = mono-combustion 2nd campaign, C2 = co-combustion 2nd campaign M3 = mono-combustion 3rd campaign.

Campaign and date of receiving	Ash type (sampling spot)	Origin	Acronym	Image
1st campaign 29/09/2021	Bottom ash (BA) Dried SS used for incineration was in form of pellets. After ash collection only residual pellets was separated and delivered for P recovery.	Co-combustion with SSF July 2021	BA_C1	
	Ash residue of BA_C1 Collection of solid residue after acid leaching of BA_C1 operated by the company		R-BA_C1	

2nd campaign 21/03/2022	Cyclone (FA)	Mono-combustion of dried SS 28-29/09/2021	CYC-FA_M2	
	Boiler ash (FA)		BO-FA_M2	
	Bottom ash (BA)		BA_M2	
	Boiler ash (FA)	Co-combustion with SSF 18/03/2022	BO-FA_C2	
	Cyclone (FA) stabilized with water and concrete		CYC-FA_C2	
	Bag filter ash (FA)		BF-FA_C2	

	Bottom ash (BA) Dried SS used for incineration was in form of pellets. After ash collection no separation between residual pellets and incinerated SSF was made.		BA_C2	
3rd campaign 14/06/2022	Cyclone (FA) stabilized with water and concrete	Mono-combustion of dried SS 17/05/2022	CYC-FA_M3	
	Boiler ash (FA)		BO-FA_M3	
	Bag filter ash (FA)		BF-FA_M3	
	Bottom ash (BA)		BA_M3	

Table 6.2 shows the results of X-Ray Fluorescence analysis (XRF) on raw ash samples according to UNI EN 15309:2007 provided by A2A Ambiente S.pA. The main elemental composition is reported. In general, Na content is less than 1 % in all the ash, except in BA_C2 and in BF-FA_C2 and BF-FA_M3, where the amount is close to 10 %. In the case of co-incinerated bottom ash, the sample from 2nd campaign (BA_C2) is richer of Na, compared to the sample from 1st campaign (BA_C1). In the second case, the ash deriving from bag filters are probably concentrated in residual sodium chemicals, due to the emission dry treatment, where sodium bicarbonate $NaHCO_3$ is injected in the flue gas, and the produced solids are collected and removed by the filters [273]. This method is very common and considered one of the best available techniques for acid gas removal in waste incinerators [274]. For the same reason, S content is higher in the bag filter ash, in accordance with the dry treatment of the flue gas that may form sodium sulphates. The highest Al content is in the mono-combusted ash from 2nd campaign (CYC-FA_M2, BO-FA_M2 and BA_M2), with concentration > 5 % in boiler ash and bottom ash of 2nd and 3rd campaign (BO-FA_C2, BO-FA_M3, BA_C2 and BA_M3). Si is very concentrated in all the bottom ash, according to the nature of the plant, where usually sand (consisting of quartz and silica SiO_2) is used as bedding material for the fluidized bed combustion system. The highest P content is recorded for BO-FA_M3 (5.1 %), and in general fly ash from mono-incineration presents more P in the matrix compared to the same co-combusted fly ash. K, the other main macronutrient normally investigated for fertilizer application, is in these samples very low (not more than 1.6 %), especially compared with the common content of K in PLA (see Table 2.2). Ca has a quite high concentration in all the ash, with more than 20% in the bag filters fly ash, probably due to the use of calcium compounds, such as lime, limestone or calcium hydroxide, during the dry flue gas treatment with sodium bicarbonate [274]. Fe content varies depending on the ash type and campaign (the final concentration is variable in function of the SS and SSF composition sent to incineration). The highest concentration is recorded for BO-FA_C2, equal to 5.3 %.

Table 6.2: XRF results for main constituent elements of solid raw ash sample. *Quantification carried out according to UNI EN 13657:2004 and UNI EN ISO 11885:2009 (solid sample mineralization and subsequent ICP-OES analysis).

							Element (%)								
Sample	**Na**		**Mg**		**Al**		**Si**		**P**		**S**		**K**		**Ca**	**Fe**
BA_C1	0.69 ± 0.20	1.31 ± 0.42	* 3.77 ± 1.10	16.10 ± 4.80	3.44 ± 1.09	0.30 ± 0.09	1.50 ± 0.47	8.87 ± 0.72	* 3.54 ± 1.10
R-BA_C1	0.99 ± 0.29	0.80 ± 0.26	* 1.29 ± 0.39	16.40 ± 4.90	0.89 ± 0.28	1.10 ± 0.33	1.07 ± 0.33	3.50 ± 0.93	* 0.95 ± 0.28
CYC-FA_M2	0.72 ± 0.22	1.44 ± 0.43	8.5 ± 2.5	15.2 ± 4.6	4.4 ± 1.3	0.26 ± 0.08	1.50 ± 0.45	12.3 ± 3.7	4.7 ± 1.4
BO-FA_M2	0.94 ± 0.28	1.14 ± 0.34	6.5 ± 1.9	14.4 ± 4.3	3.22 ± 0.97	0.80 ± 0.24	1.60 ± 0.48	10.5 ± 3.1	4.0 ± 1.2
BA_M2	0.72 ± 0.22	1.3 ± 0.39	6.7 ± 2.0	15.2 ± 4.6	3.8 ± 1.1	0.43 ± 0.13	1.40 ± 0.42	11.2 ± 3.3	4.0 ± 1.2
BO-FA_C2	0.53 ± 0.16	0.89 ± 0.27	5.0 ± 1.5	9.5 ± 2.9	3.6 ± 1.1	0.263 ± 0.079	1.54 ± 0.46	13.2 ± 4.0	5.3 ± 1.6
CYC-FA_C2	0.81 ± 0.24	1.14 ± 0.34	3.8 ± 1.1	6.3 ± 1.9	1.80 ± 0.54	0.89 ± 0.27	0.83 ± 0.25	13.3 ± 4.0	2.79 ± 0.84
BF-FA_C2	10.6 ± 3.2	1.10 ± 0.33	2.38 ± 0.71	2.97 ± 0.89	1.16 ± 0.35	3.28 ± 0.98	0.89 ± 0.27	23.7 ± 7.1	1.80 ± 0.54
BA_C2	3.10 ± 0.93	1.05 ± 0.31	5.6 ± 1.7	24.4 ± 7.3	0.66 ± 0.20	0.271 ± 0.081	1.43 ± 0.43	8.2 ± 2.5	1.94 ± 0.58
CYC-FA_M3	0.39 ± 0.12	1.51 ± 0.45	2.51 ± 0.75	9.6 ± 2.9	2.88 ± 0.86	0.72 ± 0.21	1.03 ± 0.31	9.5 ± 2.9	2.7 ± 0.83
BO-FA_M3	0.65 ± 0.20	1.80 ± 0.54	5.2 ± 1.6	15.8 ± 4.8	5.1 ± 1.5	0.60 ± 0.18	1.46 ± 0.44	13.2 ± 3.9	4.1 ± 1.2
BF-FA_M3	9.5 ± 2.8	1.70 ± 0.51	2.58 ± 0.77	6.8 ± 2.0	2.51 ± 0.75	4.4 ± 1.3	0.50 ± 0.15	21.6 ± 6.5	1.82 ± 0.55
BA_M3	0.99 ± 0.30	2.48 ± 0.74	5.5 ± 1.6	19.7 ± 5.9	4.2 ± 1.3	0.38 ± 0.11	1.48 ± 0.45	9.9 ± 3.0	3.22 ± 0.97

6.2.2.   Characterization techniques

Crystalline composition of the samples was investigated with X-ray diffraction (XRD) as described in section 2.2.2.

The comprehensive study performed on the SSA from 1st campaign involved TXRF analysis of HM as described in section 2.2.2. and P quantification via UV-Vis method. Analysis was carried out using Hach Lange spectrophotometer DR3800 and Hach Lange LCK 348 phosphate analytical kits. Appropriate dilution with MilliQ water of the leachate solutions was applied to respect the proper range of $P-PO_4^{3-}$ concentration (0.5 – 5.0 mg/L) insured by the analytic kit.

During experimental part on SSA from 2nd and 3rd campaigns, inductively coupled plasma optical emission spectroscopy (ICP-OES) was used for elemental quantification of P, HM and other elements present in the leachate samples; this was possible thanks to the access in the A2A Ambiente S.p.A. internal laboratory.

6.2.3.   Wet chemical extraction and precipitation

SSA from 1st campaign was subjected to the simultaneous P and SiO_2 recovery procedure with the same parameters mentioned in section 4.2.3.: acid leaching of BA_C1 with 0.2 mol/L of H_2SO_4, L/S ratio equal to 20 and contact time of 2 h, and alkali leaching of R-BA_C1 with NaOH 4 mol/L, L/S ratio of 10, and constant stirring at 80 °C for 4 h, followed by H_2SO_4 5 mol/L addition dropwise under constant stirring at room temperature, to reach pH around 9 for gel formation. SiO_2 extraction efficiency (SEE) was calculated following **Equation (4.1)**. This double recovery was investigated on these specific samples, to better understand the behavior of a co-incinerated SSA and the role of contaminants in P and SiO_2 recovery. Unlike the SSA studied in chapter 4, in this work also HM metal content in the leachate and the P-precipitates was monitored.

The P precipitation was then conducted based on the procedure already explained in section 4.2.4., performing the alkali titration of 7 aliquots of acid leachate with lime solution $Ca(OH)_2$ 1% w/w to reach different pH values, from 2 to 8. In this case, the titrated solutions were left to rest for 24 h before separation and analysis of the filtrate solution to quantify P and HM. Starting from the results obtained from the wet chemical extraction and precipitation of P from BA_C1, only a pH value was chosen for P precipitation from the other SSA leachate sample. Percentage of P in each precipitate (P precipitate) was calculated using the **Equation (4.2)** and **(4.3)**, and P precipitation efficiency (PPE) following the **Equation (4.4)**. In addition, concentration of HM in the precipitates (C HM, precipitate) was calculated, in accordance with **Equation (5.1)**.

6.2.4.   Thermochemical microwave treatment

SSA samples collected from 2nd and 3rd campaign were tested with an innovative microwave thermochemical procedure. The method and used chambers were patented under Italian legislation

(nr. 102022000002351) and won the 2022 EIT RAW MATERIALS business idea competition on Critical Raw Materials (EIT) [275]. It is based on a hybrid heating mechanism: a MW absorber is added to the samples to efficiently transfer the heat it absorbs from the MW radiation [276]. In addition, an external susceptor is used. It is a secondary microwave absorbent that absorbs microwaves and converts the energy into heat, allowing it to be transferred to the sample through conventional heat transfer modes. The susceptor is coupled with a MW transparent material (with low microwave absorption, allowing the MW penetration) to beneficiate of thermal insulation of heat generated in the sample and by the susceptor. The objective is not only to ensure homogeneous heating of the sample, but also to limit its thermal losses from its surface [277]. For this activity, great focus must be devoted to the selection of suitable MW transparent materials, because their transition to a MW absorbing material depends on the temperature that is reached in the chamber. Then, the material reaches a higher temperature and uniform heating compared to a simple direct microwave heating. The MW transparent material allows to beneficiate of thermal insulation for the generated heat.

The core process is based on already established thermochemical reactions occurring in a devoted kiln, where the SSA is mixed with a sodium source and a reducing agent (for example dry sewage sludge, anthracite, graphite) and treated at temperature operating around 1000°C for more than 15 min [44]. Usually, a fuel is also added to take advantage of the temperature rise. The reaction is based on the calcium ions partial replacement by sodium ions in the phosphates. The expected result is the formation of a soluble $CaNaPO_4$ compound. In the present work, to demonstrate the process feasibility, sodium bicarbonate is used as a sodium ions source, due to its relatively low cost and high availability. Anthracite is used as the absorber. In particular, the SSA source corresponds to 60% of the sample mass, where 25% of $NaHCO_3$ and 15% of carbon are added. All the as-received samples were treated in the same way: after the $NaHCO_3$ and anthracite addition they were placed in the dedicated chamber and inserted into the oven (a 2.4 GHz Panasonic commercial MW oven used for food treatment). The treatment was made on 0.4 g of sample, by setting the MW power at 1000 W for 15 minutes.

The susceptor-assisted microwave heating is referred as a hybrid microwave heating. In the present case, the use of the chamber enhances the microwave heating efficiency. The combined effect of a susceptor and a chamber has several advantages: increased heating efficiency and temperature (better energy transfer), reduced heat loss, enhanced process reproducibility, rapid heating, non-contact heating, quick start-up and stopping, better resource use, reduced costs, the possibility to optimize the susceptor and chamber design, lower manipulation of dangerous substances or chemicals, the ability to treat waste in-situ, and the portability of equipment and processes. Increase in carbon content can allow to reduce the time and/or the power for MW carbothermal reduction reactions.

Leaching tests in MIlliQ water according to Benassi et al. [30] were provided on the as-received samples (RAW SSA) and on the corresponding samples (with $NaHCO_3$ and anthracite added) after MW treatment (MW-SSA). The aim was to evaluate the formation of bioavailable P and the increase of P

solubility in water. XRD analysis was used to verify crystalline structure of SSA before and after the thermochemical recovery.

6.3.   Results and discussion

6.3.1.   SSA characterization

Figure 6.2 shows XRD spectra for samples from 1st campaign BA_C1 and R-BA_C1. Crystalline phases identification confirmed the presence of quartz [SiO_2], albite [$NaAlSi_3O_8$] and iron oxide [Fe_2O_3] in both ashes. In addition, potassium chloride [KCl] and calcium aluminum phosphate [$Ca_9Al(PO_4)_7$] are present in BA_C1, while in R-BA_C1, after the acid leaching operated by the company, no P phases are detected. Gypsum [$CaSO_4 \cdot 2H_2O$] in R-BA_C1 suggests the use of sulfuric acid for P recovery with consequent calcium sulphate formation.
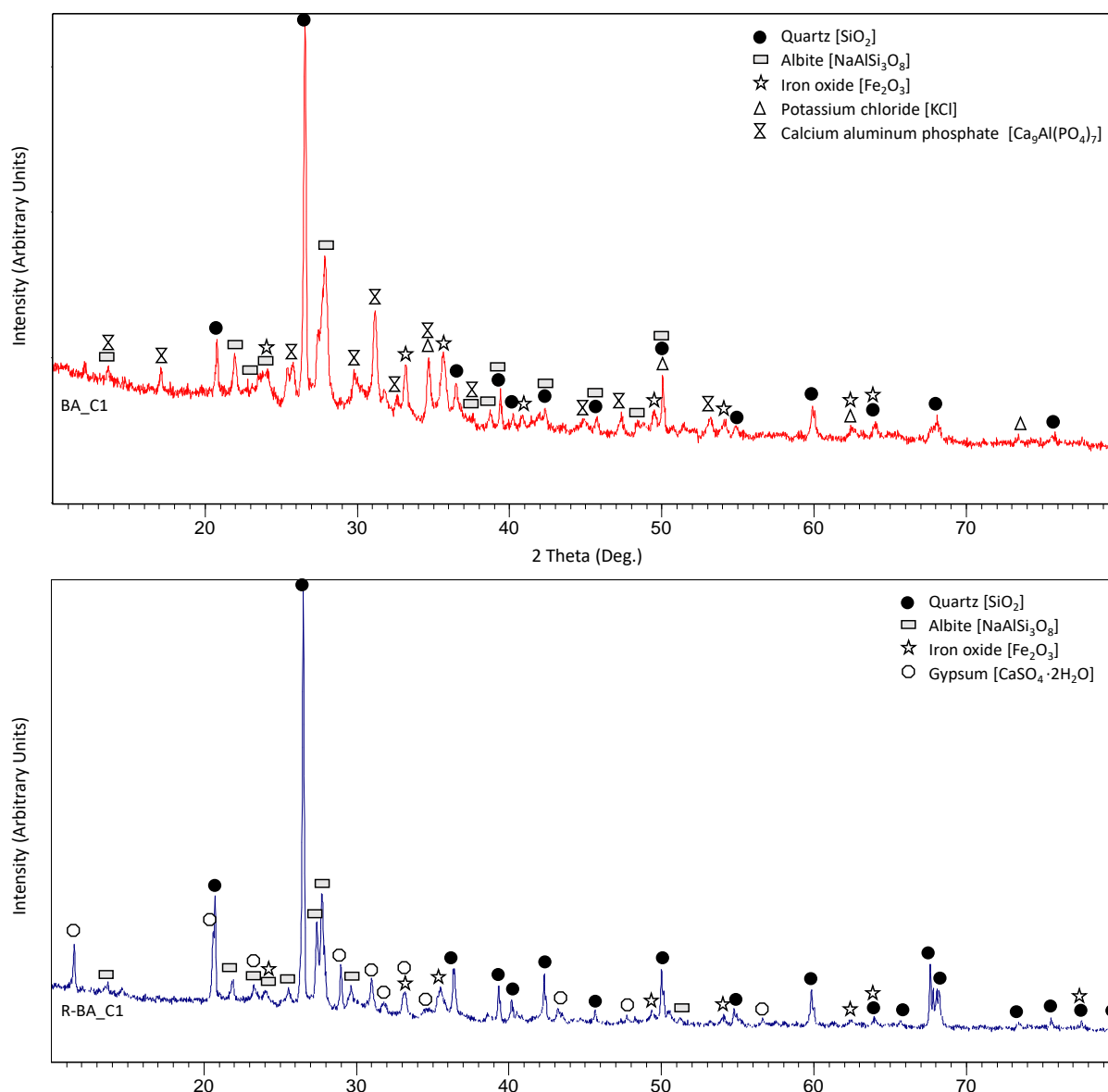
Figure 6.1: XRD patterns of SSA from first campaign: BA_C1 (red spectrum) and R-BA_C1 (blue spectrum).

Table 6.3 reports the crystalline composition recognized from XRD patterns of raw SSA from 2nd and 3rd campaign.

Table 6.3: *Crystalline phases identified by XRD for raw SSA from 2nd and 3rd campaign.*

Crystalline phase	SSA										
	CYC-FA_M2	BO-FA_M2	BA_M2	BO-FA_C2	CYC-FA_C2	BF-FA_C2	BA_C2	CYC-FA_M3	BO-FA_M3	BF-FA_M3	BA_M3
Quartz SiO_2	X	X	X	X	X		X	X	X	X	X
Whitlockite $Ca_{18}Mg_2H_2(PO_4)_{14}$	X	X		X	X	X		X	X	X	X
Calcium iron phosphate hydroxide hydrate $Ca_8Fe(PO_4)_6OH \cdot 10H_2O$									X		
Albite $NaAlSi_3O_8$	X	X	X					X	X		X
Labradorite $(Ca,\underline{Na})(Si,Al)_4O_8$							X				
Anorthite $CaAl(SiO_4)_2$				X	X						
Potassium feldspar $KAlSi_3O_8$			X					X			X
Olivine $MgSiO_4$			X					X			X
Clinoenstatite $(Mg,Fe)(SiO_3)$								X	X		
Iron oxide/Hematite Fe_2O_3				X	X	X	X	X	X		
Lime CaO					X						
Portlandite $Ca(OH)_2$						X				X	
Calcite $CaCO_3$	X			X	X	X		X	X	X	
Calcium chloride hydroxide $CaClOH$						X					
Anhydrite $CaSO_4$						X			X		
Thernadite Na_2SO_4										X	
Sodium chloride/Halite $NaCl$					X	X				X	

All the SSA samples presents quartz [SiO_2] in the matrix except BF-FA_C2, and the main crystalline P compound is whitlockite [$Ca_{18}Mg_2H_2(PO_4)_{14}$] that is missing only in the two bottom ashes from 2nd campaign (BA_M2 and BA_C2). The one other P phase is calcium iron phosphate hydroxide hydrate [$Ca_8Fe(PO_4)_6OH·10H_2O$] detected only in BF-FA_M3. Several different Na-Mg-Al-K-Ca silicates (Albite $NaAlSi_3O_8$, Labradorite $(Ca,Na)(Si,Al)_4O_8$, Anorthite $CaAl(SiO_4)_2$, Potassium feldspar $KAlSi_3O_8$, Olivine $MgSiO_4$, and Clinoenstatite $(Mg,Fe)SiO_3$) are recognized in all samples except in the bag filters fly ash BF-FA_C2 and BF-FA_M3. Iron oxide/hematite [Fe_2O_3] is missing in the mono-incinerated ash from 2nd campaign and in the mono-incinerated BF-FA_M3 and BA_M3 from 3rd campaign. Lime [CaO] is present only in BO-FA_C2, calcium chloride hydroxide [$CaClOH$] only in BF-FA_C2, while portlandite [$Ca(OH)_2$] only in BF-FA_C2 and BF-FA_M3, according to what explained in section 6.2.1. about the addition of Ca compound before the bag filters to perform the dry treatment of the acid flue gas. Probably for the same reason, Ca and Na residual compounds (Anhydrite $CaSO_4$, Thernadite Na_2SO_4 and Sodium chloride/Halite $NaCl$) are also detected in bag filters fly ash. Calcite [$CaCO_3$] is present in all samples except bottom ashes and BO-FA_M2.

6.3.2.   Feasibility study of simultaneous P recovery and SiO_2 from 1st campaign

Starting from 40 g of BA_C1, the results of UV-Vis kit and TXRF analysis on the acid leachate and filtrate solutions after titration at different pH, are visually reported in **Figure 6.2**. P is strongly concentrated in the acid leachate and starting from pH 2 its concentration in the filtrate decreases constantly increasing pH. The main HM (Fe, Cu and Zn) manifest the same behavior. Ca is countertrend due to its addition as titrant to reach higher pH.
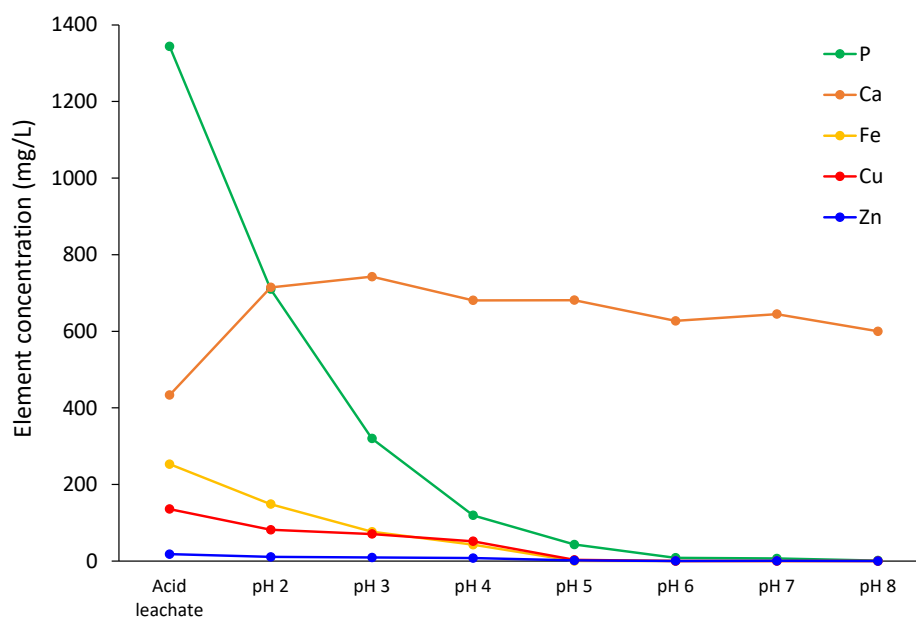
Figure 6.2: Main element concentration in solution (mg/L), after the acid leaching and the titration with Ca(OH)$_2$ 1% w/w at different pH. P content evaluated with spectrophotometric analysis, metals content with TXRF analysis.

The PEE of BA_C1 wet chemical extraction was assumed in an improper way, using P concentration in the raw SSA obtained from XRF analysis (reported in **Table 6.2**), and P concentration in the acid leachate derived from spectrophotometric analysis (see **Figure 6.2**) and converted with **Equation (2.1)**. PEE calculation was made following **Equation (3.1)** to give an idea of the effectiveness of the process. The resulting PEE = 77.9 % suggests a good extraction capability of the selected parameters also for co-combusted SSA.

Using **Equation (4.3)** and **(5.1)** P and HM concentration was assessed, and through **Equation (4.4)**, P precipitation efficiency (PPE) at different pH was calculated. The results are presented in **Figure 6.3** and **Figure 6.4**. P concentration in the precipitates varies from 4.4 to 6.2 % (**Figure 6.3**), showing the best outcome in precipitate at pH 5. In this specific SSA sample (BA_C1), the decreasing trend of P concentration in precipitates in function of increasing pH, recorded for SSA analyzed in chapter 4 (section 4.3.3), is not evident. Also precipitate at pH 8 manifest a satisfying P content (5.6 %) compared to the other pH and the results about PPE are improved: PPE equal to 92 % is recorded already at pH 5, with a percentage very close to 100% for pH 6, 7 and 8 (**Figure 6.4**).
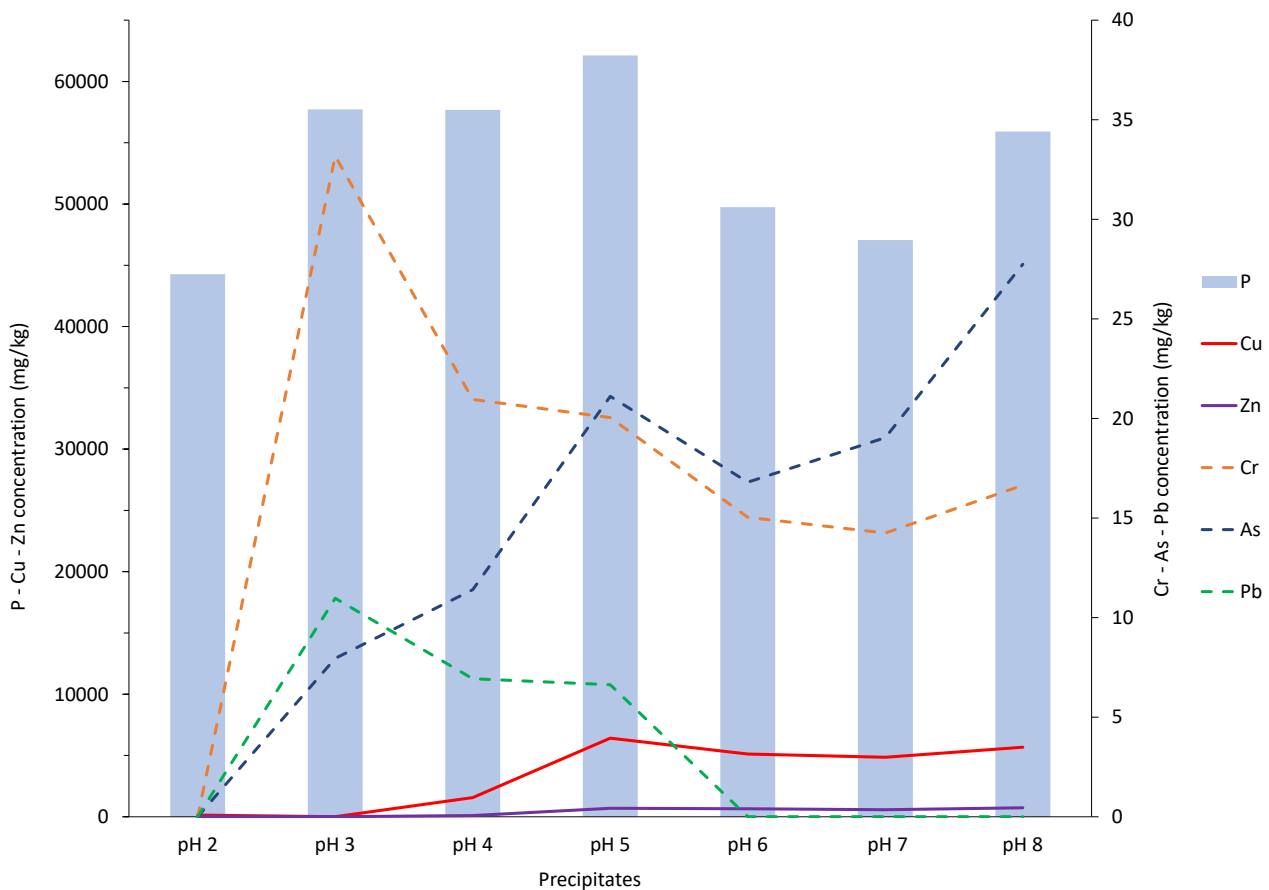
Figure 6.3: *Concentration of elements in precipitates, estimated by mass balance. The concentrations of P, Cu and Zn (represented by a solid line) refer to the left ordinate axis, while the concentrations of Cr tot, As and Pb (represented by dashed lines) refer to the right ordinate axis.*
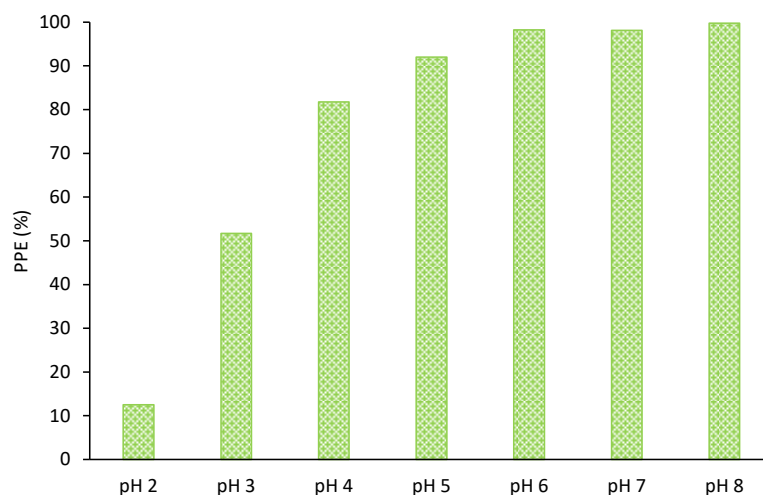
Figure 6.4*: P precipitation efficiency (PPE) during titration at different pH.*

Despite the fulfilling observations, the total P content in precipitates is about a third of that obtained for mono-incinerated SSA in section 4.3.3. (6.2 % versus 17.9 % at pH 5).

Furthermore, the concentration of HM identified in the precipitates (**Figure 6.3**) must be compared with the recent limits defined by Regulation (EU) 1009/2019 [154] for fertilizers and soil improvers presented in **Table 5.5**. All the precipitates at different pH coming from the acid leaching of BA_C1 complain this regulation unless copper (Cu). Cu concentration in the precipitates at pH 4, 5, 6, 7 and 8 was evaluated equal to 1564 mg/Kg, 6413 mg/Kg, 5121 mg/Kg, 4851 mg/Kg and 5668 mg/kg respectively, exceeding a lot the European limit of 600 mg/Kg. In addition, it should be noted that data for Cr in **Figure 6.3** refer to total chromium and not to the hexavalent form regulated, because TXRF technique cannot return the elemental speciation. The coloration of recovered precipitates also suggests the Cu contamination because precipitate at pH 2 is clearly white, while precipitate at pH 8 is light green, as stated in **Figure 6.5**.

Figure 6.5*: P-precipitate at pH 2 (left) and P-precipitates at pH 8 (right) from BA_C1.*

To conclude, considering the proportional precipitation capacity of P and HM in function of increasing pH (see **Figure 6.2**), a suitable pH value to perform the precipitation need to be selected, to achieve a good balance between maximum P and minimum HM content in the precipitates, and a sufficient PPE.

Based on the results presented in this section and what obtained in chapter 4, pH 5 was considered the appropriate point that satisfy the minimal conditions required and combines various favourable aspects. Then, pH 5 was chosen as unique point at which perform the P precipitation of the SSA samples from the other campaigns. It is important to remind that HM contamination in the precipitates is affected by the initial HM concentration in the SSA: co-incinerated ashes are normally richer in metals and their absence in the phosphatic precipitate cannot be guaranteed.

Regarding SiO_2 extraction from R-BA_C1, the procedure allowed to recover 1.54 g of amorphous dried gel, that was characterized with XRD. **Figure 6.6** shows the XRD pattern, free of crystalline peaks as already noted in other samples (see chapter 4). This suggests a minimal contamination of secondary reaction by-products like Na_2SO_4 but the visual inspection of the recovered silica, shows a greenish coloration of the powder (on the right in **Figure 6.6**), with possible other contaminants, such as Cu salts, which presence was already demonstrated in the P precipitates. This is plausible given the SS co-incineration with SSF.

Moreover, it was possible to calculate SiO_2 extraction efficiency (SSE) getting the SiO_2 concentration in R-BA_C1 based on the Si content (16.40 %) detected with XRF from **Table 6.2** and using the conversion factor Si/SiO_2 = 0.468. Considering the 40 g of R-BA_C1 used for silica recovery, $SiO_{2\ ash\ residue}$ results to be 14.02 g. The recovered mass of amorphous SiO_2 corresponds to 1.54 g, thus SEE = 10.98 %, according to **Equation (4.1).** This result is particularly unsatisfactory compared to that obtained in chapter 4 (SEE > 45 %), where a mono-incinerated SSA was investigated. The data suggests that SiO_2 recovery procedure is not suitable for co-incinerated SSA. Must be noted that, as already declares in chapter 4, this calculation is approximate, since it assumes that all the Si present in the solid matrix of ash residue is in form of SiO_2.
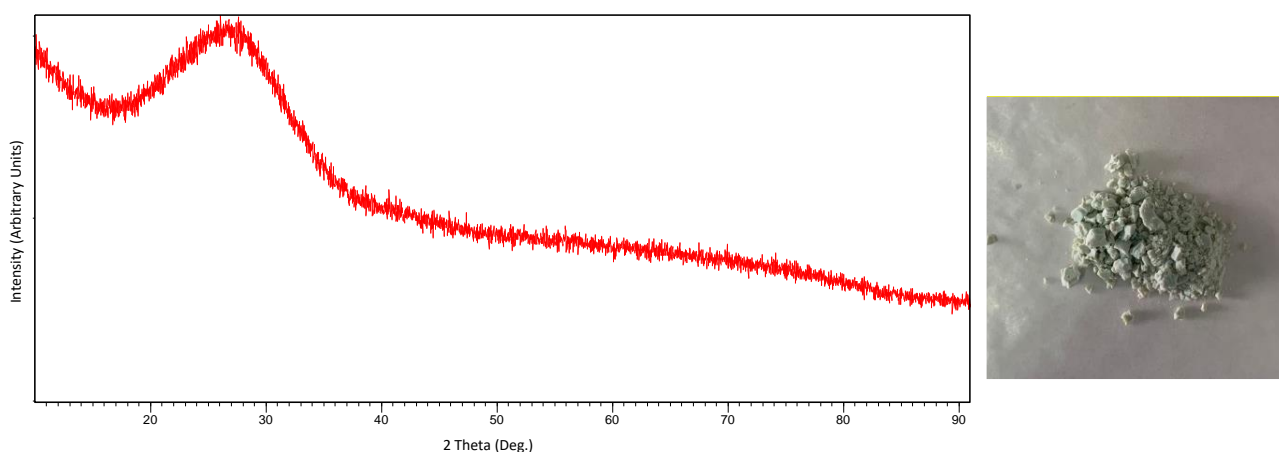
Figure 6.6*: XRD pattern of recovered SiO_2 from R-BA_C1 and image of recovered powder.*

6.3.3. P wet chemical extraction and precipitation

According to what declares in section 6.3.2., pH 5 was adopted for P precipitation trials after acid leaching of the SSA samples. Due to difficulties of pH solution stabilization, it was not possible to always achieve pH 5 during the titration. **Figure 6.7** presents different pH reached after acid leaching, alkali titration, and after recovered precipitates separation. The great alkalinity of bag filters ashes (BF-FA_C2 and BF-FA_M3) can be explained by the addition of basic compounds for the dry treatment of the flue gas discussed in section 6.2.1., while alkalinity of CYC-FA_C2 can be given by the ash stabilization with water and concrete performed in the plant (see **Table 6.1**). All the other SSA present pH < 2.5 after acid leaching.
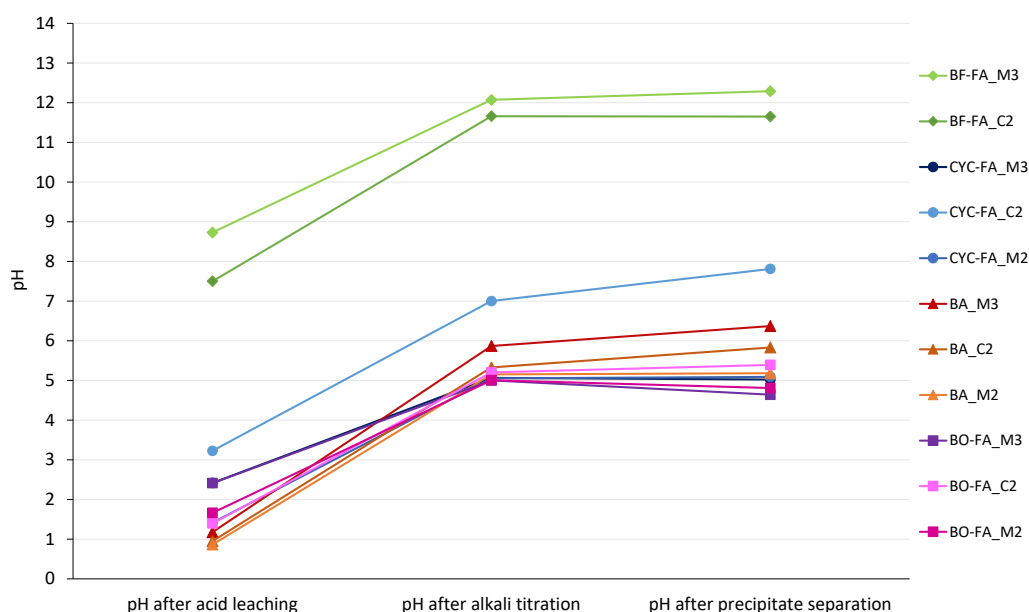
Figure 6.7*: pH variations during P recovery procedure in different SSA samples.*

Figure 6.8 shows PPE and PEE for the SSA from 2nd and 3rd campaign. Remembering that not all the sample titrations were able to reach pH 5, also PPE at different pH was reported. Samples marked with asterisk belong to this category: CYC-FA_C2 at pH = 7.0, BF-FA_C2 at pH = 11.7 and BF-FA_M3 at pH = 12.1. These three samples are indeed the more alkaline ashes that consequently manifest lower PEE (blue squares), very close to zero. The cause is given by higher acid volume or concentration required to leach P in an alkaline ash, because a large amount of acid is used initially to buffer the basic system. As mentioned in section 6.3.2., PEE was calculated based on **Equation (3.1)** using P concentration from two different analytic techniques (XRF results reported in **Table 6.2** for raw SSA, and in this specific case, ICP-OES results converted with **Equation (2.1)** for acid leachate). This is the reason why the PEE results in **Figure 6.8** are not consistent, exceeding 100 %. These data must be considered as an indicative estimate that does not contemplate the measurement uncertainties of the two techniques. More in general, the three boiler fly ashes (BO-FA_M2, BO-FA_C2 and BO-FA_M3) show a

very high PEE, together with CYC-FA_M3. Lower PEE was recorded for bottom ashes (BA_M2, BA_C2 and BA_M3), while PEE of cyclone fly ashes (CYC-FA_M2, CYC-FA_C2 and CYC-FA_M3) is very variable. The last results are interesting and need a more in-depth study because CYC-FA_M3 shows the higher PEE, but it was stabilized with water and concrete in the plant (see **Table 6.1**) exactly as CYC-FA_C2 that instead presents the lower PEE. CYC-FA_M2 was not stabilized with alkaline solution and has a middle PEE.
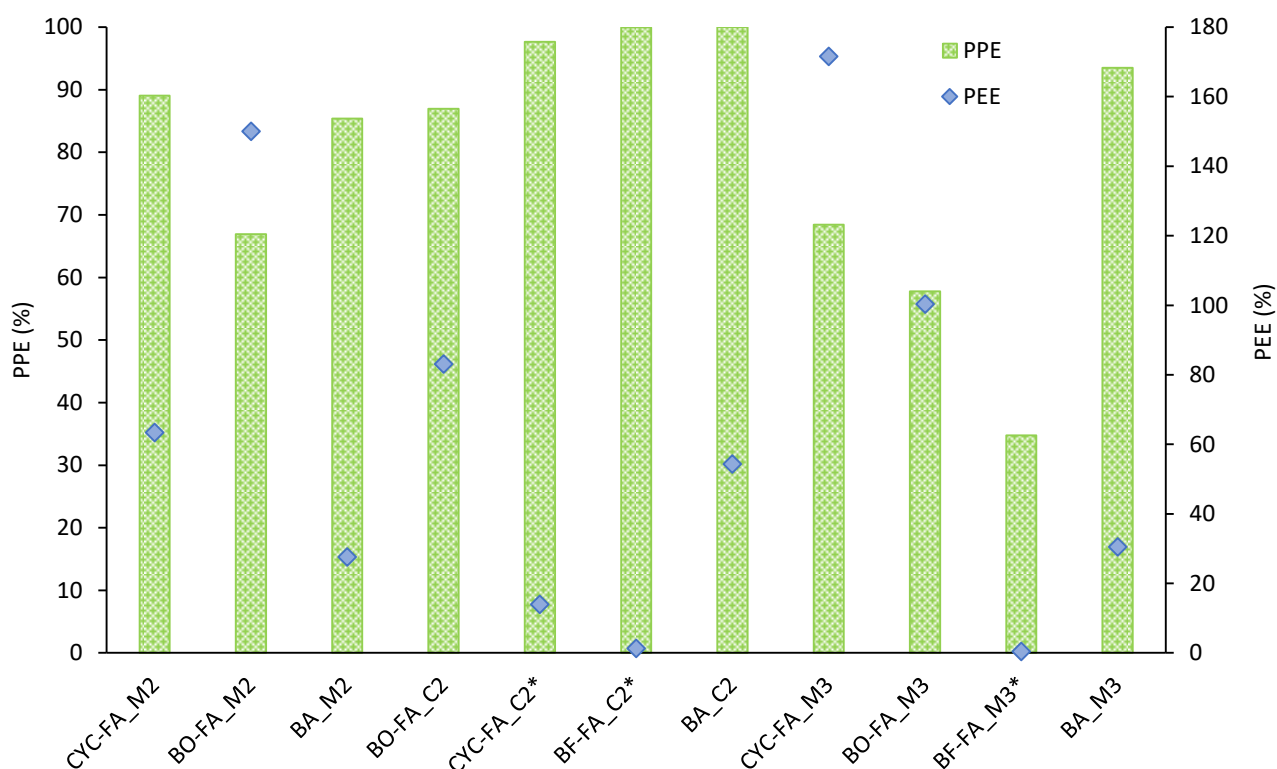
Figure 6.8: *P precipitation efficiency (PPE) at pH 5 as green bars and P extraction efficiency (PEE) as blue squares for all the SSA sample from 2nd and 3rd campaign. *Sample for which precipitation (and PPE) was performed at different pH: CYC-FA_C2 pH = 7.0, BF-FA_C2 pH = 11.7 and BF-FA_M3 pH = 12.1.*

Regarding P and HM content in the precipitate, **Table 6.4** reports the results of the mass balance calculation, expressed in mg/Kg for metals and in P_2O_5 % for P, thanks to conversion factor P/ P_2O_5 = 0.436. Data that do not comply the limits are highlighted in orange in the table. As result, only precipitate from BA_M3 is free of HM and respects the limit. Several samples present Cu above the limit, as already noted for sample BA_C1 from 1st campaign. Anyway, these mass balance calculations should be verified with a complete characterization of the recovered product, such as elemental analysis composition of the matrix to confirm this high HM content that prevents applications in fertilizer sector.

Table 6.4: *HM concentration compared with regulation limits from Table 5.5 and P content, as P_2O_5, in the precipitates at pH 5. *Sample for which precipitation was performed at different pH: CYC-FA_C2 pH = 7.0, BF-FA_C2 pH = 11.7 and BF-FA_M3 pH = 12.1. nd = not detected.*

Element	Limit EU 1009/2019	CYC-FA_M2	BO-FA_M2	BA_M2	BO-FA_C2	CYC-FA_C2*	BF-FA_C2*	BA_C2	CYC-FA_M3	BO-FA_M3	BF-FA_M3*	BA_M3
						mg/kg						
As	40	13	18	4	18	62	129	41	4	0.5	132	9
Cd	1.5-3	0.5	2.4	nd	3.5	55	87	nd	10.3	9.6	nd	1.2
Cr tot	2 (VI)	75	55	28	82	494	nd	253	48	51	1	73
Cu	300-600	105	1248	1166	2411	3443	1719	9550	1756	1819	11	322
Hg	1	nd	nd	nd	nd	nd	nd	nd	nd	nd	nd	nd
Ni	50-100	nd	nd	nd	6.9	188	88	45	nd	nd	nd	12
Pb	120	29	16	13	70	23	3	57	8	10	nd	12
Zn	800-1500	1901	1159	275	6792	32486	748	1386	1780	1560	8	171
						mass % wt						
P_2O_5	12	15.37	24.38	4.17	19.86	6.20	0.43	2.03	34.2	34.5	0.1	6.4

Commenting on the P content in precipitates, P_2O_5 results were reported in **Table 6.4** to compare the values with the minimum percentage fixed by the regulation 1009/2019. These specific P recovered products from SSA could be defined as straight solid inorganic macronutrient fertilizer [154]. A straight solid inorganic macronutrient fertilizer that contains only P as macronutrient shall have a declared content at least of 12 % by mass of total phosphorus pentoxide (P_2O_5). This condition is reached by the samples CYC-FA_M2, BO-FA_M2, BO-FA_C2, CYC-FA_M3 and BO-FA_M3, highlighted in green in the table. The P content in the precipitates reflects the trends displayed in **Figure 6.8**, where the three boiler fly ashes (BO-FA_M2, BO-FA_C2 and BO-FA_M3) showed the highest PEE, together with CYC-FA_M3. Moreover, PPE at pH 5 of boiler fly ashes ranged between 58 % and 87 %, ensuring a final P_2O_5 content in precipitates (BO-FA_M2 = 24.4 %, BO-FA_C2 = 19.9 % and BO-FA_M3 = 34.5 %) close to the minimum content declared for commercial fertilizers i.e., concentrated superphosphate P_2O_5 = 25 %, single superphosphate P_2O_5 = 16 %, and triple super-phosphate (TSP) or dicalcium phosphate P_2O_5 = 38 % [153]. Overall, mono-incinerated boiler fly ashes have higher P_2O_5 concentration in the precipitates. Regarding the cyclone fly ashes, PEE of CYC-FA_M2 was assessed around 60 %, with a PPE around 89 %, allowing to obtain more than 15 % of P_2O_5 in the corresponding precipitate. A lower PPE was recorded for CYC-FA_M3 (circa 68 %), leading however to a very good P_2O_5 content in the corresponding precipitate (34.2 %), probably due to the high PEE. On the other hand, CYC-FA_C2 that present just P_2O_5 = 6.2 % in the precipitate, is also the more contaminated product by HM, considering also that precipitation was performed at pH 7 and not 5, due to the alkalinity of the ash.

Bottom ashes seem to be not appropriate for wet chemical P recovery with the proposed procedure because the P_2O_5 content in the precipitates is low (4.17 %, 2.03 % and 6.4 % for BA_M2, BA_C2 and

BA_M3 respectively), even if all the PPE were attested > 85% (see **Figure 6.8**). Anyway, the P content in precipitates from mono-incinerated BA is higher than co-incinerated BA. In contrary BA_C1 leached and titrated at pH 5 showed a higher final P content in the precipitate equal to 6.2 % and corresponding to 14.2 % of P_2O_5 (see **Figure 6.3**).

The results about P content in the precipitates from bag filters fly ashes, definitely exclude these samples from the opportunity to carry out this wet chemical practice, due to the alkalinity of the ashes. The more suitable SSA for this type of P recovery are mono-incinerated cyclone fly ashes and mono and co-incinerated boiler fly ashes, always monitoring the HM content in the final precipitates.

6.3.4.   P recovery via thermochemical microwave treatment

Table 6.5 reports the XRD crystalline composition of the SSA treated with MW. It can be highlighted the formation of $NaCaPO_4$ in several samples due to MW treatment. Buchwaldite is present in all the MW-SSA except bottom ashes (BA_M2, BA_C2 and BA_M3) and BO-FA_C2. Other crystalline phases containing P (Calcium Magnesium Phosphate $CaMg(P_2O_7)$, Calcium Phosphate $Ca_3(PO)_2$, Berlinite $AlPO_4$, Barringerite Fe_2P, and Sodium Calcium Phosphate Silicate $Na_2Ca_4(PO_4)_2SiO_4$) were also found in various samples; they are different from the P crystalline compounds in the raw SSA before the MW treatment reported in **Table 6.3** (Whitlockite $Ca_{18}Mg_2H_2(PO_4)_{14}$ and Calcium iron phosphate hydroxide hydrate $Ca_8Fe(PO_4)_6OH \cdot 10H_2O$) confirming the chemical reaction and reduction occurred during the intensive heating. BA_M3 is the only MW-SSA that does not present crystalline P forms: considering its XRD spectrum it was essentially amorphous with a broad band from 15 to 35 2ϑ, where only quartz and cristobalite were detected. Several silicates (Sodium Calcium Phosphate Silicate $Na_2Ca_4(PO_4)_2SiO_4$, Nepheline $NaAlSiO_4$, Sodium Aluminum Silicate $Na_6Al_4Si_4O_{17}$, Sodium Calcium Silicate Na_2CaSiO_4, Grossular $Ca_3Al_2(SiO_4)_3$) were identified but not in the bottom ashes and in CYC-FA_M2 and BF-FA_C2. Aluminum oxide compounds were detected in the bag filters ash, as well as Oldhamite CaS and Lime CaO.

In general, the heating mechanism due to microwaves is different from that deriving from conventional ones, with interesting results in terms of temperatures that can be reached in a very brief time frame. Literature reports that calcium phosphates i.e. $Ca_3(PO_4)_2$ conversion to $CaNaPO_4$ occurs at temperatures ranging from 900 to 1000°C [44]. This transformation was confirmed by XRD results in **Table 6.5** suggesting the achievement of high temperatures in a short time. In addition, in the present case, process optimization was not realized. For example, it is reported that the reaction to produce $NaCaPO_4$ can be competitive with Na consumption by the silicon oxides in the SSA [82]. It is evident that a change in MW power and treatment time allows obtaining different experimental setups. Furthermore, a different selection of the raw materials typologies, such as more suitable reactants and quantities used for mixing with SSA, permits to optimize not only the characteristics of the final products but also the process sustainability.

Anyway, the quantification of bioavailable P is not accurate only considering the crystalline composition, because some other P soluble phases could be present in the MW-SSA as amorphous compounds. To test the effective achievement of P soluble form, the results of leaching test in MilliQ water in **Table 6.6** were commented. It is clear a change in the P solubility in water, due to the thermochemical treatment: the availability of P in several MW samples is higher than the RAW SSA by about two orders of magnitude, which strongly support the possibility of directly reusing the products obtained as fertilizers. This result also allows to preform further promising studies about P solubility in ammonium citrate or citric acid, as required by the standard methods for P bioavailability determination in a fertilizer [44]. The procedure is not totally efficient, because for two cyclone fly ashes (MW-CYC-FA_C2, MW-CYC-FA_M3), two bottom ashes (MW-BA_C2, MW-BA_M3) and MW-BF-FA_C2, the increasing of P solubility is minimal or equal to zero. The results suggest dissimilar composition and behavior during MW treatment of the cyclone fly ashes, because on the other hand MW-CYC-FA_M2 shows increased P solubility. Even MW bottom ashes, in which buchwaldite was not present in the matrix, show different performance since MW-BA_M2 clearly manifests P soluble during the leaching test. On the contrary, in MW-BO-FA_C2 buchwaldite was not detected, but its P solubility is evident, like for MW-BO-FA_M3. Moreover, the two MW bag filters ashes display two opposite P solubility, demonstrating that the mono-incinerated one performs better.

Table 6.5: *Crystalline phases identified by XRD for SSA from 2nd and 3rd campaign after microwave thermochemical treatment (MW).*

Crystalline phase	MW-SSA										
	CYC-FA_M2	BO-FA_M2	BA_M2	BO-FA_C2	CYC-FA_C2	BF-FA_C2	BA_C2	CYC-FA_M3	BO-FA_M3	BF-FA_M3	BA_M3
Quartz/Cristobalite SiO_2	X	X	X	X						X	X
Buchwaldite $NaCa(PO_4)$	X	X			X	X		X	X	X	
Calcium Magnesium Phosphate $CaMg(P_2O_7)$				X	X						
Calcium Phosphate $Ca_3(PO)_2$										X	
Berlinite $AlPO_4$			X	X							
Barringerite Fe_2P	X	X	X				X	X	X		
Sodium Calcium Phosphate Silicate $Na_2Ca_4(PO_4)_2SiO_4$								X	X	X	
Nepheline $NaAlSiO_4$		X		X	X						
Sodium Aluminum Silicate $Na_6Al_4Si_4O_{17}$								X	X		
Sodium Calcium Silicate Na_2CaSiO_4										X	
Grossular $Ca_3Al_2(SiO_4)_3$										X	
Calcium silicide $CaSi_2$										X	
Calcium Aluminum Oxide $Ca_5Al_6O_{14}$						X					
Sodium Aluminum Oxide $NaAlO_2$										X	
Iron Sulfide FeS				X	X						
Oldhamite CaS						X				X	
Lime CaO					X	X				X	
Portlandite $Ca(OH)_2$					X						
Silicon carbide SiC							X				
Periclase MgO										X	

Table 6.6: *Elemental concentration (mg/L) resulting from ICP-OES analysis of leaching test in MilliQ water of RAW and MW SSA. nd = not detected, < LOQ = below instrumental limit of quantification. Continues in next page.*

Element	Sample	CYC-FA_M2	BO-FA_M2	BA_M2	BO-FA_C2	CYC-FA_C2	BF-FA_C2
				mg/L			
P	RAW	0.05 ± 0.01	< LOQ	0.12 ± 0.03	0.1 ± 0.02	< LOQ	< LOQ
	MW	18.8 ± 4.4	18.9 ± 4.4	14.9 ± 3.5	15 ± 3.5	1.1 ± 0.3	< LOQ
Al	RAW	7.7 ± 1.5	0.22 ± 0.04	0.2 ± 0.04	2.2 ± 0.4	31 ± 6	0.13 ± 0.03
	MW	12 ± 2	1.9 ± 0.4	0.45 ± 0.09	12.1 ± 2.4	0.11 ± 0.02	128 ± 25
As	RAW	< LOQ	0.03 ± 0.01	< LOQ	< LOQ	< LOQ	< LOQ
	MW	0.02 ± 0.004	< LOQ	0.02 ± 0.005	< LOQ	< LOQ	< LOQ
Ba	RAW	0.16 ± 0.04	0.12 ± 0.03	0.04 ± 0.01	1.65 ± 0.42	0.25 ± 0.06	2.83 ± 0.72
	MW	0.22 ± 0.06	0.11 ± 0.03	0.12 ± 0.03	0.15 ± 0.04	0.28 ± 0.07	9.5 ± 2.41
Ca	RAW	173 ± 32	160 ± 29	152 ± 28	413 ± 76	332 ± 61	2486 ± 457
	MW	1.8 ± 0.5	2.5 ± 0.6	3.8 ± 1	1.6 ± 0.4	49 ± 13	261 ± 67
Cr	RAW	0.03 ± 0.01	0.02 ± 0.004	0.13 ± 0.03	< LOQ	0.02 ± 0.01	0.07 ± 0.02
	MW	< LOQ	< LOQ	< LOQ	< LOQ	< LOQ	nd
Cu	RAW	< LOQ	< LOQ	< LOQ	0.59 ± 0.13	< LOQ	0.94 ± 0.21
	MW	0.09 ± 0.02	0.07 ± 0.02	0.05 ± 0.01	0.85 ± 0.19	0.03 ± 0.01	0.12 ± 0.03
Fe	RAW	nd	nd	nd	nd	nd	nd
	MW	0.4 ± 0.08	0.41 ± 0.08	0.77 ± 0.15	0.33 ± 0.06	< LOQ	nd
K	RAW	12 ± 3	12 ± 3	11 ± 2	22 ± 5	369 ± 86	1090 ± 255
	MW	30 ± 7	29 ± 7	6 ± 1	27 ± 6	57 ± 13	57 ± 13
Mg	RAW	5.5 ± 1	3.6 ± 0.7	5.9 ± 1.1	< LOQ	< LOQ	< LOQ
	MW	0.3 ± 0.05	0.48 ± 0.09	0.85 ± 0.15	0.3 ± 0.05	4.4 ± 0.8	< LOQ
Na	RAW	6.7 ± 1.6	4.9 ± 1.2	13.4 ± 3.2	27.2 ± 6.5	268 ± 64	8369 ± 1997
	MW	84 ± 20	108 ± 26	68 ± 16	115 ± 27	165 ± 39	142 ± 34
Pb	RAW	< LOQ	nd	< LOQ	0.34 ± 0.11	< LOQ	17.71 ± 5.75
	MW	< LOQ	< LOQ	< LOQ	< LOQ	nd	nd
Ti	RAW	nd	nd	nd	nd	nd	nd
	MW	0.05 ± 0.01	0.07 ± 0.02	0.03 ± 0.01	0.03 ± 0.01	< LOQ	nd
Zn	RAW	< LOQ	nd	nd	0.69 ± 0.19	< LOQ	1.73 ± 0.47
	MW	0.11 ± 0.03	0.05 ± 0.01	0.08 ± 0.02	0.06 ± 0.02	< LOQ	0.18 ± 0.05

Element	Sample	BA_C2	CYC-FA_M3	BO-FA_M3	BF-FA_M3	BA_M3
				mg/L		
P	RAW	< LOQ	< LOQ	< LOQ	< LOQ	0.02 ± 0.004
	MW	1.2 ± 0.3	0.25 ± 0.06	14 ± 3.3	15.3 ± 3.6	2.7 ± 0.6
Al	RAW	11 ± 2	2.4 ± 0.5	0.35 ± 0.07	0.7 ± 0.1	0.73 ± 0.15
	MW	0.1 ± 0.02	6.3 ± 1.3	2.3 ± 0.5	1520 ± 302	0.8 ± 0.2
As	RAW	< LOQ	nd	nd	< LOQ	< LOQ
	MW	0.03 ± 0.01	< LOQ	0.06 ± 0.01	1.1 ± 0.2	0.02 ± 0.005
Ba	RAW	0.05 ± 0.01	0.13 ± 0.03	0.4 ± 0.1	0.23 ± 0.06	0.03 ± 0.01
	MW	0.94 ± 0.24	0.4 ± 0.1	0.13 ± 0.03	0.4 ± 0.1	0.04 ± 0.01
Ca	RAW	47 ± 9	505 ± 93	745 ± 137	469 ± 86	96 ± 18
	MW	36 ± 9	30 ± 6	1.4 ± 0.3	22 ± 4	0.3 ± 0.06
Cr	RAW	0.11 ± 0.03	0.04 ± 0.01	0.03 ± 0.01	0.04 ± 0.01	0.03 ± 0.01
	MW	< LOQ	< LOQ	< LOQ	nd	< LOQ
Cu	RAW	< LOQ	< LOQ	< LOQ	< LOQ	< LOQ
	MW	< LOQ	< LOQ	0.14 ± 0.03	< LOQ	0.1 ± 0.02
Fe	RAW	nd	< LOQ	nd	nd	nd
	MW	0.04 ± 0.01	nd	1.2 ± 0.2	0.7 ± 0.1	0.1 ± 0.02
K	RAW	2.5 ± 0.6	45 ± 11	24 ± 6	120 ± 28	6.4 ± 1.5
	MW	20 ± 5	47 ± 11	7.5 ± 1.7	370 ± 87	3.2 ± 0.75
Mg	RAW	< LOQ	4.2 ± 0.8	0.06 ± 0.01	< LOQ	1.2 ± 0.2
	MW	1 ± 0.2	0.31 ± 0.06	0.6 ± 0.1	0.04 ± 0.01	0.22 ± 0.04
Na	RAW	8 ± 2	24 ± 6	9 ± 2	13898 ± 3316	94 ± 22
	MW	124 ± 30	246 ± 59	61 ± 15	12259 ± 2925	73 ± 17
Pb	RAW	< LOQ	nd	nd	0.13 ± 0.04	nd
	MW	nd	nd	< LOQ	nd	nd
Ti	RAW	nd	nd	nd	nd	nd
	MW	nd	nd	0.03 ± 0.01	< LOQ	< LOQ
Zn	RAW	nd	nd	nd	0.03 ± 0.01	nd
	MW	0.02 ± 0.01	0.03 ± 0.01	0.09 ± 0.02	0.18 ± 0.05	0.05 ± 0.01

In order to propose the possible direct use of MW-SSA samples as fertilizers, the leachable metals must also be evaluated. **Table 6.6** shows that the water solubility of Pb and Cr is decreased after the treatment. This is another clear advantage of the thermochemical method: literature reports that the main components of the SSA are generally not transferred into the gaseous phases except potassium [87]. Instead, thermochemical treatment has the advantage that HM can be transferred into a gaseous phase and eventually separated in the off-gas treating system [87]. As a consequence, potassium chloride and HM chlorides are the main expected components that are generally found in the off-gas. HM removal is normally improved by adjusting temperature, generally resulting in a low concentration of leachable form after thermochemical treatment at 1000°C [81,87]. Additionally, some non-volatile HM such as As, Cr and Ni can show low removal rates even at high temperatures [83,86].

However, these literature results should be investigated in more detail to enhance the present treatment because this is the first work about MW treatments of SSA to realize thermochemical reactions. A process optimization can be highly onerous and time-consuming if the thermochemical conventional method is used [278], while the new MW proposed technology results feasible with the need for low treatment times (15 minutes in the present work), making the technology optimization very promising and low time-consuming.

6.4. Conclusions

In this chapter an overall comparison of two different P recovery techniques applied to the same SSA was addressed. A final conclusion about the suitability of each method in function of the ash origin can be made.

The first investigation of simultaneous P and SiO_2 recovery from co-combusted bottom ash of the 1st sampling (BA_C1 and R-BA_C1) proved that wet chemical extraction of P can be successfully applied also to a co-incinerated ash (SS + SSF). It was possible to obtain a very good PPE already starting from pH 5 (> 92 %) and reaching at the same pH the higher P content in the precipitate equal to 6.2 % (corresponding to 14.2 % of P_2O_5). Only Cu affected the purity of the precipitates, exceeding a lot the European limit of 600 mg/Kg at pH 4, 5, 6, 7 and 8. It is important to underline that the types of fuel used in the combustion chamber and their ratio (SS and SSF) can influence the HM concentration in the ash. So, a preventive selection of the fuel type at the plant can also overcome the Cu contamination problem in the P recovered precipitates. According to these considerations, pH 5 was chosen as appropriate value for P precipitation of SSA from 2nd and 3rd sampling. On the other side, SiO_2 recovery from R-BA_C1 produced an amorphous silica free from any salts according to XRD analysis but contaminated by colored greenish pollutants. An SSE around 11% was calculated, leading a not satisfying result and discouraging SiO_2 recovery from the residue of a co-combusted SSA.

The comprehensive study carried out on the other 11 SSA samples, based on amount of recovered P, confirmed that the more suitable SSA for P wet chemical extraction are mono-incinerated cyclone fly ashes and mono and co-incinerated boiler fly ashes. Bag filters fly ashes are inadequate for this recovery method due to their alkalinity and the large consumption of acid needed to achieve a minimal PEE. Mono and co-incinerated bottom ashes present different performances in the two campaigns, with PEE lower than 54 % but PPE higher than 85 %. In any case, all the precipitates resulted contaminated (except BA_M3) by at least one of the HM ruled by the current legislation (As, Cd, Cu, Ni and Zn). For this reason, always a screening of the HM content in the final precipitates must be performed also using additional analysis on the recovered products.

To conclude, the selection of the best recovery route is complex, due to the multicriteria evaluation that is necessary. Origin and alkalinity of the ash, P extraction efficiency (PEE), P precipitation efficiency (PPE), P concentration in the recovered precipitates and HM contamination that must comply EU regulation, are all relevant aspects that should be taken into account.

Contextually, in this work a new thermochemical microwave technology to obtain soluble P from SSA is presented. It is based on a patented chamber that allows samples to rapidly absorb MW energy and maintain internal thermal insulation to optimize the treatment. This results in faster heating, with limited reaction times, and lower energy consumption compared with conventional heating systems.

Then a reduced environmental impact in comparison with conventional thermochemical processes is also envisaged.

The results of the research are very promising in terms of the P bioavailability of the treated ash, thanks to the formation of buchwaldite $CaNaPO_4$. In particular, P appears to increase its solubility in water by about two orders of magnitude in all the boiler fly ashes (mono and co-combusted). Cyclone fly ashes manifest variable performances, as already noted for the wet chemical extraction, showing increased P solubility only in sample CYC-FA_M2. The same for bottom ashes, for which, in this case, only BA_M2 has relevant P soluble content. Surprisingly, one of the most underdog samples (bag filter ash BF-FA_M3) gave an excellent result in terms of P solubility. In general, a more in-depth study should be conducted on the nature of the starting ash and additives, and on the control of the reaction conditions in the chamber, such as temperature and amount and homogeneity of the introduced mass. Moreover, solubility of HM (Pb and Cr) is also reduced because of the treatment.

To conclude, the new proposed technologies open different scenarios, connected with new strategies concerning SSA management: SSA not suited for wet chemical extraction to produce P rich precipitates can be treated with the eco-friendly thermochemical MW method to generate MW-SSA to be used as raw fertilizers, and vice versa. This is the example of BF-FA_M3 that is clearly not eligible for wet chemical extraction but suitable for P solubility conversion with the MW treatment. Vice versa, MW-BA_M3 does not present high bioavailability of P, but from BA_M3 can be recovered a P precipitate without any HM contaminant and with a P_2O_5 content equal to 6.4%.

Acknowledgements

7. CONCLUSIONS

The characterization of rice husk poultry litter ash and a first attempt of P recovery from it confirmed this biomass as a valuable secondary P source, using the acid leaching method. More in general, it is a waste with a low heavy metals content and its exploitation for P recovery could be cleverly adopted, following the Portuguese example of mono-incineration. The optimization of the recovery process from a statistical and environmental point of view, allowed to propose the better solution for this type of waste, not yet thoroughly studied like other biomasses. Moreover, the evaluation of ash residues as basis for other eco-materials was investigated through the amorphous silica extraction. The experience resulted to be feasible but not effective, especially considering the environmental sustainability of the process and the low yield.

The widely applied wet chemical extraction was then adopted to treat Italian and foreign sewage sludge ash, pushing the procedure towards the subsequent step of P precipitation. With different acid leaching parameters, a more satisfying P recovery rate was achieved, according to the results already presented in literature. The additional monitoring of P and heavy metals precipitation grade, allowed to confirm the strong dependence of both phosphate and metal compounds saturation on the pH of the leachate. The issue of co-precipitation of contaminants, prevents the use of the recovered products as fertilizers, forcing to choose a compromise between higher P precipitation efficiency and lower heavy metals content. Furthermore, in the case of sewage sludge ash, silica recovery reached a higher extraction efficiency, probably thanks to the higher initial amount of silicon in the ash.

Alongside, to overcome the problem of heavy metals contamination in the sewage sludge ash, alternative preparation of the sample before the acid extraction was performed. Taking advantage of pozzolanic and carbonation reactions, was demonstrated that a storage period of the ash before the P recovery could be beneficial for heavy metals stabilization.

In addition, a complementary comparison among extraction efficiency of P from ashes, pyrochars and hydrochars was studied. Using wet chemical extraction and precipitation, was confirmed that the recovered products could be advantageous fertilizers, thanks to their P content. Anyway, a more exhaustive analysis could be done only after evaluation of their heavy metals content.

In the end, a novel microwave patented method, that exploits thermochemical reactions, was applied to investigate the ash change of use, avoiding further processing (like wet chemical extraction) for P recovery. The transformation of P crystalline structure in the ash, allowed to obtain a more soluble P phase, useful for the application of the ash as fertilizer as-is, consuming very low energy compared to the traditional thermochemical treatments.

To conclude, as declared in the introduction, this research across different samples and different techniques for P recovery, is intended to give to national authorities and companies the basis to enter

the field of study with the appropriate scientific evaluations to keep up with the EU. The occasion to investigate so many different samples let to the opportunity to compare the national and the foreign results about P recovery operated by wet chemical extraction. Moreover, as future perspectives, the innovative thermochemical treatment, for now applied only to Italian samples, could be proposed also for other sewage sludge and poultry litter ash samples. Of course, considerations done in these three years should be followed by a techno-economic assessment of the affordable investment to industries, to complete the work and transforming academic research in technology transfer.

8. REFERENCES

1.   Ruttenberg, K.C. Phosphorus Cycle. *Encycl. Ocean Sci.* 2001, 401–412.

2.   Mackey, K.R.M.; Paytan, A. Phosphorus Cycle. *Encycl. Microbiol.* **2009**, 322–334, doi:10.1016/B978-012373944-5.00056-0.

3.   U.S. Geological Survey *Mineral Commodity Summaries 2022*; 2022; ISBN 9780333227794.

4.   Desmidt, E.; Ghyselbrecht, K.; Zhang, Y.; Pinoy, L.; Van Der Bruggen, B.; Verstraete, W.; Rabaey, K.; Meesschaert, B. Global phosphorus scarcity and full-scale P-recovery techniques: A review. *Crit. Rev. Environ. Sci. Technol.* **2015**, *45*, 336–384, doi:10.1080/10643389.2013.866531.

5.   Reijnders, L. Phosphorus resources, their depletion and conservation, a review. *Resour. Conserv. Recycl.* **2014**, *93*, 32–49, doi:10.1016/j.resconrec.2014.09.006.

6.   Samreen, S.; Kausar, S. Phosphorus Fertilizer: The Original and Commercial Sources. In *Phosphorus*; Zhang, T., Ed.; IntechOpen: Rijeka, 2019.

7.   Cordell, D.; Drangert, J.O.; White, S. The story of phosphorus: Global food security and food for thought. *Glob. Environ. Chang.* **2009**, *19*, 292–305, doi:10.1016/j.gloenvcha.2008.10.009.

8.   Food and Agriculture Organization of the United Nations (FAO) *World fertilizer trends and outlook to 2022*; Rome, 2019;

9.   Liu, Y.; Chen, J. Phosphorus Cycle. In *Encyclopedia of Ecology (Second Edition)*; Fath, B.B.T.-E. of E. (Second E., Ed.; Elsevier: Oxford, 2014; pp. 181–191 ISBN 978-0-444-64130-4.

10.   Jupp, A.R.; Beijer, S.; Narain, G.C.; Schipper, W.; Slootweg, J.C. Phosphorus recovery and recycling-closing the loop. *Chem. Soc. Rev.* **2021**, *50*, 87–101, doi:10.1039/d0cs01150a.

11.   Mayer, B.K.; Baker, L.A.; Boyer, T.H.; Drechsel, P.; Gifford, M.; Hanjra, M.A.; Parameswaran, P.; Stoltzfus, J.; Westerhoff, P.; Rittmann, B.E. Total Value of Phosphorus Recovery. *Environ. Sci. Technol.* **2016**, *50*, 6606–6620, doi:10.1021/acs.est.6b01239.

12.   United Nations General Assembly *Transforming our world: the 2030 Agenda for Sustainable Development*; 2015; Vol. 16301;.

13.   European Commission *Study on the EU's list of Critical Raw Materials (2020) - Final Report*; 2020;

14.   European Commission *Circular Economy Action Plan*; 2015;

15.   Diakosavvas, D.; Frezal, C. Bio-economy and the sustainability of the agriculture and food system: Opportunities and policy challenges. *OECD Food, Agric. Fish. Pap.* **2019**, doi:10.1787/d0ad045d-en.

16.   Eurostat Consumption of inorganic fertilizers Available online: https://www.fao.org/3/ca6746en/ca6746en.pdf.

17.   Chojnacka, K.; Moustakas, K.; Witek-Krowiak, A. Bio-based fertilizers: A practical approach towards circular economy. *Bioresour. Technol.* **2020**, *295*, doi:10.1016/j.biortech.2019.122223.

18.   Blackwell, M.; Darch, T.; Haslam, R. Phosphorus use efficiency and fertilizers: Future opportunities for improvements. *Front. Agric. Sci. Eng.* **2019**, *6*, 332–340, doi:10.15302/J-FASE-2019274.

19.   Kominko, H.; Gorazda, K.; Wzorek, Z. Potentiality of sewage sludge-based organo-mineral fertilizer production in Poland considering nutrient value, heavy metal content and phytotoxicity for rapeseed crops. *J. Environ. Manage.* **2019**, *248*, 109283,

doi:10.1016/j.jenvman.2019.109283.

20. Ohtake, H.; Tsuneda, S. *Phosphorus Recovery and Recycling*; 2019; ISBN 9780470740774.

21. Delgado, L.; Catarino, A.S.; Eder, P.; Litten, D.; Luo, Z.; Villanueva, A. *End of waste criteria - Final report*; 2008; Vol. 14; ISBN 9789279134227.

22. Nättorp, A.; Kabbe, C.; Matsubae, K.; Ohtake, H. Development of Phosphorus Recycling in Europe and Japan. In *Phosphorus Recovery and Recycling*; Ohtake, H., Tsuneda, S., Eds.; Springer Singapore: Singapore, 2019; pp. 3–27 ISBN 978-981-10-8031-9.

23. Ott, C.; Rechberger, H. The European phosphorus balance. *Resour. Conserv. Recycl.* **2012**, *60*, 159–172, doi:10.1016/J.RESCONREC.2011.12.007.

24. van Dijk, K.C.; Lesschen, J.P.; Oenema, O. Phosphorus flows and balances of the European Union Member States. *Sci. Total Environ.* **2016**, *542*, 1078–1093, doi:10.1016/J.SCITOTENV.2015.08.048.

25. Cieślik, B.; Konieczka, P. A review of phosphorus recovery methods at various steps of wastewater treatment and sewage sludge management. The concept of "no solid waste generation" and analytical methods. *J. Clean. Prod.* **2017**, *142*, 1728–1740, doi:10.1016/j.jclepro.2016.11.116.

26. Zuthi, M.F.R.; Guo, W.S.; Ngo, H.H.; Nghiem, L.D.; Hai, F.I. Enhanced biological phosphorus removal and its modeling for the activated sludge and membrane bioreactor processes. *Bioresour. Technol.* **2013**, *139*, 363–374, doi:10.1016/j.biortech.2013.04.038.

27. Woods, N.C.; Sock, S.M.; Daigger, G.T. Phosphorus recovery technology modeling and feasibility evaluation for municipal wastewater treatment plants. *Environ. Technol. (United Kingdom)* **1999**, *20*, 663–679, doi:10.1080/09593332008616862.

28. Williams, S. Struvite precipitation in the sludge stream at slough wastewater treatment plant and opportunities for phosphorus recovery. *Environ. Technol. (United Kingdom)* **1999**, *20*, 743–747, doi:10.1080/09593332008616869.

29. Eurostat Sewage sludge production and disposal Available online: https://ec.europa.eu/eurostat/databrowser/view/ENV_WW_SPD__custom_4522968/default/table?lang=en.

30. Benassi, L.; Zanoletti, A.; Depero, L.E.; Bontempi, E. Sewage sludge ash recovery as valuable raw material for chemical stabilization of leachable heavy metals. *J. Environ. Manage.* **2019**, *245*, 464–470, doi:10.1016/j.jenvman.2019.05.104.

31. Hudcová, H.; Vymazal, J.; Rozkošný, M. Present restrictions of sewage sludge application in agriculture within the European Union. *Soil Water Res.* **2019**, *14*, 104–120, doi:10.17221/36/2018-SWR.

32. Kratz, S.; Vogel, C.; Adam, C. *Agronomic performance of P recycling fertilizers and methods to predict it : a review*; Springer Netherlands, 2019; Vol. 115; ISBN 0123456789.

33. Köninger, J.; Lugato, E.; Panagos, P.; Kochupillai, M.; Orgiazzi, A.; Briones, M.J.I. Manure management and soil biodiversity: Towards more sustainable food systems in the EU. *Agric. Syst.* **2021**, *194*, doi:10.1016/j.agsy.2021.103251.

34. Langeveld, K. Phosphorus Recovery into Fertilizers and Industrial Products by ICL in Europe. In *Phosphorus Recovery and Recycling*; Ohtake, H., Tsuneda, S., Eds.; Singapore, 2019; pp. 235–251.

35. Komiyama, T.; Ito, T. The characteristics of phosphorus in animal manure composts. *Soil Sci. Plant Nutr.* **2019**, *65*, 281–288, doi:10.1080/00380768.2019.1615384.

36. Guan, Q.; Zeng, G.; Song, J.; Liu, C.; Wang, Z.; Wu, S. Ultrasonic power combined with seed

materials for recovery of phosphorus from swine wastewater via struvite crystallization process. *J. Environ. Manage.* **2021**, *293*, 112961, doi:10.1016/j.jenvman.2021.112961.

37. Rabinovich, A.; Heckman, J.R.; Lew, B.; Rouff, A.A. Magnesium supplementation for improved struvite recovery from dairy lagoon wastewater. *J. Environ. Chem. Eng.* **2021**, *9*, 105628, doi:10.1016/j.jece.2021.105628.

38. Nusselder, S.; de Graaff, L.G.; Odegard, I.Y.R.; Vandecasteele, C.; Croezen, H.J. Life cycle assessment and nutrient balance for five different treatment methods for poultry litter. *J. Clean. Prod.* **2020**, *267*, 121862, doi:10.1016/j.jclepro.2020.121862.

39. Kacprzak, M.; Malińska, K.; Grosser, A.; Sobik-Szołtysek, J.; Wystalska, K.; Dróżdż, D.; Jasińska, A.; Meers, E. Cycles of carbon, nitrogen and phosphorus in poultry manure management technologies–environmental aspects. *Crit. Rev. Environ. Sci. Technol.* **2022**, *0*, 1–25, doi:10.1080/10643389.2022.2096983.

40. Eurostat Production of meat: poultry Available online: https://ec.europa.eu/eurostat/databrowser/view/tag00043/default/map?lang=en.

41. Eurostat Glossary: Biomass Available online: https://ec.europa.eu/eurostat/statistics-explained/index.php?title=Glossary:Biomass.

42. European Comission *Disposal and recycling routes for sewage sludge - part 2: regulatory report*; 2001; Vol. 0;

43. Takahashi, M.; Kato, S.; Shima, H.; Sarai, E.; Ichioka, T.; Hatyakawa, S.; Miyajiri, H. Technology for recovering phosphorus from incinerated wastewater treatment sludge. *Chemosphere* **2001**, *44*, 23–29, doi:10.1016/S0045-6535(00)00380-5.

44. Zhu, Y.; Zhai, Y.; Li, S.; Liu, X.; Wang, B.; Liu, X.; Fan, Y.; Shi, H.; Li, C.; Zhu, Y. Thermal treatment of sewage sludge: A comparative review of the conversion principle, recovery methods and bioavailability-predicting of phosphorus. *Chemosphere* **2022**, *291*, 133053, doi:10.1016/j.chemosphere.2021.133053.

45. Kwapinski, W.; Kolinovic, I.; Leahy, J.J. Sewage Sludge Thermal Treatment Technologies with a Focus on Phosphorus Recovery: A Review. *Waste and Biomass Valorization* **2021**, *12*, 5837–5852, doi:10.1007/s12649-020-01280-2.

46. Havukainen, J.; Thanh, M.; Hermann, L.; Horttanainen, M.; Mikkilä, M.; Deviatkin, I.; Linnanen, L. Potential of phosphorus recovery from sewage sludge and manure ash by thermochemical treatment. *Waste Manag.* **2016**, *49*, 221–229, doi:10.1016/j.wasman.2016.01.020.

47. Hu, M.; Ye, Z.; Zhang, H.; Chen, B.; Pan, Z. Thermochemical conversion of sewage sludge for energy and resource recovery : technical challenges and prospects. *Environ. Pollut. Bioavailab.* **2021**, *33*, 145–163, doi:10.1080/26395940.2021.1947159.

48. Hu, M.; Hu, H.; Ye, Z.; Tan, S.; Yin, K.; Chen, Z.; Guo, D.; Rong, H.; Wang, J.; Pan, Z.; et al. A review on turning sewage sludge to value-added energy and materials via thermochemical conversion towards carbon neutrality. *J. Clean. Prod.* **2022**, *379*, 134657, doi:10.1016/j.jclepro.2022.134657.

49. Cyr, M.; Coutand, M.; Clastres, P. Technological and environmental behavior of sewage sludge ash (SSA) in cement-based materials. *Cem. Concr. Res.* **2007**, *37*, 1278–1289, doi:10.1016/j.cemconres.2007.04.003.

50. Donatello, S.; Tong, D.; Cheeseman, C.R. Production of technical grade phosphoric acid from incinerator sewage sludge ash (ISSA). *Waste Manag.* **2010**, *30*, 1634–1642, doi:10.1016/j.wasman.2010.04.009.

51. Paneque, M.; de la Rosa, J.M.; Patti, A.F.; Knicker, H. Changes in the bio-availability of phosphorus in pyrochars and hydrochars derived from sewage sludge after their amendment to

soils. *Agronomy* **2021**, *11*, doi:10.3390/agronomy11040623.

52. Xue, X.; Chen, D.; Song, X.; Dai, X. Hydrothermal and Pyrolysis Treatment for Sewage Sludge: Choice from Product and from Energy Benefit. *Phys. Procedia* **2015**, *66*, 301–304, doi:10.1016/j.egypro.2015.02.064.

53. Chen, C.; Wei, R.; Shi, F.; Ma, X.; Zhou, X.; Xiong, Q. Analysis of the effects of prepyrolysis hydrothermal treatment on phosphorus recovery from sewage sludge using a life cycle assessment. *J. Clean. Prod.* **2022**, *377*, 134312, doi:10.1016/j.jclepro.2022.134312.

54. Zhu, Y.; Zhao, Q.; Li, D.; Li, J.; Guo, W. Performance comparison of phosphorus recovery from different sludges in sewage treatment plants through pyrolysis. *J. Clean. Prod.* **2022**, *372*, 133728, doi:10.1016/j.jclepro.2022.133728.

55. De Filippis, P.; Scarsella, M.; Verdone, N.; Zeppieri, M. Poultry litter valorization to energy. *Trans. Ecol. Environ.* **2008**, *109*, 261–267, doi:10.2495/WM080281.

56. Bolan, N.S.; Szogi, A.A.; Chuasavathi, T.; Seshadri, B.; Rothrock, M.J.; Panneerselvam, P. Uses and management of poultry litter. *Worlds. Poult. Sci. J.* **2010**, *66*, 673–698, doi:10.1017/S0043933910000656.

57. Kelleher, B.P.; Leahy, J.J.; Henihan, A.M.; O'Dwyer, T.F.; Sutton, D.; Leahy, M.J. Advances in poultry litter disposal technology – a review. *Bioresour. Technol.* **2002**, *83*, 27–36, doi:10.1007/s11668-016-0088-z.

58. Billen, P.; Costa, J.; Van Der Aa, L.; Van Caneghem, J.; Vandecasteele, C. Electricity from poultry manure: A cleaner alternative to direct land application. *J. Clean. Prod.* **2015**, *96*, 467–475, doi:10.1016/j.jclepro.2014.04.016.

59. Lynch, D.; Henihan, A.M.; Bowen, B.; Lynch, D.; McDonnell, K.; Kwapinski, W.; Leahy, J.J. Utilisation of poultry litter as an energy feedstock. *Biomass and Bioenergy* **2013**, *49*, 197–204, doi:10.1016/j.biombioe.2012.12.009.

60. Quiroga, G.; Castrillón, L.; Fernández-Nava, Y.; Marañón, E. Physico-chemical analysis and calorific values of poultry manure. *Waste Manag.* **2010**, *30*, 880–884, doi:10.1016/j.wasman.2009.12.016.

61. Leng, L.; Bogush, A.A.; Roy, A.; Stegemann, J.A. Characterisation of ashes from waste biomass power plants and phosphorus recovery. *Sci. Total Environ.* **2019**, *690*, 573–583, doi:10.1016/j.scitotenv.2019.06.312.

62. Maj, I.; Kalisz, S.; Ciukaj, S. Properties of Animal-Origin Ash—A Valuable Material for Circular Economy. *Energies* **2022**, *15*, 1274.

63. Kaikake, K.; Sekito, T.; Dote, Y. Phosphate recovery from phosphorus-rich solution obtained from chicken manure incineration ash. *Waste Manag.* **2009**, *29*, 1084–1088, doi:10.1016/j.wasman.2008.09.008.

64. Rivera, R.M.; Chagnes, A.; Cathelineau, M.; Boiron, M.C. Conditioning of poultry manure ash for subsequent phosphorous separation and assessment for a process design. *Sustain. Mater. Technol.* **2022**, *31*, e00377, doi:10.1016/j.susmat.2021.e00377.

65. Pandey, D.S.; Kwapinska, M.; Leahy, J.J.; Kwapinski, W. Fly ash from poultry litter gasification - Can it be utilised in agriculture systems as a fertiliser? *Energy Procedia* **2019**, *161*, 38–46, doi:10.1016/j.egypro.2019.02.056.

66. Blake, J.P.; Hess, J.B. Poultry litter ash as a replacement for dicalcium phosphate in broiler diets. *J. Appl. Poult. Res.* **2014**, *23*, 101–107, doi:10.3382/japr.2013-00838.

67. Cempa, M.; Olszewski, P.; Wierzchowski, K.; Kucharski, P.; Białecka, B. Ash from Poultry Manure Incineration as a Substitute for Phosphorus Fertiliser. *Materials (Basel).* **2022**, *15*,

doi:10.3390/ma15093023.

68. Komiyama, T.; Kobayashi, A.; Yahagi, M. The chemical characteristics of ashes from cattle, swine and poultry manure. *J. Mater. Cycles Waste Manag.* **2013**, *15*, 106–110, doi:10.1007/s10163-012-0089-2.

69. Fang, L.; Wang, Q.; Li, J. shan; Poon, C.S.; Cheeseman, C.R.; Donatello, S.; Tsang, D.C.W. Feasibility of wet-extraction of phosphorus from incinerated sewage sludge ash (ISSA) for phosphate fertilizer production: A critical review. *Crit. Rev. Environ. Sci. Technol.* **2020**, 1–33, doi:10.1080/10643389.2020.1740545.

70. Fang, L.; Li, J. shan; Guo, M.Z.; Cheeseman, C.R.; Tsang, D.C.W.; Donatello, S.; Poon, C.S. Phosphorus recovery and leaching of trace elements from incinerated sewage sludge ash (ISSA). *Chemosphere* **2018**, *193*, 278–287, doi:10.1016/j.chemosphere.2017.11.023.

71. Liang, S.; Chen, H.; Zeng, X.; Li, Z.; Yu, W.; Xiao, K.; Hu, J.; Hou, H.; Liu, B.; Tao, S.; et al. A comparison between sulfuric acid and oxalic acid leaching with subsequent purification and precipitation for phosphorus recovery from sewage sludge incineration ash. *Water Res.* **2019**, *159*, 242–251, doi:10.1016/j.watres.2019.05.022.

72. Petzet, S.; Peplinski, B.; Cornel, P. On wet chemical phosphorus recovery from sewage sludge ash by acidic or alkaline leaching and an optimized combination of both. *Water Res.* **2012**, *46*, 3769–3780, doi:10.1016/j.watres.2012.03.068.

73. Biswas, B.K.; Inoue, K.; Harada, H.; Ohto, K.; Kawakita, H. Leaching of phosphorus from incinerated sewage sludge ash by means of acid extraction followed by adsorption on orange waste gel. *J. Environ. Sci.* **2009**, *21*, 1753–1760, doi:10.1016/S1001-0742(08)62484-5.

74. Meng, X.; Liu, X.; Huang, Q.; Gao, H.; Tay, K.; Yan, J. Recovery of phosphate as struvite from low-temperature combustion sewage sludge ash (LTCA) by cation exchange. *Waste Manag.* **2019**, *90*, 84–93, doi:10.1016/j.wasman.2019.04.045.

75. Fahimi, A.; Bilo, F.; Assi, A.; Dalipi, R.; Federici, S.; Guedes, A.; Valentim, B.; Olgun, H.; Ye, G.; Bialecka, B.; et al. Poultry litter ash characterisation and recovery. *Waste Manag.* **2020**, *111*, 10–21, doi:10.1016/j.wasman.2020.05.010.

76. Fahimi, A.; Federici, S.; Depero, L.E.; Valentim, B.; Vassura, I.; Ceruti, F.; Cutaia, L.; Bontempi, E. Evaluation of the sustainability of technologies to recover phosphorus from sewage sludge ash based on embodied energy and CO2 footprint. *J. Clean. Prod.* **2021**, *289*, 125762, doi:10.1016/j.jclepro.2020.125762.

77. Egle, L.; Rechberger, H.; Krampe, J.; Zessner, M. Phosphorus recovery from municipal wastewater: An integrated comparative technological, environmental and economic assessment of P recovery technologies. *Sci. Total Environ.* **2016**, *571*, 522–542, doi:10.1016/j.scitotenv.2016.07.019.

78. Herzel, H.; Stemann, J.; Simon, S.; Adam, C. Comparison of thermochemical treatment of sewage sludge ash with sodium sulphate in laboratory-scale and pilot-scale experiments. *Int. J. Environ. Sci. Technol.* **2022**, *19*, 1997–2006, doi:10.1007/s13762-021-03252-y.

79. Herzel, H.; Krüger, O.; Hermann, L.; Adam, C. Sewage sludge ash — A promising secondary phosphorus source for fertilizer production. *Sci. Total Environ.* **2016**, *542*, 1136–1143, doi:10.1016/J.SCITOTENV.2015.08.059.

80. Vogel, C.; Krüger, O.; Adam, C. Thermochemical treatment of sewage sludge ash with sodium additives under reducing conditions analyzed by thermogravimetry. *J. Therm. Anal. Calorim.* **2016**, *123*, 1045–1051, doi:10.1007/s10973-015-5016-z.

81. Smol, M.; Adam, C.; Kugler, S.A. Thermochemical treatment of Sewage Sludge Ash (SSA)-potential and perspective in Poland. *Energies* **2020**, *13*, 1–17, doi:10.3390/en13205461.

82. Stemann, J.; Peplinski, B.; Adam, C. Thermochemical treatment of sewage sludge ash with sodium salt additives for phosphorus fertilizer production - Analysis of underlying chemical reactions. *Waste Manag.* **2015**, *45*, 385–390, doi:10.1016/j.wasman.2015.07.029.

83. Jeon, S.; Kim, D.J. Enhanced phosphorus bioavailability and heavy metal removal from sewage sludge ash through thermochemical treatment with chlorine donors. *J. Ind. Eng. Chem.* **2018**, *58*, 216–221, doi:10.1016/J.JIEC.2017.09.028.

84. Wang, Y.; Yu, L.; Yuan, H.; Ying, D.; Zhu, N. Improved removal of phosphorus from incinerated sewage sludge ash by thermo-chemical reduction method with CaCl2 application. *J. Clean. Prod.* **2020**, *258*, 120779, doi:10.1016/J.JCLEPRO.2020.120779.

85. Li, R.; Zhao, W.; Li, Y.; Wang, W.; Zhu, X. Heavy metal removal and speciation transformation through the calcination treatment of phosphorus-enriched sewage sludge ash. *J. Hazard. Mater.* **2015**, *283*, 423–431, doi:10.1016/J.JHAZMAT.2014.09.052.

86. Nowak, B.; Frías Rocha, S.; Aschenbrenner, P.; Rechberger, H.; Winter, F. Heavy metal removal from MSW fly ash by means of chlorination and thermal treatment: Influence of the chloride type. *Chem. Eng. J.* **2012**, *179*, 178–185, doi:10.1016/J.CEJ.2011.10.077.

87. Adam, C.; Peplinski, B.; Michaelis, M.; Kley, G.; Simon, F.G. Thermochemical treatment of sewage sludge ashes for phosphorus recovery. *Waste Manag.* **2009**, *29*, 1122–1128, doi:10.1016/j.wasman.2008.09.011.

88. Vogel, C.; Adam, C. Heavy Metal Removal from Sewage Sludge Ash by Thermochemical Treatment with Gaseous Hydrochloric acid. *Environ. Sci. Technol.* **2011**, *45*, 7445–7450, doi:10.1021/es2007319.

89. Uzkurt Kaljunen, J.; Al-Juboori, R.A.; Khunjar, W.; Mikola, A.; Wells, G. Phosphorus recovery alternatives for sludge from chemical phosphorus removal processes – Technology comparison and system limitations. *Sustain. Mater. Technol.* **2022**, *34*, e00514, doi:10.1016/j.susmat.2022.e00514.

90. Utilitalia *Libro Bianco sull'incenerimento dei rifiuti urbani*; 2020;

91. Utilitalia Termovalorizzatori, quanti sono in Italia (e come funzionano) Available online: https://www.utilitalia.it/notizia/5de4a273-432f-4b09-b479-6a71604971f9.

92. ISPRA - Istituto Superiore per la Protezione e la Ricerca Ambientale;; Sistema Nazionale per la Protezione dell'Ambiente *Rapporto Rifiuti Urbani*; 2021;

93. Gruppo A2A Il Termovalorizzatore di Brescia Available online: https://www.gruppoa2a.it/it/chi-siamo/nostri-impianti/termovalorizzatore-brescia.

94. Gruppo A2A Il termovalorizzatore di Corteolona Available online: https://www.gruppoa2a.it/it/chi-siamo/nostri-impianti/termovalorizzatore-corteolona.

95. Gruppo HERA Impianto di trattamento fanghi industriali di Bologna Available online: https://ha.gruppohera.it/lista-impianti/impianto-di-trattamento-fanghi-industriali-di-bologna.

96. GIDA S.p.A. GIDA I.D.L. Baciacavallo Available online: https://www.gida-spa.it/idl-baciacavallo.

97. MM S.p.A. Il progetto FANGHI Available online: https://www.mmspa.eu/wps/portal/mmspa/it/home/servizio-idrico/il-progetto-fanghi.

98. Gruppo CAP; ZeroC Bio Piattaforma Lab Available online: https://biopiattaformalab.it/.

99. Gallina, G.; Passoni, S. *Il piano fanghi nell'ambito del nuovo programma regionale di gestione dei rifiuti (PRGR)*; 2022;

100. *Rapporto Rifiuti Speciali Edizione 2022*; 2022;

101. Phosphorus Platform European Sustainable Phosphorus Platform Available online: https://www.phosphorusplatform.eu/.

102. ENEA Piattaforma Italiana Fosforo Available online: https://www.piattaformaitalianafosforo.it/.

103. University of Porto DEASPHOR Project Available online: https://www.fc.up.pt/deasphor/.

104. Gruppo CAP PerFORM WATER 2030 Project Available online: http://www.performwater2030.it/index_en.php.

105. A2A Ambiente S.p.A. FANGHI Project Available online: https://www.gruppoa2a.it/it/progetti/partnership/fanghi-sostenibilita.

106. Swerim PHIGO Project Available online: https://www.swerim.se/en/phigo.

107. United Nations Sustainable Development Goals (SDGs) Available online: https://sdgs.un.org/goals.

108. Pode, R. Potential applications of rice husk ash waste from rice husk biomass power plant. *Renew. Sustain. Energy Rev.* **2016**, *53*, 1468–1485, doi:10.1016/j.rser.2015.09.051.

109. Garcês, A.; Afonso, S.M.S.; Chilundo, A.; Jairoce, C.T.S. Evaluation of different litter materials for broiler production in a hot and humid environment: 1. Litter characteristics and quality. *J. Appl. Poult. Res.* **2013**, *22*, 168–176, doi:10.3382/japr.2012-00547.

110. Bodie, A.R.; Micciche, A.C.; Atungulu, G.G.; Rothrock, M.J.; Ricke, S.C. Current Trends of Rice Milling Byproducts for Agricultural Applications and Alternative Food Production Systems. *Front. Sustain. Food Syst.* **2019**, *3*, 1–13, doi:10.3389/fsufs.2019.00047.

111. Sharma, G.; Kaur, M.; Punj, S.; Singh, K. Biomass as a sustainable resource for value-added modern materials: a review. *Biofuels, Bioprod. Biorefining* **2020**, *14*, 673–695, doi:10.1002/bbb.2079.

112. Zanoletti, A.; Bilo, F.; Depero, L.E.; Zappa, D.; Bontempi, E. The first sustainable material designed for air particulate matter capture: An introduction to Azure Chemistry. *J. Environ. Manage.* **2018**, *218*, 355–362, doi:10.1016/j.jenvman.2018.04.081.

113. Pasquali, M.; Zanoletti, A.; Benassi, L.; Federici, S.; Depero, L.E.; Bontempi, E. Stabilized biomass ash as a sustainable substitute for commercial P-fertilizers. *L. Degrad. Dev.* **2018**, *29*, 2199–2207, doi:10.1002/ldr.2915.

114. Bilo, F.; Pandini, S.; Sartore, L.; Depero, L.E.; Gargiulo, G.; Bonassi, A.; Federici, S.; Bontempi, E. A sustainable bioplastic obtained from rice straw. *J. Clean. Prod.* **2018**, *200*, 357–368, doi:10.1016/j.jclepro.2018.07.252.

115. Halada, K.; Yamamoto, R. The current status of research and development on ecomaterials around the world. *MRS Bull.* **2001**, *11*, 871–879.

116. Assi, A.; Bilo, F.; Zanoletti, A.; Ponti, J.; Valsesia, A.; La Spina, R.; Depero, L.E.; Bontempi, E. Review of the Reuse Possibilities Concerning Ash Residues from Thermal Process in a Medium-Sized Urban System in Northern Italy. *Sustainability* **2020**, *12*, 4193, doi:10.3390/su12104193.

117. Assi, A.; Bilo, F.; Zanoletti, A.; Ponti, J.; Valsesia, A.; La Spina, R.; Zacco, A.; Bontempi, E. Zero-waste approach in municipal solid waste incineration: Reuse of bottom ash to stabilize fly ash. *J. Clean. Prod.* **2020**, *245*, 118779, doi:10.1016/j.jclepro.2019.118779.

118. Zanoletti, A.; Bilo, F.; Federici, S.; Borgese, L.; Depero, L.E.; Ponti, J.; Valsesia, A.; La Spina, R.; Segata, M.; Montini, T.; et al. The first material made for air pollution control able to sequestrate fine and ultrafine air particulate matter. *Sustain. Cities Soc.* **2020**, *53*, 101961, doi:10.1016/j.scs.2019.101961.

119. Benassi, L.; Dalipi, R.; Consigli, V.; Pasquali, M.; Borgese, L.; Depero, L.E.; Clegg, F.; Bingham, P.A.; Bontempi, E. Integrated management of ash from industrial and domestic combustion: a new sustainable approach for reducing greenhouse gas emissions from energy conversion. *Environ. Sci. Pollut. Res.* **2017**, *24*, 14834–14846, doi:10.1007/s11356-017-9037-y.

120. Prasad, R.; Pandey, M. Rice Husk Ash as a Renewable Source for the Production of Value Added Silica Gel and its Application: An Overview. *Bull. Chem. React. Eng. Catal.* **2012**, *7*, 1–25, doi:10.9767/bcrec.7.1.1216.1-25.

121. Hossain, S.S.; Mathur, L.; Roy, P.K. Rice husk/rice husk ash as an alternative source of silica in ceramics: A review. *J. Asian Ceram. Soc.* **2018**, *6*, 299–313, doi:10.1080/21870764.2018.1539210.

122. Setiawan, W.K.; Chiang, K.-Y. Crop Residues as Potential Sustainable Precursors for Developing Silica Materials: A Review. *Waste and Biomass Valorization* **2020**, doi:10.1007/s12649-020-01126-x.

123. Bontempi, E.; Zacco, A.; Borgese, L.; Gianoncelli, A.; Ardesi, R.; Depero, L.E. A new method for municipal solid waste incinerator (MSWI) fly ash inertization, based on colloidal silica. *J. Environ. Monit.* **2010**, *12*, 2093, doi:10.1039/c0em00168f.

124. Luyckx, L.; de Leeuw, G.H.J.; Van Caneghem, J. Characterization of Poultry Litter Ash in View of Its Valorization. *Waste and Biomass Valorization* **2020**, *11*, 5333–5348, doi:10.1007/s12649-019-00750-6.

125. Codling, E.E.; Chaney, R.L.; Sherwell, J. Poultry Litter Ash as a Potential Phosphorus Source for Agricultural Crops. *J. Environ. Qual.* **2002**, *31*, 954–961, doi:10.2134/jeq2002.9540.

126. Hermann, L.; Schaaf, T. Outotec Manure, Slurry, and Sludge Processing Technology. In *Phosphorus Recovery and Recycling*; Ohtake, H., Tsuneda, S., Eds.; Springer Singapore: Singapore, 2019; pp. 403–417 ISBN 9789811080319.

127. Luyckx, L.; Sousa Correia, D.S.; Van Caneghem, J. Linking Phosphorus Extraction from Different Types of Biomass Incineration Ash to Ash Mineralogy, Ash Composition and Chemical Characteristics of Various Types of Extraction Liquids. *Waste and Biomass Valorization* **2021**, *12*, 5235–5248, doi:10.1007/s12649-021-01368-3.

128. Welcome to BIOdat Available online: https://biodat.eu/pages/Home.aspx.

129. Andò, S. Gravimetric separation of heavy minerals in sediments and rocks. *Minerals* **2020**, *10*, 273, doi:10.3390/min10030273.

130. Assi, A.; Federici, S.; Bilo, F.; Zacco, A.; Depero, L.E.; Bontempi, E. Increased sustainability of carbon dioxide mineral sequestration by a technology involving fly ash stabilization. *Materials (Basel).* **2019**, *12*, 2714, doi:10.3390/ma12172714.

131. Klockenkämper, R.; von Bohlen, A. *Total-Reflection X-Ray Fluorescence Analysis and Related Methods*; Second.; Wiley, 2015;

132. Borgese, L.; Dalipi, R.; Riboldi, A.; Bilo, F.; Zacco, A.; Federici, S.; Bettinelli, M.; Bontempi, E.; Depero, L.E. Comprehensive approach to the validation of the standard method for total reflection X-ray fluorescence analysis of water. *Talanta* **2018**, *181*, 165–171, doi:10.1016/j.talanta.2017.12.087.

133. Romanian Standard Association *STAS 9621: 82 Solid mineral fuels. Coke and semicoke. Determination of phosphorus content, Part 3, Photocolorimetric method*; 1982;

134. Bosio, A.; Gianoncelli, A.; Zacco, A.; Borgese, L.; Rodella, N.; Zanotti, D.; Depero, L.E.; Siviero, G.; Cinosi, A.; Bingham, P.A.; et al. A new nanotechnology of fly ash inertization based on the use of silica gel extracted from rice husk ash and microwave treatment. *Proc. Inst. Mech. Eng. Part N J. Nanoeng. Nanosyst.* **2014**, *228*, 27–32, doi:10.1177/1740349913490683.

135. Kamath, S.R.; Proctor, A. Silica gel from rice hull ash: Preparation and characterization. *Cereal Chem.* **1998**, *75*, 484–487, doi:10.1094/CCHEM.1998.75.4.484.

136. Sinkó, K. Influence of chemical conditions on the nanoporous structure of silicate aerogels. *Materials (Basel).* **2010**, *3*, 704–740, doi:10.3390/ma3010704.

137. Santana Costa, J.A.; Paranhos, C.M. Systematic evaluation of amorphous silica production from rice husk ashes. *J. Clean. Prod.* **2018**, *192*, 688–697, doi:10.1016/j.jclepro.2018.05.028.

138. Kalapathy, U.; Proctor, A.; Shultz, J. A simple method for production of pure silica from rice hull ash. *Bioresour. Technol.* **2000**, *73*, 257–262, doi:10.1016/s0140-6701(01)80487-2.

139. Thongma, B.; Chiarakorn, S. Recovery of silica and carbon black from rice husk ash disposed from a biomass power plant by precipitation method. *IOP Conf. Ser. Earth Environ. Sci.* **2019**, *373*, 012026, doi:10.1088/1755-1315/373/1/012026.

140. Alvarez, J.; Lopez, G.; Amutio, M.; Bilbao, J.; Olazar, M. Upgrading the rice husk char obtained by flash pyrolysis for the production of amorphous silica and high quality activated carbon. *Bioresour. Technol.* **2014**, *170*, 132–137, doi:10.1016/j.biortech.2014.07.073.

141. Terzioğlu, P.; Yücel, S.; Kuş, Ç. Review on a novel biosilica source for production of advanced silica-based materials: Wheat husk. *Asia-Pacific J. Chem. Eng.* **2019**, *14*, 2262, doi:10.1002/apj.2262.

142. Stammeier, J.A.; Purgstaller, B.; Hippler, D.; Mavromatis, V.; Dietzel, M. In-situ Raman spectroscopy of amorphous calcium phosphate to crystalline hydroxyapatite transformation. *MethodsX* **2018**, *5*, 1241–1250, doi:10.1016/j.mex.2018.09.015.

143. Staroń, P.; Kowalski, Z.; Staroń, A.; Seidlerová, J.; Banach, M. Residues from the thermal conversion of waste from the meat industry as a source of valuable macro- and micronutrients. *Waste Manag.* **2016**, *49*, 337–345, doi:10.1016/j.wasman.2016.01.018.

144. Valentim, B.; Flores, D.; Guedes, A.; Guimarães, R.; Shreya, N.; Paul, B.; Ward, C.R. Notes on the occurrence of phosphate mineral relics and spheres (phosphospheres) in coal and biomass fly ash. *Int. J. Coal Geol.* **2016**, *154–155*, 43–56, doi:10.1016/j.coal.2015.12.009.

145. Rodella, N.; Bosio, A.; Dalipi, R.; Zacco, A.; Borgese, L.; Depero, L.E.; Bontempi, E. Waste silica sources as heavy metal stabilizers for municipal solid waste incineration fly ash. *Arab. J. Chem.* **2017**, *10*, S3676–S3681, doi:10.1016/j.arabjc.2014.04.006.

146. Bosio, A.; Zacco, A.; Borgese, L.; Rodella, N.; Colombi, P.; Benassi, L.; Depero, L.E.; Bontempi, E. A sustainable technology for Pb and Zn stabilization based on the use of only waste materials: A green chemistry approach to avoid chemicals and promote CO_2 sequestration. *Chem. Eng. J.* **2014**, *253*, 377–384, doi:10.1016/j.cej.2014.04.080.

147. Alvarez, J.; Lopez, G.; Amutio, M.; Bilbao, J.; Olazar, M. Physical Activation of Rice Husk Pyrolysis Char for the Production of High Surface Area Activated Carbons. *Ind. Eng. Chem. Res.* **2015**, *54*, 7241–7250.

148. Hong, K.-J.; Tarutani, N.; Shinya, Y.; Kajiuchi, T. Study on the Recovery of Phosphorus from Waste-Activated Sludge Incinerator Ash. *J. Environ. Sci. Heal. Part A* **2005**, *40*, 617–631, doi:10.1081/ESE-200046614.

149. Xu, H.; He, P.; Gu, W.; Wang, G.; Shao, L. Recovery of phosphorus as struvite from sewage sludge ash. *J. Environ. Sci. (China)* **2012**, *24*, 1533–1538, doi:10.1016/S1001-0742(11)60969-8.

150. Semerci, N.; Ahadi, S.; Coşgun, S. Comparison of dried sludge and sludge ash for phosphorus recovery with acidic and alkaline leaching. *Water Environ. J.* **2020**, *0*, wej.12633, doi:10.1111/wej.12633.

151. Smol, M.; Kulczycka, J.; Henclik, A.; Gorazda, K.; Tarko, B.; Wzorek, Z. Sewage Sludge Ash (SSA)

as a Phosphate Fertilizer in the Aspect of Legal Regulations. In; 2015; pp. 323–328 ISBN 9781138028821.

152. Kominko, H.; Gorazda, K.; Wzorek, Z.; Wojtas, K. Sustainable Management of Sewage Sludge for the Production of Organo-Mineral Fertilizers. *Waste and Biomass Valorization* **2018**, *9*, 1817–1826, doi:10.1007/s12649-017-9942-9.

153. Parliament, E. *Regulation (EC) No 2003/2003 of the European Parliament and of the Council relating to fertilizers*; 2003; pp. 1–176;.

154. European Parliament *Regulation (EU) 2019/1009 of the European Parliament and of the Council laying down rules on the making available on the market of EU fertilising products*; 2019; pp. 1–114;.

155. Fang, L.; Li, J. shan; Donatello, S.; Cheeseman, C.R.; Wang, Q.; Poon, C.S.; Tsang, D.C.W. Recovery of phosphorus from incinerated sewage sludge ash by combined two-step extraction and selective precipitation. *Chem. Eng. J.* **2018**, *348*, 74–83, doi:10.1016/j.cej.2018.04.201.

156. Wang, Q.; Li, J. shan; Tang, P.; Fang, L.; Poon, C.S. Sustainable reclamation of phosphorus from incinerated sewage sludge ash as value-added struvite by chemical extraction, purification and crystallization. *J. Clean. Prod.* **2018**, *181*, 717–725, doi:10.1016/j.jclepro.2018.01.254.

157. Thant Zin, M.M.; Kim, D.J. Struvite production from food processing wastewater and incinerated sewage sludge ash as an alternative N and P source: Optimization of multiple resources recovery by response surface methodology. *Process Saf. Environ. Prot.* **2019**, *126*, 242–249, doi:10.1016/j.psep.2019.04.018.

158. Rech, I.; Kamogawa, M.Y.; Jones, D.L.; Pavinato, P.S. Synthesis and characterization of struvite derived from poultry manure as a mineral fertilizer. *J. Environ. Manage.* **2020**, *272*, 111072, doi:10.1016/j.jenvman.2020.111072.

159. Luyckx, L.; Geerts, S.; Van Caneghem, J. Closing the phosphorus cycle: Multi-criteria techno-economic optimization of phosphorus extraction from wastewater treatment sludge ash. *Sci. Total Environ.* **2020**, *713*, 135543, doi:10.1016/j.scitotenv.2019.135543.

160. Liu, Y.; Qu, H. Design and optimization of a reactive crystallization process for high purity phosphorus recovery from sewage sludge ash. *J. Environ. Chem. Eng.* **2016**, *4*, 2155–2162, doi:10.1016/j.jece.2016.03.042.

161. Castillo, D.; Cruz, J.C.; Trejo-Arroyo, D.L.; Muzquiz, E.M.; Zarhri, Z.; Gurrola, M.P.; Vega-Azamar, R.E. Characterization of poultry litter ashes as a supplementary cementitious material. *Case Stud. Constr. Mater.* **2022**, *17*, e01278, doi:10.1016/j.cscm.2022.e01278.

162. Li, J.; Chen, Z.; Wang, Q.; Fang, L.; Xue, Q.; Cheeseman, C.R.; Donatello, S. Change in re-use value of incinerated sewage sludge ash due to chemical extraction of phosphorus. *Waste Manag.* **2018**, *74*, 404–412, doi:10.1016/j.wasman.2018.01.007.

163. Donatello, S. Characteristics of incinerated sewage sludge ashes: Potential for phosphate extraction and re-use as a pozzolanic material in construction products, Imperial College London, 2009.

164. Zanoletti, A.; Cornelio, A.; Bontempi, E. A post-pandemic sustainable scenario: What actions can be pursued to increase the raw materials availability? *Environ. Res.* **2021**, *202*, 111681, doi:10.1016/j.envres.2021.111681.

165. Bontempi, E.; Sorrentino, G.P.; Zanoletti, A.; Alessandri, I.; Depero, L.E.; Caneschi, A. Sustainable Materials and their Contribution to the Sustainable Development Goals (SDGs): A Critical Review Based on an Italian Example. *Molecules* **2021**, *26*, 1407, doi:10.3390/molecules26051407.

166. Sousa, P.M.S.; Martelo, L.M.; Marques, A.T.; M.S.M. Bastos, M.; M.V.M. Soares, H. A closed and

zero-waste loop strategy to recycle the main raw materials (gold, copper and fiber glass layers) constitutive of waste printed circuit boards. *Chem. Eng. J.* **2022**, *434*, 1–10, doi:10.1016/j.cej.2022.134604.

167.   Zaman, A.U. A strategic framework for working toward zero waste societies based on perceptions surveys. *Recycling* **2017**, *2*, 1, doi:10.3390/recycling2010001.

168.   Juta, D.; Lienite, L. PRINCIPLES OF A CIRCULAR ECONOMY IN THE FOOD SECTOR : A SYSTEMATIC LITERATURE REVIEW. *J. Reg. Econ. Soc. Dev.* **2018**, *14*, 20–28.

169.   Yontar, E. Critical success factor analysis of blockchain technology in agri-food supply chain management: A circular economy perspective. *J. Environ. Manage.* **2023**, *330*, 117173, doi:10.1016/j.jenvman.2022.117173.

170.   Assi, A.; Bilo, F.; Zanoletti, A.; Ducoli, S.; Ramorino, G.; Gobetti, A.; Zacco, A.; Federici, S.; Depero, L.E.; Bontempi, E. A circular economy virtuous example-use of a stabilized waste material instead of calcite to produce sustainable composites. *Appl. Sci.* **2020**, *10*, 754, doi:10.3390/app10030754.

171.   Fahimi, A.; Bontempi, E.; Fiameni, L.; Guedes, A.; Guimarães, R.; Moreira, K.; Santos, A.C.; Valentim, B.; Predeanu, G.; Bălănescu, M.; et al. Incineration of Aviary Manure: the Case Studies of Poultry Litter and Laying Hens Manure. *Submitt. to BIOMASS WASTE VALORIZATION* **2022**.

172.   Fiameni, L.; Assi, A.; Fahimi, A.; Valentim, B.; Moreira, K.; Predeanu, G.; Slăvescu, V.; Vasile, B.; Nicoară, A.I.; Borgese, L.; et al. Simultaneous amorphous silica and phosphorus recovery from rice husk poultry litter ash. *RSC Adv.* **2021**, *11*, 8927–8939, doi:10.1039/d0ra10120f.

173.   Neves, A.; Godina, R.; Azevedo, S.G.; Matias, J.C.O. A comprehensive review of industrial symbiosis. *J. Clean. Prod.* **2020**, *247*, doi:10.1016/j.jclepro.2019.119113.

174.   Taqi, H.M.M.; Meem, E.J.; Bhattacharjee, P.; Salman, S.; Ali, S.M.; Sankaranarayanan, B. What are the challenges that make the journey towards industrial symbiosis complicated? *J. Clean. Prod.* **2022**, *370*, 133384, doi:10.1016/j.jclepro.2022.133384.

175.   Jama-Rodzeńska, A.; Sowiński, J.; Koziel, J.A.; Białowiec, A. Phosphorus recovery from sewage sludge ash based on cradle-to-cradle approach—Mini-review. *Minerals* **2021**, *11*, 1–17, doi:10.3390/min11090985.

176.   Liu, H.; Hu, G.; Basar, I.A.; Li, J.; Lyczko, N.; Nzihou, A.; Eskicioglu, C. Phosphorus recovery from municipal sludge-derived ash and hydrochar through wet-chemical technology: A review towards sustainable waste management. *Chem. Eng. J.* **2021**, *417*, 129300, doi:10.1016/j.cej.2021.129300.

177.   Boniardi, G.; Turolla, A.; Fiameni, L.; Gelmi, E.; Malpei, F.; Bontempi, E.; Canziani, R. Assessment of a simple and replicable procedure for selective phosphorus recovery from sewage sludge ashes by wet chemical extraction and precipitation. *Chemosphere* **2021**, *285*, 131476, doi:10.1016/j.chemosphere.2021.131476.

178.   Luyckx, L.; Van Caneghem, J. Recovery of phosphorus from sewage sludge ash: Influence of incineration temperature on ash mineralogy and related phosphorus and heavy metal extraction. *J. Environ. Chem. Eng.* **2021**, *9*, 106471, doi:10.1016/j.jece.2021.106471.

179.   Luyckx, L.; Caneghem, J. Van Recovery of phosphorus from sewage sludge ash: Influence of chemical addition prior to incineration on ash mineralogy and related phosphorus and heavy metal extraction. *J. Environ. Chem. Eng.* **2022**, *10*, 108117, doi:10.1016/j.jece.2022.108117.

180.   Fang, L.; Li, L.; Wang, Q.; Li, J. shan; Poon, C.S. Agronomic effectiveness of recovered phosphate fertilizer produced from incinerated sewage sludge ash. *Waste Dispos. Sustain. Energy* **2022**, *4*, 157–167, doi:10.1007/s42768-022-00097-0.

181.   Uysal, A.; Tuncer, D.; Kir, E.; Koseoglu, T.S. Phosphorus recovery from hydrolysed sewage sludge

liquid containing metals using donnan dialysis. In Proceedings of the Proceedings of the 2nd World Congress on New Technologies; 2016.

182. Barbosa, S.G.; Peixoto, L.; Meulman, B.; Alves, M.M.; Pereira, M.A. A design of experiments to assess phosphorous removal and crystal properties in struvite precipitation of source separated urine using different Mg sources. *Chem. Eng. J.* **2016**, *298*, 146–153, doi:10.1016/j.cej.2016.03.148.

183. Tasca, A.L.; Mannarino, G.; Gori, R.; Vitolo, S.; Puccini, M. Phosphorus recovery from sewage sludge hydrochar: Process optimization by response surface methodology. *Water Sci. Technol.* **2020**, *82*, 2331–2343, doi:10.2166/wst.2020.485.

184. Khaing, K.T.; Polprasert, C.; Mahasandana, S.; Pimpeach, W.; Patthanaissaranukool, W.; Polprasert, S. Phosphorus Recovery and Bioavailability from Chemical Extraction of Municipal Wastewater Treatment's Waste Activated Sludge: A Case of Bangkok Metropolis, Thailand. *Environ. Nat. Resour. J.* **2022**, *20*, 369–378, doi:10.32526/ennrj/20/202200024.

185. Shim, S.; Won, S.; Reza, A.; Kim, S.; Ahmed, N.; Ra, C. Design and optimization of fluidized bed reactor operating conditions for struvite recovery process from swine wastewater. *Processes* **2020**, *8*, 422, doi:10.3390/PR8040422.

186. Ownby, M.; Desrosiers, D.-A.; Vaneeckhaute, C. Phosphorus removal and recovery from wastewater via hybrid ion exchange nanotechnology: a study on sustainable regeneration chemistries. *npj Clean Water* **2021**, *4*, doi:10.1038/s41545-020-00097-9.

187. Benassi, L.; Pasquali, M.; Zanoletti, A.; Dalipi, R.; Borgese, L.; Depero, L.E.; Vassura, I.; Quina, M.J.; Bontempi, E. Chemical Stabilization of Municipal Solid Waste Incineration Fly Ash without Any Commercial Chemicals: First Pilot-Plant Scaling Up. *ACS Sustain. Chem. Eng.* **2016**, *4*, 5561–5569, doi:10.1021/acssuschemeng.6b01294.

188. Bosio, A.; Rodella, N.; Gianoncelli, A.; Zacco, A.; Borgese, L.; Depero, L.E.; Bingham, P.A.; Bontempi, E. A new method to inertize incinerator toxic fly ash with silica from rice husk ash. *Environ. Chem. Lett.* **2013**, *11*, 329–333, doi:10.1007/s10311-013-0411-9.

189. Li, X.; Chen, Q.; Zhou, Y.; Tyrer, M.; Yu, Y. Stabilization of heavy metals in MSWI fly ash using silica fume. *Waste Manag.* **2014**, *34*, 2494–2504, doi:10.1016/J.WASMAN.2014.08.027.

190. Fahimi, A.; Ducoli, S.; Federici, S.; Ye, G.; Mousa, E.; Frontera, P.; Bontempi, E. Evaluation of the sustainability of technologies to recycle spent lithium-ion batteries, based on embodied energy and carbon footprint. *J. Clean. Prod.* **2022**, *338*, 130493, doi:10.1016/j.jclepro.2022.130493.

191. Ducoli, S.; Fahimi, A.; Mousa, E.; Ye, G.; Federici, S.; Frontera, P.; Bontempi, E. ESCAPE approach for the sustainability evaluation of spent lithium-ion batteries recovery: Dataset of 33 available technologies. *Data Br.* **2022**, *42*, 108018, doi:10.1016/j.dib.2022.108018.

192. Fahimi, A.; Zanoletti, A.; Cornelio, A.; Mousa, E.; Ye, G.; Frontera, P.; Depero, L.E.; Bontempi, E. Sustainability Analysis of Processes to Recycle Discharged Lithium-Ion Batteries, Based on the ESCAPE Approach. *Materials (Basel).* **2022**, *15*, doi:10.3390/ma15238527.

193. Ducoli, S.; Zacco, A.; Bontempi, E. Incineration of sewage sludge and recovery of residue ash as building material: A valuable option as a consequence of the COVID-19 pandemic. *J. Environ. Manage.* **2021**, *282*, 111966, doi:10.1016/j.jenvman.2021.111966.

194. Bontempi, E.; Zanoletti, A.; Bilo, F.; Tushtev, K.; Valente, G.; Zappa, D.; Treccani, L.; Depero, L.E. New Sustainable Hybrid Porous Materials for Air Particulate Matter Trapping. *Mater. Sci. Forum* **2018**, *941*, 2237–2242.

195. Bontempi, E. A new approach for evaluating the sustainability of raw materials substitution based on embodied energy and the CO2 footprint. *J. Clean. Prod.* **2017**, *162*, 162–169, doi:10.1016/j.jclepro.2017.06.028.

196.   Bontempi, E. *Raw Materials Substitution Sustainability*; 2017; ISBN 978-3-319-60830-3.

197.   Fang, L.; Wang, Q.; Li, J. shan; Poon, C.S.; Cheeseman, C.R.; Donatello, S.; Tsang, D.C.W. Feasibility of wet-extraction of phosphorus from incinerated sewage sludge ash (ISSA) for phosphate fertilizer production: A critical review. *Crit. Rev. Environ. Sci. Technol.* **2020**, *51*, 939–971, doi:10.1080/10643389.2020.1740545.

198.   Assi, A.; Bilo, F.; Zanoletti, A.; Ponti, J.; Valsesia, A.; La Spina, R.; Zacco, A.; Bontempi, E. Zero-waste approach in municipal solid waste incineration: Reuse of bottom ash to stabilize fly ash. *J. Clean. Prod.* **2020**, *245*, 118779, doi:10.1016/j.jclepro.2019.118779.

199.   Montgomery, D.C. *Design and Analysis of Experiments*; Ninth Edit.; Wiley, 2017; ISBN 9781119113478.

200.   Rosales, E.; Sanromán, M.A.; Pazos, M. Application of central composite face-centered design and response surface methodology for the optimization of electro-Fenton decolorization of Azure B dye. *Environ. Sci. Pollut. Res.* **2012**, *19*, 1738–1746, doi:10.1007/s11356-011-0668-0.

201.   Granta Design Cambridge Engineering Selector (CES) 2019.

202.   GreenDelta openLCA is a free, professional Life Cycle Assessment (LCA) and footprint software with a broad range of features and many available databases Available online: http://www.openlca.org/.

203.   Rodríguez, C. *ecoinvent v.3.3 in openLCA*; 2016;

204.   Ashby, M.F. Chapter 10 - Eco-informed materials selection. In; Ashby, M.F.B.T.-M. and the E. (Second E., Ed.; Butterworth-Heinemann: Boston, 2013; pp. 275–317 ISBN 978-0-12-385971-6.

205.   Xu, H.; Zhang, H.; Shao, L.; He, P. Fraction distributions of phosphorus in sewage sludge and sludge ash. *Waste and Biomass Valorization* **2012**, *3*, 355–361, doi:10.1007/s12649-011-9103-5.

206.   International Organization for Standardization *ISO 6878:2004 Water quality - Determination of phosphorus - Ammonium molybdate spectrometric method*; 2004;

207.   Habashi, F.; Awadalla, F.T.; Yao, X. The hydrochloric acid route for phosphate rock. *J. Chem. Technol. Biotechnol.* **1987**, *38*, 115–126, doi:10.1002/jctb.280380208.

208.   Abdellaoui, I.; Islam, M.M.; Sakurai, T.; Hamzaoui, S.; Akimoto, K. Impurities removal process for high-purity silica production from diatomite. *Hydrometallurgy* **2018**, *179*, 207–214, doi:10.1016/j.hydromet.2018.06.009.

209.   Fiameni, L.; Assi, A.; Fahimi, A.; Valentim, B.; Moreira, K.; Predeanu, G.; Slăvescu, V.; Vasile, B.; Nicoară, A.I.; Borgese, L.; et al. Simultaneous amorphous silica and phosphorus recovery from rice husk poultry litter ash. *RSC Adv.* **2021**, *11*, 8927–8939, doi:10.1039/d0ra10120f.

210.   Danish, A.; Ozbakkaloglu, T. Greener cementitious composites incorporating sewage sludge ash as cement replacement: A review of progress, potentials, and future prospects. *J. Clean. Prod.* **2022**, *371*, 133364, doi:10.1016/j.jclepro.2022.133364.

211.   Tipraj; Shanmugapriya, T. A comprehensive analysis on optimization of Sewage sludge ash as a binding material for a sustainable construction practice: A state of the art review. *Mater. Today Proc.* **2022**, *64*, 1094–1101, doi:10.1016/j.matpr.2022.05.479.

212.   Zdeb, T.; Tracz, T.; Adamczyk, M. Physical, mechanical properties and durability of cement mortars containing fly ash from the sewage sludge incineration process. *J. Clean. Prod.* **2022**, *345*, 131055, doi:10.1016/j.jclepro.2022.131055.

213.   Prabhakar, A.K.; Krishnan, P.; Lee, S.S.C.; Lim, C.S.; Dixit, A.; Mohan, B.C.; Teoh, J.H.; Pang, S.D.; Tsang, D.C.W.; Teo, S.L.M.; et al. Sewage sludge ash-based mortar as construction material:

Mechanical studies, macrofouling, and marine toxicity. *Sci. Total Environ.* **2022**, *824*, 153768, doi:10.1016/j.scitotenv.2022.153768.

214. Chang, Z.; Long, G.; Xie, Y.; Zhou, J.L. Chemical effect of sewage sludge ash on early-age hydration of cement used as supplementary cementitious material. *Constr. Build. Mater.* **2022**, *322*, 126116, doi:10.1016/j.conbuildmat.2021.126116.

215. Świerczek, L.; Cieślik, B.M.; Konieczka, P. Challenges and opportunities related to the use of sewage sludge ash in cement-based building materials – A review. *J. Clean. Prod.* **2021**, *287*, doi:10.1016/j.jclepro.2020.125054.

216. Salihoglu, G.; Mardani-Aghabaglou, A. Characterization of sewage sludge incineration ashes from multi-cyclones and baghouse dust filters as possible cement substitutes. *Environ. Sci. Pollut. Res.* **2021**, *28*, 645–663, doi:10.1007/s11356-020-10507-7.

217. Chang, Z.; Long, G.; Zhou, J.L.; Ma, C. Valorization of sewage sludge in the fabrication of construction and building materials: A review. *Resour. Conserv. Recycl.* **2020**, *154*, 104606, doi:10.1016/j.resconrec.2019.104606.

218. Lu, J.X.; Zhou, Y.; He, P.; Wang, S.; Shen, P.; Poon, C.S. Sustainable reuse of waste glass and incinerated sewage sludge ash in insulating building products: Functional and durability assessment. *J. Clean. Prod.* **2019**, *236*, 117635, doi:10.1016/j.jclepro.2019.117635.

219. Smol, M.; Kulczycka, J.; Henclik, A.; Gorazda, K.; Wzorek, Z. The possible use of sewage sludge ash (SSA) in the construction industry as a way towards a circular economy. *J. Clean. Prod.* **2015**, *95*, 45–54, doi:10.1016/j.jclepro.2015.02.051.

220. Zhou, Y.; Li, J.; Poon, C.S. Sustainable utilization of incinerated sewage sludge ash. In *Low Carbon Stabilization and Solidification of Hazardous Wastes*; Elsevier, 2022; pp. 211–225 ISBN 9780128240045.

221. Dassekpo, J.B.M.; Ning, J.; Zha, X. Potential solidification/stabilization of clay-waste using green geopolymer remediation technologies. *Process Saf. Environ. Prot.* **2018**, *117*, 684–693, doi:10.1016/j.psep.2018.06.013.

222. Assi, A.; Bilo, F.; Federici, S.; Zacco, A.; Depero, L.E.; Bontempi, E. Bottom ash derived from municipal solid waste and sewage sludge co-incineration: First results about characterization and reuse. *Waste Manag.* **2020**, *116*, 147–156, doi:10.1016/j.wasman.2020.07.031.

223. Assi, A.; Bilo, F.; Zanoletti, A.; Borgese, L.; Depero, L.E.; Nenci, M.; Bontempi, E. Stabilization of municipal solid waste fly ash, obtained by co-combustion with sewage sludge, mixed with bottom ash derived by the same plant. *Appl. Sci.* **2020**, *10*, 6075, doi:10.3390/app10176075.

224. Ma, W.; Meng, F.; Qiu, D.; Tang, Y. Co-stabilization of Pb/Cu/Zn by beneficial utilization of sewage sludge incineration ash: Effects of heavy metal type and content. *Resour. Conserv. Recycl.* **2020**, *156*, doi:10.1016/j.resconrec.2019.104671.

225. Donatello, S.; Cheeseman, C.R. Recycling and recovery routes for incinerated sewage sludge ash (ISSA): A review. *Waste Manag.* **2013**, *33*, 2328–2340, doi:10.1016/j.wasman.2013.05.024.

226. Donatello, S.; Freeman-Pask, A.; Tyrer, M.; Cheeseman, C.R. Effect of milling and acid washing on the pozzolanic activity of incinerator sewage sludge ash. *Cem. Concr. Compos.* **2010**, *32*, 54–61, doi:10.1016/j.cemconcomp.2009.09.002.

227. Liang, S.; Yang, L.; Chen, H.; Yu, W.; Tao, S.; Yuan, S.; Xiao, K.; Hu, J.; Hou, H.; Liu, B.; et al. Phosphorus recovery from incinerated sewage sludge ash (ISSA) and reutilization of residues for sludge pretreated by different conditioners. *Resour. Conserv. Recycl.* **2021**, *169*, 105524, doi:10.1016/j.resconrec.2021.105524.

228. Zheng, M.; Chen, J.; Zhang, L.; Cheng, Y.; Lu, C.; Liu, Y.; Singh, A.; Trivedi, M.; Kumar, A.; Liu, J. Metal organic frameworks as efficient adsorbents for drugs from wastewater. *Mater. Today*

Commun. **2022**, *31*, 103514, doi:10.1016/j.mtcomm.2022.103514.

229. Manyangadze, M.; Chikuruwo, N.M.H.; Narsaiah, T.B.; Chakra, C.S.; Charis, G.; Danha, G.; Mamvura, T.A. Adsorption of lead ions from wastewater using nano silica spheres synthesized on calcium carbonate templates. *Heliyon* **2020**, *6*, e05309, doi:10.1016/j.heliyon.2020.e05309.

230. Ezeuko, A.S.; Ojemaye, M.O.; Okoh, O.O.; Okoh, A.I. Influence of different chaotropic salts on etched mesoporous silica nanoparticles for the removal of bacteria DNA conveying antibiotic resistance genes from hospital wastewater. *J. Clean. Prod.* **2022**, *381*, 135157, doi:10.1016/j.jclepro.2022.135157.

231. Natarajan, R.; Banerjee, K.; Kumar, P.S.; Somanna, T.; Tannani, D.; Arvind, V.; Raj, R.I.; Vo, D.V.N.; Saikia, K.; Vaidyanathan, V.K. Performance study on adsorptive removal of acetaminophen from wastewater using silica microspheres: Kinetic and isotherm studies. *Chemosphere* **2021**, *272*, 129896, doi:10.1016/j.chemosphere.2021.129896.

232. Kalmykova, Y.; Karlfeldt Fedje, K. Phosphorus recovery from municipal solid waste incineration fly ash. *Waste Manag.* **2013**, *33*, 1403–1410, doi:10.1016/j.wasman.2013.01.040.

233. Numviyimana, C.; Warchoł, J.; Khalaf, N.; Leahy, J.J.; Chojnacka, K. Phosphorus recovery as struvite from hydrothermal carbonization liquor of chemically produced dairy sludge by extraction and precipitation. *J. Environ. Chem. Eng.* **2022**, *10*, doi:10.1016/j.jece.2021.106947.

234. US Geological Survey PHREEQC Version 3 Available online: https://www.usgs.gov/software/phreeqc-version-3.

235. vminteq Visual MINTEQ.

236. Li, B.; Huang, H.M.; Boiarkina, I.; Yu, W.; Huang, Y.F.; Wang, G.Q.; Young, B.R. Phosphorus recovery through struvite crystallisation: Recent developments in the understanding of operational factors. *J. Environ. Manage.* **2019**, *248*, 109254, doi:10.1016/j.jenvman.2019.07.025.

237. Daneshgar, S.; Vanrolleghem, P.A.; Vaneeckhaute, C.; Buttafava, A.; Capodaglio, A.G. Optimization of P compounds recovery from aerobic sludge by chemical modeling and response surface methodology combination. *Sci. Total Environ.* **2019**, *668*, 668–677, doi:10.1016/j.scitotenv.2019.03.055.

238. Sun, L.; Yang, Y.; Yuan, W.; Wu, X.; Cui, Z.; Wang, H.; Deng, H.; Zhu, X.; Li, R. Struvite purity prediction by response surface methodology and chemical equilibrium modeling combination. *Environ. Technol. Innov.* **2023**, *29*, 103016, doi:10.1016/j.eti.2023.103016.

239. Li, M.; Sun, H.; Zhang, H.; Mohammed, A.; Liu, Y.; Lu, Q. Phosphorus recovery from synthetic biosolid digestion supernatant through lignin-induced struvite precipitation. *J. Clean. Prod.* **2020**, *276*, 124235, doi:10.1016/j.jclepro.2020.124235.

240. Jia, G.; Zhang, H.; Krampe, J.; Muster, T.; Gao, B.; Zhu, N.; Jin, B. Applying a chemical equilibrium model for optimizing struvite precipitation for ammonium recovery from anaerobic digester effluent. *J. Clean. Prod.* **2017**, *147*, 297–305, doi:10.1016/j.jclepro.2017.01.116.

241. Warmadewanthi, I.D.A.A.; Zulkarnain, M.A.; Ikhlas, N.; Kurniawan, S.B.; Abdullah, S.R.S. Struvite precipitation as pretreatment method of mature landfill leachate. *Bioresour. Technol. Reports* **2021**, *15*, 100792, doi:10.1016/j.biteb.2021.100792.

242. de Azevedo Basto, P.; Savastano Junior, H.; de Melo Neto, A.A. Characterization and pozzolanic properties of sewage sludge ashes (SSA) by electrical conductivity. *Cem. Concr. Compos.* **2019**, *104*, 103410, doi:10.1016/j.cemconcomp.2019.103410.

243. Magdziarz, A.; Dalai, A.K.; Koziński, J.A. Chemical composition, character and reactivity of renewable fuel ashes. *Fuel* **2016**, *176*, 135–145, doi:10.1016/j.fuel.2016.02.069.

244. Kabbe, C. *Inventory of phosphorus "recovery and /or recycling" facilities operating or under*

construction at or downstream of wastewater treatment installations; 2023;

245. Fan, C.; Wang, B.; Zhang, T. Review on cement stabilization/solidification of municipal solid waste incineration fly ash. *Adv. Mater. Sci. Eng.* **2018**, *2018*, doi:10.1155/2018/5120649.

246. Mehta, C.M.; Khunjar, W.O.; Nguyen, V.; Tait, S.; Batstone, D.J. Technologies to Recover Nutrients from Waste Streams: A Critical Review. *Crit. Rev. Environ. Sci. Technol.* **2015**, *45*, 385–427, doi:10.1080/10643389.2013.866621.

247. Huang, R.; Fang, C.; Zhang, B.; Tang, Y. Transformations of Phosphorus Speciation during (Hydro)thermal Treatments of Animal Manures. *Environ. Sci. Technol.* **2018**, *52*, 3016–3026, doi:10.1021/acs.est.7b05203.

248. Wang, T.; Camps-Arbestain, M.; Hedley, M. The fate of phosphorus of ash-rich biochars in a soil-plant system. *Plant Soil* **2014**, *375*, 61–74, doi:10.1007/s11104-013-1938-z.

249. Rose, T.J.; Schefe, C.; Weng, Z. (Han); Rose, M.T.; van Zwieten, L.; Liu, L.; Rose, A.L. Phosphorus speciation and bioavailability in diverse biochars. *Plant Soil* **2019**, *443*, 233–244, doi:10.1007/s11104-019-04219-2.

250. Bergfeldt, B.; Tomasi Morgano, M.; Leibold, H.; Richter, F.; Stapf, D. Recovery of Phosphorus and other Nutrients during Pyrolysis of Chicken Manure. *Agriculture* **2018**, *8*, doi:10.3390/agriculture8120187.

251. Duboc, O.; Santner, J.; Golestani Fard, A.; Zehetner, F.; Tacconi, J.; Wenzel, W.W. Predicting phosphorus availability from chemically diverse conventional and recycling fertilizers. *Sci. Total Environ.* **2017**, *599–600*, 1160–1170, doi:10.1016/J.SCITOTENV.2017.05.054.

252. Pachón Gómez, E.M.; Domínguez, R.E.; López, D.A.; Téllez, J.F.; Marino, M.D.; Almada, N.; Gange, J.M.; Moyano, E.L. Chicken litter: A waste or a source of chemicals? Fast pyrolysis and hydrothermal conversion as alternatives in the valorisation of poultry waste. *J. Anal. Appl. Pyrolysis* **2023**, *169*, 105796, doi:10.1016/J.JAAP.2022.105796.

253. Chen, B.; Zhou, D.; Zhu, L. Transitional Adsorption and Partition of Nonpolar and Polar Aromatic Contaminants by Biochars of Pine Needles with Different Pyrolytic Temperatures. *Environ. Sci. Technol.* **2008**, *42*, 5137–5143, doi:10.1021/es8002684.

254. Méndez, A.; Paz-Ferreiro, J.; Araujo, F.; Gascó, G. Biochar from pyrolysis of deinking paper sludge and its use in the treatment of a nickel polluted soil. *J. Anal. Appl. Pyrolysis* **2014**, *107*, 46–52, doi:10.1016/J.JAAP.2014.02.001.

255. Huang, R.; Tang, Y. Speciation Dynamics of Phosphorus during (Hydro)Thermal Treatments of Sewage Sludge. *Environ. Sci. Technol.* **2015**, *49*, 14466–14474, doi:10.1021/acs.est.5b04140.

256. Bridle, T.R.; Pritchard, D. Energy and nutrient recovery from sewage sludge via pyrolysis. *Water Sci. Technol. a J. Int. Assoc. Water Pollut. Res.* **2004**, *50*, 169–175.

257. Meng, X.; Huang, Q.; Xu, J.; Gao, H.; Yan, J. A review of phosphorus recovery from different thermal treatment products of sewage sludge. *Waste Dispos. Sustain. Energy* **2019**, *1*, 99–115, doi:10.1007/s42768-019-00007-x.

258. Acharya, B.; Dutta, A.; Minaret, J. Review on comparative study of dry and wet torrefaction. *Sustain. Energy Technol. Assessments* **2015**, *12*, 26–37, doi:10.1016/J.SETA.2015.08.003.

259. Wang, L.; Chang, Y.; Li, A. Hydrothermal carbonization for energy-efficient processing of sewage sludge: A review. *Renew. Sustain. Energy Rev.* **2019**, *108*, 423–440, doi:10.1016/J.RSER.2019.04.011.

260. Mau, V.; Arye, G.; Gross, A. Poultry litter hydrochar as an amendment for sandy soils. *J. Environ. Manage.* **2020**, *271*, 110959, doi:10.1016/J.JENVMAN.2020.110959.

261. Heilmann, S.M.; Molde, J.S.; Timler, J.G.; Wood, B.M.; Mikula, A.L.; Vozhdayev, G. V; Colosky, E.C.; Spokas, K.A.; Valentas, K.J. Phosphorus Reclamation through Hydrothermal Carbonization of Animal Manures. *Environ. Sci. Technol.* **2014**, *48*, 10323–10329, doi:10.1021/es501872k.

262. Ghanim, B.M.; Pandey, D.S.; Kwapinski, W.; Leahy, J.J. Hydrothermal carbonisation of poultry litter: Effects of treatment temperature and residence time on yields and chemical properties of hydrochars. *Bioresour. Technol.* **2016**, *216*, 373–380, doi:10.1016/J.BIORTECH.2016.05.087.

263. Sun, K.; Ro, K.; Guo, M.; Novak, J.; Mashayekhi, H.; Xing, B. Sorption of bisphenol A, 17α-ethinyl estradiol and phenanthrene on thermally and hydrothermally produced biochars. *Bioresour. Technol.* **2011**, *102*, 5757–5763, doi:10.1016/J.BIORTECH.2011.03.038.

264. Huang, R.; Tang, Y. Evolution of phosphorus complexation and mineralogy during (hydro)thermal treatments of activated and anaerobically digested sludge: Insights from sequential extraction and P K-edge XANES. *Water Res.* **2016**, *100*, 439–447, doi:10.1016/j.watres.2016.05.029.

265. Takhim, M.; Sonveaux, M.; de Ruiter, R. The Ecophos Process: Highest Quality Market Products Out of Low-Grade Phosphate Rock and Sewage Sludge Ash. In *Phosphorus Recovery and Recycling*; Ohtake, H., Tsuneda, S., Eds.; Springer Singapore: Singapore, 2019; pp. 209–218.

266. Boniardi, G.; Turolla, A.; Fiameni, L.; Gelmi, E.; Bontempi, E.; Canziani, R. Phosphorus recovery from a pilot-scale grate furnace: influencing factors beyond wet chemical leaching conditions. *Water Sci. Technol.* **2022**, *85*, 2525–2538, doi:10.2166/wst.2022.132.

267. Gorazda, K.; Tarko, B.; Wzorek, Z.; Kominko, H.; Nowak, A.K.; Kulczycka, J.; Henclik, A.; Smol, M. Fertilisers production from ashes after sewage sludge combustion – A strategy towards sustainable development. *Environ. Res.* **2017**, *154*, 171–180, doi:10.1016/J.ENVRES.2017.01.002.

268. Abis, M.; Calmano, W.; Kuchta, K. Innovative technologies for phosphorus recovery from sewage sludge ash. *Detritus* **2018**, *1*, 23–29, doi:10.26403/detritus/2018.23.

269. Li, X.; Shen, S.; Xu, Y.; Guo, T.; Dai, H.; Lu, X. Mining phosphorus from waste streams at wastewater treatment plants: a review of enrichment, extraction, and crystallization methods. *Environ. Sci. Pollut. Res.* **2023**, doi:10.1007/s11356-023-25388-9.

270. Edmond, C.R. Direct Determination of Fluoride in Phosphate Rock Samples Using Specific Ion Electrode. *Anal. Chem.* **1969**, *41*, 1327–1328, doi:10.1021/ac60279a050.

271. Severin, M.; Breuer, J.; Rex, M.; Stemann, J.; Adam, C.; Van den Weghe, H.; Kücke, M. Phosphate fertilizer value of heat treated sewage sludge ash. *Plant, Soil Environ.* **2014**, *60*, 555–561, doi:10.17221/548/2014-pse.

272. Furszyfer Del Rio, D.D.; Sovacool, B.K.; Foley, A.M.; Griffiths, S.; Bazilian, M.; Kim, J.; Rooney, D. Decarbonizing the ceramics industry: A systematic and critical review of policy options, developments and sociotechnical systems. *Renew. Sustain. Energy Rev.* **2022**, *157*, 112081, doi:10.1016/j.rser.2022.112081.

273. Dal Pozzo, A.; Guglielmi, D.; Antonioni, G.; Tugnoli, A. Sustainability analysis of dry treatment technologies for acid gas removal in waste-to-energy plants. *J. Clean. Prod.* **2017**, *162*, 1061–1074, doi:10.1016/j.jclepro.2017.05.203.

274. Neuwahl, F.; Cusano, G.; Benavides, J.G.; Holbrook, S.; Serge, R. *Best Available Techniques (BAT) Reference Document for Waste Incineration*; 2019;

275. EIT-SusCritMOOC business idea competition on Critical Raw Materials Available online: https://eitrawmaterials.eu/ (accessed on May 20, 2022).

276. Siddique, I.J.; Salema, A.A.; Antunes, E.; Vinu, R. Technical challenges in scaling up the microwave technology for biomass processing. *Renew. Sustain. Energy Rev.* **2022**, *153*, 111767,

doi:10.1016/j.rser.2021.111767.

277. Bhattacharya, M.; Basak, T. A review on the susceptor assisted microwave processing of materials. *Energy* **2016**, *97*, 306–338, doi:10.1016/j.energy.2015.11.034.

278. Agrawal, S.; Rayapudi, V.; Dhawan, N. Comparison of microwave and conventional carbothermal reduction of red mud for recovery of iron values. *Miner. Eng.* **2019**, *132*, 202–210, doi:10.1016/J.MINENG.2018.12.012.

9. SCIENTIFIC CONTRIBUTION

International peer reviewed journal publications:

o Fahimi A., Bilo F., Assi A., Dalipi R., Federici S., Guedes A., Valentim B., Olgun H., Ye G., Bialecka B., **Fiameni L.**, Borgese L., Cathelineau M., Boiron M., Predeanu G., Bontempi E., Poultry litter ash characterisation and recovery. *Waste Management* (2020), **111**, 10-21. https://doi.org/10.1016/j.wasman.2020.05.010

o **Fiameni L.**, Assi A., Fahimi A., Valentim B., Moreira K., Predeanu G., Slăvescu V., Vasile B. Ş., Nicoară A. I., Borgese L., Boniardi G., Turolla A., Canziani R., Bontempi E., Simultaneous amorphous silica and phosphorus recovery from rice husk poultry litter ash. *RSC Advances* (2021), **11**, 8927-8939. https://doi.org/10.1039/d0ra10120f

o **Fiameni L.**, Fahimi A., Marchesi C., Sorrentino G. P., Zanoletti A., Moreira K., Valentim B., Predeanu G., Depero L. E., Bontempi E., Phosphorous and silica recovery from rice husk poultry litter ash: a sustainability analysis using a zero-waste approach. *Materials* (2021), **14** (21), 6297. https://doi.org/10.3390/ma14216297

o Boniardi G., Turolla A., **Fiameni L.**, Gelmi E., Malpei F., Bontempi B., Canziani R., Assessment of a simple and replicable procedure for selective phosphorus recovery from sewage sludge ashes by wet chemical extraction and precipitation. *Chemosphere* (2021), **285**, 131476. https://doi.org/10.1016/j.chemosphere.2021.131476

o Fahimi A., Bontempi E., **Fiameni L.**, Guedes A., Guimarães R., Moreira K., Santos A. C., Valentim B., Predeanu G., Bălănescu M., Olgun H., Boiron M., Cathelineau M., Incineration of aviary manure: the case studies of poultry litter and laying hens manure. *Waste and Biomass Valorization* (2022), **13**, 3335-3357. https://doi.org/10.1007/s12649-022-01739-4

o Boniardi G., Turolla A., **Fiameni L.**, Gelmi E., Bontempi E., Canziani R., Phosphorus recovery from a pilot-scale grate furnace: influencing factors beyond wet chemical leaching conditions. *Water Science & Technology* (2022), **85** (9), 2525–2538. https://doi.org/10.2166/wst.2022.132

o **Fiameni L.**, Fahimi A., Federici S., Cornelio A., Depero L. E., Bontempi E., A new breakthrough in the P recovery from sewage sludge ash by thermochemical processes. *Green Chemistry* (2022), **24**, 6836-6839. https://doi.org/10.1039/D2GC02328H

International conference proceedings:

o **Fiameni L.**, Fahimi A., Marchesi C., Sorrentino G. P., Bontempi E., The sustainability analysis of a zero-waste process combined with a statistical optimization: the case of rice husk poultry litter ash for phosphorous and silica recovery. *2nd International Conference Strategies toward Green Deal Implementation - Water, Raw Materials & Energy*. ISBN 978-83-963280-3-8.

Oral and poster presentations at international conferences:

o **Fiameni L.**, Boniardi G., Turolla A., Canziani R., Bontempi E., Simultaneous phosphorus and amorphous silica recovery from incinerated sewage sludge ash. *CLIMATE EXP0 - A fusion of science and policy advancing a resilient, zero-carbon world*, May 17-21, 2021, online conference. Poster and pre-recorded video presentation. https://doi.org/10.33774/coe-2022-zm3m7

o **Fiameni L.**, Fahimi A., Valentim B., Predeanu G., Bontempi E., Zero-waste phosphorus recovery from rice husk poultry litter ash. *ERA-MIN 2 Final Conference and Final review of Call 2017 projects*, November 19, 2021, online conference. Poster presentation and **winner of the Poster Competition Award.** https://www.era-min.eu/event/era-min-2-final-conference-and-final-seminar-call-2017-projects

o **Fiameni L.**, Fahimi A., Marchesi C., Sorrentino G. P., Bontempi E., The sustainability analysis of a zero-waste process combined with a statistical optimization: the case of rice husk poultry litter ash for phosphorous and silica recovery. *2nd International Conference Strategies toward Green Deal Implementation - Water, Raw Materials & Energy*, December 8-10, 2021, online conference. Poster and pre-recorded video presentation. https://greendeal2021.pl/pl/posters/

o **Fiameni L.**, Boniardi G., Turolla A., Canziani R., Bontempi E., Heavy metal stabilization in sewage sludge ash with poultry litter ash to enhance phosphorus recovery. *4th European Sustainable Phosphorus Conference ESPC4 and 5th European Phosphorus Research Meeting PERM5*, June 20-22, 2022, Vienna, Austria. Oral Presentation.

o **Fiameni L.**, Özaydin S., Yanik J., Bontempi E., An example of critical raw material recovery from biological waste: phosphorus extraction from Turkish chicken manure and sewage sludge. *9th International Conference on Engineering for Waste and Biomass Valorisation*, June 27-30, 2022, Copenhagen, Denmark. Poster presentation.

MODULO DI EMBARGO DELLA TESI
(da compilare solo se si richiede un periodo di segretazione della tesi)

Il/La sottoscritto/a…Fiameni Laura………………………… Nato/a il……17/02/1991…………………..
a (indicare anche l'eventuale paese estero)……Manerbio………………………………………………..
provincia di (ovvero sigla del paese estero)……Brescia………………………………………………….
Dottorato di Ricerca in …Ingegneria Meccanica e Industriale…………………………………………………

DICHIARA

- che il contenuto della tesi **non può essere immediatamente consultabile per il seguente motivo**

Le informazioni contenute in alcuni capitoli della tesi sono oggetto di attuale studio a seguito di deposito di un brevetto.

La motivazione deve essere dettagliata e controfirmata obbligatoriamente dal Tutor e/o Relatore
(Brevetto, segreto industriale, motivi di priorità nella ricerca, motivi editoriali, altro)

- che il testo completo della tesi potrà essere reso consultabile dopo:

□ 6 mesi dalla data di conseguimento titolo
■ 12 mesi dalla data di conseguimento titolo
□ 24 mesi dalla data di conseguimento titolo
□ altro periodo _____

- che sarà comunque consultabile immediatamente l'abstract della tesi, che viene caricato in Esse3, profilo studente.

Luogo e Data
Manerbio, 30/04/2023

Firma del Dichiarante
Laura Fiameni
_____

Controfirma del Tutor e/o Relatore del Dottorato
per la motivazione di embargo e il periodo.

Elsa Bontempi
_____